# Higher Strength Cold-Formed Steel Framed / Steel Shear Walls for Mid-Rise Construction

By

Robert Rizk

Research Project Director

Colin A.Rogers



Department of Civil Engineering and Applied Mechanics McGill University, Montréal, Canada August 2017

A thesis submitted to McGill University in partial fulfillment of the requirements of the degree of Masters of Engineering

©Robert Rizk 2017

## **ABSTRACT**

The current North American Standards, AISI S240 (2015) & AISI S400 (2015), provide design information for steel sheathed shear walls having a maximum sheathing thickness of 0.84mm (0.33") and a 1.37mm (0.54") thick frame. The specimens tested as part of past research programs composed of these members developed a shear resistance close to 30 kN/m (2058lb/ft) (#10 screws @ 50 mm (2") o.c.). There is a demand to be able to design all-steel shear walls that are capable of developing lateral resistance beyond 100 kN/m to bridge the gap between cold-formed steel and hot-rolled steel lateral framing shear wall systems. DaBreo (2012) showed that the full blocking increased the resistance of the shear walls by up to 25%.

The objectives of the current research project are; 1) to analyze the influence of the wall length for shear walls designed and built with quarter point blocking elements, and 2) to determine the influence of the framing thickness on the performance of the shear walls. In total, 28 specimens (14 configurations) were tested under monotonic and CUREE reversed cyclic loading protocols. The data analysis conducted to extract various design parameters for Canada was based on the Equivalent Energy Elastic-Plastic (EEEP) methodology. The equivalent design parameters were also determined for the United States of America and Mexico.

First, the results of this research program indicate that the shear resistance (normalized to length) is not be affected by the wall length for walls having an aspect ratio (h:w) less than (2:1). Walls having an aspect ratio (h:w) of 4:1 reached equivalent levels of ultimate resistance but had to be pushed to large displacement in order to attain those load levels. Second, the data collected showed that specimens constructed with a thicker framing developed a higher shear capacity. Lastly, the testing program showed that the quarter point blocking reinforcement reduced the distortion of the chord studs of the 2' (610 mm), 4' (1220 mm) and 6' (1830 mm) long walls. The full blocking did not restrict effectively the overall out-of-plane deformation of the 8' walls.

The recommended Canadian limits states design resistance factor  $\phi$  for shear walls with blocking reinforcement designed to carry lateral wind loads is 0.7. For the USA and Mexico, a resistance factor  $\phi$ =0.6 was recommended. Further, the reduction factor of 2w/h listed in the AISI S400 (2015) Standard for high aspect ratio walls is applicable for the design of blocked shear walls. The recommended factors of safety, calculated for limit states design (LSD) and allowable strength design (ASD) are respectively 2.06 and 2.88. For Canada, an overstrength value of 1.4 was recommended for the blocked specimens. Finally, for CFS framed / steel sheathed shear walls, the measured "test based" Canadian seismic force modification factors for ductility are  $R_d$ =2.0 and for overstrength,  $R_o$ =1.3.

The FEMA P795 methodology was applied in order to determine if the cold-formed steel shear walls designed with full frame blocking and thick sheathing / framing members is equivalent to line A.16 in Table 12.2-1 of ASCE/SEI (2010), which reads "Light-Frame (cold-formed steel) walls sheathed with wood structural panels rated for shear resistance or steel sheets." The results obtained from the analysis were not conclusive, some of the requirements listed by the FEMA P-795 to confirm the equivalency were not met. It is recommended to apply the FEMA P-695 methodology, in which R values are evaluated using a non-linear response history dynamic analyses of representative structures, whose load-deformation response is modelled after the results of the shear wall tests.

## RESUMÉ

Les normes nord-américaines actuelles, AISI S240 (2015) et AISI S400 (2015), fournissent des informations de conception pour les murs de refend (dotés de cadres et de revêtements en acier laminé à froid) ayant une épaisseur de revêtement maximale de 0,84 mm (0,33 ") et un cadre de 1,37 mm (0,54 ") d'épaisseur. Les spécimens testés dans le cadre de programmes de recherche passés composés de ces membres ont développé une résistance au cisaillement de 30 kN / m (2058 lb / pi) (vis # 10 à 50 mm (2 ") o.c.). Il est nécessaire de concevoir des murs de refend (dotés de cadres et de revêtements en acier laminé à froid) capables de développer une résistance latérale au-delà de 100 kN / m pour combler l'écart entre l'acier formé à froid et les systèmes de paroi latérale à charpente latérale en acier laminé à chaud. DaBreo (2012) a montré que le dispositif de blocage de l'armature augmentait la résistance des murs de cisaillement jusqu'à 25%

Les objectifs du projet de recherche actuel sont les suivants : 1) analyser l'influence de la longueur des murs sur la performance des murs de refend conçus et construits avec un dispositif de blocage de l'armature, et 2) déterminer l'influence de l'épaisseur des cadres sur la performance des murs de refend. Au total, 28 spécimens (14 configurations) ont été testés sous protocoles de chargement monotone et cyclique. L'analyse des données menée pour extraire divers paramètres de conception pour le Canada repose sur la méthodologie Equivalent Energy Elastic-Plastic (EEEP). Les paramètres de conception équivalents ont également été déterminés pour les États-Unis d'Amérique et le Mexique.

Tout d'abord, les résultats de ce programme de recherche indiquent que la résistance au cisaillement (normalisée à la longueur) n'est pas affectée par la longueur des murs de refend ayant un rapport d'aspect (h:w) inférieur à (2:1). Les murs de refend ayant un rapport d'aspect (h:w) de 4:1 ont atteint des niveaux équivalents de résistance ultime mais ont dû être poussés à un grand déplacement afin d'atteindre ces niveaux de charge. Deuxièmement, les données recueillies ont montré que les spécimens construits avec un cadrage plus épais ont développé une capacité de cisaillement plus élevée. Enfin, le programme de test a montré que dispositif de blocage de l'armature réduisait la distorsion

des éléments verticaux des murs de 2 '(610 mm), 4' (1220 mm) et 6 '(1830 mm). Le dispositif de blocage de l'armature n'a pas restreint efficacement la déformation globale hors-plan des murs 8 '.

Pour le Canada, un facteur de résistance  $\phi$ =0.7 a été recommandé . Pour les États-Unis et le Mexique, un facteur de résistance  $\phi$ =0.6 a été recommandé. En outre, le facteur de réduction de 2w / h indiqué dans la norme AISI S400 (2015) pour les murs à haut rapport d'aspect s'applique à la conception des murs de refend dotés d'un dispositif de blocage de l'armature. Les facteurs de sécurité recommandés, calculés pour la conception des états limites (LSD) et la conception admissible de la résistance (ASD) sont respectivement de 2,06 et 2,88. Pour le Canada, une valeur de sur-résistance de 1,4 était recommandée pour les spécimens bloqués. Enfin, pour les murs de refend dotés d'un dispositif de blocage de l'armature, les facteurs de modification de la force sismique canadienne mesurés à base de test pour la ductilité sont  $R_d$  = 2,0 et pour la sur-résistance,  $R_o$  = 1,3.

La méthodologie FEMA P795 a été appliquée pour déterminer si les murs de refend dotés d'un dispositif de blocage de l'armature sont équivalents à la ligne A.16 du tableau 12.2-1 de l'ASCE / SEI (2010) "Light-Frame (cold-formed steel) walls sheathed with wood structural panels rated for shear resistance or steel sheets." Les résultats obtenus à partir de l'analyse n'étaient pas concluants, certaines des exigences listées par FEMA P-795 pour confirmer l'équivalence n'ont pas été respectée. Il est donc recommandé d'appliquer la méthodologie FEMA P-695.

## **ACKNOWLEDGEMENTS**

I would like to thank first Prof.Rogers. It was a great opportunity to work under his supervision. I learned a lot from this experience on the professional level and on the personal level.

I would like to thank also the team that helped me in my work in the laboratory: Vincent Briere and Veronica Santos. A special thanks for John Bartczak and Damon Kiperchuk for their great contribution, they were as involved as anyone else on the team to complete this project.

On the personal level I would like to thank both my parents Mounir and Gisele for their support throughout all my academic years, my brothers Roger and Richard, and Jad Irani and Elias Yared.

Finally, I would like to thank the sponsors of this research program: The American Iron and Steel Institute (AISI), the Natural Sciences and Engineering Research Council of Canada (NSERC), the Canadian Sheet Steel Building Institute (CSSBI), Simpson Strong-Tie Co. Inc, Bailey Metal Products limited, Ontario Tools and Fasteners (OTF) and Arcelor Mittal.

## TABLE OF CONTENTS

A	BSTR	ACT		i
R	ESUM	1É		iii
A	CKNO	OWL	EDGEMENTS	v
T	ABLE	OF	CONTENTS	Vi
T	ABLE	OF	FIGURES	X
T.	ABLE	OF	TABLES	xiii
1	CH	IAPT	TER 1 – INTRODUCTION	1
	1.1	GE	NERAL OVERVIEW	1
	1.2	OB	JECTIVES	3
	1.3	SC	OPE AND LIMITATIONS OF STUDY	3
	1.4	TH	ESIS OUTLINE	4
	1.5	LIT	ERATURE REVIEW	5
	1.5	5.1	STEEL SHEATHED / CFS FRAMED SHEAR WALLS	5
	1.5	5.2	RELATED WOOD SHEATHED / CFS FRAMED SHEAR WALLS	. 27
2.	CH	IAPT	TER 2 - SHEAR WALL TEST PROGRAM	. 32
	2.1 II	NTRO	ODUCTION	. 32
	2.2	STI	EEL FRAME/ STEEL PANEL SHEAR WALLS TESTING PROGRAM.	. 34
	2.3	SPI	ECIMEN FABRICATION, TEST SETUP AND INSTRUMENTATION .	. 37
	2.3	3.1	COMPONENTS	. 37
	2.3	3.2	SPECIMEN FABRICATION	. 39
	2.3	3.3	TEST SETUP	. 42
	2.3	3.4	INSTRUMENTATION AND DATA ACQUISITION	. 43
	2.4	TE	STING PROTOCOLS	. 45
	2.4	.1	MONOTONIC TESTING PROTOCOL	. 45
	2.4	2	REVERSED-CYCLIC TESTING PROTOCOL	. 46
	2.5	OB	SERVED FAILURE MODES	. 50
	2.5	5.1	CONNECTION FAILURE	. 50
	2.5	5.2	SHEATHING FAILURE	. 54
	2.5	5.3	FRAMING	. 56
	2.5	5.4	FAILURE MODES OF SHORT WALLS	. 59
	2.5	5.5	FAILURE MODES OF LONG WALLS	. 59
	2.6	DA	TA REDUCTION	. 62
	2.6	5.1	LATERAL DISPLACEMENT	62

	2.6	.2	ENERGY DISSIPATION	62
,	2.7	TES	ST RESULTS	64
2	2.8	AN	CILLARY TESTING OF MATERIALS	70
3 DE	_		ER 3 – INTERPRETATION OF TEST RESULTS AND PRESCRIPTI	
	3.1	INT	RODUCTION	73
	3.2	EEI	EP CONCEPT, CANADA	73
	3.3	DE	SIGN PARAMETERS FOR CANADA, THE U.S.A AND MEXICO	76
	3.4	CO	MPARISON OF SHEAR WALL CONFIGURATIONS	82
	3.4	.1	EFFECT OF FASTENER SPACING	84
	3.4	.2	EFFECT OF WALL LENGTH	86
	3.4	.3	EFFECT OF FRAMING THICKNESS	89
	3.4	.4	EFFECT OF FRAME BLOCKING	91
	3.5	LIN	IIT STATES DESIGN PROCEDURE (CANADA)	96
	3.5	.1	CALIBRATION OF RESISTANCE FACTOR FOR CANADA	98
	3.5 ME		CALIBRATION OF RESISTANCE FACTOR FOR THE USA & O	103
	3.5	.3	NOMINAL SHEAR WALL RESISTANCE FOR CANADA	105
	3.5	.4	NOMINAL SHEAR WALL RESISTANCE FOR THE USA & MEXION 108	CO
	3.5 AS		VERIFICATION OF SHEAR RESISTANCE REDUCTION FOR HIG T RATIO WALLS (CANADA)	
	3.5 AS		VERIFICATION OF SHEAR RESISTANCE REDUCTION FOR HIGH	
	3.5	.7	FACTOR OF SAFETY, CANADA	115
	3.5	.8	CAPACITY BASED DESIGN, CANADA	117
	3.5	.9	CAPACITY BASED DESIGN FOR THE USA AND MEXICO	120
		.10 NAI	TEST-BASED SEISMIC FORCE MODIFICATION FACTORS FC DA 121	)R
		.11 CTO	TEST-BASED DUCTILITY-RELATED FORCE MODIFICATION $PR, R_d$	
		.12 DDIF	TEST-BASED OVERSTRENGTH-RELATED FORCE ICATION FACTOR, $R_{\scriptscriptstyle 0}$	124
		.13 E UI	TEST BASED SEISMIC FORCE MODIFICATION FACTORS FONITED STATES OF AMERICA	
	3.5	.14	INELASTIC DRIFT LIMIT	125
4	СН	АРТ	ER 4 – COMPONENT EQUIVALENCY METHODOLOGY	127

4.1	INTRODUCTION	127
4.2	COMPONENT TESTING REQUIREMENT	128
4.2	2.1 GENERAL REQUIREMENTS FOR COMPONENT TESTING	129
4.2	2.2 CYCLIC LOAD TESTING	132
4.3	MONOTONIC LOAD TESTING	134
4.4	EVALUATION OF APPLICABILITY CRITERIA	136
	4.1 REFERENCE SEISMIC-FORCE-RESISTING SYSTEM: COLLAR ERFORMANCE CRITERIA	
4.4	4.2 QUALITY RATING CRITERIA	136
4.4	4.3 GENERAL CRITERIA	137
4.5	REFERENCE COMPONENT TEST DATA	138
4.5	7.1 REFERENCE COMPONENT DESIGN SPACE	138
4.5	5.2 REFERENCE COMPONENT PERFORMANCE GROUPS	143
4.5	5.3 TEST DATA & SUMMARY STATISTICS	143
4.6	PROPOSED COMPONENT TEST DATA	155
4.6	5.1 PROPOSED COMPONENT DESIGN SPACE	155
4.6	5.2 PROPOSED COMPONENT PERFORMANCE GROUPS	158
4.6	5.3 TEST DATA & SUMMARY STATISTICS	158
4.7	EVALUATE QUALITY RATINGS	162
4.7	7.1 QUALITY RATING OF TEST DATA	162
4.7	7.2 QUALITY RATING OF DESIGN REQUIREMENTS	164
4.8	EVALUATE COMPONENT EQUIVALENCY	165
4.8	3.1 OVERVIEW	165
	3.2 REQUIREMENTS BASED ON CYCLIC-LOAD TEST DATA: RENGTH AND ULTIMATE DEFORMATION	166
	3.3 REQUIREMENTS BASED ON CYCLIC-LOAD TEST DATA: FFECTIVE DUCTILITY CAPACITY	169
	3.4 REQUIREMENTS BASED ON CYCLIC-LOAD TEST DATA: FFECTIVE INITIAL STIFFNESS	170
	B.5 REQUIREMENTS BASED ON MONOTONIC-LOAD TEST DAT LTIMATE DEFORMATION	
4.9	CONCLUSION	171
	HAPTER 5- CONCLUSIONS AND RECOMMENDATIONS	
5.1	CONCLUSIONS	
5.2	RECOMMENDATIONS FOR FUTURE STUDY	174
EEER	ENCES	176

5

APPENDIX A TEST CONFIGURATION	. 179
APPENDIX B DATA ANALYSIS	. 193
APPENDIX C LOADING PROTOCOL	. 249
APPENDIX D OBSERVATION SHEETS	277

## TABLE OF FIGURES

FIGURE 1.1 COLD-FORMED STEEL SHEAR WALL CONSTRUCTION (COURTESY OF JEF	F
ELLIS, SIMPSON STRONG-TIE)	2
FIGURE 1.2 FAILURE MODE OF $6^{\circ}\times8^{\circ}$ WALL WITH (RIGHT) AND WITHOUT (LEFT) SPECTOR (CONTINUE TO SPECTOR).	CIAL
DETAILING (YU ET AL., 2009)	9
FIGURE 1.3 FORCE VS. DISPLACEMENT TEST HYSTERESIS CURVES FOR $8^{\prime}\times4^{\prime}$ WALLS	WITH
33-MIL SHEATHING) (YU ET AL., 2009)	11
FIGURE 1.4 FORCE VS. DISPLACEMENT TEST HYSTERESIS CURVES FOR $8^{\prime}\times$ $2^{\prime}$ WALLS	WITH
33-MIL SHEATHING (YU ET AL., 2009)	12
FIGURE 1.5 COMPARISON OF REINFORCEMENT: WALL RESISTANCE VS. DISPLACEMENT	ENT OF
TESTS 9M-A,B,C (BALH, 2010)	15
FIGURE 1.6 CHORD TWISTING OF UNBLOCKED WALLS (BALH, 2010)	19
FIGURE 1.7 COMPARISON OF REINFORCEMENT: WALL RESISTANCE VS. DISPLACEMENT	ENT OF
MONOTONIC TESTS (DABREO, 2012)	20
FIGURE 1.8 COMPARISON OF REINFORCEMENT: WALL RESISTANCE VS. DISPLACEMENT	ENT OF
REVERSED-CYCLIC TESTS (DABREO, 2012)	20
FIGURE 1.9 COMPARISON OF DESIGN VALUE: EEEP CURVES OF BLOCKED WALLS VS	) <b>.</b>
UNBLOCKED WALLS (DABREO, 2012)	21
FIGURE 1.10 SCHEMATIC OF UPLIFT DEFORMATION: A) SINGLE-STOREY, AND B) DO	UBLE-
STOREY WALL (SHAMIM, 2012)	24
FIGURE 1.11 INITIAL MODEL OF SHEAR WALLS IN OPENSEES, SHAMIM (2012)	25
FIGURE 1.12 DEVELOPED MODEL OF SHEAR WALLS IN OPENSEES A) DIAGONAL BRA	CE B)
BRACE NET SHAMIM (2012)	25
FIGURE 1.13 WALL RESISTANCE VS. DISPLACEMENT CURVE FOR A TYPICAL MONOTOR $(1.13)$	ONIC
TEST, BRANSTON (2005)	29
FIGURE 2.1 SHEAR WALL TEST FRAME	33
FIGURE 2.2 TYPICAL WALL INSTALLATION IN TEST FRAME	34
FIGURE 2.3 SHEAR WALL CONFIGURATIONS W3, W1 AND W12	35
FIGURE 2.4 A) SHEAR WALL W1-M FRONT VIEW OF THE WALL, B) SHEAR WALL W1-M	М
BACK VIEW OF THE WALL	37
FIGURE 2.5- A) FRAME ASSEMBLY WITH TEMPORARY BRACE, B) SHEATHING ASSEM	IBLY 41
FIGURE 2.6 BLOCKING CONNECTION	41
FIGURE 2.7 SHEATHING COMBINATION FOR $1830 \times 2440$ MM (6'×8') SHEAR WALLS	42
FIGURE 2.8 INSTRUMENTATION LOCATIONS	43
FIGURE 2.9 LVDT PLACEMENT ON NON-STRUCTURAL STEEL PLATE	44
FIGURE 2.10 REPRESENTATIVE FORCE VS. DISPLACEMENT MONOTONIC TEST CURV	E46
FIGURE 2.11 REPRESENTATIVE CUREE DISPLACEMENT TIME HISTORY	49

FIGURE 2.12 REPRESENTATIVE FORCE VS. DISPLACEMENT CUREE REVERSED-CYCL	IC TEST
CURVE	49
FIGURE 2.13 SHEATHING STEEL BEARING	51
FIGURE 2.14 SHEATHING SCREW TILTING	51
FIGURE 2.15 SHEATHING SCREW PULL-OUT FAILURE	52
FIGURE 2.16 SCREW PULL-THROUGH SHEATHING FAILURE	53
FIGURE 2.17 SCREW TEAR-OUT FAILURE	53
FIGURE 2.18 SHEAR BUCKLING AND TENSION FIELD ACTION OF SHEATHING ; A)	
MONOTONIC TEST (1220 $\times$ 2440 MM (4' $\times$ 8')), B) REVERSED CYCLIC TEST (1220 $\times$	2440
MM (4' × 8'))	54
FIGURE 2.19 SHEAR BUCKLING AND TENSION FIELD OF SHEATHING ; A) MONOTONI	IC TEST
$(1830 \times 2440 \text{ MM } (6' \times 8')), \text{ B) REVERSED CYCLIC TEST } (1830 \times 2440 \text{ MM } (6' \times 8'))$	55
FIGURE 2.20 SHEAR BUCKLING AND TENSION FIELD OF SHEATHING : A) MONOTONI	IC TEST
$(2440 \times 2440 \text{ MM } (8' \times 8')), \text{ B) REVERSED CYCLIC TEST } (2440 \times 2440 \text{ MM } (8' \times 8'))$	55
FIGURE 2.21 FLANGE AND LIP DISTORTED UNWRAPPED AFTER TESTING : A) SPECIM	1EN W1
M, AND B) SPECIMEN W1-C	57
FIGURE 2.22 A) DEFORMATION AND UPLIFT OF BOTTOM TRACK, B) DEFORMATION	AND
UPLIFT OF TOP TRACK	58
FIGURE 2.23 LOCAL BUCKLING OF THE CHORD STUDS IN 610×2440MM (2'×8') WALLS	59
FIGURE 2.24 FLEXURAL BENDING OF FIELD STUD IN LONG WALLS	60
FIGURE 2.25 COMBINATION OF FAILURE MODES IN 1220×2440MM (4'×8') WALLS : A) I	FLANGE
AND LIP DISTORTION OF THE CHORD STUDS, B) UPLIFT OF THE BOTTOM TRAC	CKS, C)
PULL THROUGH SHEATHING	61
FIGURE 2.26 ENERGY AS AREA BELOW FORCE VS. DISPLACEMENT CURVE	63
FIGURE 2.27 PARAMETERS OF MONOTONIC TESTS	64
FIGURE 2.28 PARAMETERS OF REVERSED-CYCLIC TESTS	65
FIGURE 3.1 EEEP MODEL (BRANSTON, 2004)	74
FIGURE 3.2 RESULTING EEEP CURVE FOR THE OBSERVED MONOTONIC CURVE (TES	T W7-
M)	76
FIGURE 3.3 RESULTING EEEP CURVES FOR THE OBSERVED REVERSED-CYCLIC CUR	VE77
FIGURE 3.4 DESIGN VALUES FOR THE USA AND MEXICO (W7-M)	78
FIGURE 3.5 DESIGN VALUES FOR THE USA AND MEXICO (W7-C)	78
FIGURE 3.6 LOSS OF SHEAR RESISTANCE DUE TO SHEATHING SHEAR BUCKLING AN	1D
SHEATHING CONNECTION FAILURE (TEST W8-M)	83
FIGURE 3.7 COMPARISON OF FASTENER SPACING: WALL RESISTANCE VS. DISPLACE	EMENT
FOR COMPARISON GROUP 2	86
FIGURE 3.8 COMPARISON OF WALL LENGTH: WALL RESISTANCE VS. DISPLACEMEN	IT89

FIGURE 3.9 COMPARISON OF FRAMING THICKNESS: WALL RESISTANCE VS.
DISPLACEMENT91
FIGURE 3.10 DRIFT, $\Delta D$ , FOR SHORT WALL AT REDUCED RESISTANCE111
FIGURE 3.11 DRIFT, $\Delta D$ , FOR 1830MM (6 $\square$ ) LONG WALL AT NOMINAL RESISTANCE111
FIGURE 3.12 DRIFT, $\Delta D$ , FOR SHORT WALL AT REDUCED RESISTANCE (W5-M)113
FIGURE 3.13 DRIFT, $\Delta D$ , FOR 1830MM (6 $\square$ ) LONG WALL AT NOMINAL RESISTANCE (W9-M)
FIGURE 3.14 FACTOR OF SAFETY RELATIONSHIP WITH ULTIMATE AND FACTORED
RESISTANCES
FIGURE 3.15 OVERSTRENGTH RELATIONSHIP WITH ULTIMATE AND NOMINAL SHEAR
RESISTANCE118
FIGURE 4.1 REVERSED CYCLIC LOAD TEST DATA, ENVELOPE CURE AND PERFORMANCE
PARAMETERS, (FEMA P-795, 2011)134
FIGURE 4.2 MONOTONIC LOAD TEST DATA AND PERFORMANCE PARAMETERS, (FEMA P-
795, 2011)
FIGURE 4.3 ILLUSTRATION OF PROPOSED COMPONENT BOUNDARIES (COURTESY OF RJC
LTD)137
FIGURE 4.4 ILLUSTRATION OF MONOTONIC RESPONSE OF COLD-FORMED STEEL SHEAR
WALLS SHEATHED WITH STEEL SHEATHING, DATA FROM BALH (2010)144
FIGURE 4.5 ILLUSTRATION OF CYCLIC RESPONSE OF COLD-FORMED STEEL SHEAR WALLS
SHEATHED WITH STEEL SHEATHING, DATA FROM BALH (2010)144

## TABLE OF TABLES

TABLE 1.1BENEFITS OF COLD-FORMED STEEL (STEEL FRAMING ALLIANCE, 2017)	1
TABLE 1.2 SHEAR WALL TEST MATRIX (SERRETTE 1997)	6
TABLE 1.3 SHEAR WALL TEST MATRIX (YU ET AL., 2007)	8
TABLE 1.4 SHEAR WALL TEST MATRIX (YU ET AL., 2009)	.10
TABLE 1.5 NOMINAL SHEAR VALUES FOR ORDINARY AND BLOCKED STEEL SHEATHED	
WALLS (EL-SALOUSSY, 2010)	.13
TABLE 1.6 SHEAR WALL TEST MATRIX (BALH, 2010 & ONG-TONE, 2009)	.14
TABLE 1.7 SHEAR WALL TEST MATRIX (DABREO, 2012)	.17
TABLE 1.8 NORMALIZED PARAMETERS FOR COMPARISON OF BLOCKED TO	
CONVENTIONAL SHEAR WALL- MONOTONIC TEST (DABREO, 2012)	.18
TABLE 2.1 SHEAR WALL TEST MATRIX (NOMINAL DIMENSIONS)	.36
TABLE 2.2 CUREE PROTOCOL INPUT DISPLACEMENTS FOR TEST W8	.48
TABLE 2.3 TEST DATA SUMMARY – MONOTONIC TESTS	.66
TABLE 2.4 TEST DATA SUMMARY – POSITIVE CYCLES REVERSED CYCLIC TESTS	.67
TABLE 2.5 TEST DATA SUMMARY – NEGATIVE CYCLES REVERSED CYCLIC TESTS	.68
TABLE 2.6 TEST DATA SUMMARY – REVERSED CYCLIC TESTS AVERAGE VALUES	.69
TABLE 2.7 SUMMARY OF MATERIAL PROPERTIES	.71
TABLE 2.8 R <sub>T</sub> AND R <sub>Y</sub> VALUES OF STUDS/TRACKS/SHEATHING	.72
TABLE 3.1 DESIGN VALUES FOR MONOTONIC SHEAR WALL TESTS	.79
TABLE 3.2 DESIGN VALUES FOR REVERSED-CYCLIC SHEAR WALL TESTS: POSITIVE	
CYCLES	.80
TABLE 3.3 DESIGN VALUES FOR REVERSED-CYCLIC SHEAR WALL TESTS: NEGATIVE	
CYCLES	.81
TABLE 3.4 COMPARISON GROUPS (EFFECT OF SHEATHING FASTENER SPACING)	.84
TABLE 3.5 COMPARISON OF NORMALIZED ULTIMATE RESISTANCE FOR MONOTONIC	
TESTS (EFFECT OF SHEATHING FASTENER SPACING)	.84
TABLE 3.6 COMPARISON OF NORMALIZED ULTIMATE RESISTANCE FOR REVERSED-CYCL	JC
TESTS (EFFECT OF SHEATHING FASTENER SPACING)	.85
TABLE 3.7 COMPARISON GROUPS (EFFECT OF WALL LENGTH)	.87
TABLE 3.8 COMPARISON OF NORMALIZED ULTIMATE RESISTANCE FOR MONOTONIC	
TESTS	.87
TABLE 3.9 COMPARISON OF NORMALIZED ULTIMATE RESISTANCE FOR REVERSED-CYCL	JIC
TESTS (EFFECT OF WALL LENGTH)	.88
TABLE 3.10 COMPARISON GROUPS (EFFECT OF FRAMING THICKNESS)	.90
TABLE 3.11 COMPARISON OF NORMALIZED ULTIMATE RESISTANCE FOR MONOTONIC	
TESTS (EFFECT OF FRAMING THICKNESS)	90

TABLE 3.12 COMPARISON OF NORMALIZED ULTIMATE RESISTANCE FOR REVERSEI	)-
CYCLIC TESTS (EFFECT OF FRAMING THICKNESS)	90
TABLE 3.13 COMPARISON GROUPS AND SHEAR WALL CONFIGURATIONS	92
TABLE 3.14 NORMALIZED PARAMETERS FOR COMPARISON OF BLOCKED TO	
CONVENTIONAL SHEAR WALLS - MONOTONIC TESTS (EFFECT OF FRAME BLO	CKING)
	93
TABLE 3.15 NORMALIZED PARAMETERS FOR COMPARISON OF BLOCKED TO	
CONVENTIONAL SHEAR WALLS – REVERSED-CYCLIC TESTS (EFFECT OF FRAM	1E
BLOCKING)	94
TABLE 3.16 DESCRIPTION OF TEST SPECIMEN GROUP CONFIGURATIONS FOR LIMIT	STATES
DESIGN PROCEDURE (CANADA)	97
TABLE 3.17 STATISTICAL DATA FOR THE DETERMINATION OF RESISTANCE FACTOR	R (AISI
S100, 2016)	100
TABLE 3.18 SUMMARY OF RESISTANCE FACTOR CALIBRATION FOR DIFFERENT TY	PES OF
COMPONENTS AND FAILURE MODES (CANADA)	102
TABLE 3.19 SUMMARY OF RESISTANCE FACTORS, $\phi$ , CALIBRATION RESULTS FOR	
DIFFERENT TYPES OF COMPONENT FAILURE MODES (CANADA)	102
TABLE 3.20 SUMMARY OF RESISTANCE FACTOR CALIBRATION FOR DIFFERENT TY	PES OF
COMPONENTS AND FAILURE MODES (USA AND MEXICO)	105
TABLE 3.21 SHEATHING THICKNESS AND TENSILE STRESS MODIFICATION FACTOR	S106
TABLE 3.22 MODIFICATION FACTORS OF PAST RESEARCH ON STEEL SHEATHED SH	EAR
WALLS	106
TABLE 3.23 NOMINAL SHEAR RESISTANCE, SY, FOR CFS FRAMED/STEEL SHEATHED	)
BLOCKED SHEAR WALLS <sup>1,2,3</sup> (KN/M) (CANADA)	107
TABLE 3.24 SUMMARY OF PROPOSED NOMINAL SHEAR RESISTANCE, SY, FOR CFS	
FRAMED/STEEL SHEATHED BLOCKED SHEAR WALLS (KN/M)	108
TABLE 3.25 SUMMARY OF PROPOSED NOMINAL SHEAR RESISTANCE, SU, FOR CFS	
FRAMED/STEEL SHEATHED BLOCKED SHEAR WALLS (LB/FT)	109
TABLE 3.26 VERIFICATION OF SHEAR RESISTANCE REDUCTION FOR HIGH ASPECT I	RATIO
WALLS (CANADA)	110
TABLE 3.27 AVERAGE DRIFT VALUES, $\Delta_D$	112
TABLE 3.28 VERIFICATION OF SHEAR RESISTANCE REDUCTION FOR HIGH ASPECT I	RATIO
WALLS (USA & MEXICO)	113
TABLE 3.29 AVERAGE DRIFT VALUES, $\Delta_D$	114
TABLE 3.30 FACTOR OF SAFETY FOR THE MONOTONIC TEST SPECIMENS	116
TABLE 3.31 FACTOR OF SAFETY FOR THE REVERSED-CYCLIC TEST SPECIMENS	117
TABLE 3 32 OVERSTRENGTH DESIGN VALUES FOR MONOTONIC TESTS (CANADA)	119

TABLE 3.33 OVERSTRENGTH DESIGN VALUES FOR REVERSED-CYCLIC TESTS (CANADA)	120
TABLE 3.34 DUCTILITY AND TEST-BASED RD VALUES FOR MONOTONIC TESTS	123
TABLE 3.35 DUCTILITY AND TEST-BASED RD VALUES FOR REVERSED-CYCLIC TESTS1	123
TABLE 3.36 OVERSTRENGTH FACTORS FOR CALCULATING THE TEST-BASED	
OVERSTRENGTH-RELATED FORCE MODIFICATION FACTOR, RO	125
TABLE 3.37 DRIFTS AT $\Delta_{0.8U}$ OF MONOTONIC TESTS	126
TABLE 3.38 DRIFTS AT $\Delta_{0.8U}$ OF REVERSED-CYCLIC TESTS	126
TABLE 4.1 SUMMARY OF COLD-FORMED STEEL FRAMED SHEAR WALLS WITH STEEL	
SHEATHING CONFIGURATIONS IN THE REFERENCE COMPONENT DATA BY YU ET A	L.
(2007) PHASE 1	139
TABLE 4.2 SUMMARY OF COLD-FORMED STEEL FRAMED SHEAR WALLS WITH STEEL	
SHEATHING CONFIGURATIONS IN THE REFERENCE COMPONENT DATA BY YU ET A	L.
(2009) PHASE 2	140
TABLE 4.3 SUMMARY OF COLD-FORMED STEEL FRAMED SHEAR WALLS WITH STEEL	
SHEATHING CONFIGURATIONS IN THE REFERENCE COMPONENT DATA BY BALH	
(2010) AND ONG-TONE (2009)	142
TABLE 4.4 NOMINAL SHEAR STRENGTH [RESISTANCE] (VN) PER UNIT LENGTH FOR	
SEISMIC AND OTHER IN-PLANE LOADS FOR SHEAR WALLS WITH STEEL SHEET	
SHEATHING ON ONE SIDE OF WALL (USA AND MEXICO) (AISI S400 2015)	146
TABLE 4.5 NOMINAL SHEAR STRENGTH [RESISTANCE] (VN) PER UNIT LENGTH FOR	
SEISMIC AND OTHER IN-PLANE LOADS FOR SHEAR WALLS WITH STEEL SHEET	
SHEATHING ON ONE SIDE OF WALL (CANADA) (AISI S400 2015)	147
TABLE 4.6 SUMMARY OF IMPORTANT COMPONENT PARAMETERS FOR THE REFERENCE	
COMPONENT DATA SET -MONOTONIC TEST DATA BY YU ET AL. (2007) PHASE 1	148
TABLE 4.7 SUMMARY OF IMPORTANT COMPONENT PARAMETERS FOR THE REFERENCE	
COMPONENT DATA SET -MONOTONIC TEST DATA BY YU ET AL. (2009) PHASE 2	149
TABLE 4.8 SUMMARY OF IMPORTANT COMPONENT PARAMETERS FOR THE REFERENCE	
COMPONENT DATA SET –REVERSED CYCLIC TEST DATA BY YU ET AL. (2007) PHASE	Ξ 1
	150
TABLE 4.9 SUMMARY OF IMPORTANT COMPONENT PARAMETERS FOR THE REFERENCE	
COMPONENT DATA SET –REVERSED CYCLIC TEST DATA BY YU ET AL. (2007) PHASE	Ξ2
1	151
TABLE 4.10 SUMMARY OF IMPORTANT COMPONENT PARAMETERS FOR THE REFERENCE	2
COMPONENT DATA SET –REVERSED CYCLIC TEST DATA BY BALH (2010) AND ONG-	
TONE (2009)	152
TABLE 4.11 SUMMARY STATISTICS FOR REFERENCE COMPONENT PARAMETERS-	
MONOTONIC TESTS (43 SPECIMENS)	153

TABLE 4.12 SUMMARY STATISTICS FOR REFERENCE COMPONENT PARAMETERS-
REVERSED CYCLIC TESTS (53 SPECIMENS)
TABLE 4.13 SUMMARY OF COLD-FORMED STEEL FRAMED STEEL SHEATHED SHEAR
WALLS DESIGNED WITH FULL FRAME BLOCKING AND THICK SHEATHING / FRAMING
MEMBERS (DABREO (2012))
TABLE 4.14 SUMMARY OF COLD FORMED STEEL FRAMED STEEL SHEATHED SHEAR
WALLS DESIGNED WITH FULL FRAME BLOCKING AND THICK SHEATHING / FRAMING
MEMBERS (RIZK (2017))
TABLE 4.15 SUMMARY OF IMPORTANT COMPONENT PARAMETERS FOR THE PROPOSED.158
TABLE 4.16 SUMMARY OF IMPORTANT COMPONENT PARAMETERS FOR THE PROPOSED.159
TABLE 4.17 SUMMARY STATISTICS FOR PROPOSED COMPONENT PARAMETERS-
MONOTONIC TESTS, (17 SPECIMENS)160
TABLE 4.18 SUMMARY STATISTICS FOR PROPOSED COMPONENT PARAMETERS- REVERSED
CYCLIC TESTS, (16 SPECIMENS)161
TABLE 4.19 QUALITY RATING OF TEST DATA, (FEMA P-795, 2011)162
TABLE 4.20 QUALITY RATING OF DESIGN REQUIREMENTS, (FEMA P-795, 2011)164
TABLE 4.21 SUMMARY OF ACCEPTANCE CRITERIA (CYCLIC-LOAD TEST DATA), (FEMA P-
795, 2011)166
TABLE 4.22 SUMMARY OF ACCEPTANCE CRITERIA (MONOTONIC-LOAD TEST DATA),
(FEMA P-795, 2011)166
TABLE 4.23 PENALTY FACTOR TO ACCOUNT FOR UNCERTAINTY,167
TABLE 4.24 PENALTY FACTOR TO ACCOUNT FOR DIFFERENCES IN LOAD (STRENGTH)167
TABLE 4.25 EVALUATION OF EQUIVALENCY ACCEPTANCE CRITERIA FOR INDIVIDUAL
COMPONENT CONFIGURATIONS

## 1 CHAPTER 1 – INTRODUCTION

### 1.1 GENERAL OVERVIEW

The construction industry in North America witnessed major shifts in the past decades mainly driven by demographical, environmental and economic changes. For these reasons, and due to the multiple benefits to the builders and consumers listed in Table 1.1, the demand for cold-formed steel (CFS) has significantly increased in recent years mainly for low to mid-rise residential and commercial buildings, such as apartments, single family dwellings, multi residential units, hotels, schools, box stores and office buildings.

Table 1.1Benefits of Cold-Formed Steel (Steel Framing Alliance, 2017).

	BENEFITS								
	Builder	Consumers							
1.	Substantial discounts on builders' risk	1.	High strength results in safer structures,						
	insurance.		less maintenance and slower aging of						
2.	Lighter than other framing materials.		structure.						
3.	Non-combustible.	2.	Fire safety - does not burn or add fuel to						
4.	Easy material selection - no need to cull		the spread of a house fire.						
	or sort the pile and small punch list.	3.	Not vulnerable to termites.						
5.	Saves job-site time with ease of	4.	Not vulnerable to any type of fungi or						
	penalization off-site.		organism, including mould.						
6.	Most cost-effective mid-rise structural	5.	Less probability of foundation problems -						
	material.		less weight results in less movement.						
7.	Highest strength-to-weight ratio of any	6.	Less probability of damage in an						
	building material.		earthquake.						
8.	Price stability - price spikes are extremely	7.	Lighter structure with stronger						
	rare.		connections results in less seismic force.						
9.	Consumer perceives steel as better.	8.	Less probability of damage in high winds.						
		9.	Stronger connections, screwed versus						
			nailed						

The rate of penetration in the market place of cold-formed steel construction varies across North America. For example, research shows that 40% of residential buildings in Hawaii are built with CFS Framing (*Steel Framing alliance, 2005*). This number is significantly lower in Canada, where the rate of progression of cold-formed steel construction is relatively low. While many factors have an impact on these numbers, an important reason

is due to the deficiencies of the Canadian standards to provide guidelines for seismic design of CFS structures to structural engineers.

The use of cold-formed steel sheathed CFS framed shear walls is relatively new. In the past years, it was more common to design wood sheathed and gypsum panel cold-formed steel framed shear walls, as well as strap braced walls. For this reason, academic institutions in collaboration with the industry are investing heavily in research to better understand the performance of such structures. The intent is to be able to design all-steel shear walls that are capable of developing lateral resistance beyond 100 kN/m to bridge the gap between cold-formed steel and hot-rolled steel lateral framing shear wall systems. The current North American Standards, AISI S240 (2015) & AISI S400 (2015), provide design information for shear walls designed having a maximum sheathing thickness of 0.84mm and a 1.37mm thick frame (Balh et al. 2014, DaBreo et al. 2014, Yu 2010, Yu & Chen 2011). The specimens tested as part of past research programs composed of these elements developed a nominal shear resistance close to 30 kN/m (#10 screws @ 50 mm o.c.).

The building process of steel-sheathed CFS framed shear walls is similar to the techniques used in the past for wood-sheathed walls: Once the detailing and pre-assembling of the individual structural members of the specimens is achieved, the assembling of the different components is completed using platform or ledger framing techniques. The lateral resistance of the CFS shear walls developed to provide stability under wind or earthquake loading is dictated by the framing members, the sheathing, the sheathing fastener pattern and screw size, as well as the holdowns.



Figure 1.1 Cold-Formed Steel Shear Wall Construction (Courtesy of Jeff Ellis, Simpson Strong-Tie)

### 1.2 OBJECTIVES

The objectives of the research program are as follows:

- 1. Conduct monotonic and reversed-cyclic loading tests on single-storey steel sheathed/cold-formed steel framed shear walls built with special blocking detailing, having various aspect ratios and framing thicknesses.
- 2. Apply the Equivalent Energy Elastic Plastic (EEEP) methodology (Park, 1989 and Foliente, 1996), deemed appropriate by Branston (2004), in order to extract relevant design parameters and nominal shear resistance values for Canada for the configurations tested as part of this research program.
- 3. Extract design parameters and compute nominal shear resistance values for the U.S& Mexico for the configurations tested as part of this research program.
- 4. Compare the performance of fully blocked walls with respect to the performance of shear walls designed without special detailing.
- 5. Specify the appropriate resistance factor,  $\phi$ , for ultimate states design, and recommend the appropriate nominal shear resistance values, factor of safety, and the "test based" seismic force modification factors for ductility and overstrength,  $R_d$ ,  $R_o$  and R for Canada and for the U.S&Mexico, respectively.
- 6. Apply the FEMA P795 methodology in order to determine if the cold formed shear walls designed with full frame blocking and thick Sheathing / Framing Members is equivalent to line A.16 in Table 12.2-1 of ASCE/SEI (2010), which reads « Light-Frame (cold-formed steel) walls sheathed with wood structural panels rated for shear resistance of steel sheets. »

### 1.3 SCOPE AND LIMITATIONS OF STUDY

The shear wall testing program took place in the winter of 2016. A total of 28 walls (14 different configurations) were tested in the Jamieson Structures Laboratory in the Macdonald Engineering Building at McGill University. The steel-sheathed cold-formed steel framed shear walls were tested using two displacement based loading protocols: monotonic and reversed-cyclic CUREE displacement based loading protocols (Krawinkler

et al. 2000, ASTM E 2126, *2011*). The walls that were tested as part of this research program varied in size from 610×2440 mm (2′×8′) to 2440×2440mm (8′×8′), in configuration in terms of framing thickness (1. 37mm (0.054″), 1.73 mm (0.068″), 2.46 mm (0.097″)) and fastener spacing (50mm (2″), 75mm (3″), 100 mm (4″) and 150 mm (6″)). The thickness of the sheathing fastened to the CFS frame for all 14 different configurations was 0.762mm (0.03″). A Matlab algorithm was implemented in order to perform the data analysis and extract the required design parameters for both Canada and the US, using the equivalent energy elastic plastic (EEEP) analysis approach for Canadian design values to be consistent with the tabulated shear wall strength values currently found in AISI S400 and S240. For calibration purposes, material properties of the various component of the test shear walls were also obtained.

### 1.4 THESIS OUTLINE

The content of the thesis is segmented as follows:

Chapter 2 contains a description of the Phase 1 of shear wall testing program.

It contains information about:

- 1. The specifications of the materials and members.
- 2. The list of the configurations tested.
- 3. The construction methodology.
- 4. The test set-up and the instrumentation.
- 5. The testing protocol.
- 6. The observed failure modes.
- 7. The ancillary testing of material.

Chapter 3 contains the analysis performed on the data collected from the testing program and the prescriptive design recommendations for the U.S and Canada. The EEEP methodology was adopted to conduct the data analysis. A Matlab algorithm designed by Rizk (2017) was used to improve the efficiency of the data analysis process.

Chapter 4 presents the application the FEMA P795 methodology in order to determine if the cold formed shear walls designed with full frame blocking and thick Sheathing / Framing Members is equivalent to line A.16 in Table 12.2-1 of ASCE/SEI (2010), which reads « Light-Frame (cold-formed steel) walls sheathed with wood structural panels rated for shear resistance of steel sheets. »

Chapter 5 provides the conclusions of this research program and the recommendations for future research on steel sheathed/CFS frame shear walls.

### 1.5 LITERATURE REVIEW

In the following subsections, an overview is provided of previous research programs conducted on CFS shear walls which were relied upon to formulate the design provisions currently available in the AISI S400 and S240 design standards.

#### 1.5.1 STEEL SHEATHED / CFS FRAMED SHEAR WALLS

The first research program conducted on all-steel shear walls took place at the University of Santa Clara in the United States of America, where Prof. Serrette and his graduate students analyzed the performance of cold-formed steel framed walls with sheet steel sheathing on one side. Table 1.2 provides the different configurations included in the test matrix and their respective nominal shear strength monitored under monotonic and reversed cyclic loading (Serrette 1997).

Table 1.2 Shear wall test matrix (Serrette 1997)

		Monotonic Tests		
Configuration	Sheathing	#8 Screw Spacing	Wall Aspect	Nominal
	Thickness	Edge	Ratio	Shear
	(in.)	(in.)/field(in.)	(h:w)	Strength (plf)
1	0.018	6/12	4:1 (8' x2')	491
2	0.018	6/12	2:1 (8' x 4')	483
3	0.027	4/12	4:1 (8'x2')	990
l.		Cyclic Tests		
1	0.018	6/12	2:1 (8'x 4')	392
2	0.027	4/12	4:1 (8'x2')	1003
3	0.027	2/12	4:1 (8'x 2')	1171

All specimens used nominal 33 ksi yield strength material, SSMA 350S162-33 studs, SSMA 350T125-33 track, and No.8  $\times$  1/2 inch self-drilling screws.

As a result of this research program and the recommendations provided by Serrette (1997), the design data in the 1997 Uniform Building Code (UBC, 1997) was updated. In addition to that, the results of this research program were included in the 2000 International Building Code (IBC, 2000), and the American Iron and Steel Institute (AISI) S213 Standard (2004) for Cold-Formed Steel Framing – Lateral Design.

In an effort to expand the number of steel sheathed steel shear wall configurations found in AISI S213, Yu et al. (2007) conducted two series of tests at the of University of North Texas. The first series consisted of determining the nominal shear strength for wind loads. For this purpose, monotonic tests were conducted following the recommendation of the ASTM E564-06 Standard, "Standard Practice for Static Load Test for Shear Resistance of Framed Walls for Buildings." The second series of tests focused on addressing the nominal shear strength for seismic loads. For this purpose, reversed cyclic tests were conducted in accordance with the CUREE (Consortium of Universities for Research in Earthquake Engineering) protocol in accordance with ICCES AC130 "Acceptance Criteria for prefabricated Wood Shear Panels" (2004). The data collected from the two series of tests provided design values for 0.030-in. And 0.033-in. Steel sheet sheathed shear walls with

2:1 and 4:1 aspect ratios and 0.027-in. Sheet steel shear walls with 2:1 aspect ratio and 6-in., 4-in., 3-in., and 2-in. Fastener spacing at panel edges.

All specimens were designed having the flat steel sheathing fastened on one side of the wall. The first series of tests consisted of subjecting each specimen to monotonic loading in order to extract the shear strength for wind loads. The second series of tests consisted of subjecting the walls to reversed-cyclic testing to determine shear strengths for seismic loads. The data collected from this research indicated that no significant improvement of the shear resistance of the sheet steel wall assemblies was driven by the use of No. 10  $\times$ 3/4" flat truss self-drilling tapping screws because the shear failure of the fasteners did not dominate the failure mechanism in the tests. In addition, the specimens designed with a (2"/12") screw spacing suffered from flange distortion of the boundary studs. For this reason, it was recommended to conduct more tests on the staggered fastener pattern to confirm two specific aspects. First, to confirm the results that showed that that a staggered screw pattern on both flanges of the boundary studs or installing screws on the inner flange of the boundary studs would improve the shear strength of the walls. Second, that it would reduce at the same time the distortion of the stud flanges. Moreover, the post-testing analysis showed that the performance of the shear walls may be improved if thicker framing members were used, hence the recommendation to test 0.030-in. And 0.033-in. Sheet steel walls 54-mil or thicker framing members, and the 0.027-in. Sheet steel walls with 43-mil or thicker framing members. The shear wall test matrix of Yu et al. (2007) is presented in Table 1.3.

Table 1.3 Shear wall test matrix (Yu et al., 2007)

Wall dimensions (height x Width x	Steel Sheet	Fastener Spacing	Number of	Number of	- Fastener Size
Framing	Thickness	Perimeter/Field	Monotonic	Cyclic	(No.)
Thickness)	(in.)	(in./in.)	Tests	tests	(= . 5 .)
.8'x 4' x 43 mil	0.033	2/12	2	.2	.8
8' x 4' x 43 mil	0.033	4/12	2	2	8
.8' x 4' x 43 mil	.0.033	6/12	2	.2	8
.8' x 4' x 43 mil	0.030	2/12	2	.2	8
8' x 4' x 43 mil	0.030	4/12	2	2	8
.8' x 4' x 43 mil	0.030	6/12	2	.2	8
.8' x 4' x 33 mil	0.027	2/12	2	.2	8
8' x 4' x 33 mil	0.027	4/12	2	2	8
.8' x 4'x 33 mil	0.027	6/12	2	.2	8
.8' x 2' x 43 mil	0.033	2/12	2	.2	8
8' x 2' x 43 mil	0.033	4/12	2	2	8
8' x 2' x 43 mil	0.033	6/12	2	2	8
.8' x 2' x 43 mil	0.030	2/12	2	.2	8
8' x 2' x 43 mil	0.030	4/12	2	2	8
.8' x 2' x 43 mil	0.030	6/12	2	.2	8

Phase 2 of the research program (Yu et al., 2009) was conducted at the materials testing laboratory of the University of North Texas. The tests performed and the data collected contributed to accomplishing two main objectives: 1) Confirm the published nominal shear strength of 27-mil and 18-mil sheet steel shear walls and if discrepancy was warranted, provided revised nominal strength; and 2) Develop a special seismic detailing for 6'×8', 4'×8', and 2'×8' walls to increase the nominal strength in addition to improving the ductility of the shear wall. The special detailing consisted of installing blocking and strapping at the wall's mid-height, using No. 10x3/4-in. Self-drilling screws staggered at boundary and joint studs. In addition, the post-testing analysis resulted in the recommendation to use a single stud at the sheet joint. The data collected from the testing program showed significant improvement due to the special detailing for the 6'×8' walls. For example, the special detailing contributed to an increase of the shear strength and ductility on average by 11.4% and 21.7% respectively for the 54-mil framed shear walls. Figure 1.2 shows the

effect of the special detailing in restricting the flexural buckling of the interior studs. The shear wall test matrix of Yu et al. (2009) is presented in Table 1.4.



Figure 1.2 Failure mode of 6'×8' wall with (right) and without (left) special detailing (Yu et al., 2009)

Table 1.4 Shear wall test matrix (Yu et al., 2009)

Test Label	.Wall dimensions (height (ft.) x Width (ft.))	Nominal Steel Sheet Thickness (in.)	Nominal Framing thickness (in.)	Fastener spacing at edge (in.)	Test protocol	Fastener Size (No.) / Pattern
.8×2×350- 33×27-2-C1	.8x2	0.027	0.033	2	Cyclic - SPD	.8
8×2×350- 33×27-6-M1	8x2	0.027	0.033	6	Monotonic -ASTM E564	8
.8×2×350- 33×27-6-M2	.8x2	0.027	0.033	6	Monotonic -ASTM E564	.8
.8×2×350- 33×27-6-C1	.8x2	.0.027	0.033	6	Cyclic - CUREE	.8
8×2×350- 33×27-6-C2	8x2	0.027	0.033	6	Cyclic - CUREE	8
8×4×350- 33×18-6-M1	8x4	0.018	0.033	6	Monotonic -ASTM E564	8
.8×4×350- 33×18-6-M2	.8x4	.0.018	0.033	.6	Monotonic -ASTM E564	.8
8×4×350- 33×18-6-C1	8x4	0.018	0.033	6	Cyclic - CUREE	8
8×4×350- 33×18-6-C2	8x4	0.018	0.033	6	Cyclic - CUREE	8
.8×2×350- 33×27-2-M1	.8x2	.0.027	0.033	.2	Monotonic -ASTM E564	.8
8×2×350- 33×27-2-M2	8x2	0.027	0.033	2	Monotonic -ASTM E564	8
.8×2×350- 33×27-2-M3	8x2	.0.027	0.033	.2	Monotonic -ASTM E564	.8
.8×2×350- 33×27-2-C2	.8x2	.0.027	0.033	.2	Cyclic - CUREE	.8
8×2×350- 33×27-2-C3	8x2	0.027 .	0.033	2	Cyclic - CUREE	8

In order to analyze the impact of the special detailing on the performance of cold-formed steel shear walls with a broader range of aspect ratios, tests were performed on 8'.×4' and 8'×2'. Shear walls. The data collected from two 8'.×4' shear walls with 33-mil sheathing and 2-in. Screw spacing at panel edges subjected to cyclic loading is presented in Figure 1.3.

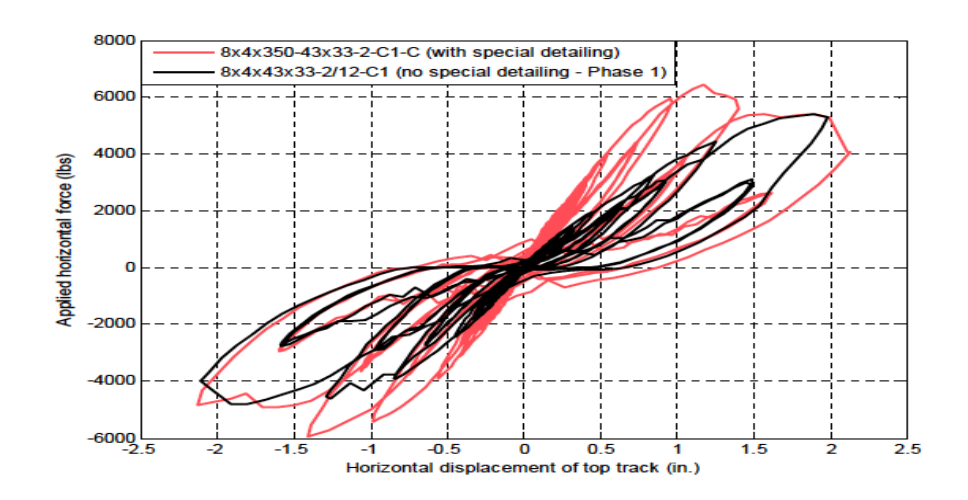


Figure 1.3 Force vs. Displacement test hysteresis curves for  $8' \times 4'$  walls with 33-mil sheathing) (Yu et al., 2009)

These results indicated that the special detailing influenced significantly the elastic stiffness and increased the nominal shear strength of the walls by an average of 16.7%. Similar to the performance observed for the  $6'\times8'$  walls, the interior stud of the walls designed with an aspect ratio of two, did not suffer from flexural buckling. The failure of the shear walls was driven by the screw pull- out at the centre of the interior stud and at the corners of the sheathing. In addition, as shown in Figure 1.4, the shear walls having an aspect ratio of four designed with the special detailing, 33-mil sheathing and 2-in. Fastener spacing at panel edges, witnessed an increase of shear resistance by 18.3%.

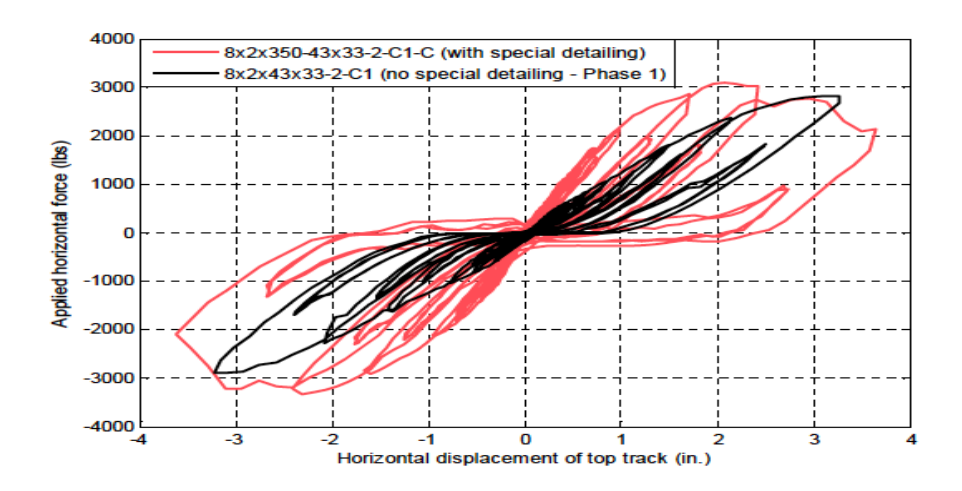


Figure 1.4 Force vs. Displacement test hysteresis curves for 8'× 2' walls with 33-mil sheathing (Yu et al., 2009)

As a result of these research program, two journal papers were published:

- Yu C. Shear resistance of cold-formed steel framed shear walls with 0.686-mm,
   0.762-mm, and 0.838-mm steel sheet sheathing. *Engineering Structures*, 2010
   32(6) 1522–1529.
- ii) Yu C, Chen Y. Detailing recommendations for 1.83-m wide cold-formed steel shear walls with steel sheathing. *Journal of Constructional Steel Research*, 2011 67(1) 93–101.

As part of a group of research projects conducted at McGill University, El-Saloussy (2010) analyzed the data collected from the CFS shear wall tests carried out at the University of North Texas using the equivalent energy elastic-plastic (EEEP) analysis technique for both monotonic and reversed-cyclic testing, as recommended by Branston (2004), developed by Park (1989), and further modified by Foliente (1996). It is important to mention that the EEEP analysis method is in-line with the approach used to develop Canadian design parameters for other wood sheathed and steel-sheathed shear walls found in AISI S240 and S400. The data analysis that was executed and the interpretation of the available US test data allowed to extract several conclusions and propose recommendations for further studies. Among other useful insights, the data collected and the post-testing analysis

performed showed that 6'×8' all-steel shear walls yielded similar or increased nominal shear resistance to 4'×8' walls, and mid-height blocking in accordance with the AISI S230 Standard for Cold-Formed Steel Framing allowed to improve the nominal shear resistance of the walls. Moreover, El-Saloussy recommended to conduct additional testing on the impact of blocking on the performance of shear walls, especially by testing different variations of blocking locations. Table 1.5 presents a comparison of nominal shear values between ordinary walls and blocked walls.

Table 1.5 Nominal shear values for ordinary and blocked steel sheathed walls (El-Saloussy, 2010)

Sheathing mm-in	Max Aspect Ratio (h/w)	Fastener Spacing at Panel Edges mm-in 50  (2)  Nominal Shear kN/m (lb/ft)	Mid-Height Blocking		
	2:1	13.95 (956)	No		
0.84-0.33	2.1	14.67 (1005)	Yes		
	4:3	18.15 (1244)	No		
	7.5	20.85 (1429)	Yes		

With the main objective to develop design guidelines for cold-formed steel frame / steel-sheathed shear walls that can be used in conjunction with the National Building Code of Canada (NBCC, 2010), Ong-Tone (2009) and Balh (2010) conducted at McGill University a research program comprised of shear wall testing. A total of 54 steel sheathed single-storey shear walls under two loading protocols: monotonic and CUREE reversed-cyclic were completed. The shear wall test matrix of Balh (2010) and Ong-Tone (2009) is presented in Table 1.6.

Table 1.6 Shear wall test matrix (Balh, 2010 & Ong-Tone, 2009)

Configuration	Sheathing Thickness (mm)	Wall Length (mm)	Wall Height (mm)	Fastener Spacing (mm)	Framing Thickness (mm)	Number of Tests and Protocol
1	0.46	1220	2440	150/300	1.09	3M & 2C
2	0.46	1220	2440	50/300	1.09	2M & 2C
3	0.46	1220	2440	150/300	0.84	2M & 3C
4	0.76	1220	2440	150/300	1.09	2M & 2C
5	0.76	1220	2440	100/300	1.09	3M & 2C
6	0.76	1220	2440	50/300	1.09	3M & 2C
7	0.76	1220	2440	100/300	0.84	1M
8	0.76	610	2440	100/-	1.09	2M & 2C
9	0.76	610	2440	50/-	1.09	3M & 2C
10	0.76	610	2440	100/-	0.84	1M
11	0.76	2440	2440	100/300	1.09	2M & 2C
12	0.76	1830	2440	100/300	1.09	1M
13	0.76	1830	2440	50/300	1.09	1M
14	0.76	1220	2440	50/300	0.84	4M
15	0.76	1220	2440	100/300	1.09	1M
16	0.76	1830	2440	100/-	1.09	1M
17	0.46	1220	2440	-/300	1.09	2M
18	0.46	1220	2440	75/300	1.09	1M

The post-testing analysis of the data allowed the extraction of several useful insights. First, the results showed that the nominal resistance of the shear walls was driven by three main detailing parameters: the sheathing thickness, framing thickness and fastener spacing. It was observed that the shear resistance increased as the fastener spacing decreased. The use of a thick sheathing of 0.76mm (0.030") and 1.09mm (0.043") framing thickness allowed the development of higher lateral resistance of the cold-formed steel shear walls. Second, the nominal shear resistances obtained from the testing of 1830 mm x 2440 mm were similar to the results obtains for the 1220 mm x 2440 mm. Third, the results collected from the tests performed on specimens 9M-c, 5M-c and 6M-c, showed that the three rows of bridging that were added to the initial design of configurations 9, 5 and 6, successfully reduced the damage to the chord study due to twisting. This bridging reinforcement increased the shear resistance of the walls as illustrated in Figure 1.5. But, the results show that it compromised to some extent the ductility of the specimens. Moreover, at high level of in-plane lateral displacements, the bridging channels suffered from lateral torsional buckling and failed to restrict the twisting of the chord studs. This is why it was judged more efficient to add full blocking, and it was recommended to conduct additional experimental research in order to be able to collect useful data on this topic. The recommendations from Balh (2010), Ong-Tone (2009) and El-Saloussy (2012) were all used to provide Canadian design values in the S400 and S240 standards.

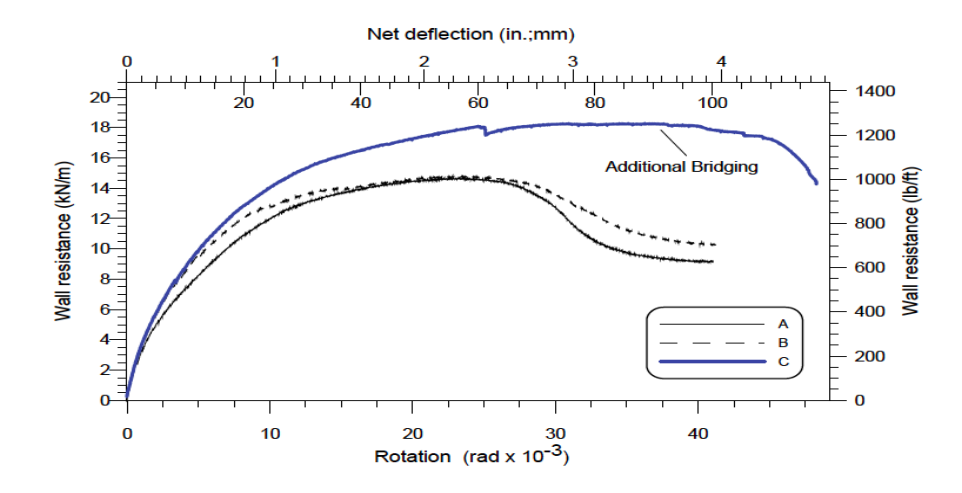


Figure 1.5 Comparison of reinforcement: wall resistance vs. Displacement of tests 9M-a,b,c (Balh, 2010)

Some specimens tested as part of the research programs of Balh (2010), Ong-Tone (2009), Yu et al., (2007) and Yu et al. (2009) suffered from severe damage due to unfavourable twisting deformations of the chord studs and local buckling. Moreover, all the tests conducted at McGill University and in the US, consisted only of imposing lateral in-plane loading to the shear walls. In order to address this unfavourable failure mode witnessed during the previous testing programs, and to account for combined gravity and lateral loading DaNreo (2012) conducted a subsequent test-based research program at McGill University. The objective was to evaluate the performance of cold-formed steel framed / steel-sheathed shear walls, constructed with blocked stud members, to address the issue of excessive chord stud twisting, and to evaluate the influence of combined gravity and shear loading. The results of this research were published. The article in question is:

"DaBreo J, Balh N, Ong-Tone C, Rogers C.A. Steel sheathed - cold-formed steel framed shear walls subjected to lateral and gravity loading. *Thin-Walled Structures*, 2014 (74) 232-245."

A total of 14 single storey shear walls (8 configurations) were tested under Monotonic and CUREE reversed-cyclic lateral loading protocols. Specimens were limited to 1220×2440mm (4′×8′) in dimension, and varied in configuration in terms of framing thickness, sheathing thickness and fastener spacing. Table 1.7 provides a detailed description of the eight different configurations of the testing program by DaBreo. Table 1.8 provides a summary of test results for the blocked walls tested by DaBreo (2012) and the nominally identical conventional walls tested in previous research programs (Balh, 2010; Ong-Tone, 2009)

Table 1.7 Shear wall test matrix (DaBreo, 2012)

Test Label	Protocol	Test Specimen	Wall Size (mm)	Fastener Spacing (mm)	Sheathing Thickness (mm)	Framing Thickness (mm)
B1	Monotonic	B1-M	1220 x 2440	50/300	0.76	1.37
<b>D</b> 1	Cyclic	B1-R	1220 x 2440	50/300	0.76	1.37
B2	Monotonic	B2-M	1220 x 2440	50/300	0.46	1.09
D2	Cyclic	B2-R	1220 x 2440	50/300	0.46	1.09
В3	Monotonic	B3-M	1220 x 2440	100/300	0.76	1.09
	Cyclic	B3-R	1220 x 2440	100/300	0.76	1.09
B4	Monotonic	B4-M	1220 x 2440	150/300	0.76	1.09
Д-Т	Cyclic	B4-R	1220 x 2440	150/300	0.76	1.09
B5	Monotonic	B5-M	1220 x 2440	100/300	0.46	1.09
<b>D</b> 3	Cyclic	B5-R	1220 x 2440	100/300	0.46	1.09
В6	Monotonic	B6-M	1220 x 2440	150/300	0.46	1.09
<b>D</b> 0	Cyclic	B6-R	1220 x 2440	150/300	0.46	1.09
В7	Monotonic	B7-M	1220 x 2440	75/300	0.76	1.37
В8	Monotonic	B8-M	1220 x 2440	75/300	0.46	1.37

Table 1.8 Normalized parameters for comparison of blocked to conventional shear wall- Monotonic Test (DaBreo, 2012)

Comparison group	Test Specimen	Ultimate Resistance S <sub>u</sub> (kN/m)	sistance at 0.8 S <sub>u</sub> Resistance Stiffness, k <sub>e</sub> Ductility.µ Dissipat		Energy Dissipation (Joules)	on			Prope	erties			
								$S_{\mathrm{u}}$	$\Delta_{net,0.8u}$	$S_y$	Ke	M	Е
	B2-M	16.91	68.26	15.55	1.10	4.85	1161	1.70	0.72	1.69	1.09	0.46	1.14
1	2M-a <sup>†</sup>	10.10	90.42	9.00	0.91	9.10	937	1.00	1.00	1.00	1.00	1.00	1.00
	2M-b <sup>†</sup>	9.81	100	9.36	1.11	11.91	1094	1.00	1.00	1.00	1.00	1.00	1.00
	B6-M	9.31	65.98	8.44	1.19	9.30	643	1.43	1.36	1.44	1.20	1.19	1.98
2	1M-a <sup>†</sup>	6.50	72.99	5.87	0.79	9.79	496	1.00	00 1.00	1.00	1.00	1.00	
2	1M-b <sup>†</sup>	6.63	37.07	5.85	0.94	5.97	242						1.00
	1M-c <sup>†</sup>	6.41	35.73	5.83	1.26	7.7	238						
	В3-М	19.40	51.22	17.43	1.11	3.27	922	1.41	0.88	1.38	0.61	0.39	1.09
3	5M-a*	14.19	52.6	12.90	1.87	7.61	773	1.00	1.00	1.00	1.00	1.00	1.00
	5M-b*	13.39	64.45	12.41	1.77	9.18	922	1.00	1.00	1.00	1.00	1.00	1.00
	B4-M	16.83	53.95	14.85	1.67	6.08	896	1.53	0.83	1.48	0.97	0.54	1.17
4	4M-a*	11.02	67.57	10.08	1.67	11.19	793	1.00	1.00	1.00	1.00	1.00	1.00
	4M-b*	10.98	62.97	10.03	1.78	11.17	735	1.00   1.00	1.00	1.00	1.00	1.00	1.00

The data listed in Table 1.8 indicate that the nominal design resistance values of the blocked walls exceed their nominally identical counterparts by 37% to 80%. Moreover, the data analysis indicates that the blocked shear wall specimens tested by DaBreo (2012) exhibited reduced ductile behaviour compared with their unblocked counterparts tested by (Balh, 2010; Ong-Tone, 2009) and unfavourable rates of strength degradation. For these reasons, it was recommended to conduct more research on a hybrid shear wall system designed with strapped braces incorporated into the flat steel panel in order to improve inelastic post peak behaviour. The result of this research were published. The article in question is:

Balh N, DaBreo J, Ong-Tone C, El-Saloussy K, Yu C, Rogers C.A. Design of steel sheathed cold-formed steel framed shear walls. *Thin-Walled Structures*, 2014 (75) 76-86.

Figure 1.6 illustrated the twisting of the chord studs of the unblocked shear walls observed during the testing programs of Balh (2010), and Ong-Tone (2009).



Figure 1.6 Chord twisting of unblocked walls (Balh, 2010)

Figures 1.7 and 1.8 illustrate the increase in the nominal shear resistance of the blocked walls compared to their conventional counterparts (unblocked walls). Figure 1.9 shows the differences in the design values between the blocked walls and their conventional counterparts.

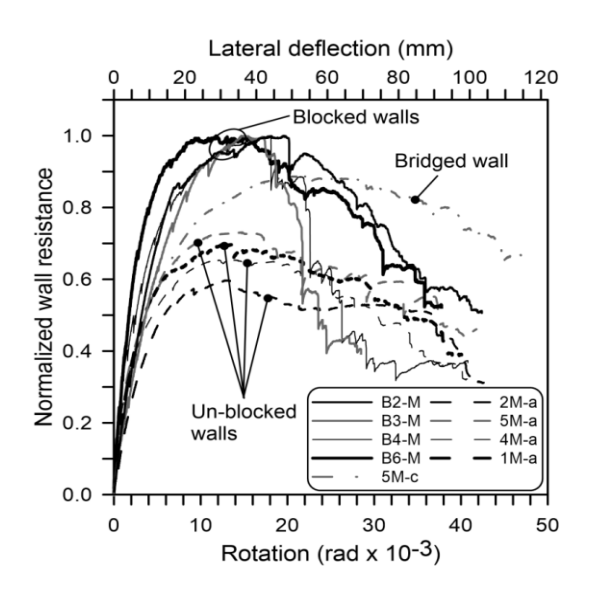


Figure 1.7 Comparison of reinforcement: wall resistance vs. displacement of monotonic tests (DaBreo, 2012)

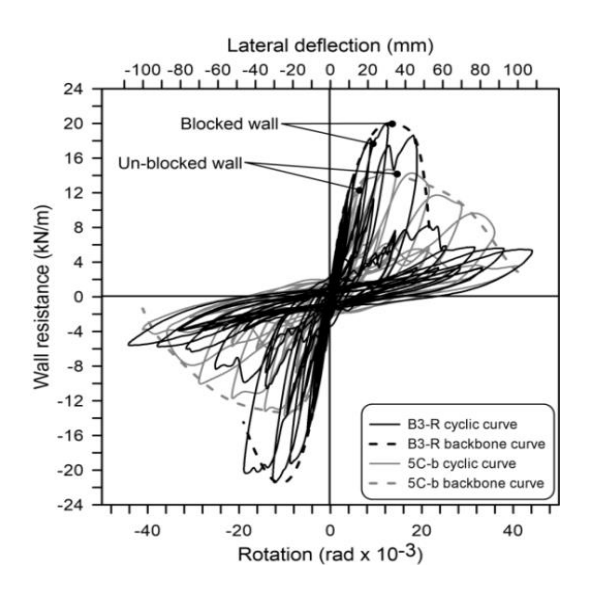


Figure 1.8 Comparison of reinforcement: wall resistance vs. Displacement of reversed-cyclic tests (DaBreo, 2012)

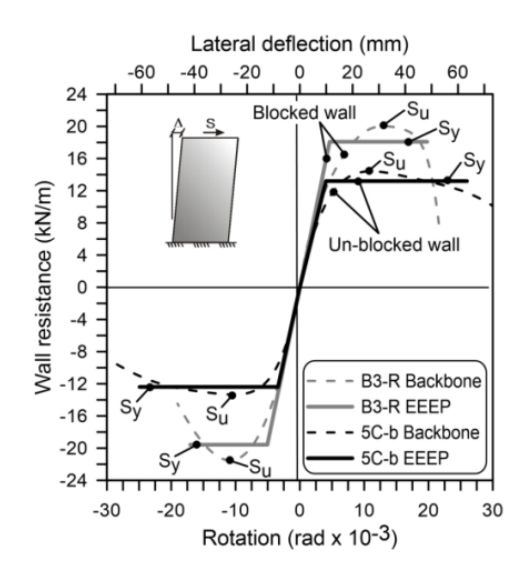


Figure 1.9 Comparison of Design value: EEEP curves of blocked walls vs. Unblocked walls (DaBreo, 2012)

Shamim (2012) conducted a research program in order to develop seismic design provisions for structures designed having a seismic force resisting system (SFRS) composed of CFS framed shear walls that can be proposed for inclusion in the National Building Code of Canada (NBCC) and AISI S213; which has since been replaced by AISI S400. In addition, an investigation of the seismic performance of wood sheathed cold-formed steel framed shear walls was conducted by means of dynamic tests and numerical models.

In order to meet the objectives of the research program, the methodology consisted of:

- Dynamic testing of single- and double-storey CFS framed shear walls on a shake table
- ii) Numerical modelling of the tested shear walls in opensees
- iii) Incremental Dynamic Analyses (IDA) following the Federal Emergency Management Agency (FEMA) P695 (2009) methodology.

The result of this research were published. The three journal papers in question are:

- i) Shamim I, DaBreo J, Rogers C.A. Dynamic testing of single- and double-story steel sheathed cold-formed steel framed shear walls. *Journal of Structural Engineering* ASCE, 2013 139(5): 807-817.
- ii) Shamim I., Rogers C.A. (2015), "Numerical evaluation: AISI S400 steel-sheathed CFS framed shear wall seismic design method", *Thin-Walled Structures* 95: 48-59.
- iii) Shamim I, Rogers C.A. Steel sheathed CFS framed shear walls under dynamic loading: numerical modelling and calibration. *Thin-Walled Structures* 2013; 71: 57-71.

The shake table testing consisted of five single- and five double-storey full-scale steel sheathed CFS framed shear walls in addition to three single- and four double-storey wood sheathed CFS framed shear walls. The one-directional shake table test program was conducted in order to meet four specific objectives:

- i) To monitor for the first time, the seismic performance of single- and doublestorey wood and steel sheathed/CFS framed shear walls under dynamic loading.
- ii) To determine if the specimens performed similarly when subjected to dynamic loading and when tested under displacement based loading (i.e. Monotonic and reversed cyclic) protocols.
- iii) To monitor the shear force vs. Lateral displacement hysteresis response of the specimens in addition to determining their dynamic properties (damping ratio and natural frequency).
- iv) To study the influence of the second storey and floor detailing by conducting tests on double-storey specimens.

The dynamic analyses were conducted with the purpose to first, develop and calibrate a non-linear dynamic model based on the data collected from the shake table testing program. Second, the dynamic analyses allowed the evaluation and recommendation of a seismic design method implementing the FEMA P695 methodology.

The average damping ratio of all specimen was determined as being equal to 6%, excluding the second mode damping ratio in averaging. In addition, the natural frequency of the specimens determined based on the specimen shear stiffness and the test set-up mass and that measured from the test were similar. The values of the period obtained differed from the results obtained using the empirical equation provided by the NBCC for structures designed with a shear wall lateral resisting system ( $T_a = 0.05h^{3/4}$ ). However, it was judged adequate to use the NBCC specified fundamental period value as a conservative estimate of the building's fundamental period of vibration at the initial design stage.

The data collected from the dynamic testing program indicates that walls designed with blocking members between studs developed higher yield shear strength S<sub>v</sub>, compared to the values obtained from the static tests conducted by Balh (2010), Ong-Tone (2009), Yu et al. (2007) and Serrette (1997). The specimens tested under monotonic and reversedcyclic loading were not designed with blocking members. However, DaBreo (2012) showed that when nominally identical blocked walls were subjected to monotonic and reversed cyclic protocols, the  $S_v$  values computed following the EEEP methodology were similar to the values obtained from the dynamic tests. It was then concluded that the dynamic nature of the loading did not influence the shear resistance developed by the specimen. The same conclusion was drawn for wood sheathed shear walls. It was noted that the blocking members increased the shear wall strength by 50% for specimens designed with a 50mm (2in.) fastener spacing and by 35 % for specimen designed with fastener spacing higher than 50 mm (2in.). The average damping ratio of all specimens was determined as being equal to 7.6%, excluding the second mode damping ratio in averaging. In addition, the natural frequency of the specimens determined based on the shear stiffness and the test set-up mass and that measured from the test were similar. The values obtained differed from the results obtained using the empirical equation provided by the NBCC for structures designed with a shear wall lateral resisting system ( $T_a = 0.05h^{3/4}$ ).

With the purpose to examine the ability of the representative numerical models to predict the seismic performance of the shear wall test specimens subjected to dynamic loading, non-linear time history dynamic analyses were performed. The numerical modelling of the elastic and enhanced dynamic tests of the CFS framed wood and steel sheathed specimens was completed using the opensees software (McKenna, 1997). Pinching04 hysteretic material was used in order to model the shear strength-shear displacement hysteresis of the specimens subjected to cyclic loading. Several parameters were captured using the Pinching04 material: stiffness, strength, strength degradation and pinching behaviour. Holdown anchor rods were modeled using linear elastic spring. Hence, the in-plane lateral displacement of the specimen was driven by two factors: First, the shear displacement simulating the wood/steel sheathed CFS frame displacement caused by the lateral forces. Second, the uplift displacement representing the rigid rotation of the wall due to anchor rod elongation. Figure 1.10 illustrates the deformation of a single- and double-storey wall due to the uplift.

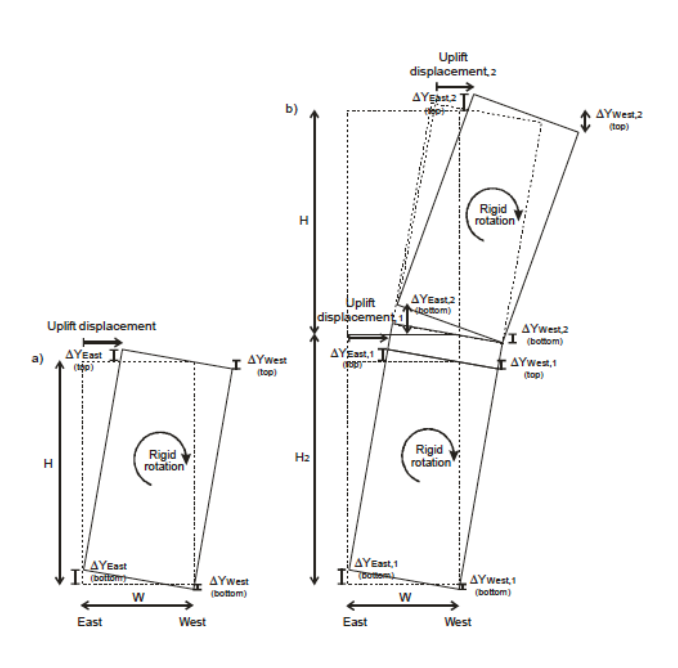


Figure 1.10 Schematic of uplift deformation: a) single-storey, and b) double-storey wall (Shamim, 2012)

Elastic beam-column elements, rigid beam-column elements and elastic truss members were used to model respectively the chord stud members, the tracks and the floor structure. The flexural stiffness of the blocked bare frame without sheathing was modeled using

rotational springs. Figures 1.11 and 1.12 illustrate the Initial model and Developed model of shear walls in opensees.

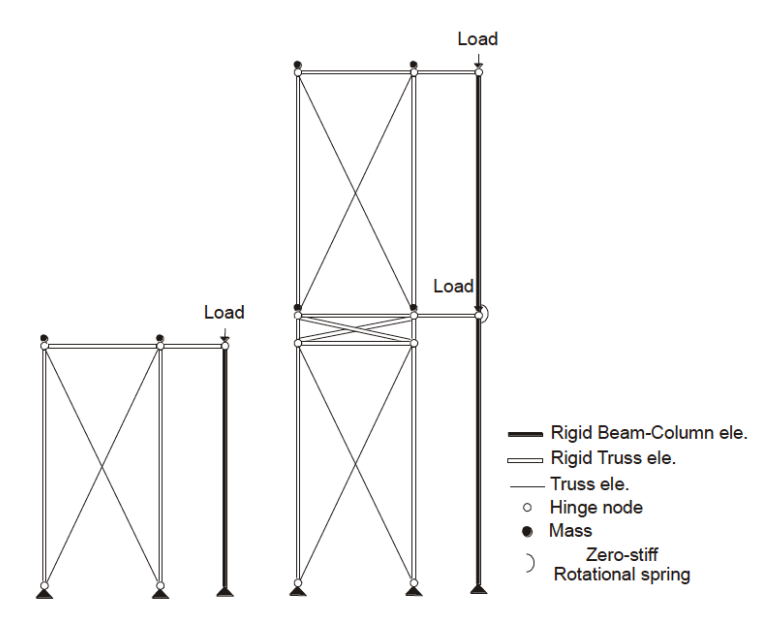


Figure 1.11 Initial model of shear walls in opensees, Shamim (2012)

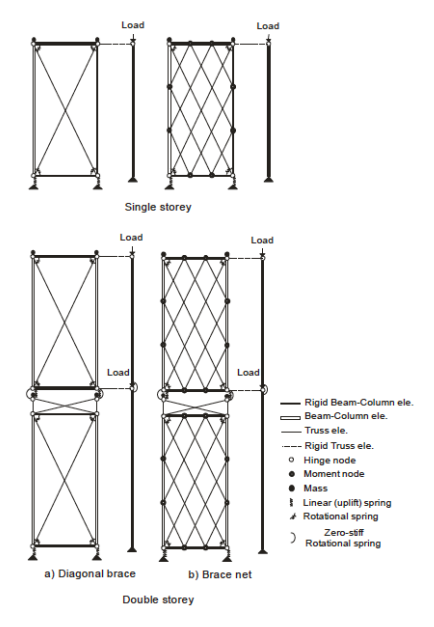


Figure 1.12 Developed model of shear walls in opensees a) diagonal brace b) brace net Shamim (2012)

The calibration process of the numerical model for each dynamic test specimen, at both the enhanced and elastic level, contained an adjustment of the Pinching04 parameters and Rayleigh damping ratio. Other parameter impacting the response of the specimen numerical model were directly extracted from the data collected during the dynamic tests. The results obtained from the numerical model indicate a convergence with the test results in terms of hysteresis response overall shape and the strength and displacement response time histories for all the wood and steel sheathed shear wall specimens.

#### 1.5.2 RELATED WOOD SHEATHED / CFS FRAMED SHEAR WALLS

In the past decades, several testing programs for wood sheathed / cold-formed steel framed shear walls were conducted at various academic institutions in North America and Europe to better understand their behaviour under lateral loading and to develop and improve the relevant design codes.

The data collected from previous research programs show that cold-formed steel walls subjected to lateral loads exhibit highly non-linear behaviour from the onset of loading. For this reason, and in order to be able to evaluate certain design parameters, i.e. Yield force, ductility, stiffness and energy dissipation, Branston (2004) recommended to implement the Equivalent Energy Elastic-Plastic (EEEP) data analysis approach.

Park (1989) was the first to propose the concept of equivalent energy. Foliente (1996) presented a modified form of the equivalent energy, and then was adopted by Virginia Polytechnic Institute and State University by various researchers (Dolan and Heine, 1997a, 1997b, 1997c; Dolan and Johnson, 1997a, 1997b; Heine, 1997; Johnson, 1997; Johnson and Dolan, 1996; Salenikovich and Dolan, 1999b; Salenikovich et al., 2000a, 2000b). Several data interpretation techniques were explored, but the EEEP methodology was considered the best technique to represent the performance of cold-formed steel frame / wood panel shear walls subject to both monotonic and reversed-cyclic loads. Moreover, Serrette (1998) recommended to implement a detailed energy based methodology for the interpretation of the data collected during the research programs of shear walls.

The EEEP methodology consists of modeling the energy dissipated by the shear wall specimen subjected to monotonic or reversed-cyclic loading using a bi-linear curve. The EEEP curve illustrates the behaviour of a perfectly elastic/plastic shear wall. The perfectly elastic zone of the EEEP curve illustrated the behaviour of the specimen until the yield point and the perfectly plastic zones models its behaviour until failure.

Branston (2004) conducted a research program on cold-formed steel stud shear walls sheathed with wood panels (CSP, DFP, OSB) at McGill University. Forty-three steel frame / wood panel shear wall specimens were tested under monotonic and reversed-cyclic loading protocols. In total, 109 shear walls were tested in collaboration with Boudreault (2005) and Chen (2004). The specimens consisted of 1220 x 2440 mm (4'. X 8') walls designed having a 1.12 mm thick cold-formed steel framing members of 230 MPa grade and using 12.5 mm Canadian Softwood Plywood (CSP) (CSA 0151, 1978), 12.5 mm Douglas Fir Plywood (DFP) (CSA 0121, 1978) or 11 mm Oriented Strand Board (OSB) (CSA 0325, 1992) as sheathing to provide lateral stability. The different fastener pattern that were tested consisted of: 3" (75 mm), 4" (100 mm) or 6" (150 mm) around the perimeter of the panel. All field fasteners were spaced at 12" (305 mm). The data analysis that was performed on the results obtained from the tests indicates that a resistance factor of 0.7 provided sufficient reliability and a reasonable factor of safety for wind loading cases.

Boudreault (2005) presented in his thesis an overview of the monotonic protocol and the four of the most commonly reversed-cyclic protocols adopted by the scientific society-SPD (Sequential Phased Displacement), ATC-24 (Applied Technology Council), ISO 16670 (International Organization of Standardization) and CUREE (Consortium of Universities for Research in Earthquake Engineering).

Even though the American Society for Testing and Materials Standard E 564 (ASTM, 1995) is used for static testing of the specimens, some researchers adapted and modified this standard with the goal to obtain some results that were not provided by the ASTM E 564 (ASTM, 1995). Branston (2005) adopted the monotonic protocol used by Serrette et al. (1996, 1997, 2002). This protocol consists of unloading the shear wall to zero force at displacements of 12.7 mm (0.5") and 38.1 mm (1.5") in order to evaluate permanent set as shown in Figure 1.13.

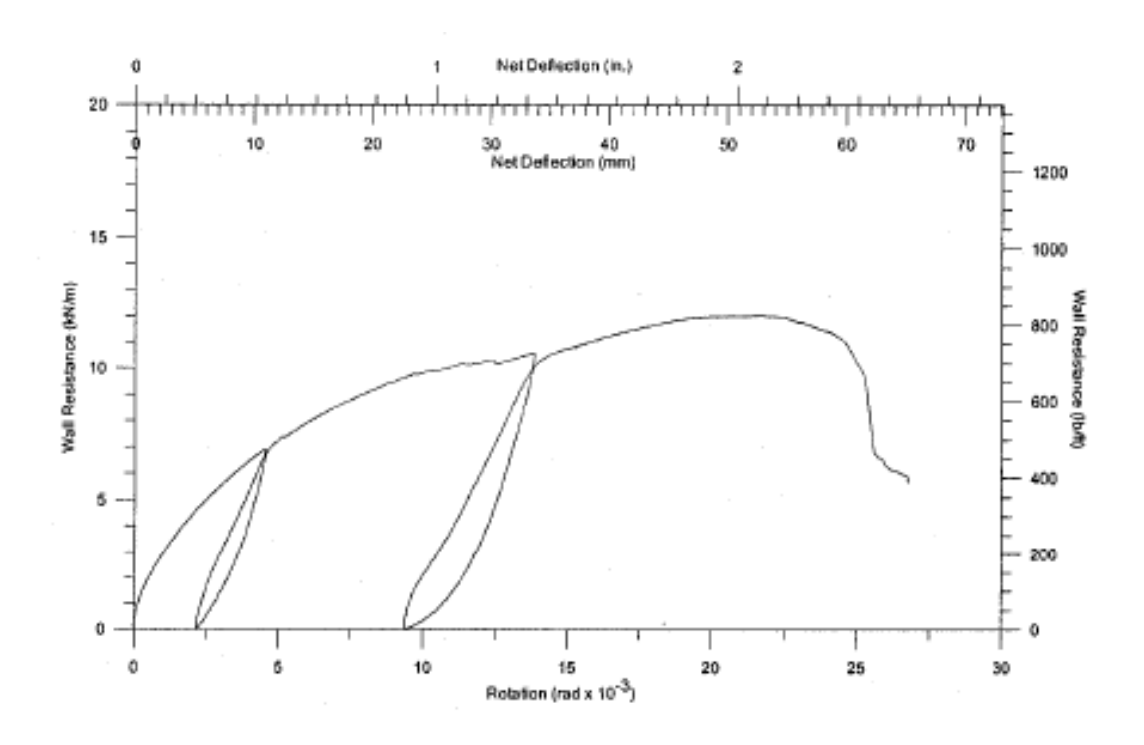


Figure 1.13 Wall resistance vs. Displacement curve for a typical monotonic test, Branston (2005)

The CUREE loading protocol was judged by Boudreault (2005) to be adequate for the testing of CFS framed shear walls. The CUREE loading protocol is considered to be an accurate scientific derivation from actual earthquake demands, and its displacement history is based on a measure of the ultimate displacement rather than yield displacement (Heine, 2001). In addition, the concept of cumulative damage was implemented in order to transform the time history responses into representative displacement history, a method judged more representative of the demand imposed on light framed shear wall during an earthquake (Krawinkler et al., 2000). It is important to mention that this protocol has its own flaws, mainly due to the fact that all the natural acceleration records used to design the CUREE protocol were from Los Angeles and thus do not represent accurately the earthquake events that may occur elsewhere. In addition, the CUREE protocol aims to represent ordinary ground motions characterized by a probability 10 % of exceedance within a time span of 50 years. This characteristic does not meet the criteria listed in the 2005 Edition of the National Building Code of Canada (NRCC, 2004). The listed probability of exceedance is 2% in 50 years.

In order to simulate the demand that would be imposed on the cold-formed steel stud shear walls sheathed with wood panels (CSP, DFP, OSB) under seismic loading, Boudreault (2005), Branston (2004) and Chen (2004) chose to perform the laboratory testing on the specimens with the CUREE Ordinary Ground Motions loading protocol (Krawinkler *et al.*, 2000; ASTM E2126, 2005). The primary objectives of this research program consisted of first, providing a preliminary recommendation of seismic force modification factors for ductility and over strength for use with the 2005 National Building Code of Canada, second to determine a hysteretic model that corresponds to the shear resistance vs. Lateral displacement behaviour of a CFS steel frame / wood panel shear wall subjected to a reversed cyclic loading protocol.

Based on the analysis of the data collected that was performed using the Equivalent Energy Elastic-Plastic (EEEP) method, a ductility related ( $R_d$ ) and an over strength related ( $R_o$ ) force modification factor of 1.8 and 2.5 were respectively determined, provided that a maximum aspect ratio (height:length) of 2: 1 for shear walls is respected. Boudreault (2005) judged that it was appropriate to use of the Stewart hysteretic model in order to represent strength and stiffness characteristics of a steel frame / wood panel shear wall tested in accordance to a reversed cyclic loading protocol. It was observed that this hysteretic rule model properly the pinching and degrading stiffness characteristics, and the difference in dissipated energy between the experimental tests and the models was found to be low.

#### **1.5.3 SUMMARY**

In summary, the previous research programs contributed to the development of loading protocols that accurately represents the actual earthquake demands, and the data interpretation techniques to accurately extract the various design parameters of the cold-formed steel framed shear walls. In addition, several research programs were developed in order to better understand the performance of cold-formed steel shear walls (wood or steel sheathed). However, the specimens tested so far were limited to walls constructed of a CFS frame and steel sheathing is limited to a maximum of 0.84 mm thick sheathing and 1.37

mm thick framing. Such configurations developed shear resistances close to 30 kN/m (#10 screws @ 50 mm o.c.). For this reason, and in order to reach resistance approaching 100kN/m, and to analyze the influence of wall length for shear walls constructed with full quarter point frame blocking, various configuration having aspect ratio of 4:3 and 1:1 were tested. In addition, shear walls constructed with heavier frames were included in this research program to better understand its behavior, its modes of failure, and how much increase in shear resistance it will provide to the specimen.

# 2. CHAPTER 2 - SHEAR WALL TEST PROGRAM

#### 2.1 INTRODUCTION

During the winter, summer and fall semesters of 2016, and as part of the Cold-Formed Steel Frame – Steel Sheathed Shear Walls research program: Improved range of Shear Strength Values Accounting for Effect of Full Frame Blocking and Thick Sheathing / Framing Members research program, 59 walls (30 different configurations) were tested in the Jamieson Structures Laboratory, located in the Macdonald Engineering Building at McGill University. The Phase 1 research project of the author of this thesis comprised the building and testing of 28 shear walls, as well as the analysing of data. Fourteen wall configurations out of the thirty were included, each of which was tested according to monotonic and reversed-cyclic displacement-based lateral loading protocols. The laboratory component of the first phase of this research program ended the 31st of May 2016, whereas the remaining wall configurations were tested in the summer and fall semesters of 2016, as part of the Phase 2 and 3 research projects by Santos (2017) and Brière (2017).

During the summer of 2010, with the intent of eliminating the occurrence of twisting deformations, DaBreo (2012) tested 14 single-storey steel sheathed shear walls that were constructed with blocked framing members. The results indicated that the shear resistance increased up to 25% compared with an un-blocked wall suffering from chord stud damage. A total of eight different configurations were tested, but designs were limited to  $1220 \times 2440 \text{ mm}$  (4' × 8') walls. One of the objectives of Phase 1 of this research program consisted of identifying the influence of wall length for shear walls constructed with frame blocking elements. For this reason, the testing program included 12 configurations of shear walls constructed with a single side sheathing and frame blocking elements, having three different aspect ratios (4:1, 4:3, 1:1). Various fastener spacings were tested, i.e. 50mm (2"), 75mm (3"), 100mm (4") and 150mm (6"). In addition, and with the purpose to bridge the gap between cold-formed steel and hot-rolled steel lateral framing shear wall systems, two configurations of walls were tested having an aspect ratio of 2:1, constructed with heavier

frames- 1.73 mm (0.068") and 2.46mm (0.097"), as well as with a single side sheathing and frame blocking components.

Once the detailing of every individual component of the specimens for Phase 1 had been completed, the walls were assembled horizontally on the ground using the platform framing technique, and then installed vertically in the testing frame, designed specifically for the in-plane shear loading (Figures 2.1 and 2.2). The top of the shear walls was connected to a loading beam. The in-plane longitudinal displacement of the loading beam was controlled by a 250 kN MTS actuator with a  $\pm 125$ mm (5") stroke that was incorporated into the testing frame. In order to restrict any out-of-plane movement of the specimens, the loading beam was braced using HSS lateral supports. A detailed review of the properties of the testing frame can be found in Zhao (2002).

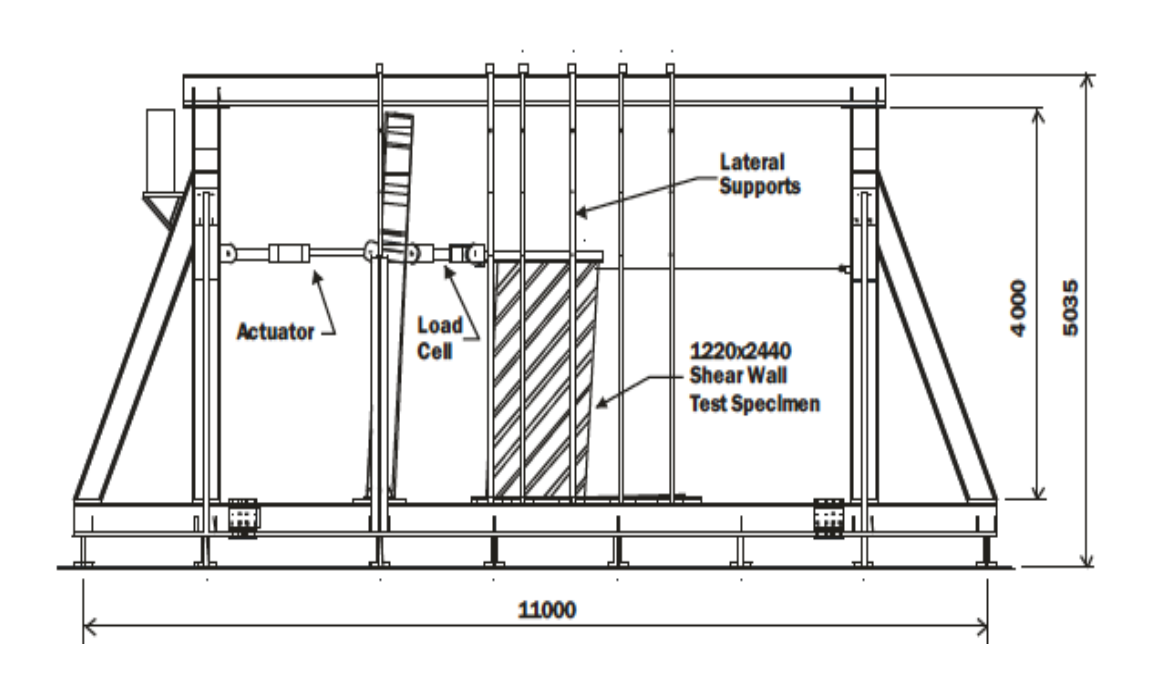


Figure 2.1 Shear wall test frame



Figure 2.2 Typical wall installation in test frame

# 2.2 STEEL FRAME/ STEEL PANEL SHEAR WALLS TESTING PROGRAM

The testing program consisted of 14 different configurations of fully blocked cold-formed steel shear walls. The walls were designed and built with a single sided cold-formed steel sheathing having a nominal thickness of 0.76mm (0.03") connected to a cold-formed steel frame. As shown in Table 2.1, specimens having different wall length, framing thickness (wall studs, blockings and tracks), and fastener spacing were tested under monotonic and reversed cyclic loading.

# The testing matrix consisted of:

- i) Two wall configurations having an aspect ratio of  $2:1 1220 \times 2440 \text{ mm } (4' \times 8') \text{designed}$  and built with heavier frames 1.73mm (0.068") and 2.46mm (0.09"), respectively, and a fastener spacing of 50mm (2").
- ii) Four wall configurations having an aspect ratio of 4:1  $610 \times 2440$  mm (2'  $\times$  8') designed and built with a framing thickness of 1.37mm (0.054"), and four fastener

spacing patterns (50mm (2"), 75mm (3"), 100mm (4") and 150mm (6")).

- iii) Four wall configurations having an aspect ratio of  $4:3 1830 \times 2440 \text{ mm } (6' \times 8') \text{designed}$  and built with a framing thickness of 1.37 mm (0.054''), and four fastener spacing patterns (50mm (2"), 75mm (3"), 100mm (4") and 150mm (6").
- iv) Four wall configurations having an aspect ratio of 1:1  $2440 \times 2440 \text{ mm}$  (8' × 8') designed and built with a framing thickness of 1.37 mm (0.054"), and four fastener spacing patterns (50mm (2"), 75mm (3"), 100mm (4") and 150mm (6")).

A more detailed description of the 14 different wall configurations under the scope of study of this thesis can be found in Appendix A. Figure 2.3 contains schematic drawings of three of the configurations W1, W3 and W12, for illustrative purposes.

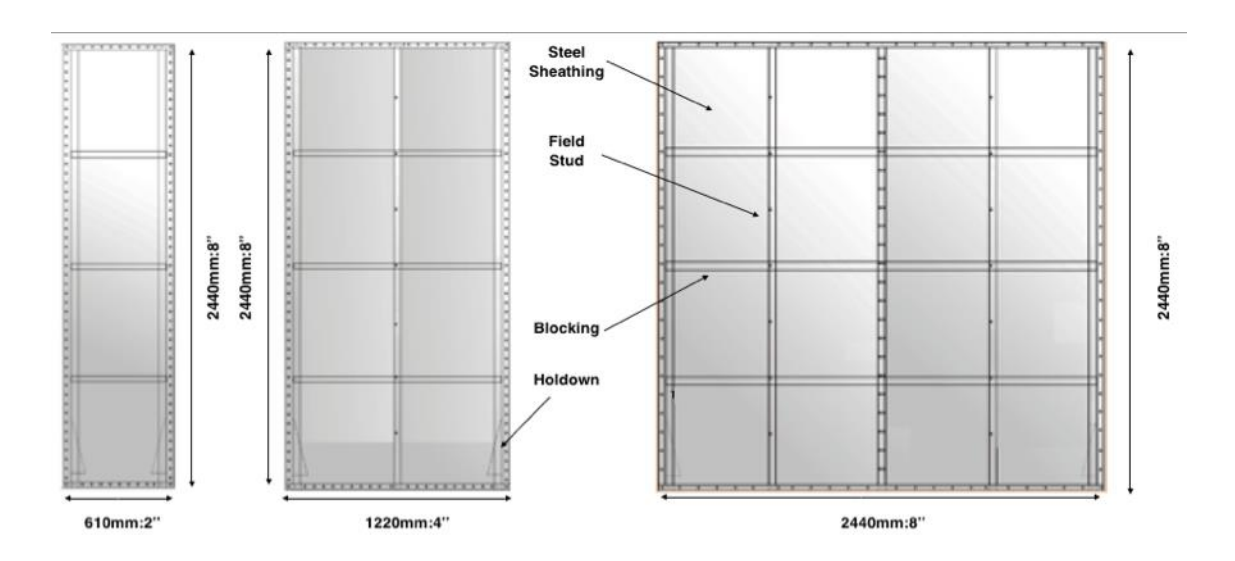


Figure 2.3 Shear wall configurations W3, W1 and W12

**Table 2.1 Shear wall test matrix (Nominal dimensions)** 

Configuration	Sheathing Thickness (in:mm)	Wall Length (ft:mm)	Wall Height (ft:mm)	Fastener Spacing (in:mm)	Framing Thickness (in:mm)	Number Of Tests And Protocol
W1	0.03:0.76	4:1220	8:2440	2/12 : 50/300	0.068:1.73	1M&1C
W2	0.03:0.76	4:1220	8:2440	2/12 : 50/300	0.097:2.46	1M&1C
W3	0.03:0.76	2:610	8:2440	2/12 : 50/300	0.054:1. 37	1M&1C
W4	0.03:0.76	2:610	8:2440	3/12 : 75/300	0.054:1. 37	1M&1C
W5	0.03:0.76	2:610	8:2440	4/12 : 100/300	0.054:1. 37	1M&1C
W6	0.03:0.76	2:610	8:2440	6/12 : 150/300	0.054:1. 37	1M&1C
W7	0.03:0.76	6:1830	8:2440	2/12: 50/300	0.054:1. 37	1M&1C
W8	0.03:0.76	6:1830	8:2440	3/12 : 75/300	0.054:1. 37	1M&1C
W9	0.03:0.76	6:1830	8:2440	4/12 : 100/300	0.054:1. 37	1M&1C
W10	0.03:0.76	6:1830	8:2440	6/12 : 150/300	0.054:1. 37	1M&1C
W11	0.03:0.76	8:2440	8:2440	2/12: 50/300	0.054:1. 37	1M&1C
W12	0.03:0.76	8:2440	8:2440	3/12 : 75/300	0.054:1. 37	1M&1C
W13	0.03:0.76	8:2440	8:2440	4/12 : 100/300	0.054:1. 37	1M&1C
W14	0.03:0.76	8:2440	8:2440	6/12 : 150/300	0.054:1. 37	1M&1C

The wall shown in Figure 2.4 (a&b) corresponds to configuration W1, the first specimen tested as part of Phase 1 of this research project. The sheathing and framing details are illustrated.

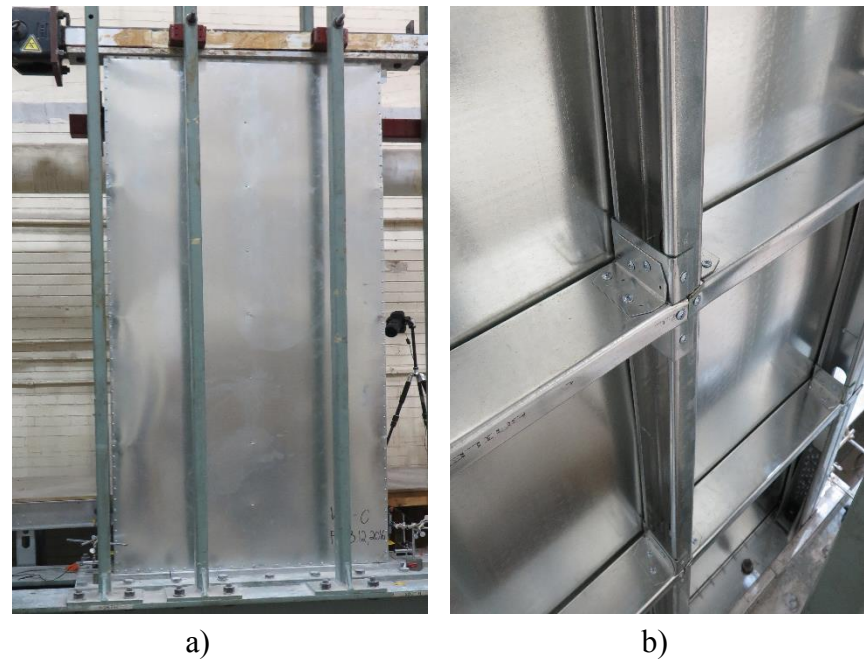


Figure 2.4 a) Shear wall W1-M front view of the wall, b) Shear wall W1-M back view of the wall

# 2.3 SPECIMEN FABRICATION, TEST SETUP AND INSTRUMENTATION

The following subsections provide a description of the different components used in the construction of the wall specimens, in addition to the test setup and instrumentation.

#### 2.3.1 COMPONENTS

In this subsection, an overview of the components used in the construction of the coldformed steel shear walls of the Phase 1 research program is provided:

 0.76mm (0.03") nominal thickness cold-formed steel sheet of ASTM A653 (2015) Grade 230 MPa (33ksi). Specimen's sheathing mounted vertically on one side of the cold-formed steel frame with direction of rolled coil aligned vertically.

- ii) 1.37mm (0.054") nominal thickness cold-formed steel stud of ASTM A653 (2015) Grade 340 MPa (50ksi). The nominal dimensions of the web, flange and lip of the C-section studs were respectively 92.1mm  $\times$  1.3mm  $\times$ 12.7mm (3-5/8"  $\times$  1-5/8"  $\times$  1/2").
- iii) 1.73mm (0.064") nominal thickness cold-formed steel stud of ASTM A653 (2015) Grade 340 MPa (50ksi). The nominal dimensions of the web, flange and lip of the C-section studs were respectively 92.1mm  $\times$  41.3mm  $\times$  12.7mm (3-5/8"  $\times$  1-5/8"  $\times$  1/2").
- iv) 2.46mm (0.097") nominal thickness cold-formed steel stud of ASTM A653 (2015) Grade 340 MPa (50ksi). The nominal dimensions of the web, flange and lip of the C-section studs were respectively 92.1mm×41.3mm×12.7mm (3-5/8" × 1-5/8" × 1/2").
- v) 1.37mm (0.054") nominal thickness cold-formed steel channel track of ASTM A653 (2015) Grade 340 MPa (50ksi). The nominal dimensions of the web and flange of the channel section tracks were respectively 92.1mm×31.8mm (3-5/8" × 1-1/4").
- vi) The blockings were cut from the channel section track listed in (v).
- vii) 1.73mm (0.064") nominal thickness cold-formed steel channel track of ASTM A653 (2015) Grade 340 MPa (50ksi). The nominal dimensions of the web and flange of the channel section tracks were respectively 92.1mm  $\times$  31.8mm (3-5/8"  $\times$  1-1/4").
- viii) 2.46mm (0.097") nominal thickness cold-formed steel channel track of ASTM A653 (2015) Grade 340 MPa (50ksi). The nominal dimensions of the web and flange of the channel section tracks were respectively 92.1mm  $\times$  31.8mm (3-5/8"  $\times$  1-1/4").
- ix) No.8 gauge 19mm (3/4") self-drilling Phillips wafer head screws used to fasten the structural components of the cold-formed steel frame. (tracks, studs, blockings).
- x) No.8 gauge 19mm (3/4") self-drilling pan head screws used to fasten the flat sheathing panel to the cold-formed steel frame with an edge distance of 9.5mm (3/8").

- xi) No.10 gauge 25.4mm (1") self-drilling hex head screws were used to connect the C-section cold-formed studs back-to-back to construct the chord studs.
- xii) Simpson Strong-Tie S/HD 10S holdown connectors were fastened to the webs of the pre-built chord studs using No.14 gauge 25.4mm (1") self-drilling hex head screws. 22.2mm (7/8") ASTM A193 (2016) grade B7 threaded anchor rods were used to connect the holdowns to the base of the testing frame and to the loading beam

#### 2.3.2 SPECIMEN FABRICATION

All the individual structural components that belonged to the different walls having the same aspect ratio were prepared and detailed prior to the assembly of the walls. First, the chord studs were pre-built using two No-10 gauge 19.1mm screws spaced at 300mm (12"), to connect back-to-back the two C-studs. The holdowns located at each end of the chord studs were offset by 2mm from their respective ends, properly centred along the centreline of the studs, and then connected to the webs of the C-studs using 24 No-14 gauge screws. As shown in Figure 2.5, in order to be able to connect properly the 610 mm (2') channel section tracks used as blocking to the chord studs and field studs, 125mm (5") long track sections were fastened every 610 mm (2') to each flange of the studs using two No.8 wafer head screws. Second, the top and bottom tracks were predrilled using the templates available for each wall configuration, in order to be able to connect the shear walls to the test frame and the loading beam using (3/4") A325 shear bolts along the length of the tracks, and (7/8") threaded anchor rods at each end of the track at the holdown locations. Then, using the chop saw, the 610mm (2') channel section tracks were detailed properly in accordance to the recommendations given by the AISI 230-15 Standard for Cold-Formed Steel Framing-Prescriptive Method for One and Two Family Dwellings (AISI S230, 2015) Section E (Figure E4-3), in order to be able to connect them properly to the chord studs and the field study using No.8 wafer head screws. Once the detailing and pre-assembling of the individual structural members of the specimens was achieved, the assembling of the different components was completed using platform building techniques. Two No.8 wafer head screws were used to connect the bottom and top tracks to chord studs at each corner of the walls on both sides. Except for the walls having an aspect ratio of 4:1 ( $610 \times 2440$ mm  $(2' \times 8')$ , the field study spaced 610 mm (2') apart, were connected to the top and bottom tracks using No.8 wafer head screws. The three rows of full blocking, 610 mm (2') apart along the height of the specimens, were fastened to the cold-formed steel study using No.8 wafer head screws. Bridging clip angles were then used to connect each end of the 610 mm (2') channel section tracks to the 125 mm (5") long track sections added on the studs as shown in Figure 2.6. In order for the frames to remain square during the construction operation, they were braced using a temporary diagonal C-channel as shown in Figure 2.5. Once the assembly of the CFS framing was achieved, the flat sheathing panels were fastened on one side to the tracks, chord studs and field stud(s) using No.8gauge pan head screws, as per the spacing listed in Table 2.1 and as shown in Figure 2.4. The screws' edge distance used for all 14 configurations was 9.5 mm (3/8"). For the 1220mm (4'), 1830 (6') and 2440 mm (8') long walls, the screw spacing used to connect the sheathing to the field studs was 12". The flat steel sheathing panels used in the construction of the 28 walls were available in two sizes; 610×2440mm (2'×8') and  $1220\times2440$ mm (4'  $\times$  8'). For the walls having an aspect ratio of 2:1 and 4:1 (610 mm (2') and 1220mm (4') long walls), a single flat steel sheathing panel was used, whereas for the 1830mm (6') and 2440mm (8') long walls, two panels were used side by side. For the 1830mm (6') walls, a combination of both sheathings' dimensions was used as shown in Figure 2.7. In order to connect both panels to the frame, they were placed side-by-side in full edge contact, and then screw fastened to the field stud using No.8-gauge pan head screws. Once the sheathing was fastened to the cold-formed steel framing, the temporary diagonal brace was removed.

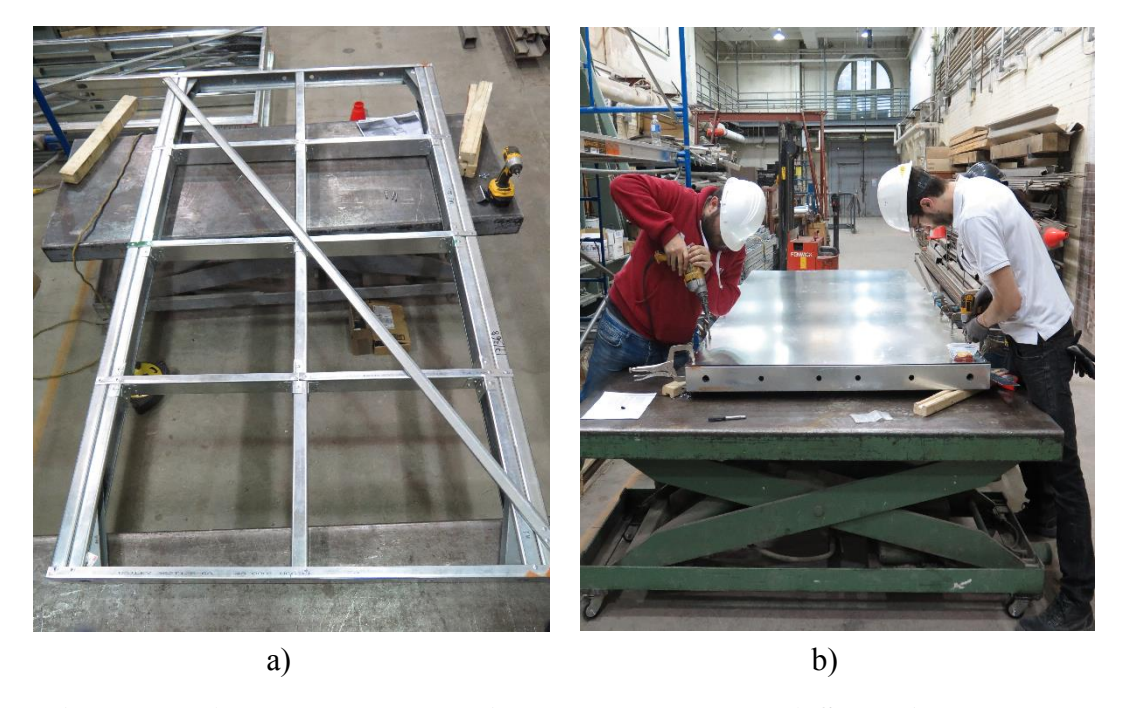


Figure 2.5- a) Frame assembly with temporary brace, b) Sheathing assembly



Figure 2.6 Blocking connection



Figure 2.7 Sheathing combination for 1830×2440 mm (6'×8') shear walls

# 2.3.3 TEST SETUP

Once all the wall configurations having the same aspect ratio were built, the appropriate loading beam was installed in the testing frame. The specimens were transferred from the construction zone to the testing frame, either manually for the light walls, or by securely using the forklift for the heavier ones. Once in position, the anchoring operations of the bottom and top tracks to the testing frame and the loading beam, respectively, were carried out. The 3/4" A325 shear bolts were placed in the tracks through the predrilled holes, and the 7/8" anchor threaded rods at the four corners of the wall at the holdown locations. In order to minimize damage to the tracks caused by bearing, cut washers were placed before installing the nuts of the shear bolts and anchor rods.

# 2.3.4 INSTRUMENTATION AND DATA ACQUISITION

To capture the data measured during the tests, and to monitor the behaviour of the specimens, instruments were installed and connected to the data acquisition system. As shown in Figures 2.8 and 2.9, two linear variable differential transformers (lvdts) were installed at the north and south bottom corner of the walls, in order to monitor the uplift and in-plane slip. A string potentiometer was attached to the south top corner of the walls in order to capture the in-plane lateral displacement. The lateral load applied to the walls was recorded by the load cell imbedded in the MTS actuator; in addition, the displacement of the actuator was also recorded. The measurement instruments were connected to Vishay Model 5100B scanners that were used to record data using the Vishay System 5000 strainsmart software (2 data/second for the monotonic tests, 100 data/second for the reversed-cyclic tests).



**Figure 2.8 Instrumentation locations** 



Figure 2.9 LVDT placement on non-structural steel plate

#### 2.4 TESTING PROTOCOLS

The steel-sheathed / cold-formed steel framed shear walls were tested according to two displacement-based loading protocols, the same as those used for all previous research programs (Balh (2010), Ong-Tone (2010), DaBreo (2012)) on this type of wall at McGill University. This included a monotonic protocol and the CUREE (Consortium of universities for research in earthquake engineering) reversed-cyclic protocol (Krawinkler et al. (2000).

#### 2.4.1 MONOTONIC TESTING PROTOCOL

Each specimen of the 14 configurations was tested according to the monotonic protocol. In order to avoid any strain rate effects and to simulate a static lateral loading or a wind loading, the wall was subjected to a constant rate of lateral displacement of 5mm/min. The loading operation consisted of pushing the shear walls from the point of zero displacement, which is considered to be the level at which the specimen was not subjected to any lateral loading. The displacement was increased up to the point where the monitored load on the specimen degraded severely or, an in-plane lateral displacement of approximately 125 mm (5") was reached, which is beyond the allowable inelastic seismic drift limit prescribed by the 2010 NBCC (NRCC, 2010) (2.5% of the wall height: 61mm (2.4"). Figure 2.10 represents a typical relationship between resistance and displacement for a monotonic test.

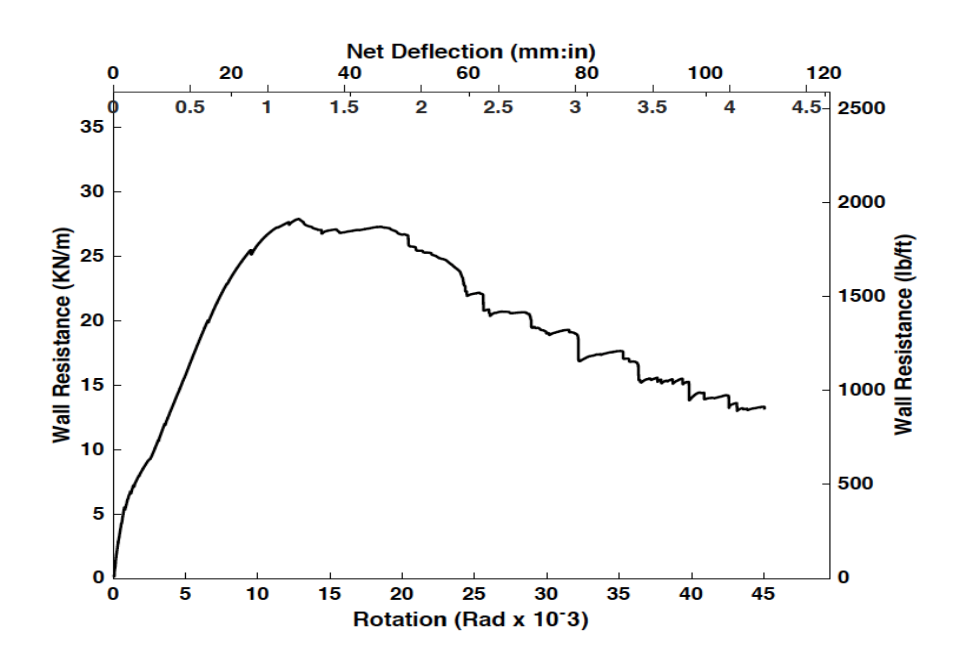


Figure 2.10 Representative force vs. Displacement monotonic test curve

# 2.4.2 REVERSED-CYCLIC TESTING PROTOCOL

Once the data was collected from the monotonic test performed for each configuration, the walls were tested under the reversed-cyclic loading protocol, which was based on the CUREE (Consortium of Universities for Research in Earthquake Engineering) ordinary ground motions protocol. The CUREE protocol, described in-depth by Krawinkler et al. (2000) and ASTM E2126 (2007), represents the demand expected during a design level earthquake with a 2% in 50 year return period

The amplitudes of the displacement cycles of the CUREE protocol are proportional to a reference displacement  $\Delta$ , obtained from the data captured during the monotonic test of the same wall configuration. The reference displacement  $\Delta$  corresponds to 60% of the post-peak displacement  $\Delta_m$ , which is defined as the displacement corresponding to 80% of the post ultimate load ( $S_u$ ) reached and collected during the monotonic test. The frequency at which all the tests were performed was 0.25Hz. Three principal cycles form the core of the CUREE protocol; a detailed description of each will follow. The in-plane lateral

movements to which the walls were subjected are multiples of the reference displacement  $\Delta$ . At first, the specimens were subjected to 6 cycles, also known as the initiation cycles, having an amplitude of  $0.050\Delta$ . The purpose of these 6 cycles, that push the walls through their elastic ranges, is to ensure that every detail is working as planned; more specifically, the instrumentation and the data acquisition system are capturing all the signals, the wall under testing is properly anchored to the testing set up and the cameras are properly capturing the pictures needed for the post-test analysis. Following the initiation cycles, the specimens were pushed through their inelastic ranges with a series of primary cycles having different amplitudes. The first primary cycle's amplitude represents 7.5% of the reference displacement  $\Delta$ . The following cycles' amplitudes are respectively:  $0.1\Delta$ ,  $0.2\Delta$ ,  $0.3\Delta$ ,  $0.4\Delta$ ,  $0.7 \Delta$  and  $1.0\Delta$ . Additional cycles following the same pattern, with an increase of  $0.5 \Delta$ , until the amplitude of 125 mm is reached. Between every two different primary cycles, the specimens are subjected to a trailing cycle having an amplitude equal to 75% of the preceding primary cycle's amplitude. Once the amplitude of 125mm is reached, the wall is subjected to one last trailing cycle at a frequency of 0.125Hz. The loading protocols of all 14 configurations are presented in the Appendix C. As an example, Table 2.2 provides the reversed cyclic loading protocol of Configuration 8, and Figure 2.11 represents the CUREE displacement time history. The hysteretic curve shown in Figure 2.12 provides an example of a typical relationship between resistance and displacement for a reversed-cyclic test.

Table 2.2 CUREE protocol input displacements for test W8

Wall Configuration:	W8		
Screw Pattern:	3"/12"		
$\Delta_{ m m}$	60.230mm		
Δ=0.6 Δ <sub>m</sub>	36.13mm		
Di1	Actuator	Number of	Cools Torre
Displacement	Input (mm)	Cycles	Cycle Type
0.05 Δ	1.807	6	Initiation
0.075 Δ	2.710	1	Primary
0.056 Δ	2.014	6	Trailing
0.1 Δ	3.614	1	Primary
0.075 Δ	2.710	6	Trailing
0.2 Δ	7.228	1	Primary
0.15 Δ	5.421	3	Trailing
0.3 Δ	10.841	1	Primary
0.225 Δ	8.131	3	Trailing
0.4 Δ	14.455	1	Primary
0.3 Δ	10.841	2	Trailing
0.7 Δ	25.30	1	Primary
0.525 Δ	18.972	2	Trailing
1.0 Δ	36.138	1	Primary
0.75 Δ	27.104	2	Trailing
1.5 Δ	54.207	1	Primary
1.125 Δ	40.655	2	Trailing
2.0 Δ	72.726	1	Primary
1.5 Δ	54.207	2	Trailing
2.5 Δ	90.345	1	Primary
1.875 Δ	67.759	2	Trailing
3.0 Δ	108.414	1	Primary
2.250 Δ	81.301	2	Trailing
3.5 Δ	125	1	Primary
2.625 Δ	94.862	2	Trailing

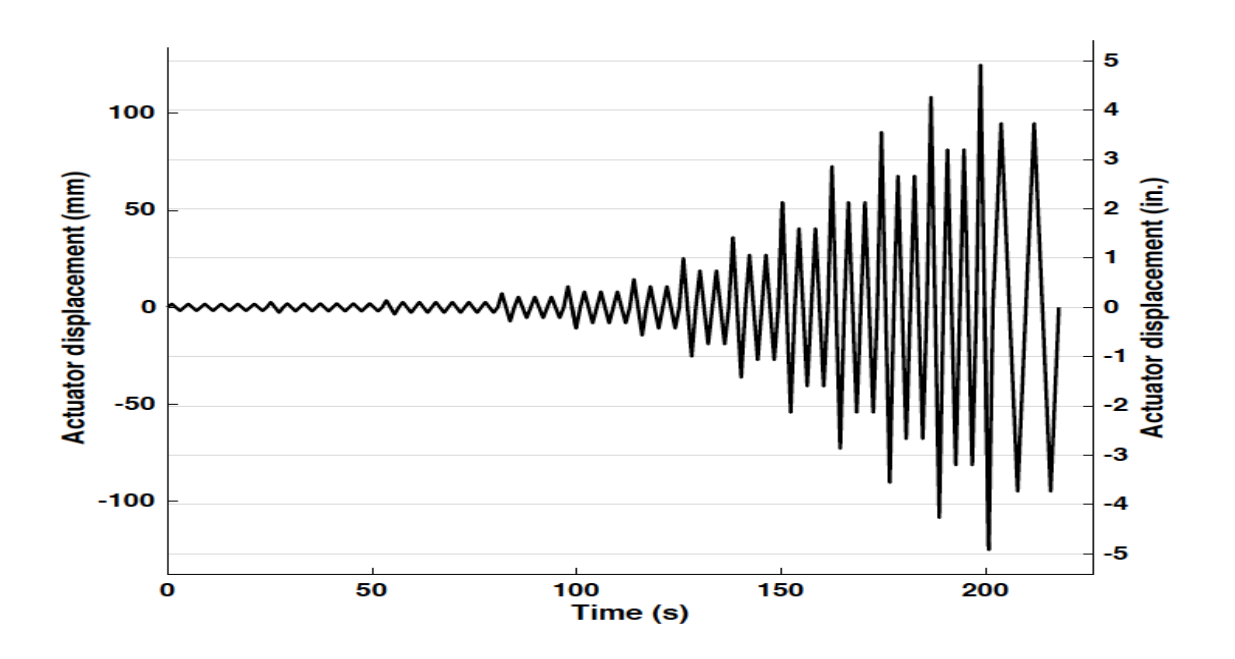


Figure 2.11 Representative CUREE displacement time history

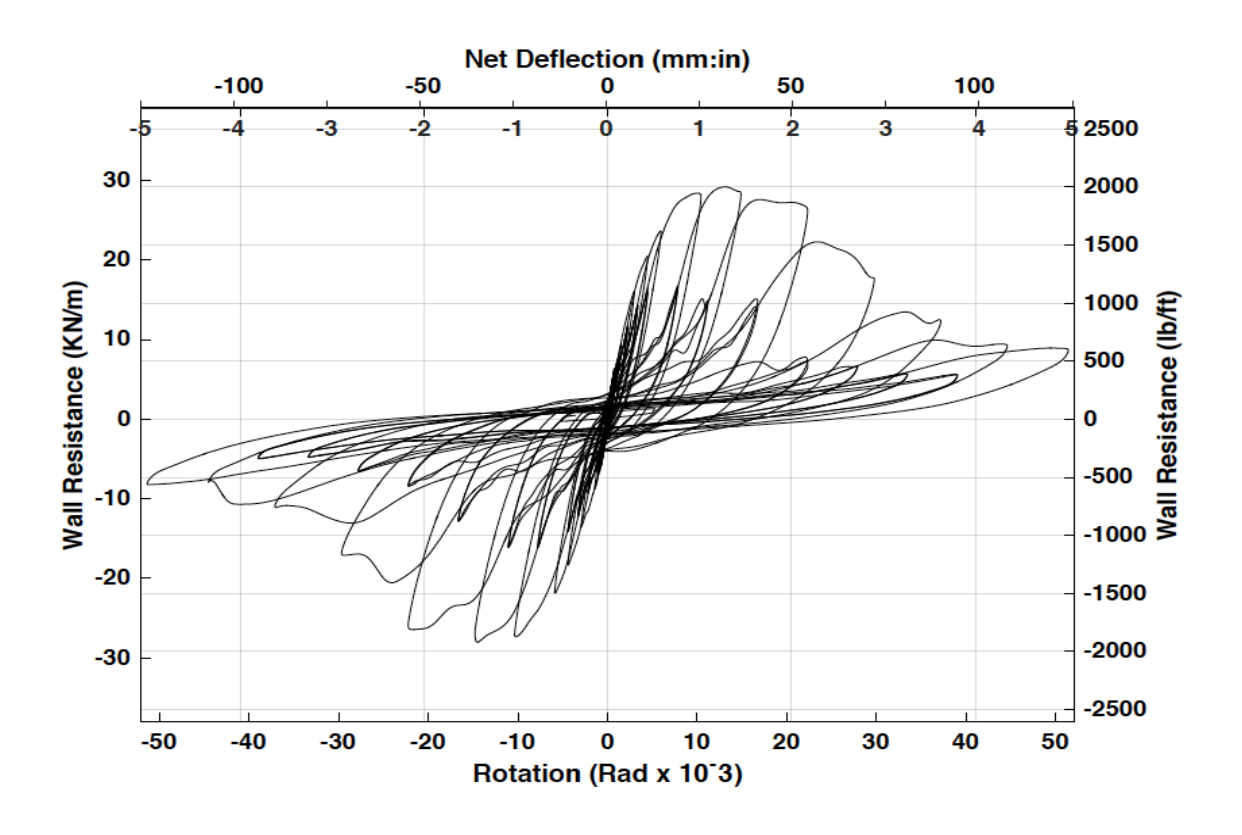


Figure 2.12 Representative force vs. Displacement CUREE reversed-cyclic test curve

#### 2.5 OBSERVED FAILURE MODES

A description of each mode of failure that occurred during the testing of the shear walls is provided in the following subsections. In the initial stages of loading the elastic shear buckling of the steel sheathing was dominant. This phenomenon represented by a diagonal out-of-plane deformation pattern was developed due to the compression stresses. In addition, tension stresses occurred in the sheathing, which led to the development of large tension forces acting on the corners of the shear walls. Subsequently, these large concentrated tension forces caused failures to the steel sheathing connections; damage to the cold-formed steel framing was also observed in some cases. Even though the structural components of the frame suffered from several modes of failure during the testing of the 28 specimens, it is important to emphasize that the dominant mode of failure was in most cases located at the screw connection between the sheathing and the cold-formed steel frame. In addition, the damage caused to the specimens during the tests was typically the result of a combination of several of the failure modes. The test observation sheets that were used to record all the damage patterns for each wall are provided in Appendix D.

# 2.5.1 CONNECTION FAILURE

### 2.5.1.1 BEARING SHEATHING FAILURE (SB)

Since the sheathing was relatively thin compared with the framing, and as the movement of the sheathing during the in-plane loading of the wall was independent of the frame response, failure of the sheathing by bearing in the area surrounding the fastener was observed as shown in Figure 2.13.



Figure 2.13 Sheathing steel bearing

# 2.5.1.2 TILTING OF SHEATHING SCREW (TS)

The first mechanism that is responsible for triggering the connection failure process is the tilting of the sheathing screws as shown in Figure 2.14. This phenomenon is the result of the eccentric shear forces acting on the fastener. Localized bearing of the sheathing and the frame were also observed around the tilted screw, which resulted in loosening of the connection.



Figure 2.14 Sheathing screw tilting

# 2.5.1.3 PULL-OUT FAILURE OF SHEATHING SCREW (PO)

Bearing damage occurred to the frame as a result of screw bearing on the edge of the screw hole, which led gradually to the enlargement of the diameter of the hole in the frame. Depending on the level of the forces in action, the screw was either partially pulled out (PPO) or fully pulled out of the framing. In some cases, the fastener remained intact within the sheathing as shown in Figure 2.15.



Figure 2.15 Sheathing screw pull-out failure

# 2.5.1.4 PULL-THROUGH SHEATHING FAILURE (PT)

The pull through sheathing failure mode, was observed more frequently along the field studs and during the testing of the specimens having thicker structural components composing the frame (configurations W1 and W2). This phenomenon was triggered by the shear buckling of the sheathing. The buckles caused the sheathing to pull away -normal direction- from the wall framing while the screws remained connected to the cold-formed steel frame as shown in Figure 2.16.



Figure 2.16 Screw pull-through sheathing failure

# 2.5.1.5 TEAR-OUT SHEATHING FAILURE (TO)

All the screws connecting the sheathing to the cold-formed steel frame were placed at a specific distance of 9.5mm (3/8") with respect to the panel's edge. During the test, as the bearing damage in the sheathing became more pronounced, the fastener progressively tore out from the edge of the steel sheathing, Figure 2.17.



Figure 2.17 Screw tear-out failure

#### 2.5.2 SHEATHING FAILURE

# 2.5.2.1 SHEAR BUCKLING AND TENSION FIELD ACTION OF SHEATHING

In the very early stages of the in-plane loading of the wall specimens, elastic shear buckling of the flat sheathing panels was noted. The observed diagonal pattern across the sheathing during the tests was caused by the compression field action. This was accompanied by the development of a tension field also running diagonally (opposite direction) across the sheathing. The walls tested according to the monotonic protocol witnessed the deformation pattern of the compression field and tension field action of the sheathing in one direction; whereas in the reversed-cyclic cases, these phenomena were noted in both directions as shown in Figures 2.18 a) and b). In wall configurations where two flat sheathing panels were used, the development of the tension field action and the shear buckling of the sheathing was observed in each panel as shown in Figures 2.19 and 2.20.

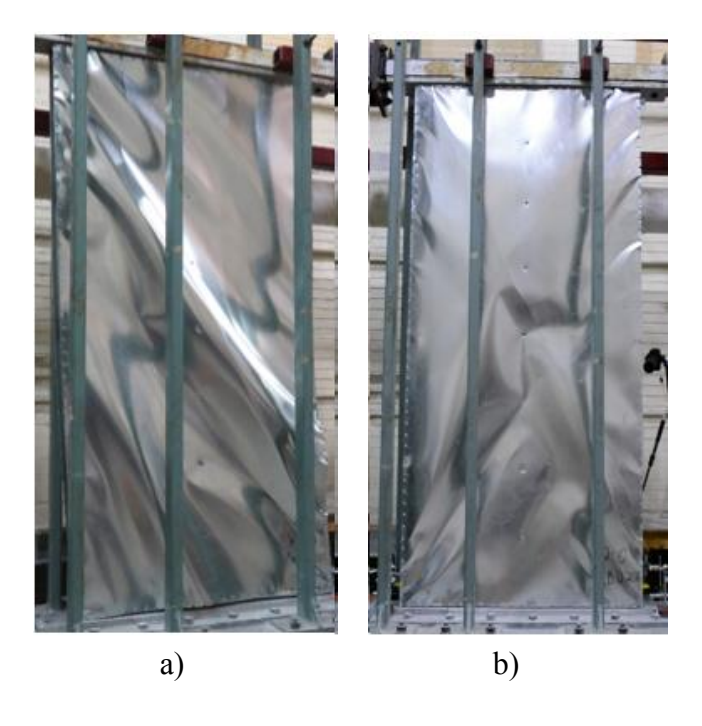


Figure 2.18 Shear buckling and tension field action of sheathing; a) Monotonic test  $(1220 \times 2440 \text{ mm } (4' \times 8'))$ , b) Reversed cyclic test  $(1220 \times 2440 \text{ mm } (4' \times 8'))$ 

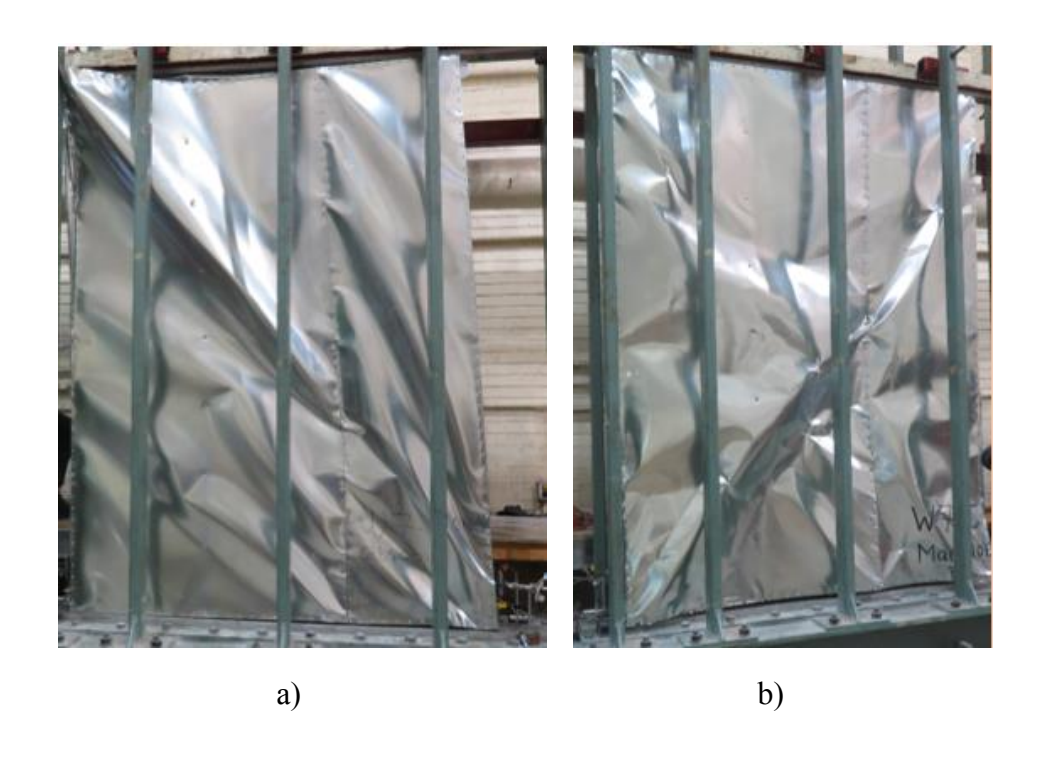


Figure 2.19 Shear Buckling and Tension Field of Sheathing; a) Monotonic Test  $(1830 \times 2440 \text{ mm } (6' \times 8'))$ , b) Reversed Cyclic test  $(1830 \times 2440 \text{ mm } (6' \times 8'))$ 

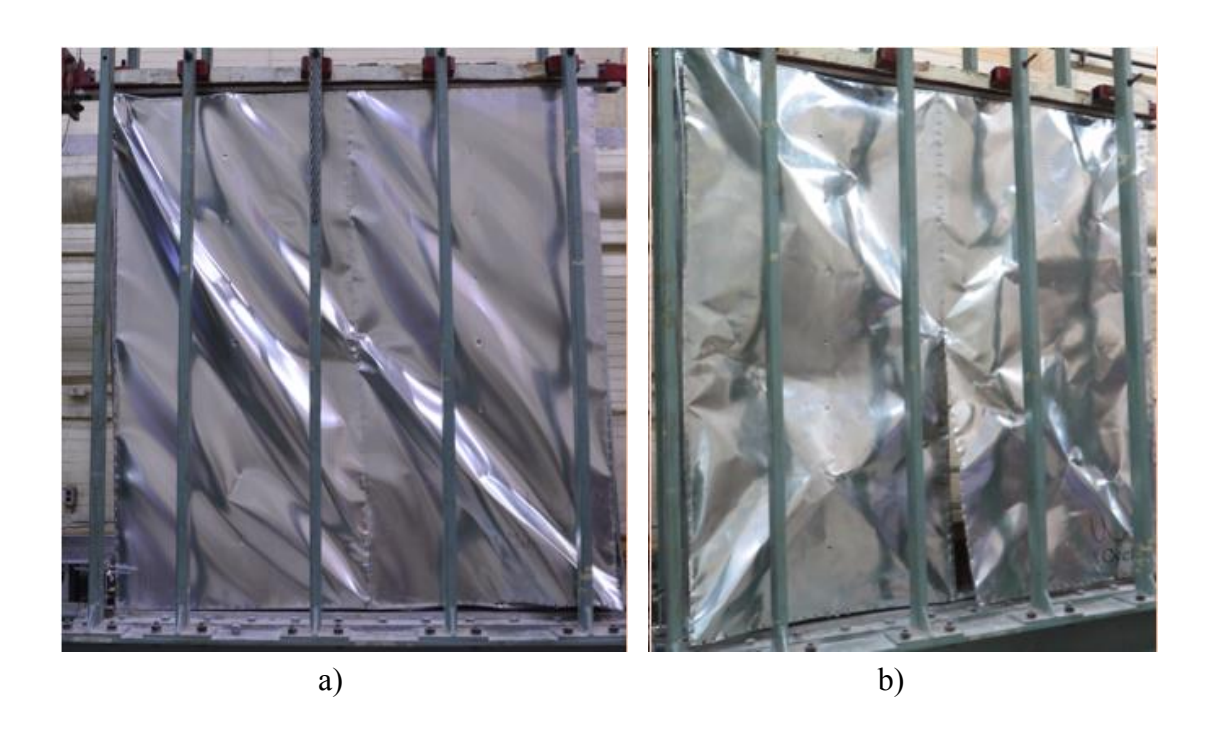


Figure 2.20 Shear buckling and tension field of sheathing : a) Monotonic test (2440  $\times$  2440 mm (8'  $\times$  8 ')), b) Reversed cyclic test (2440  $\times$  2440 mm (8'  $\times$  8'))

#### 2.5.3 FRAMING

In addition to the connection failure modes and to the shear buckling / tension field development of the flat sheathing panels, damage was also observed at the level of the structural components of the cold-formed steel framing. These phenomena resulted first from the asymmetry of the walls, i.e. The sheathing was placed on one side of each wall, and the horizontal and vertical components of the tension field forces action. In addition, the shear buckles observed in the sheathing created normal forces that pushed into the wall and exacerbated the overall bending of the structural components of the cold-formed steel frame. The latter was mainly observed in long walls.

#### 2.5.3.1 FLANGE AND LIP DISTORTION (FLD) OF CHORD STUDS

Once the specimens were pushed into their inelastic ranges, twisting and distortion of the flanges and lips of the chord studs were observed, mainly in the configurations designed with closely spaced sheathing fasteners, i.e. 50mm (2") and 75mm (3"). This behaviour resulted from the asymmetry of the walls and the action of the horizontal component of the tension field force on the chord studs. The sheathing panels were fastened to the framing only on one side; thus the mid-line of the wall, where the in-plane lateral loading was applied, did not coincide with the location where the shear resistance was being developed. Hence, a direct torque was placed on the chord studs over the corresponding width of the tension field in the sheathing. On one hand, the frame blocking reinforcement that was integrated in the design of the shear walls, reduced to a large extent the overall twisting failure of the studs, a failure mode commonly observed in previous research programs (Ong-Tone (2009) and Balh (2010)). On the other hand, and more precisely for the walls with the closely spaced sheathing fasteners, the horizontal component of the tension field force caused the flange / lip component of the chord studs to distort or "unwrap", at the top and bottom corners of the walls as shown in Figure 2.21.

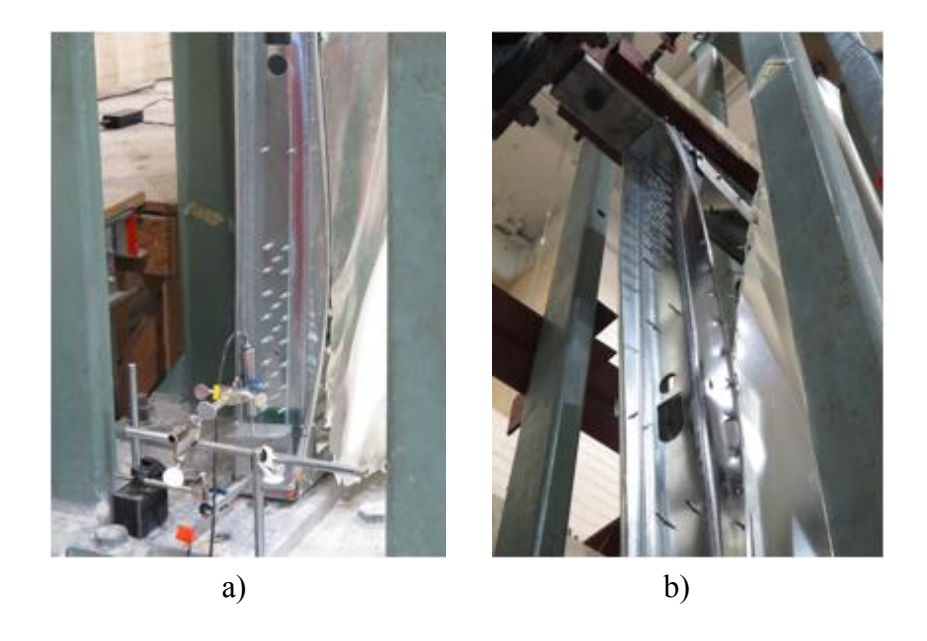


Figure 2.21 Flange and lip distorted unwrapped after testing : a) Specimen W1-M, and b) Specimen W1-C

## 2.5.3.2 DEFORMATION AND UPLIFT OF TRACKS

The uplift deformations of the tracks were mostly observed during the testing of the walls having closely spaced sheathing connectors. These configurations experienced the development of a high level of tension field action within the sheathing. The vertical component of this force is the main reason that uplift deformations occurred in the track members as shown in Figure 2.22 a and b.



Figure 2.22 a) Deformation and uplift of bottom track, b) Deformation and uplift of top track

#### 2.5.4 FAILURE MODES OF SHORT WALLS

## Configurations W3 to W6: 610×2440mm (2'×8')

Walls having an aspect ratio of 4:1, constructed with frames having a thickness of 1.37mm (0.054"), single side sheathing and frame blocking elements were tested as part of Phase 1 of this research program. The data collected and the post-test analysis show that the slender walls witnessed high level of in-plane rotation. The flat sheathing panels suffered from tear out at the bottom corners. In addition, as shown in Figure 2.23 the chord studs suffered from local buckling caused by a combination of axial compression and bending, a mode of failure that was dominant in the case of slender walls.



Figure 2.23 Local Buckling of the chord studs in 610×2440mm (2'×8') walls

## 2.5.5 FAILURE MODES OF LONG WALLS

As part of the Phase 1 tests, walls of size 1830×2440mm (6'×8') and 2440×2440mm (8'×8') designed with full blocking were tested. These walls were designed and built using two cold-formed steel panels placed side by side, which were screw connected to a single field

stud. As the amplitude of the lateral displacement increased, the perimeter connections, sheathing and structural components of the cold-formed steel frame suffered from a combination of failure modes as presented in Subsections 2.5.1 to 2.5.3. In addition, the field stud connecting both sheathing panels did suffer from damage caused by the overall bending of the walls as shown in Figure 2.24. This phenomenon was observed during the testing of the long shear walls,  $1830 \times 2440 \text{ mm}$  (6'×8') and  $2440 \times 2440 \text{ mm}$  (8'×8'), designed with closely spaced sheathing fasteners, 50 mm (2") and 75 mm (3"). The full blocking did not restrict effectively the overall out-of-plane deformation of these walls.

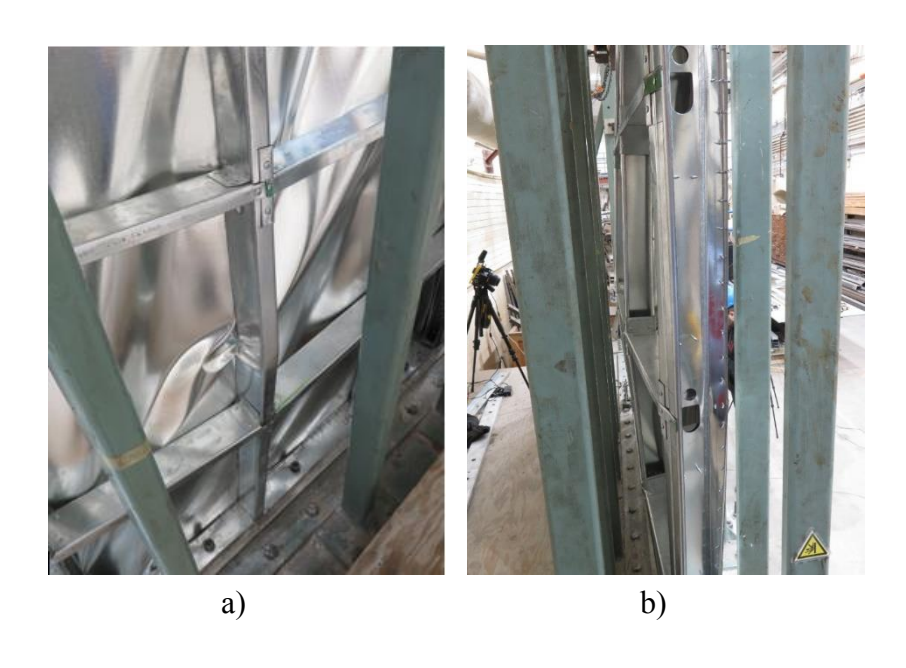


Figure 2.24 Flexural bending of field Stud in long walls

### Configurations W1 &W2 :1220×2440mm (4'×8')

Walls having an aspect ratio of 2:1, constructed with heavier frames (1.73 mm (0.068") and 2.46mm (0.097")) a single side sheathing and frame blocking elements were tested as part of Phase 1 of this research program. Overall, as the amplitude of the lateral displacement increased, the perimeter connections, sheathing and structural components of the cold-formed steel frame suffered from a combination of several modes of failures as presented in Subsections 2.5.1 to 2.5.3. More precisely, configurations W1 and W2 under

monotonic and reversed-cyclic loading suffered from flange and lip distortion of the chord studs at the top and bottom corner and tear out of the sheathing at the bottom corners. In addition, pull through sheathing failure mode more along the field studs and deformations of the upper tracks and uplift of the bottom tracks were observed. Figure 25 a,b and c show the several modes of failures detailed in this subsection.

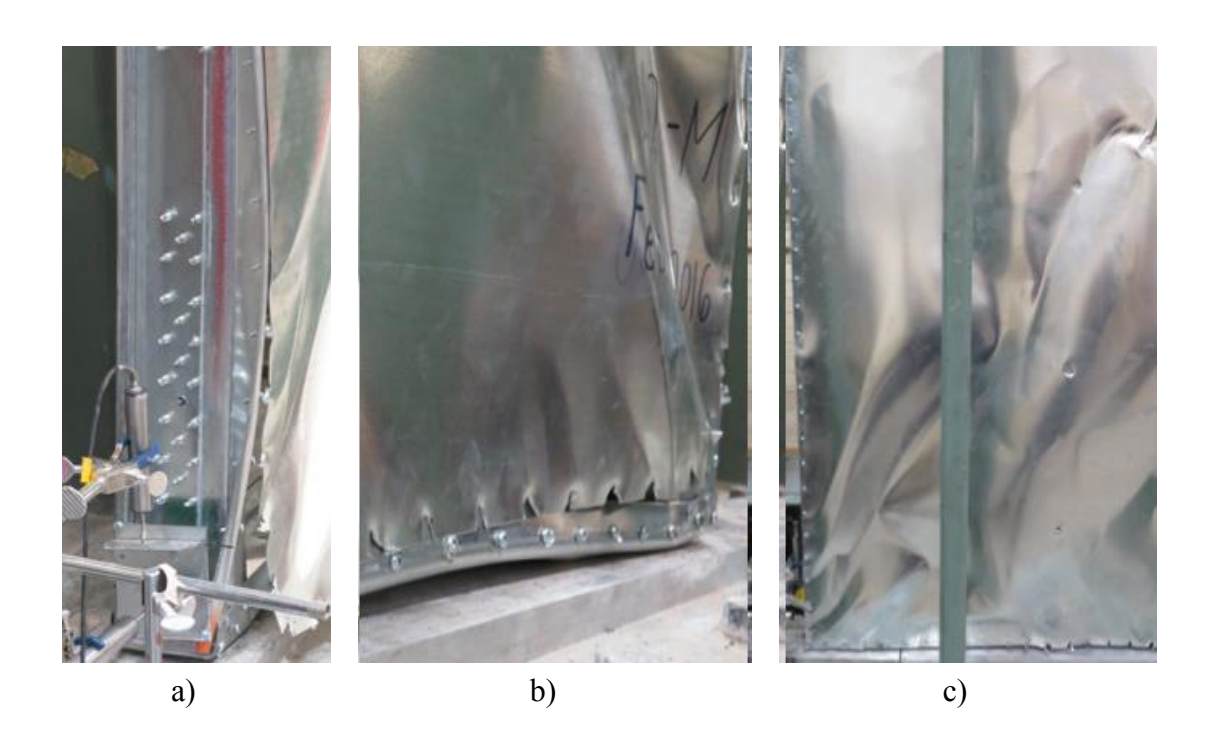


Figure 2.25 Combination of failure modes in 1220×2440mm (4'×8') walls : a) Flange and lip distortion of the chord studs, b) Uplift of the bottom tracks, c) Pull through sheathing

### 2.6 DATA REDUCTION

#### 2.6.1 LATERAL DISPLACEMENT

Equations 2.1 and 2.2 were used to compute the net lateral displacement ( $\Delta_{net}$ ) in addition to the rotations ( $\theta_{net}$ ) experienced by the wall specimens under loading.

$$\Delta_{net} = \Delta_{top} \tag{2-1}$$

$$\theta_{net} = \frac{\Delta_{net}}{H} \tag{2-2}$$

Where,

 $\Delta_{net}$ : Net lateral displacement (mm);

 $\Delta_{top}$ : Top wall lateral displacement as measured (mm);

 $\Theta_{net}$ : Net rotation of wall (radians);

H: Height of wall (mm);

#### 2.6.2 ENERGY DISSIPATION

The energy dissipated by the specimens subjected to both displacement-based loading protocols was computed using Equations 2.3 and 2.4. As shown in Figure 2.26, the energy dissipated during a test is represented by the integrated area under the load-displacement curve obtained from the testing program.

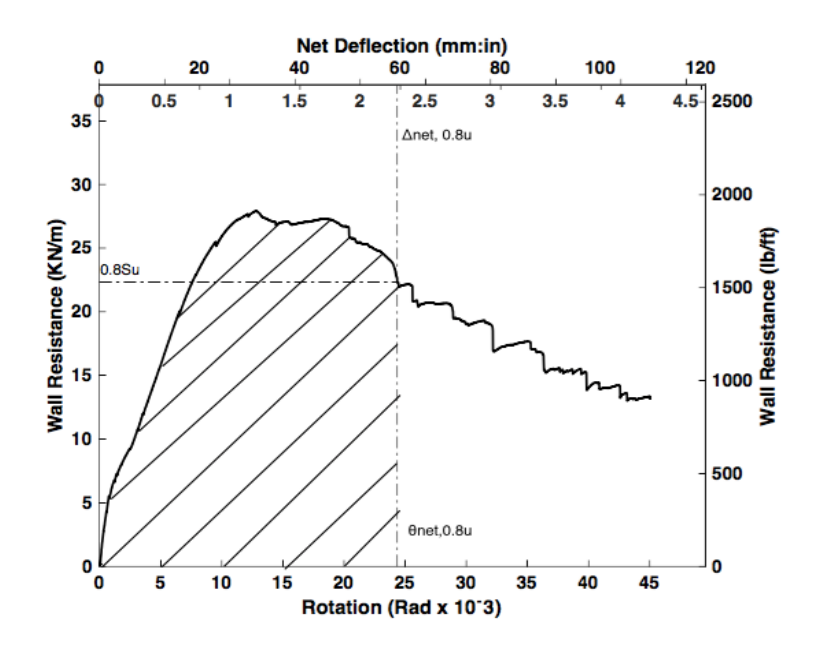


Figure 2.26 Energy as area below force vs. Displacement curve

The energy was calculated using an incremental approach:

$$E_i = \frac{F_i + F_{i-1}}{2} \times \left(\Delta_{top,i} - \Delta_{top,i-1}\right) \tag{2-3}$$

$$E_{Total} = \sum_{i=1}^{n} E_i \tag{2-4}$$

## Where,

 $E_i$ : Energy between two consecutive points;

 $F_i$ : Shear force between two consecutive data points;

 $\Delta_{top,i}$ : Measured wall top displacement;

*E*<sub>total</sub>: Cumulative Energy Dissipation;

### 2.7 TEST RESULTS

Once all specimens were tested and the data was collected, a Matlab algorithm was designed in order to extract the parameters summarized in Tables 2.3, 2.4 and 2.5. Table 2.3 lists the maximum wall resistance,  $S_u$ , wall resistance at 40% of  $S_u$ , 0.4  $S_u$  and the wall resistance at 80% of  $S_u$ , 0.8  $S_u$ , in addition to their respective level of in-plane lateral displacement recorded during the tests  $\Delta_{net,u}$ ,  $\Delta_{net,0.4u}$  and  $\Delta_{net,0.8u}$ . Moreover, and based on Equations 2.2 and 2.3, the rotations at  $S_u$  ( $\theta_u$ ), 40%  $S_u$  ( $\theta_{0.4u}$ ), 80%  $S_u$  ( $\theta_{0.8u}$ ) and the total energy dissipated  $E_{total}$ , were computed and presented. The same parameters were extracted from the data recorded during the 14 tests performed based on the CUREE protocol. Table 2.4 displays the results obtained from the positive region of the curve, whereas the values extracted from the negative region are provided in Table 2.5. Figures 2.27 and 2.28 represent graphically the results obtained from the monotonic and reversed-cyclic tests performed on specimen W8.

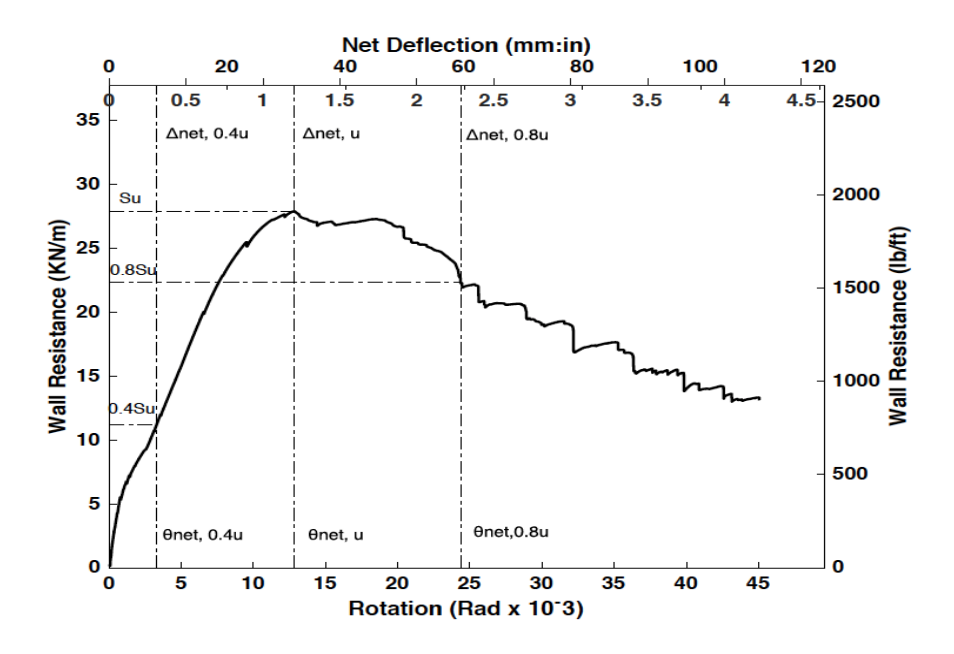


Figure 2.27 Parameters of monotonic tests

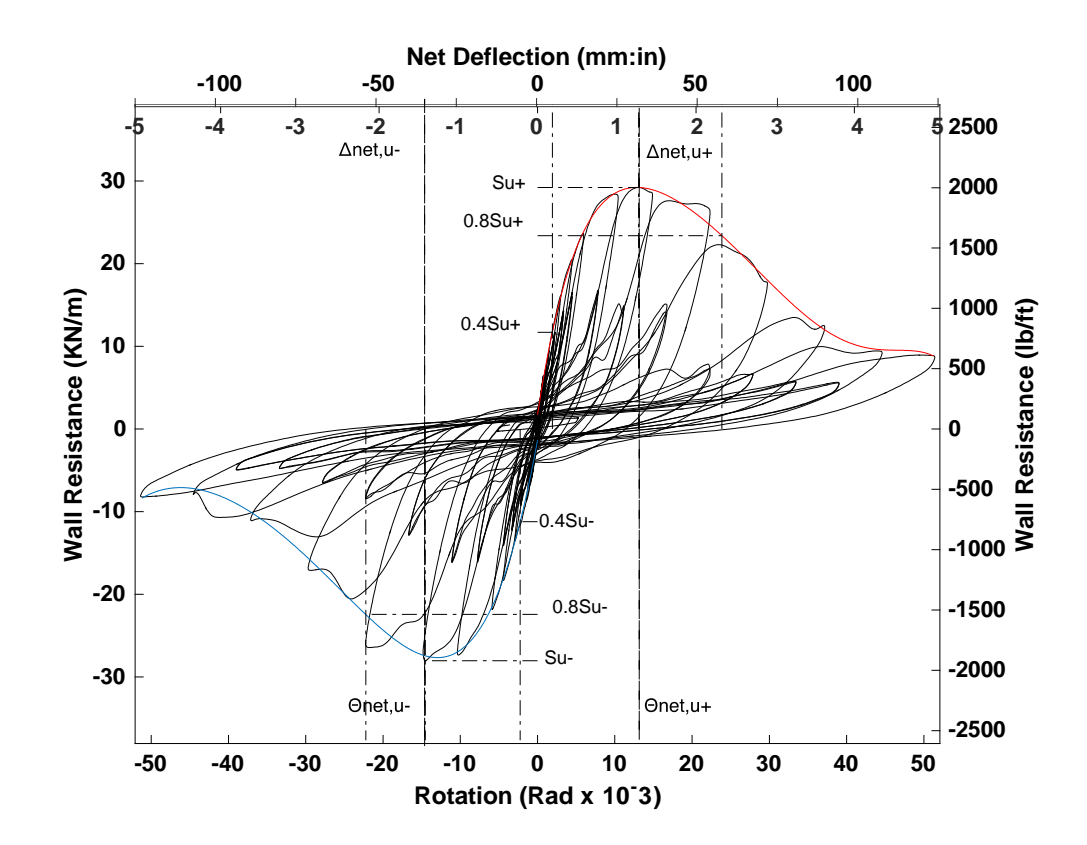


Figure 2.28 Parameters of reversed-cyclic tests

Table 2.3 Test data summary – Monotonic tests

Specimen	Maximum Wall Resistance S <sub>u</sub> (kN/m)	$\begin{array}{c} \text{Displacement} \\ \text{at } S_u  \Delta_{\text{net},u} \\ \text{(mm)} \end{array}$	$\begin{array}{c} Displacement \\ at \ 0.4S_u \ \Delta_{net,0.4u} \\ (mm) \end{array}$	$\begin{array}{c} Displacement \\ at \ 0.8S_u \ \Delta_{net0.8u} \\ (mm) \end{array}$	$\begin{array}{c} \text{Rotation at } S_u \\ \theta_{\text{net},u} \\ (\text{rad} \times 10^{-3}) \end{array}$	Rotation at $0.4S_u \; \theta_{net,0.4u}$ (rad $\times 10^{-3}$ )	Rotation at $0.8S_u$ $\Theta_{net,0.8u}$ $(rad \times 10^{-3})$	Energy Dissipation, E (Joules)
W1	34.88	52.76	11.42	83.65	21.64	4.68	34.31	3370
W2	39.13	52.38	9.64	85.87	21.48	3.95	35.22	4121
W3	35.32	101.87	16.7	100.00	41.78	6.85	41.01	2114
W4	29.97	85.56	13.18	100.00	35.09	5.41	41.01	1820
W5	25.41	58.14	9.71	83.03	23.84	3.98	34.05	1474
W6	20.13	58.03	12.81	81.73	23.80	5.25	33.52	1018
W7	33.46	28.8	5.20	75.48	11.81	2.13	30.95	5671
W8	27.92	31.25	7.99	59.38	12.82	3.28	24.35	3973
W9	25.55	40.19	5.35	67.04	16.48	2.19	27.49	3030
W10	18.94	39.59	5.26	50.04	16.24	2.16	20.52	1790
W11	32.87	36.31	4.79	86.77	14.89	1.96	35.58	7742
W12	28.81	32.83	6.48	54.03	13.46	2.66	22.16	3836
W13	24.68	24.20	3.97	42.37	9.92	1.63	17.38	3088
W14	47.56	28.35	3.14	42.77	11.63	1.29	17.54	2310

Table 2.4 Test data summary – Positive cycles reversed cyclic tests

Specimen	Maximum Wall Resistance Su'+ (kN/m)	$\begin{array}{c} Displacement \\ at \ S_{u'+}, \\ \Delta_{net,u+}(mm) \end{array}$	$\begin{array}{c} Displacement \\ at \ 0.8S_{u^{'}+}, \\ \Delta_{net, \ 0.8u+}(mm) \end{array}$	$\begin{array}{c} Displacement \\ at \ 0.4S_{u^{'}+}, \\ \Delta_{net,0.4u+(}mm) \end{array}$	Rotation at $S_{u'+}$ , $\theta_{net,u+}$ (rad $x10^{-3}$ )	Rotation at $0.4Su'_+$ , $\theta_{net,0.4u+}$ (rad x10 <sup>-3</sup> )	Rotation at $0.8Su'_+$ , $\theta_{net,0.8u+}$ (rad $\times 10^{-3}$ )	Energy Dissipation, E (Joules)
W1	36.70	41.68	9.80	60.10	17.09	4.02	24.65	17470
W2	40.35	48.29	7.90	64.50	19.80	3.24	26.45	16150
W3	38.65	85.80	17.30	100.00	35.19	7.09	41.01	12642
W4	29.00	70.79	14.00	100.00	29.03	5.74	41.01	5807
W5	26.67	47.13	8.40	74.20	19.33	3.44	30.43	4958
W6	19.98	67.27	7.30	80.80	27.59	2.99	33.14	4353
W7	31.34	29.54	5.00	77.80	12.11	2.05	31.91	32114
W8	29.22	31.92	4.70	58.20	13.09	1.93	23.87	22742
W9	25.71	27.89	4.80	51.80	11.44	1.97	21.24	18462
W10	20.47	29.05	4.00	48.70	11.91	1.64	19.97	14748
W11	35.20	32.66	5.30	62.70	13.39	2.17	25.71	42939
W12	30.22	31.90	4.30	48.00	13.08	1.76	19.69	25814
W13	24.82	29.57	5.20	41.20	12.13	2.13	16.90	19645
W14	19.19	24.64	3.80	38.50	10.10	1.56	15.79	16022

Table 2.5 Test data summary – Negative cycles reversed cyclic tests

Specimen	Maximum Wall Resistance Su'.(kN/m)	Displacement at $S_u'$ -, $\Delta_{net,u}$ -(mm)	Displacement at $0.4S_u$ '-, $\Delta_{net,0.8u}$ -(mm)	Displacement at $0.8S_u'$ ., $\Delta_{net,0.4u}$ -(mm)	Rotation at $S_{u'}$ -, $\Theta_{net,u}$ - (rad $x10^{-3}$ )	Rotation at $0.4S_{u'}$ , $\theta_{net,0.4u}$ (rad $\times 10^{-3}$ )	Rotation at $0.8S_u'$ -, $\theta_{net,0.8u}$ - (rad $\times 10^{-3}$ )	Energy Dissipation, E (Joules)
W1	35.22	44.16	9.60	67.00	18.11	3.94	27.48	17470
W2	41.54	49.97	9.00	56.90	20.49	3.69	23.33	16150
W3	36.02	79.80	15.50	100.00	32.73	6.36	41.01	12642
W4	27.56	71.12	15.00	100.00	29.17	6.15	41.01	5807
W5	26.39	69.21	10.30	100.00	28.38	4.22	41.01	4958
W6	19.55	78.40	10.60	95.40	32.15	4.35	39.12	4353
W7	30.24	31.42	6.20	85.70	12.89	2.54	35.15	32114
W8	28.04	35.41	5.50	54.20	14.52	2.26	22.23	22742
W9	24.29	27.97	5.80	44.00	11.47	2.38	18.04	18462
W10	19.36	29.05	3.20	45.10	11.91	1.31	18.50	14748
W11	32.14	36.77	4.20	65.80	15.08	1.72	26.98	42939
W12	29.02	31.92	4.60	41.00	13.09	1.89	16.81	25814
W13	23.75	25.14	4.90	37.80	10.31	2.01	15.50	19645
W14	18.13	25.62	3.70	33.90	10.51	1.52	13.90	16022

Table 2.6 Test data summary – Reversed cyclic tests average values

Specimen	Maximum Wall Resistance Su (kN/m)	Displacement at $S_u$ , $\Delta_{net,u}(mm)$	$\begin{array}{c} Displacement \ at \\ 0.4S_u, \\ \Delta_{net,0.4u}(mm) \end{array}$	$\begin{array}{c} \text{Displacement at} \\ 0.8S_u, \\ \Delta_{\text{net, 0.8u}}(mm) \end{array}$	$ \begin{array}{c} \text{Rotation at } S_u, \\ \theta_{\text{net},u} \\ \text{(rad } x10^{\text{-}3}) \end{array} $	Rotation at $0.4S_u$ , $\Delta_{net,0.4u}(mm)$ (rad x10 <sup>-3</sup> )	$ \begin{array}{c} \text{Rotation at} \\ 0.8S_u, \\ \Delta_{\text{net, 0.8u}}(\text{mm}) \\ (\text{rad} \times 10^{-3}) \end{array} $	Energy Dissipation, E (Joules)
W1	35.96	42.92	9.70	63.55	17.60	3.98	26.06	17470
W2	40.94	49.13	8.45	60.70	20.15	3.47	24.89	16150
W3	37.34	82.80	16.40	100.00	33.96	6.73	41.01	12642
W4	28.28	70.96	14.50	100.00	29.10	5.95	41.01	5807
W5	26.53	58.17	9.35	87.10	23.86	3.83	35.72	4958
W6	19.77	72.84	8.95	88.10	29.87	3.67	36.13	4353
W7	30.79	30.48	5.60	81.75	12.50	2.30	33.53	32114
W8	28.63	33.67	5.10	56.20	13.81	2.09	23.05	22742
W9	25.00	27.93	5.30	47.90	11.45	2.17	19.64	18462
W10	19.92	29.05	3.60	46.90	11.91	1.48	19.23	14748
W11	33.67	34.72	4.75	64.25	14.24	1.95	26.35	42939
W12	29.62	31.91	4.45	44.50	13.09	1.82	18.25	25814
W13	24.28	27.36	5.05	39.50	11.22	2.07	16.20	19645
W14	18.66	25.13	3.75	36.20	10.31	1.54	14.85	16022

#### 2.8 ANCILLARY TESTING OF MATERIALS

In order to measure and thus verify the various thicknesses and the mechanical properties of the structural components of the shear walls an ancillary testing program was performed by testing three coupons of each source coil based on the requirements provided by ASTM A370 (2014). It is important to mention that the structural components (tracks, studs, sheathings) having the same thickness were cold-rolled from the same coil. In total, the ancillary testing program consisted of 24 coupons (3 coupons for every different thickness of studs, 3 coupons for every different thickness of tracks, and 6 coupons for the flat sheathing panel- 3 in longitudinal and 3 in transverse orientation with respect to the rolling direction). As specified by ASTM A653 (2015), all steels were grade 340 MPa (50ksi) with the exception of the cold-formed steel sheathing of thickness 0.76mm (0.03") which was 230 MPa (33ksi). To measure the longitudinal elongation of the coupons at the end of the tests, gauge marks were punched (gauge length 50.4mm) prior to launching the test. In addition, a 50mm (2") extensometer was attached to the coupons in order to monitor and record the variation of their longitudinal elongation throughout the test as a function of the tensile load applied. The cross-head movement rate was 0.002mm/s throughout the elastic range of the specimens, then it was increased to 0.01mm/s after the yield point was reached and the behaviour was characterized by a plastic plateau. When strain hardening of the material was observed, the cross-head rate was raised to 0.1mm/s until the rupture of the specimen. Once the tensile testing program of the coupons was completed, the zinc coating was removed with a 25% hydrochloric acid solution (hcl). The area of the base metal was used in order to determine the Yield Stress (F<sub>v</sub>) and Ultimate Stress (F<sub>u</sub>). Table 2.6 provides a summary of the measured material properties of the cold-formed steel studs and sheathing.

**Table 2.7 Summary of material properties** 

Nominal Material Thickness(mm)	Member	Base Metal Thickness (mm)	Yield Stress, F <sub>y</sub> (MPa)	Tensile Stress, F <sub>u</sub> (MPa)	$F_u / F_y$	% Elong. 50 mm Gauge
1.37	Stud	1.37	381	462	1.21	34.2
1.37	Track	1.37	345	432	1.25	32.5
1.73	Stud	1.77	352	452	1.21	34.2
1.73	Track	1.75	372	456	1.23	31.9
2.43	Stud	2.49	370	450	1.22	33.1
2.43	Track	2.50	341	427	1.25	35.5
0.76	Sheathing	0.76	333	406	1.21	29.3

The results indicate that all coupons meet the minimum requirements specified in the CSA-S136 Standard (2016) and AISI S100 Standard (2016) stating that the ratio of tensile strength to yield stress is not less than 1.08 and the minimum elongation is greater than or equal to 10% in a two-inch (50-mm) gauge length. The values for the ratio of the measured yield stress to minimum specified yield stress R<sub>y</sub>, and measured tensile stress to minimum specified tensile stress, R<sub>t</sub>, are listed in the AISI S400 (2015). Referring to Section A3.2-1 of the AISI S400, it is permitted to use values of R<sub>y</sub>, other than those listed in Table A3.2-1, if the values were determined by testing specimens representative of the product thickness and source. Table 2.8 lists the R<sub>y</sub> and R<sub>t</sub> value computed based on the results obtained from testing of the materials.

Table 2.8  $R_t$  and  $R_y$  Values of Studs/Tracks/Sheathing

Member	Thickness (mm)	$R_{y}$	$R_{t}$
Stud	1.37	1.12	1.03
Track	1.37	1.01	0.96
Stud	1.73	1.04	1.01
Track	1.73	1.09	1.01
Stud	2.43	1.09	1.00
Track	2.43	1.00	0.95
Sheathing	0.76	1.45	1.31

# 3 CHAPTER 3 – INTERPRETATION OF TEST RESULTS AND PRESCRIPTIVE DESIGN

#### 3.1 INTRODUCTION

Throughout this chapter, data analysis will be performed to provide to structural engineers the design parameters required to design and build higher strength cold-formed steel sheathed shear walls for low and mid-rise buildings (up to 5 storeys) in high seismic regions. These design parameters will be provided for use in Canada, the US and Mexico. Due to the non-linear nature of the data recorded during previous phases of the testing program, the Equivalent Energy Elastic Plastic (EEEP) (*Park*, 1989 and Foliente, 1996) method was used for the analysis of the shear wall test data intended for use with the Canadian design provisions of AISI S400. The EEEP analysis approach, recommended by Branston et al. (2004), was the preferred method used to analyse the data obtained from previous research performed on wood sheathed shear walls at the Jamieson Structures Laboratory at McGill. The EEEP method was also used by El-Saloussy (2010), DaBreo (2012), Balh (2010) and Ong-Tone (2009) in order to develop the Canadian design shear resistance values for steel sheathed shear walls presently found in the AISI S400 (2015) and S240 (2015) design standards. Several design parameters were extracted from this analysis: yield resistance, in-plane displacement, ductility, stiffness and energy dissipation. In order to make the analysis process more efficient, a Matlab© algorithm was developed.

### 3.2 EEEP CONCEPT, CANADA

In order to simplify the non-linear results obtained during the testing of the monotonic and reversed-cyclic shear wall specimens the Equivalent Energy Elastic Plastic (EEEP) analysis method was used to determine shear wall design values for use in Canada. The core of this method is based on the assumption that the energy dissipated by the test specimen up to 80% of the post-peak load, which is considered to be the ultimate failure, can be modeled by a bilinear elastic-plastic curve having the same level energy dissipation. In addition, and as shown in Figure 3.1, the

integrated area (A1) under the observed response (or backbone curve) is equal to the area A2 under the bilinear elastic plastic curve.

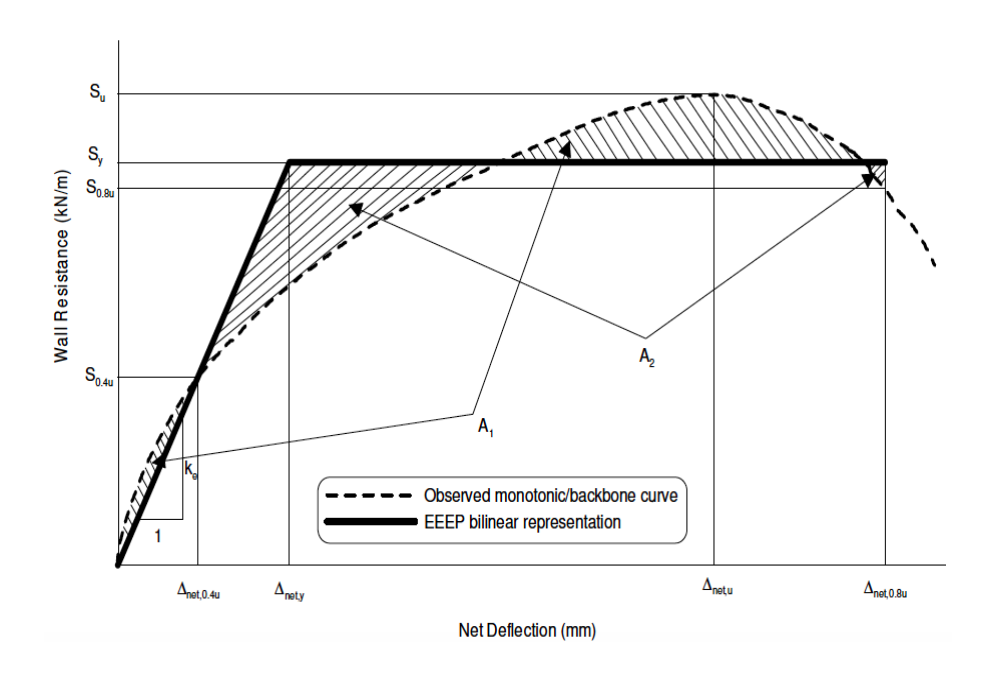


Figure 3.1 EEEP model (Branston, 2004)

Based on the data collected during the testing program, two different definitions of the ultimate displacement for use with the EEEP methodology were applied:

- i) In most cases the point of ultimate failure  $0.8S_u$  (80% post peak load) and its corresponding displacement  $\Delta_{net,0.8Su}$  were utilized.
- ii) In a limited number of cases for walls with a 4:1 aspect ratio the post peak resistance did not decrease to  $0.8S_u$  prior to reaching the limit of the actuator stroke. The ultimate displacement  $\Delta_{net,0.8Su}$  was hence defined as 100mm (4"), or the maximum lateral displacement if this point was not attained.

Three important parameters must be extracted from the data collected during the tests to develop the bilinear elastic-plastic EEEP curve: The wall's peak resistance ( $S_u$ ) in addition to the resistance corresponding to  $0.4S_u$  and  $0.8S_u$  (post peak), and their respective measured displacements,  $\Delta_{net,u}$ ,

 $\Delta_{net,0.4u}$  and  $\Delta_{net,0.8u}$ , obtained either from the monotonic curve, when analysing specimens subjected to the monotonic protocol, or from the backbone curve when performing the analysis for specimens tested under reversed-cyclic loading. Based on these parameters, and using Equations 3-1, 3-2, 3-3 and 3-4, the different parameters needed to model the bilinear elastic-plastic EEEP curve for every specimen, were obtained: the unit elastic stiffness,  $k_e$ , the yield wall resistance,  $S_y$ , its corresponding yield displacement,  $\Delta_{net,y}$ , and the ductility,  $\mu$ . The equations used to model the EEEP curves were derived based on equating the integrated areas  $A_1$  to  $A_2$  as shown in Figure 3.1.

$$k_e = \frac{0.4S_u}{\Delta_{\text{Net,0.4u}}} \tag{3-1}$$

$$S_y = \frac{-\Delta_{\text{Net,0.8u}} \pm \sqrt{\Delta_{\text{Net,0.8u}}^2 - \frac{2A}{k_e}}}{\frac{1}{k_e}}$$
(3-2)

$$\Delta_{\text{Net,y}} = \frac{s_y}{k_e} \tag{3-3}$$

$$\mu = \frac{\Delta_{\text{Net,0.8u}}}{\Delta_{\text{Net,v}}} \tag{3-4}$$

Where

 $S_y$ : Yield wall resistance (kN/m)

 $S_u$ : Ultimate wall resistance (kN/m)

A: Area under observed curve up to  $\Delta_{net,0.8u}$ 

 $K_e$ : Unit elastic stiffness ((kN/m)/mm))

 $\Delta_{net,0.8u}$ : Displacement at  $0.8S_u$  (post-peak)(mm)

 $\Delta_{net,y}$ : Yield displacement at  $S_y(mm)$ 

 $\mu$ : ductility of shear wall

#### 3.3 DESIGN PARAMETERS FOR CANADA, THE U.S.A AND MEXICO

Tables 3.1, 3.2 and 3.3 display a summary of the design parameters for the monotonic tests, as well as the positive and negative cycles of the reversed-cyclic tests, respectively. The analysis performed on the data obtained from the specimens subjected to reversed-cyclic loading is similar to that used for the monotonic tests, but requires some additional data handling. The curves modeling the force vs. Deformation performance of the walls subjected to cyclic loading are characterized by hysteretic loops. In order to be able to analyze these tests in a similar manner to the results obtained from the monotonic tests, it was necessary to model the backbone curve that envelops these hysteretic loops. The EEEP analysis (for Canada) was then performed separately and independently on the positive and negative regions of the backbone curves. Figures 3.2 and 3.3 display for illustrative purposes, the EEEP curves obtained from the analysis performed on the data collected during the monotonic and reversed-cyclic tests of the wall W7.

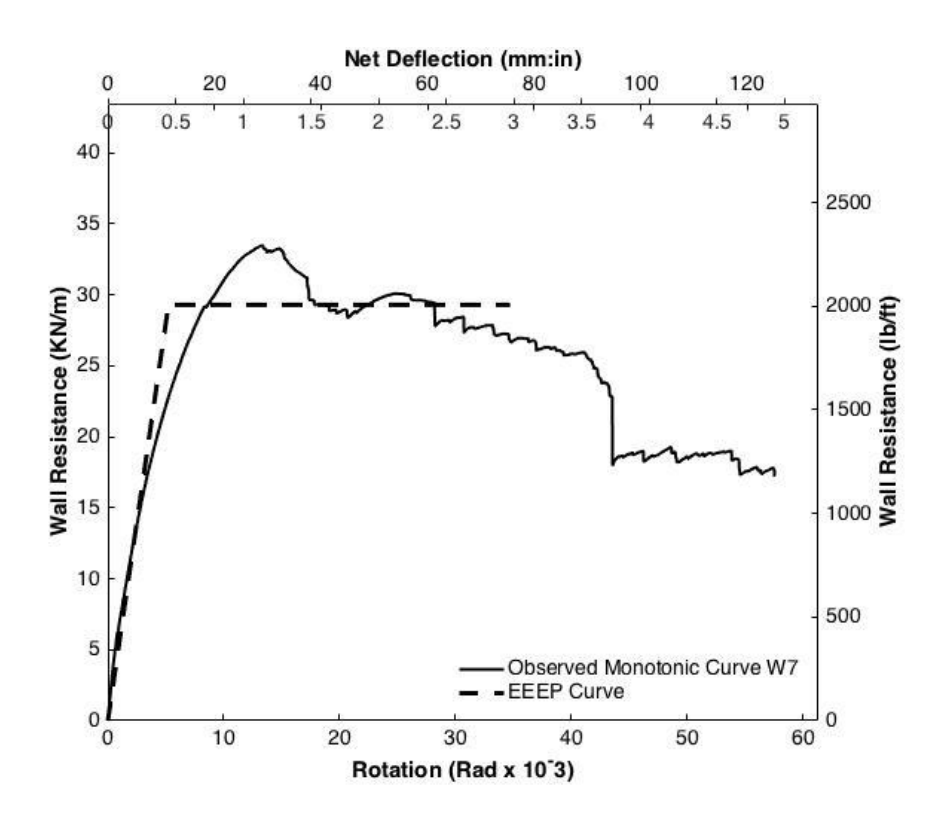


Figure 3.2 Resulting EEEP curve for the observed monotonic curve (test W7-M)

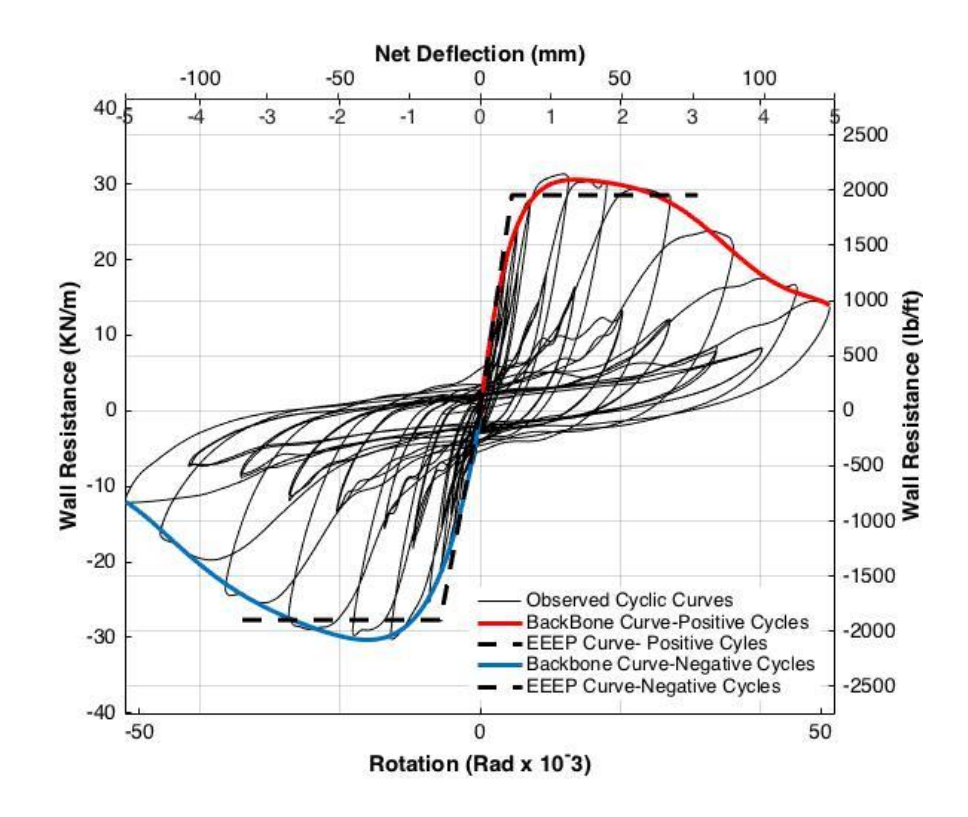


Figure 3.3 Resulting EEEP curves for the observed reversed-cyclic curve

For the United States of America and Mexico, the design parameters for the monotonic tests, as well as the positive and negative cycles of the reversed cyclic tests are listed in Tables 3.1, 3.2 and 3.3. The design values consist of the maximum wall resistance ( $S_u$ ), the displacement at  $S_u$  ( $\Delta_{net,u}$ ) and the rotation at  $S_u$  ( $\theta_{net,u}$ ). In order to automate the extraction of the relevant information from the test data, a Matlab algorithm was designed. Figures 3.4 and 3.5 illustrate these parameters extracted from the monotonic and reversed-cyclic tests conducted for specimen W7.

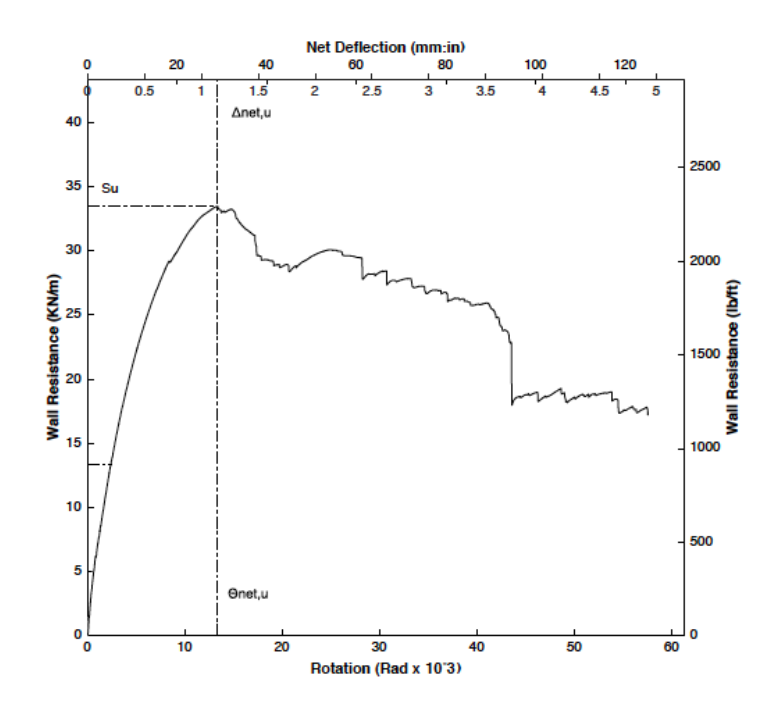


Figure 3.4 Design values for the USA and Mexico (W7-M)

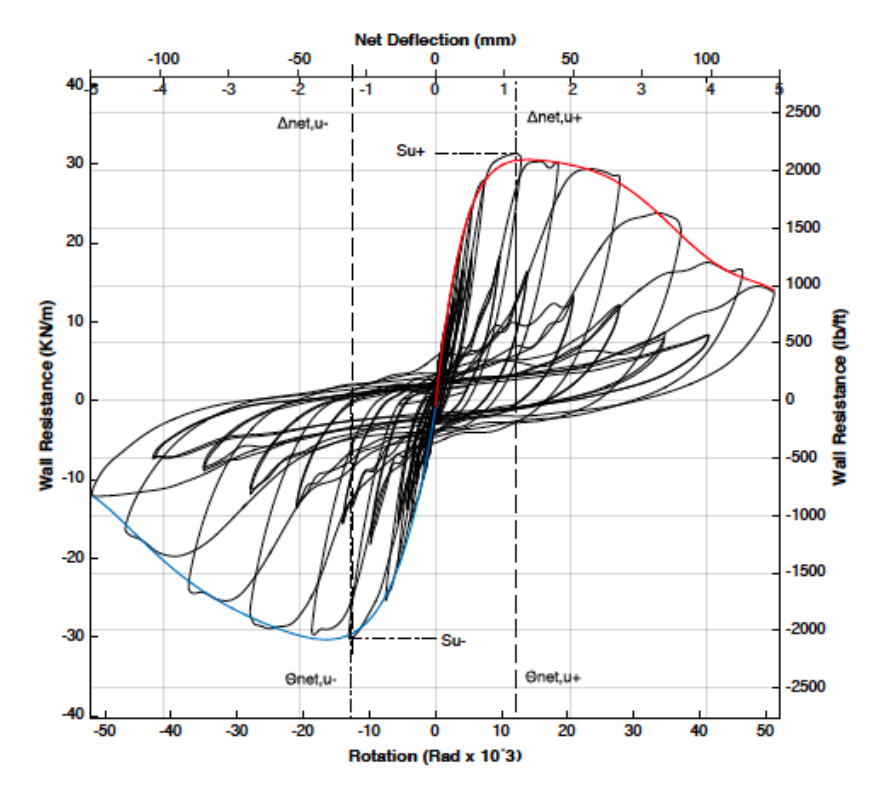


Figure 3.5 Design values for the USA and Mexico (W7-C)

Table 3.1 Design values for monotonic shear wall tests

Test Specimen	Yield Wall Resistance, S <sub>y</sub> (kN/m) <sup>1</sup>	Maximum Wall Resistance S <sub>u</sub> (kN/m) <sup>2</sup>	$\begin{array}{c} Displacement \\ at \ S_u \ \Delta_{net,u} \\ (mm) \end{array}$	$\begin{array}{c} Displacement \\ at \\ 0.4S_u, \Delta_{net,0.4u} \\ (mm) \end{array}$	$\begin{array}{c} Displacement \\ at \\ S_y, \Delta_{net,y} \\ (mm) \end{array}$	Unit Elastic Stiffness, k <sub>e</sub> (kN/m/mm)	$\begin{array}{c} Rotation \\ at \ S_u \\ \theta_{net,u} \\ (rad \\ \times 10^{-3}) \end{array}$	Rotation at $0.4S_u$ , $\theta_{net,0.4u}$ (rad)x10 <sup>-3</sup>	$\begin{array}{c} \text{Rotation} \\ \text{at } S_y, \\ \Theta_{\text{net},y} \\ \text{(rad)} \end{array}$	Ductility, μ
W1-M	32.59	34.88	52.76	11.42	26.67	1.22	21.64	4.68	10.94	3.14
W2-M	34.38	39.13	52.38	9.64	21.18	1.62	21.48	3.95	8.68	4.05
W3-M	32.02	35.32	101.87	16.70	37.86	0.85	41.78	6.85	15.53	2.64
W4-M	27.53	29.97	85.56	13.18	30.27	0.90	35.09	5.41	12.41	3.30
W5-M	22.46	25.41	58.14	9.71	21.44	1.05	23.84	3.98	8.79	3.87
W6-M	17.67	20.13	58.03	12.81	28.12	0.62	23.80	5.25	11.53	2.91
W7-M	29.29	33.46	28.8	5.20	11.37	2.58	11.81	2.13	4.66	6.64
W8-M	26.05	27.92	31.25	7.99	18.63	1.40	12.82	3.28	7.64	3.19
W9-M	23.46	25.55	40.19	5.35	12.29	1.91	16.48	2.19	5.04	5.45
W10-M	17.05	18.94	39.59	5.26	11.84	1.44	16.24	2.16	4.86	4.23
W11-M	29.60	32.87	36.31	4.79	10.78	2.75	14.89	1.96	4.42	8.05
W12-M	28.81	28.81	32.83	6.48	15.04	1.78	13.46	2.66	6.17	3.59
W13-M	22.25	24.68	24.20	3.97	8.95	2.49	9.92	1.63	3.67	4.73
W14-M	17.40	19.50	28.35	3.14	7.01	2.47	11.63	1.29	2.88	6.10

<sup>&</sup>lt;sup>1</sup>S<sub>y</sub> is the design value for Canada

 $<sup>^2</sup>S_u$  is the design value for the USA and Mexico

<sup>1</sup> kN/m=75.547 lb/ft, 1 mm= 0.0394 in

Table 3.2 Design values for reversed-cyclic shear wall tests: positive cycles

Test Specimen	Yield Wall Resistance, S <sub>y</sub> (kN/m) <sup>1</sup>	Maximum Wall Resistance Su' <sub>+</sub> (kN/m) <sup>2</sup>	Displacement at Su'+, \( \Delta net, u+(mm) \)	$\begin{array}{c} Displacement \\ at \\ 0.4S_u,  \Delta_{net,0.4u} \\ (mm) \end{array}$	$\begin{array}{c} Displacement \\ at \\ S_y, \Delta_{\text{net},y} \\ (mm) \end{array}$	Unit Elastic Stiffness, k <sub>e</sub> (kN/mm)	Rotation at $S_{u'+}$ , $\theta_{net,u+}$ (rad $x10^{-3}$ )	$\begin{array}{c} \text{Rotation} \\ \text{at} \\ 0.4S_u, \\ \theta_{\text{net},0.4u} \\ (\text{rad})x10^{-3} \end{array}$	$\begin{array}{c} \text{Rotation} \\ \text{at } S_y, \\ \Theta_{\text{net},y} \\ \text{(rad)} \end{array}$	Ductility, μ
W1-C	33.12	36.70	41.68	9.80	22.11	1.83	17.09	4.02	9.07	2.72
W2-C	35.62	40.35	48.29	7.90	17.44	2.49	19.80	3.24	7.15	3.70
W3-C	34.20	38.65	85.80	17.30	38.27	0.55	35.19	7.10	15.69	2.61
W4-C	27.04	29.00	70.79	14.00	32.64	0.51	29.03	5.74	13.39	3.06
W5-C	23.34	26.67	47.13	8.40	18.38	0.77	19.33	3.45	7.54	4.04
W6-C	17.88	19.98	67.27	7.30	16.34	0.67	27.59	2.99	6.70	4.95
W7-C	28.53	31.34	29.54	5.00	11.38	4.58	12.11	2.05	4.67	6.84
W8-C	26.63	29.22	31.92	4.70	10.71	4.55	13.09	1.93	4.39	5.44
W9-C	23.02	25.71	27.89	4.80	10.75	3.92	11.44	1.97	4.41	4.82
W10-C	18.42	20.47	29.05	4.00	9.00	3.74	11.91	1.64	3.69	5.41
W11-C	31.30	35.20	32.66	5.30	11.78	6.48	13.39	2.17	4.83	5.32
W12-C	27.96	30.22	31.90	4.30	9.95	6.85	13.08	1.76	4.08	4.83
W13-C	23.09	24.82	29.57	5.20	12.09	4.66	12.13	2.13	4.96	3.41
W14-C	17.65	19.19	24.64	3.80	8.74	4.93	10.10	1.56	3.58	4.41
C is the design	1 6 0		L		L	1		1	ı.	<u> </u>

<sup>&</sup>lt;sup>1</sup>S<sub>y</sub> is the design value for Canada

 $<sup>^2</sup>S_u$  is the design value for the USA and Mexico

<sup>1</sup> kN/m=75.547 lb/ft, 1 mm= 0.0394 in

Table 3.3 Design values for reversed-cyclic shear wall tests: negative cycles

Test Specimen	Yield Wall Resistance, S <sub>y</sub> (kN/m) <sup>1</sup>	Maximum Wall Resistance Su'-(kN/m) <sup>2</sup>	$\begin{array}{c} Displacement \\ at \ S_u'\text{-}, \\ \Delta_{net,u}\text{-}(mm) \end{array}$	$\begin{array}{c} Displacement \\ at \\ 0.4S_u,  \Delta_{\text{net},0.4u} \\ \text{(mm)} \end{array}$	$\begin{array}{c} Displacement \\ at \\ S_y, \Delta_{net,y} \\ (mm) \end{array}$	Unit Elastic Stiffness, k <sub>e</sub> (kN/mm)	Rotation at Su'-, $\Theta_{\text{net,u-}}$ (rad x10 <sup>-3</sup> )	Rotation at $0.4S_u$ , $\theta_{net,0.4u}$ (rad)x10-3	Rotation at $S_y$ , $\Theta_{net,y}$ (rad)	Ductility, μ
W1-C	31.11	35.22	44.16	9.60	21.20	1.79	18.11	3.94	8.69	3.16
W2-C	37.32	41.54	49.97	9.00	20.21	2.25	20.49	3.69	8.28	2.82
W3-C	32.12	36.02	79.80	15.50	34.55	0.57	32.73	6.36	14.17	2.90
W4-C	24.64	27.56	71.12	15.00	33.53	0.45	29.17	6.15	13.75	2.98
W5-C	23.85	26.39	69.21	10.30	23.28	0.62	28.38	4.22	9.55	4.35
W6-C	17.44	19.55	78.40	10.60	23.64	0.45	32.15	4.35	9.70	4.04
W7-C	27.70	30.24	31.42	6.20	14.19	3.57	12.89	2.54	5.82	6.04
W8-C	25.21	28.04	35.41	5.50	12.37	3.73	14.52	2.26	5.07	4.38
W9-C	21.68	24.29	27.97	5.80	12.94	3.06	11.47	2.38	5.31	3.40
W10-C	17.72	19.36	29.05	3.20	7.32	4.43	11.91	1.31	3.00	6.16
W11-C	29.31	32.14	36.77	4.20	9.57	7.46	15.08	1.72	3.93	6.87
W12-C	26.64	29.02	31.92	4.60	10.55	6.15	13.09	1.89	4.33	3.88
W13-C	21.23	23.75	25.14	4.90	10.95	4.73	10.31	2.01	4.49	3.45
W14-C	16.61	18.13	25.62	3.70	8.48	4.78	10.51	1.52	3.48	4.00
10	ha dacian valu	. C C 1.	<u> </u>				<u> </u>	<u> </u>		

<sup>&</sup>lt;sup>1</sup>S<sub>y</sub> is the design value for Canada

 $<sup>^2</sup>S_u$  is the design value for the USA and Mexico

<sup>1</sup> kN/m=75.547 lb/ft, 1 mm= 0.0394 in

#### 3.4 COMPARISON OF SHEAR WALL CONFIGURATIONS

The results summarized in Tables 2.3, 2.4, 2.5, 3.1, 3.2 and 3.3 were analysed in order to determine the impact of the various detailing factors on the performance of the steel sheathed cold-formed steel framed shear walls. Moreover, a benchmarking of the performance of the different configurations was performed with respect to the steel sheathed shear wall test results obtained by Ong-Tone (2009), Balh (2010), and DaBreo (2012).

The results obtained during the testing program are summarized in Tables 2.3, 2.4, 2.5, 3.1, 3.2 and 3.3 indicate that the performance of each configuration under Monotonic and Reversed-Cyclic loading is similar. The data collected during the reversed-cyclic loading indicate that the specimens performed better in the positive cycles in term of capacity, because the walls were first pulled in this direction, with the only exception of configuration W2 that was initially pushed in the negative direction. The damage that was caused to the structural components of the walls and the screw connections became severe when the specimens were pushed into the inelastic cycles in the positive direction; thus, the shear capacity of the walls decreased in subsequent cycles regardless of direction.

The plots of the wall resistance vs. In-plane lateral displacement of the monotonic and reversed-cyclic tests are characterized by the presence of sharp depressions/dips, which indicate the sudden loss of shear capacity. As illustrated in Figure 3.6, prior to reaching the ultimate wall resistance, smaller dips in the curve were observed, indicating the sudden shear buckling of the sheathing; whereas the larger depressions observed in the post ultimate peak domain indicate the failure of the sheathing connections coupled with the shear buckling of the sheathing. Figure 3.6 illustrates the loss of shear resistance observed during the testing of the specimen W8-M.

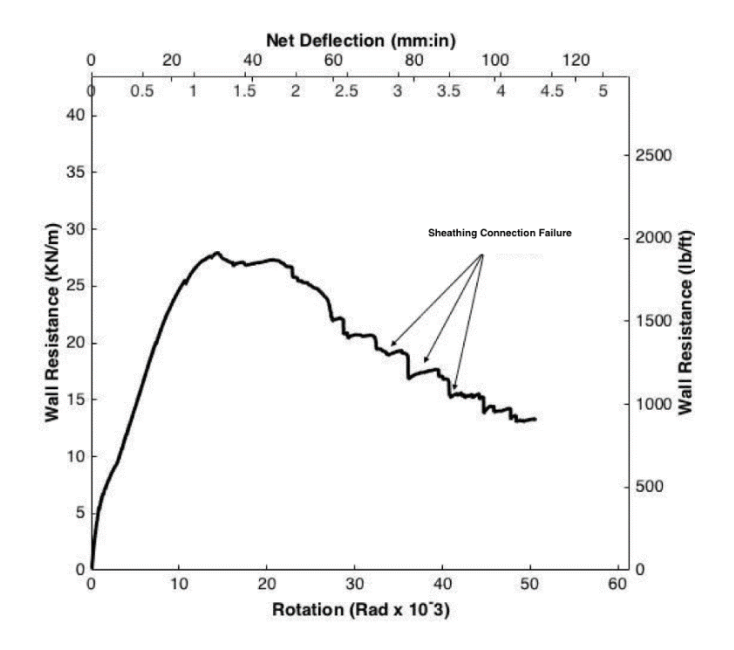


Figure 3.6 Loss of shear resistance due to sheathing shear buckling and sheathing connection failure (test W8-M)

## 3.4.1 EFFECT OF FASTENER SPACING

The comparison groups presented in Table 3.4 consist of walls having the same design parameters with the exception of the fastener spacing.

**Table 3.4 Comparison groups (Effect of sheathing fastener spacing)** 

Comparison Group	Monotonic Test Specimen	Reversed- Cyclic Test Specimen	Aspect Ratio	Fastener Spacing	Sheathing Thickness	Framing Thickness
	W3-M	W3-C		50mm (2")		
1	W4-M	W4-C	4:1	75mmm (3")		
1	W5-M	W5-C	4:1	100mm (4")		
	W6-M	W6-C		150mm (6")		
	W7-M	W7-C		50mm (2")		
2	W8-M	W8-C	4:3	75mmm (3")	0.76mm	1.37mm (0.054")
2	W9-M	W9-C	4.3	100mm (4")	(0.03")	1.5711111 (0.054 )
	W10-M	W10-C		150mm (6")		
	W11-M	W11-C		50mm (2")		
3	W12-M	W12-C	1:1	75mmm (3")		
3	W13-M	W13-C	1.1	100mm (4")		
	W14-M	W14-C		150mm (6")		

1 kN/m=75.547 lb/ft

Table 3.5 Comparison of normalized ultimate resistance for monotonic tests (Effect of sheathing fastener spacing)

Comparison Group	Monotonic Test Specimen	Ultimate Resistance, S <sub>u</sub> (kN/m)	Normalized Ultimate Resistance, Su (kN/m)
	W3-M (50 mm / 2")	35.32	1.75
1	W4-M (75 mm / 3")	29.97	1.49
1	W5-M (100 mm / 4")	25.41	1.26
	W6-M (150 mm / 6")	20.13	1.00
	W7-M (50 mm / 2")	33.47	1.77
2	W8-M (75 mm / 3")	27.92	1.47
2	W9-M (100 mm / 4")	25.55	1.35
	W10-M (150 mm / 6")	18.94	1.00
	W11-M (50 mm / 2")	32.87	1.48
3	W12-M (75 mm / 3")	28.81	1.29
3	W13-M (100 mm / 4")	24.68	1.11
	W14-M (150 mm / 6")	19.51	1.00

1 kN/m=75.547 lb/ft

Table 3.6 Comparison of normalized ultimate resistance for reversed-cyclic tests (Effect of sheathing fastener spacing)

Comparison Group	Reversed-Cyclic Test Specimen	Ultimate Resistance, S <sub>u</sub> (kN/m)	Normalized Ultimate Resistance, S <sub>u</sub> (kN/m)
	W3-C (50 mm / 2")	37.34	1.89
1	W4-C (75 mm / 3")	28.28	1.43
1	W5-C (100 mm / 4")	26.53	1.34
	W6-C (150 mm / 6")	19.77	1.00
	W7-C (50 mm / 2")	30.79	1.55
2	W8-C (75 mm / 3")	28.63	1.44
2	W9-C (100 mm / 4")	25.00	1.26
	W10-C (150 mm / 6")	19.92	1.00
	W11-C (50 mm / 2")	33.67	1.81
3	W12-C (75 mm / 3")	29.62	1.59
3	W13-C 100 mm / 4")	24.28	1.30
	W14-C (150 mm / 6")	18.66	1.00

Note: The values listed in Table 3.6 were computed using the average value of ultimate resistance collected from the positive and negative cycles of a reversed-cyclic test.

1 kN/m=75.547 lb/ft

As shown in Tables 3.5 and 3.6, the ultimate resistance  $S_u$  of each configuration in every comparison group is normalized with respect to the ultimate resistance of the specimen designed with a fastener spacing of 150mm (6"), since it developed the lowest ultimate resistance. The data collected from all the tests, presented in Tables 3.5 and 3.6 and illustrated in Figure 3.7 indicate that a wall's ultimate resistance is inversely proportional to the sheathing fastener spacing. This was expected, because sheathing fastener configurations with a smaller screw spacing behave as a group in resisting the shear forces applied to a wall. Each individual fastener in the configurations having a denser screw spacing has to resist forces of smaller magnitude compared to the connectors of the configurations designed with larger fastener spacing. Walls designed with larger sheathing connection spacing have a smaller number of screws available to resist the shear forces applied to the wall, which results in higher forces concentrated per connector, and thus leads to localised failures, which translates to lower shear capacity. These results are in line with the performance of the cold-formed steel shear walls tested as part of previous research programs conducted by DaBreo (2012), Balh (2010) and Ong-Tone (2009).

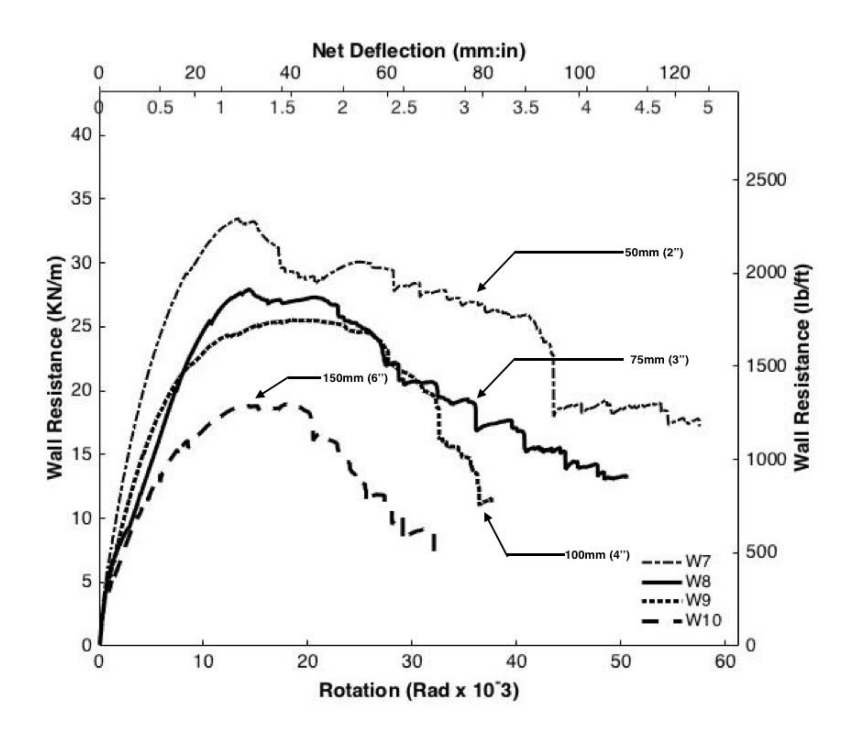


Figure 3.7 Comparison of fastener spacing: Wall resistance vs. Displacement for comparison group 2

### 3.4.2 EFFECT OF WALL LENGTH

Data from DaBreo (2012) was included in this comparison in order to analyze the effect of wall length. The comparison groups presented in Table 3.7 consist of walls having the same design parameters with the exception of the wall length. Figure 3.6 illustrates a comparison of the maximum wall resistance  $S_u$  (kN/m) measured during the testing program of the author of this thesis.

Table 3.7 Comparison groups (Effect of wall length)

Comparison Group	Monotonic Test Specimen	Reversed Cyclic Test Specimen	Aspect Ratio	Fastener Spacing	Sheathing Thickness	Framing Thickness
	W3-M	W3-C	4:1			
1	B1-M <sup>1</sup>	B1-C1	2:1	50mm (2")		
1	W7-M	W7-C	4:3			
	W11-M	W11-C	1:1			
	W4-M	W4-C	4:1	75mm (3") 0.76mm		
2	B7-M <sup>1</sup>	-	2:1		0.76mm (0.03") 1.37mm (0.054")	
	W8-M	W8-C	4:3			
	W12-M	W12-C	1:1			
3	W5-M	W5-C	4:1	100 mm (4")		
	W9-M	W9-C	4:3			
	W13-M	W13-C	1:1			
4	W6-M	W6-C	4:1			
	W10-M	W10-C	4:3	150 mm (6")		
	W14-M	W14-C	1:1			

<sup>&</sup>lt;sup>1</sup> DaBreo (2012)

Table 3.8 Comparison of normalized ultimate resistance for monotonic tests

Comparison Group	Monotonic Test Specimen	Ultimate Resistance, S <sub>u</sub> (kN/m)	Normalized Ultimate Resistance, S <sub>u</sub> (kN/m)
	W3-M (4:1)	35.32	1.07
1	B1-M <sup>1</sup> (2:1)	33.96	1.03
1	W7-M (4:3)	33.47	1.02
	W11-M (1:1)	32.87	1.00
	W4-M (4:1)	29.97	1.04
2	B7-M (2:1)	28.01	0.97
2	W8-M (4:3)	27.92	0.97
	W12-M (1:1)	28.81	1.00
3	W5-M (4:1)	25.41	1.03
	W9-M (4:3)	25.55	1.04
	W13-M (1:1)	24.68	1.00
4	W6-M (4:1)	20.13	1.06
	W10-M (4:3)	18.94	1.00
	W14-M (1:1)	19.51	1.03

<sup>&</sup>lt;sup>1</sup> DaBreo (2012)

<sup>1</sup> kN/m=75.547 lb/ft

Table 3.9 Comparison of normalized ultimate resistance for reversed-cyclic tests (Effect of wall length)

Comparison Group	Reversed Cyclic Test Specimen	Ultimate Resistance, S <sub>u</sub> (kN/m)	Normalized Ultimate Resistance, Su (kN/m)
	W3-C (4:1)	33.32	0.99
1	B1-C <sup>1</sup> (2:1)	31.52	0.94
1	W7-C (4:3)	30.79	0.91
	W11-C (1:1)	33.67	1.00
2	W4-C (4:1)	29.97	1.01
	W8-C (4:3)	28.63	0.97
	W12-C (1:1)	29.62	1.00
3	W5-C (4:1)	26.53	1.09
	W9-C (4:3)	25.00	1.03
	W13-C (1:1)	24.28	1.00
4	W6-C (4:1)	19.77	1.06
	W10-C (4:3)	19.92	1.07
	W14-C (1:1)	18.66	1.00

#### Note:

The ultimate resistance values listed in Table 3.9 were computed using the average value of ultimate resistance collected from the positive and negative cycles of a reversed-cyclic test.

The results summarized in Tables 3.8 and 3.9 confirmed the hypothesis that was set prior to the testing program, which stated that the shear resistance (normalized to length) would not be affected by the wall length for walls having an aspect ratio (h:w) less than (2:1). As shown in Figure 3.8, walls having an aspect ratio (h:w) of 4:1 reached equivalent levels of ultimate resistance but had to be pushed to large displacement in order to attain those load levels. A more detailed discussion on high aspect ratio walls is provided in Section 3.4.2.1 of this document.

<sup>&</sup>lt;sup>1</sup> DaBreo (2012)

<sup>1</sup> kN/m=75.547 lb/ft

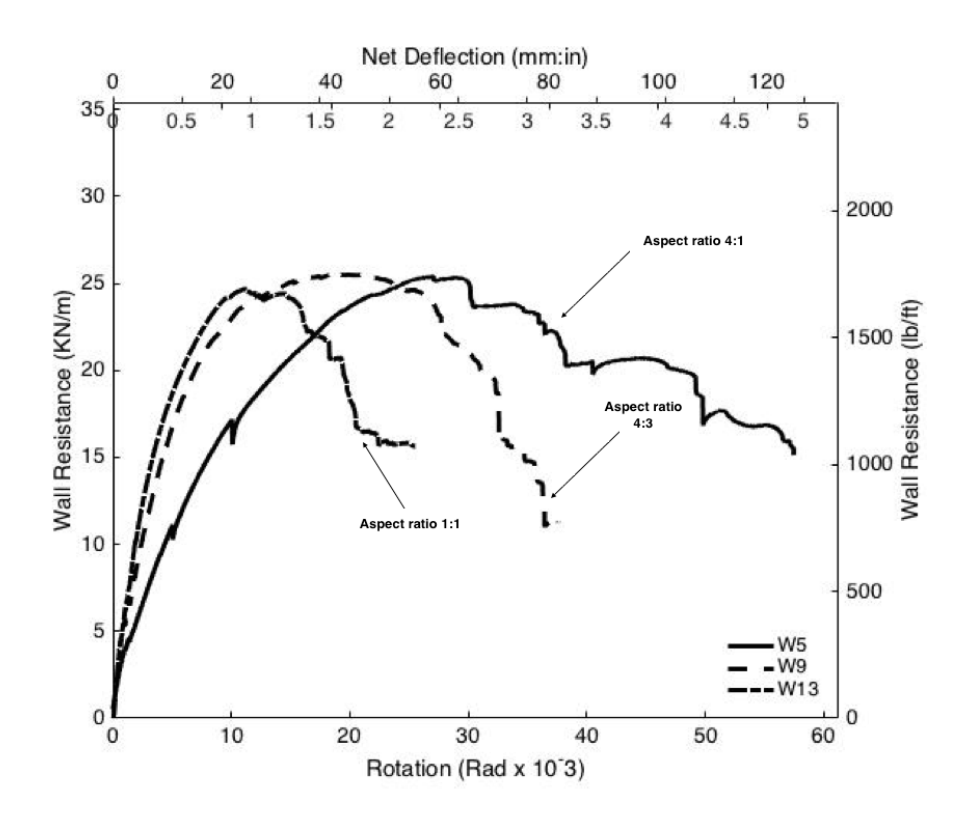


Figure 3.8 Comparison of wall length: Wall resistance vs. Displacement

## 3.4.3 EFFECT OF FRAMING THICKNESS

The comparison group presented in Table 3.10 consists of walls having the same design parameters, i.e. The fastener spacing 50 mm (2"), the aspect ratio 2:1 and the sheathing thickness 0.76mm (0.03"), with the exception of the framing thickness. The results presented in Tables 3.11 and 3.12 indicate the effect of framing thickness.

Table 3.10 Comparison groups (Effect of framing thickness)

Comparison Group	Monotonic Test Specimen	Reversed Cyclic Test Specimen	Aspect Ratio	Fastener Spacing	Sheathing Thickness	Framing Thickness
	B1-M	В1-С				1.37mm (0.054")
1	W1-M	W1-C	2:1	50mm (2")	0.76mm (0.03")	1.73mm (0.068")
	W2-M	W2-C				2.49 mm (0.097")

Table 3.11 Comparison of normalized ultimate resistance for monotonic tests (Effect of framing thickness)

Comparison Group	Monotonic Test Specimen	Ultimate Resistance, S <sub>u</sub> (kN/m)	Normalized Ultimate Resistance, S <sub>u</sub> (kN/m)
	B1-M (1.37mm / 0.054")	33.96	1.00
1	W1-M (1.73mm / 0.068")	34.88	1.03
	W2-M (2.49 mm / 0.097")	39.13	1.15

1 kN/m=75.547 lb/ft, 1 mm= 0.0394 in

Table 3.12 Comparison of normalized ultimate resistance for reversed-cyclic tests (Effect of framing thickness)

Comparison Group	Reversed Cyclic Test Specimen	Ultimate Resistance, S <sub>u</sub> (kN/m)	Normalized Ultimate Resistance, S <sub>u</sub> (kN/m)
	B1-C (1.37mm / 0.054")	31.52	1.00
1	W1-C (1.73mm / 0.068")	35.96	1.14
	W2-C (2.49 mm / 0.097")	40.95	1.30

Note:

The ultimate resistance values listed in Table 3.12 were computed using the average value of ultimate resistance collected from the positive and negative cycles of a reversed-cyclic test.

1 kN/m=75.547 lb/ft, 1 mm= 0.0394 in

As listed in Tables 3.11 and 3.12, and as shown in Figure 3.9, the specimens having a thicker framing developed a higher shear capacity. Configuration W2 developed an average shear capacity 13% higher than the capacity reached by specimen W1, and 23% higher than the shear resistance developed by specimen B1-M.

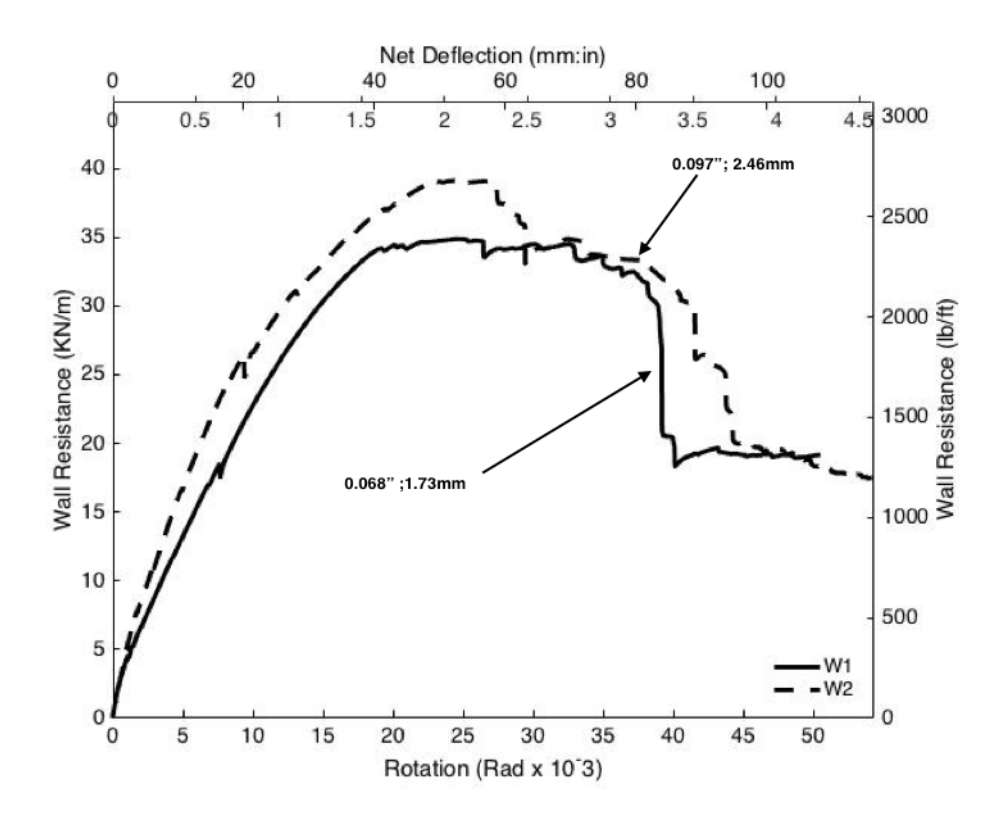


Figure 3.9 Comparison of framing thickness: Wall resistance vs. Displacement

### 3.4.4 EFFECT OF FRAME BLOCKING

In order to analyze the effect of frame blocking on the performance of the cold-formed steel shear walls, a benchmarking of relevant design values of the blocked shear walls collected during the testing programs was done with respect to the design parameters of conventional unblocked walls tested by Balh (2010) and Ong-Tone (2009). The comparison groups presented in Table 3.13 were created. These groups consist of walls having the same aspect ratio and the same configurations in terms of sheathing thickness and fastener spacing. The results of the comparison presented in Tables 3.14 and 3.15

indicate that the blocked walls developed higher ultimate shear resistances,  $S_u$ , and yield shear resistances,  $S_y$ , compared to their conventional (unblocked) counterparts. In addition, a decrease in the ductility and a significant increase in energy dissipation, E, of the blocked walls compared to their conventional (unblocked) counterparts was observed.

Table 3.13 Comparison groups and shear wall configurations

Comparison Group	Monotonic Test Specimen	Reversed Cyclic Test Specimen	Aspect Ratio	Fastener Spacing	Sheathing Thickness	Framing Thickness
	W3-M <sup>1</sup>	W3-C1		50mm		1.37mm (0.054")
1	9M-a <sup>3</sup> 9M-b <sup>3</sup>	9C-a <sup>3</sup> 9C-b <sup>3</sup>	4.1	(2")		1.09mm (0.043")
	W5-M <sup>1</sup>	W5-C1	4:1			1.37mm (0.054")
2	8M-a <sup>3</sup> 8M-b <sup>3</sup>	8C-a <sup>3</sup> 8C-b <sup>3</sup>		100mm (4")	1.09mm (0.043")	
	W1-M <sup>1</sup>	W1-C1		<i>5</i> 0	0.76mm	1.73mm (0.068")
3	$\frac{6M-a^2}{6M-b^2}$	6C-a <sup>2</sup> 6C-b <sup>2</sup>	2:1	50mm (2")	(0.03')	1.09mm (0.043")
4	W7-M <sup>1</sup>	W7-C1		50mm		1.37mm (0.054")
4	$13M-a^2$	1	4:3	(2")		1.09mm (0.043")
5	W8-M <sup>1</sup>	W8-C <sup>1</sup>	4.3	100mm		1.37mm (0.054")
3	$12M-a^2$	ı		(4")		1.09mm (0.043")
	W13-M <sup>1</sup>	W13-C1		100mm		1.37mm (0.054")
6	$\frac{11\text{M}-\text{a}^3}{11\text{M}-\text{b}^3}$	11C-a <sup>3</sup> 11C-b <sup>3</sup>	2:1	(4")		1.09mm (0.043")

<sup>&</sup>lt;sup>1</sup> Blocked walls Rizk (2017)

As listed in Tables 3.14 and 3.15, Balh (2010) and Ong-Tone (2009) tested two specimens for each configuration. In this case the normalization was done with respect to the average of the values obtained from each test. In addition, the ultimate resistance values, yield resistances, ductility and energy listed in Table 3.15 were computed using the average value of ultimate resistance collected from the positive and negative cycles of a reversed-cyclic test.

<sup>&</sup>lt;sup>2</sup> Ong-Tone (2009)

<sup>&</sup>lt;sup>3</sup>Balh (2010)

Table 3.14 Normalized parameters for comparison of blocked to conventional shear walls - Monotonic tests (Effect of frame blocking)

	Monotonic	Ultimate	Yield				Normalized	properties	
Comparison Group	Test Specimen	Resistance, S <sub>u</sub> (kN/m)	Resistance, S <sub>y</sub> (kN/m)	Ductility μ	Energy Joules	S <sub>u</sub> (kN/m)	S <sub>y</sub> (kN/m)	M	E (Joules)
	W3-M <sup>1</sup>	35.32	32.02	2.64	158	2.40	2.41	0.45	2.20
1	9M-a <sup>3</sup>	14.67	13.16	5.06	694	1.00	1.00	1.00	1.00
	9M-b <sup>3</sup>	14.78	13.40	6.67	742	1.00	1.00	1.00	1.00
	W5-M <sup>1</sup>	25.41	22.46	3.87	990	1.98	1.90	0.47	1.29
2	8M-a <sup>3</sup>	12.66	11.60	7.86	748	1.00	1.00	1.00	1.00
	8M-b <sup>3</sup>	13.02	12.01	8.73	792	1.00	1.00	1.00	1.00
	W1-M <sup>1</sup>	34.88	32.59	3.14	2794	2.08	2.14	0.36	1.95
3	6M-a <sup>2</sup>	16.93	15.47	9.75	1789	1.00	1.00	1.00	1.00
	6M-b <sup>2</sup>	16.56	15.05	7.63	1080	1.00	1.00	1.00	1.00
4	W7-M <sup>1</sup>	33.46	29.29	6.64	3739	1.81	1.73	0.95	2.22
4	13M-a <sup>2</sup>	18.53	16.89	7.02	1683	1.00	1.00	1.00	1.00
5	W8-M <sup>1</sup>	27.92	26.05	3.19	2385	1.95	1.98	0.23	1.47
3	12M-a <sup>2</sup>	14.35	13.16	13.78	1618	1.00	1.00	1.00	1.00
	W13-M <sup>1</sup>	24.68	22.25	4.73	2057	1.61	1.61	0.66	0.78
6	11M-a <sup>3</sup>	15.25	13.61	8.34	2547	1.00	1.00	1.00	1.00
	11M-b <sup>3</sup>	15.41	14.10	6.05	2708	1.00	1.00	1.00	1.00

<sup>&</sup>lt;sup>1</sup>Blocked walls Rizk (2017)

<sup>&</sup>lt;sup>2</sup> Ong-Tone (2009) <sup>3</sup>Balh (2010)

<sup>1</sup> kN/m=75.547 lb/ft

Table 3.15 Normalized parameters for comparison of blocked to conventional shear walls – Reversed-cyclic tests (Effect of frame blocking)

Comparison Group	Monotonic Test	Ultimate Resistance,	Yield Resistance,	Ductility	Energy Joules	Normalized properties				
Group	Specimen	S <sub>u</sub> (kN/m)	S <sub>y</sub> (kN/m)	μ	voules	S <sub>u</sub> (kN/m)	S <sub>y</sub> (kN/m)	M	E (Joules)	
	W3-M <sup>1</sup>	37.34	33.16	2.75	1653	2.360	2.308	0.467	2.122	
1	9M-a <sup>3</sup>	15.92	14.87	4.96	824	1.00	1.00	1.00	1.00	
	9M-b <sup>3</sup>	15.73	13.86	6.83	734	1.00	1.00	1.00	1.00	
	W5-M <sup>1</sup>	26.53	23.60	4.20	1115	1.951	1.913	0.588	1.732	
2	8M-a <sup>3</sup>	13.86	12.40	7.03	627	1.000	1.000	1.000	1.000	
	8M-b <sup>3</sup>	13.33	12.28	7.24	661	1.000	1.000	1.000	1.000	
	W1-M <sup>1</sup>	35.96	32.12	2.94	2060	2.079	2.043	0.456	1.725	
3	6M-a <sup>2</sup>	17.11	15.55	7.73	1399	1.000	1.000	1.000	1.000	
	6M-b <sup>2</sup>	17.49	15.90	5.16	989	1.000	1.000	1.000	1.000	
4	W7-M <sup>1</sup>	30.79	28.11	6.44	3872	-	-	-	-	
4	13M-a <sup>2</sup>	-	-	-	-	-	-	-	-	
5	W8-M <sup>1</sup>	28.63	25.92	4.91	2394	-	-	-	-	
3	12M-a <sup>2</sup>	-	-	-	-	-	-	-	-	
	W13-M <sup>1</sup>	24.28	22.16	3.43	1826	1.511	1.503	0.466	1.037	
6	11M-a <sup>3</sup>	16.15	14.77	7.09	1877	1.000	1.000	1.000	1.000	
	11M-b <sup>3</sup>	16.00	14.71	7.64	1646	1.000	1.000	1.000	1.000	

<sup>&</sup>lt;sup>1</sup>Blocked walls Rizk (2017)

<sup>2</sup> Ong-Tone (2009) didn't conduct reversed cyclic tests for configurations 12 and 13

<sup>3</sup>Balh (2010), ) didn't conduct reversed cyclic tests for configurations 12 and 13

<sup>1</sup> kN/m=75.547 lb/ft

The walls tested by Balh (2010) and Ong-Tone (2009) were designed and built using cold-formed steel framing having a thickness of 1.09 mm (0.043"). In contrast, the configurations tested as part of the Phase 1-blocked walls- of this research program were designed with a framing thickness of 1.37mm (0.054") for the walls having an aspect ratio (h:w) of 4:1, 4:3 and 1:1, and a framing thicknesses of 1.73mm (0.068") and 2.46mm (0.097") for the walls having an aspect ratio of 2:1-W1 and W2 respectively. This is important to mention because the comparisons listed below are not only based on the effect of the blockings, but also take into account the impact of the difference in the thickness of the frames.

## 3.4.4.1 COMPARISON OF ULTIMATE SHEAR RESISTANCE & YIELD SHEAR RESISTANCE

The data presented in Tables 3.14 and 3.15 indicate that the blocked walls developed higher ultimate shear resistances,  $S_u$ , and yield shear resistances,  $S_y$ , compared to their conventional (unblocked) counterparts. The quarter point blocking reinforcement reduced the distortion of the chord studs and allowed for higher in-plane lateral loads to be carried by the wall.

### 3.4.4.2 COMPARISON OF DUCTILITY

In addition to the length of the plastic region of the resulting bi-linear EEEP curve, where a longer plastic region indicates a higher ductility, the rate of strength degradation of the post peak monotonic curve and reversed-cyclic curve serves as a visual indicator of the shear wall's ductility. A slower rate of strength degradation is translated graphically by a slowly declining post peak curve, which indicates a more ductile behavior compared to specimens where a rapid decrease in strength was observed.

The data presented in Tables 3.14 and 3.15 indicate a general decrease in the ductility of the blocked walls compared to the conventional walls; consistent patterns for both monotonic and reserved-cyclic tests were observed. The ductility of the unblocked walls was achieved by a combination of plastic bearing deformations of sheathing at the sheathing screw connections and

plastic deformations of the chord studs as they twisted due to the eccentric loading placed on them. In the case of blocked walls, the quarter point blocking reinforcement reduced the twisting distortion of the chord stud. Hence, the ductility was largely provided by the plastic bearing deformations at the sheathing screw connections and some deformations of the elements in the studs; hence the reduction in the achieved ductility of these walls.

### 3.4.4.3 COMPARISON OF ENERGY DISSIPATION

The data presented in Tables 3.14 and 3.15 indicate a significant increase in energy dissipation, E, of the blocked walls compared to their conventional (unblocked) counterparts, with the exception of comparison group 6, where a decrease of energy dissipation was observed. Group 6 comprises walls having an aspect ratio of 1:1 ( $2440 \times 2440$ mm,  $8' \times 8'$ ). This trend was observed in both monotonic and reversed-cyclic tests. As explained in Section 2.5.5 of this thesis, the full blocking did not restrict effectively the overall out-of-plane deformation of these walls. This explains the decrease in energy dissipation. The total energy dissipation is equal to the product of the wall resistance by the wall displacement. The increase in energy dissipation is driven by the fact that blocked walls achieved higher shear resistance compared to their conventional (unblocked) counterparts.

### 3.5 LIMIT STATES DESIGN PROCEDURE (CANADA)

Balh (2010) and Ong-Tone (2009) recommended a limit states design procedure for cold-formed steel-sheathed shear walls for use with the NBCC (NRCC, 2015). A detailed explanation of the method is provided in the paper by Balh *et al.* (2013). The design procedure has been adopted by the author of this thesis and includes the resulting resistance factor, factor of safety, over-strength for capacity-based design and test-based seismic force modification factors for the blocked shear walls. Based on nominal values of wall length, framing thickness (studs, tracks, & blockings), sheathing thickness and fastener spacing, the test specimens were separated into 14 groups (Table 3.16).

Table 3.16 Description of test specimen group configurations for limit states design procedure (Canada)

Configuration		athing ckness		tud kness		astener pacing	Protocol	Test Name
_	(in.)	(mm)	(in.)	(mm)	(in.)	(mm)		
1			0.068	1.73	2	50	Monotonic	W1-M
1			0.008	1.75	2	30	Cyclic	W1-C
2			0.097	2.47	2	50	Monotonic	W2-M
2			0.097	2.47	2	50	Cyclic	W2-C
3					2	50	Monotonic	W3-M
3					2	30	Cyclic	W3-C
4					3	75	Monotonic	W4-M
7	0.03	0.76			3	73	Cyclic	W4-C
5	0.03	0.70			4	100	Monotonic	W5-M
<i>J</i>			0.054	1.37	4	100	Cyclic	W5-C
6			0.05	1.07	6	150	Monotonic	W6-M
					- U	150	Cyclic	W6-C
7					2	50	Monotonic	W7-M
·							Cyclic	W7-C
8					3	75	Monotonic	W8-M
			1				Cyclic	W8-C
9					4	100	Monotonic	W9-M
							Cyclic Monotonic	W9-C
10					6	100	Cyclic	W10-M W10-C
							Monotonic	W10-C W11-M
11					2	50	Cyclic	W11-W
	0.03	0.76	0.054	1.37			Monotonic	W12-M
12					3	75	Cyclic	W12-C
10						100	Monotonic	W13-M
13					4	100	Cyclic	W13-C
1.4						150	Monotonic	W14-M
14					6	150	Cyclic	W14-C

### 3.5.1 CALIBRATION OF RESISTANCE FACTOR FOR CANADA

In limit states design, the factored resistance of any structural member must be greater than the combined effects of the factored loads applied to it. As prescribed in Clause 4.1.3.2 of the 2015 National Building Code of Canada (NRCC, 2015), the combined effects of loads are based on the most critical load combination.

$$\phi R \ge \sum \alpha S$$
 (3-5)

Where,

φ: Resistance factor of structural element

R: Nominal resistance of structural member

α: Load factor

S: Effect of particular specified load combinations

The North American specification for the design of cold-formed steel structural members (CSA S136) (2016) and (AISI S100) (2016) specify a method for determining the resistance factor for ultimate limit states design (Equation (3-6))

$$\phi = C_{\phi}(M_m F_m P_m) e^{-\beta_o \sqrt{V_M^2 + V_F^2 + C_P V_P^2 + V_Q^2}}$$
(3-6)

Where,

 $C_{\phi}$ : Calibration coefficient

 $M_m$ : Mean value of material factor

 $F_m$ : Mean value of fabrication factor

 $P_m$ : Mean value of professional factor

*E* : *Natural logarithmic base* 

 $\beta_0$ : Target reliability index

 $V_{M:}$  Coefficient of variation of material factor

 $V_{F:}$  Coefficient of variation of fabrication factor

*V<sub>P</sub>*: Coefficient of variation of professional factor

V<sub>Q</sub>: Coefficient of variation of load effect

 $C_P$ : Correction factor for sample size

$$C_P = \frac{(1+1/n)m}{(m-2)}, \text{ for } n \ge 4$$
 (3-7)

$$C_P = 5.7, for n=3$$
 (3-8)

Where,

N: Number of tests (sample size)

M: Degrees of freedom = n-1

Mean values and their corresponding coefficients of variation of the material factor,  $M_m$  and  $V_M$ , respectively and the fabrication factor,  $F_m$  and  $V_F$  respectively are listed in the North American specification for the design of cold-formed steel structural members (CSA-S136) (2016) and (AISI S100) (2016).

These variables are based on statistical analysis of the failure modes of the components used in the design and construction of the cold-formed shear wall specimens. For the purposes of this analysis, two failure modes were considered

- 1) Under Combined Forces
- 2) Screw Connections

Table 3.17 Statistical data for the determination of resistance factor (AISI S100, 2016)

Type of Component and Failure Mode	$M_{\rm m}$	$V_{\mathrm{M}}$	F <sub>m</sub>	$V_{F}$
Type 1: Under Combined Forces	1.05	0.10	1.00	0.05
Type 2: Screw Connections	1.10	0.10	1.00	0.10

AISI S100 (2016) lists the value  $\beta_0$ , the target reliability index for structural member, which is a factor describing the probability of failure, equal to 3.0 for LSD. AISI S100 (2016) lists the value  $C_{\phi}$  equal to 1.42 for LSD. AISI S100 (2016) lists the value of  $V_Q$  equal to 0.21 for LSD.

Equation (3-9) was used to calculate the mean value of the professional factor  $P_m$ , based on the yield shear resistance,  $S_y$ , the average yield shear resistance  $S_{y,avg}$  of both monotonic and reversed cyclic tests and the sample size of each configuration, n.

$$P_m = \frac{\sum_{i=1}^n \binom{S_y}{S_{y,avg}}_i}{n} \tag{3-9}$$

$$S_{y,avg} = \frac{S_{y,mono,avg} + \frac{S_{y+,avg} + S_{y-,avg}}{2}}{2}$$
 (3-10)

Where,

 $S_{y,mono,avg}$ : Average yield wall resistance of the monotonic tests of a specific configuration

 $S_{y+,avg}$ : Average positive yield wall resistance of the reversed cyclic test of a specific Configuration

 $S_{y-,avg}$ : Average negative yield wall resistance of the reversed cyclic test of a specific configuration

$$V_p = \sigma/P_m \tag{3-11}$$

Where,

$$\sigma^{2} = \frac{1}{n-1} \sum_{i=1}^{n} \left[ \binom{S_{y}}{S_{y,avg}}_{i} - P_{m} \right]^{2}$$
 (3-12)

AISI S100 (2016) indicates that the coefficient of variation of test results must be equal or greater than 0.065.

The resistance factors  $\phi$ , determined for each failure mode are summarized in Table 3.18. The recommended Canadian limits states design resistance factor  $\phi$  for shear walls with blocking reinforcement designed to carry lateral wind loads is 0.7. As shown in Table 3.18, this value is very close to the value computed following the recommendation of the AISI S100 (2016). In addition, the recommendation of a resistance factor  $\phi$  of 0.7 in seismic design of steel sheathed CFS framed shear walls is warranted because it is used in the calculation of the equivalent static earthquake base shear where  $R_0$ , the overstrength related force modification factor is a function of  $\phi$  as shown in Equation 3-21, and in the calculation of the factored resistance of the shear walls. This value obtained is in-line with the recommendations of DaBreo (2012), Balh (2010), El- Saloussy (2010), and Ong-Tone (2009) and with the recommended value applicable to design in Canada listed in AISI S400 (2015).

Table 3.18 Summary of resistance factor calibration for different types of components and failure modes (Canada)

Type of Component and Failure Mode	$C_{\phi}$	$M_{ m m}$	F <sub>m</sub>	P <sub>m</sub>	βο	$V_{\rm m}$	$V_{\mathrm{f}}$	$V_{Q}$	N	$C_P$	$V_p$	ф
Type 1: Under Combined Forces	1.42	1.05	1.0	1.0	3.0	0.1	0.05	0.21	28	1.119	0.065	0.71
Type 2: Screw Connection	1.42	1.1	1.0	1.0	3.0	0.1	0.1	0.21	28	1.119	0.065	0.71

Table 3.19 list the summary of the average values of the resistance factors obtained from various testing programs conducted in North America for each type of component failure.

Table 3.19 Summary of Resistance Factors,  $\phi$ , calibration results for different types of component failure modes (Canada)

Type of component failure	Ong-Tone (2009)	Balh (2010)	El-Salousy (2010)	DaBreo (2012)	Rizk (2017)
Type 1	0.75	0.75	0.74	0.75	0.71
Type 2	0.78	0.77	0.77	0.78	0.71
Type 3	0.77	0.76	0.76	-	-
Type 4	0.70	0.69	0.69	-	-
Average	0.75	0.74	0.74	0.77	0.71

Type 1: connection – shear strength of screw

Type 2: connection -bearing and tilting strength of screw

Type 3: wall studs – chord stud in compression

Type 4: structural members not listed – uplift of track

#### 3.5.2 CALIBRATION OF RESISTANCE FACTOR FOR THE USA & MEXICO

For the United States of American and Mexico, the same approach followed for Canada is used in the calculation of a resistance factor. The AISI S100 Standards (2016) provides a value of  $C_{\phi}$  equal to 1.52 for LRFD. The various coefficient ( $M_m$ ,  $V_m$ ,  $F_m$  and  $V_f$ ) used for the determination of the resistance factor are the same as those used for Canada. The correction factor  $C_P$  is the same as the correction factor used for Canada. The target reliability index provided by the AISI S100 (2016) is equal to 2.5 for structural members for LRFD. The coefficient of variation of load effect is equal to 0.21 for LRFD.

The difference between Canada and the United States of America and Mexico is in the approach used to compute  $P_m$ , the mean value of the professional factor for the tested components (Equation 3.13).

$$P_{m} = \frac{\sum_{i=1}^{n} \binom{S_{u}}{S_{u,avg}}_{i}}{n}$$
 (3-13)

Where,

$$S_{u,avg} = \frac{S_{u,mono,avg} + \frac{S_{u+,avg} + S_{u-,avg}}{2}}{2}$$
(3-14)

Where,

 $S_{u,mono,avg}$ : Average maximum wall resistance of the monotonic tests of a specific configuration

 $S_{u+,avg}$ : Average positive maximum wall resistance of the reversed cyclic test of a specific configuration

 $S_{u-,avg}$ : Average negative positive maximum wall resistance of the reversed cyclic test of a specific configuration

The coefficient of variation of the test results  $V_P$  for the USA and Mexico is computed using Equations 3.15 and 3.16.

$$V_p = {}^{\sigma}\!/P_m \tag{3-15}$$

Where,

$$\sigma^{2} = \frac{1}{n-1} \sum_{i=1}^{n} \left[ \left( \frac{S_{u}}{S_{u,avg}} \right)_{i} - P_{m} \right]^{2}$$
 (3-16)

AISI S100 (2016) indicates that the coefficient of variation of the test results  $V_P$  must not be less than 0.065. Table 3.20 lists the different values of the various parameters used to calibrate the resistance factor.

Table 3.20 Summary of resistance factor calibration for different types of components and failure modes (USA and Mexico)

Type of Component and Failure Mode	$C_{\phi}$	$M_{ m m}$	F <sub>m</sub>	P <sub>m</sub>	βο	$V_{\rm m}$	$V_{\mathrm{f}}$	$V_{Q}$	N	$C_P$	$V_P$	ф
Type 1: Under Combined Forces	1.52	1.05	1.0	1.0	2.5	0.1	0.05	0.21	28	1.119	0.065	0.86
Type 2: Screw Connection	1.52	1.1	1.0	1.0	2.5	0.1	0.1	0.21	28	1.119	0.065	0.87

The resistance factor computed is higher than the recommended value listed in the AISI S400 (2015). AISI S400 (2015) recommends a resistance factor  $\phi_v$ =0.6 (LRFD). It is then recommended to use  $\phi_v$ =0.6.

### 3.5.3 NOMINAL SHEAR WALL RESISTANCE FOR CANADA

The calculated values of the yield wall resistance  $S_y$  using the EEEP analysis are dependent on the sheathing fastener connection resistances, which in turn are dependent on the material thickness and tensile stress. The ancillary tests of the steel sheathing indicated that the measured material properties of the test components were higher than the minimum specified values given by ASTM A653 (2015). The ASTM A653 Specification states that a material with a yield stress of 230 MPa (33ksi) should have a corresponding tensile stress of 310 MPa (45ksi). The measured material properties are listed in Table 3.21.

To address the higher than nominal material properties measured for the sheathing, the calculated EEEP  $S_y$  values must be reduced to provide values corresponding to the minimum specified properties. Table 3.21 lists the values of the calculated modification

factors for sheathing thickness and tensile stress that were applied to the EEEP  $S_y$  values to obtain nominal shear resistance values of the cold-formed steel frame/steel sheathed blocked shear walls. The proposed nominal shear resistances  $S_y$  are listed in Table 3.24. The same methodology was used for the development of the design values of all other steel sheathed CFS shear walls in previous research programs conducted by DaBreo (2012) Balh (2010), El-Saloussy (2010), and Ong-Tone (2009). Table 3.22 lists the different modification factors used by the author and those obtained from previous research programs on steel sheathed shear walls. Table 3.23 lists the nominal shear resistances for every configuration tested as part of this research program.

Table 3.21 Sheathing thickness and tensile stress modification factors

Member	Nominal Thickness (mm)	Measured Thickness (mm)	Thickness Modification Factor	Minimum Specified Tensile Stress, F <sub>u</sub> (MPa)	Measured Tensile Stress, F <sub>u</sub> (MPa)	Tensile Stress Modification Factor
Sheathing	0.76	0.76	1.00	310	406	0.764

Table 3.22 Modification factors of past research on steel sheathed shear walls

Research by:	Nominal Sheathing Thickness	Thickness Modification Factor	Tensile Stress Modification Factor	Overall Modification Factor
Rizk (2017)		1.000	0.764	0.764
DaBreo (2012)		0.960	0.823	0.790
Balh (2010)	0.76 (0.030")	1.000	0.831	0.831
Ong-Tone (2009)		1.000	0.831	0.831
El-Saloussy (2010) <sup>1</sup>		1.000	0.810	0.810
El-Saloussy (2010) <sup>2</sup>		1.000	0.920	0.920

<sup>1</sup> obtained from Phase 1, Yu et al (2007)

<sup>2</sup> obtained from Phase 2, Yu et al (2009)

Table 3.23 Nominal shear resistance, Sy, for CFS framed/steel sheathed blocked shear walls<sup>1,2,3</sup> (kN/m) (Canada)

Assembly	Max Aspect	Faster	•	g at Panel I	Designation Thickness, of Stud,	Required Sheathing	
Description	Ratio (h/w)	50 (2)	75 (3)	100 (4)	150 (6)	Track, and Blocking ((mm) (mils))	Screw Size
	2:1	24.66	-	-	-	1.72 (68)	8
	2:1	27.33	-	-	-	2.46 (97)	8
0.76 mm	4:1	25.04	20.17	17.74	13.49	1.37 (54)	8
(0.030")	2:18	23.31	19.88	-	-	1.37 (54)	8
	4:3	21.78	19.84	17.36	13.55	1.37 (54)	8
	1:1	22.97	20.72	16.95	13.15	1.37 (54)	8
	2:18	-	-	14.33	11.69	1.09 (43)	8
0.46 mm (0.018")	2:18	13.5	11.6	9.7	7.4	1.09 (43)	8

<sup>1)</sup> Nominal resistance,  $S_v$ , to be multiplied by the resistance factor,  $\mu = 0.7$ , to obtain factored resistance

Table 3.24 provides a summary of the proposed nominal shear resistances for CFS framed/steel sheathed blocked shear walls. The nominal shear resistances provided consist of the average of the nominal shear resistances of the specimens having the same fastener spacing, framing and sheathing thickness, sheathing screw size and having a specific maximum aspect ratio limit.

<sup>2)</sup> Sheathing must be connected vertically to steel frame

<sup>3)</sup> Nominal shear resistance values are applicable for lateral loading

<sup>4)</sup> Edge fasteners are to be placed at least 9.5mm (3/8") from the sheathing edge and field screws to be spaced 305mm (12") o/c

<sup>5)</sup> Wall stud and tracks shall be ASTM A653 grade 340 MPa(50ksi) for 1.37mm (0.054") minimum uncoated base metal thickness

<sup>6)</sup> Stud dimension: 92.1 mm (3-5/8") web, 41.3 mm (1-5/8") flange, 12.7 mm (1/2") lip, Track dimension:

<sup>92.1</sup> mm (3-5/8") web, 31.8 mm (1-1/4") flange Blockings are to be made from tracks of same designation thickness

<sup>7)</sup> Minimum No.8 x 12.7 (1/2") sheathing screws shall be used

<sup>8)</sup> Proposed nominal shear resistance based on DaBreo (2012)

Table 3.24 Summary of proposed nominal shear resistance, Sy, for CFS framed/steel sheathed blocked shear walls (kN/m)

Assembly Description	Max Aspect Ratio (h/w)	Fastei	ner Spacing (mm(	Designation Thickness, of Stud, Track, and Blocking ((mm)	Required Sheathing Screw Size		
		50 (2)	75 (3)	100 (4)	150 (6)	(mils))	
	2:1	24.7	-	-	-	1.72 (68)	8
0.76 mm	2:1	27.3	-	-	-	2.46 (97)	8
(0.030")	2:1	23.3	19.9	17.2	13.3	1.37 (54)	8
(0.030 )	2:1	-	-	14.3	11.7	1.09 (43)	8
	4:1	25	20.2	17.7	13.5	1.37 (54)	8
0.46 mm (0.018")	2:1	13.5	11.6	9.7	7.4	1.09 (43)	8

### 3.5.4 NOMINAL SHEAR WALL RESISTANCE FOR THE USA & MEXICO

The collected values of the maximum wall resistance S<sub>u</sub> are dependent on the sheathing fastener connection resistances, which in turn are dependent on the material thickness and tensile stress. The ancillary tests of the steel sheathing indicated that the measured material properties of the test components were higher than the minimum specified values given by ASTM A653 (2015). The ASTM A653 Specification states that a material with a yield stress of 230 MPa (33ksi) should have a corresponding tensile stress of 310 MPa (45ksi). The measured material properties are listed in Table 3.21.

To address the higher than nominal material properties measured for the sheathing, the monitored  $S_u$  values must be reduced to provide values corresponding to the minimum specified properties. Table 3.22 lists the values of the calculated modification factors for sheathing thickness and tensile stress that were applied to the  $S_u$  values to obtain nominal shear resistance values of the cold-formed steel frame/steel sheathed blocked shear walls. The proposed nominal shear resistances  $S_u$  are listed in Table 3.25.

Table 3.25 Summary of proposed nominal shear resistance, Su, for CFS framed/steel sheathed blocked shear walls (lb/ft)

	Max	Faste	ener Spacing (mm(		Designation Thickness, of	Dogwired	
Description Ra	Aspect Ratio (h/w)	50 (2)	75 (3)	100 (4)	150 (6)	Stud, Track, and Blocking ((mm) (mils)	Required Sheathing Screw Size
	2:1	1866	-	-	-	1.72 (68)	8
0.76 mm	2:1	2114	-	-	-	2.46 (97)	8
(0.030")	2:1			1300	1010	1.37 (54)	8
(0.000)	2:1		-	1099	900	1.09 (43)	8
	4:1	1921	1512	1371	1042	1.37 (54)	8

# 3.5.5 VERIFICATION OF SHEAR RESISTANCE REDUCTION FOR HIGH ASPECT RATIO WALLS (CANADA)

As part of the research program, four different configurations of short walls measuring 610  $\times$  2440 mm (2'  $\times$  8') were tested at McGill University in order to verify if walls having an aspect ratio of (4:1) can be utilized in design. Referring to the AISI S400 (2015) Section E.2.3.1.1, the nominal strength [resistance] for shear,  $V_n$  of Type 1 shear walls with steel sheathing having an aspect ratio (h:w) greater than 2:1, but not exceeding 4:1, shall be determined in accordance with the following:

For 
$$2 < h/w \le 4$$

$$V_n = v_n w(2w/h) \tag{3-17}$$

AISI S400 specifies that in no case shall the height-to-length aspect ratio (h:w) exceed 4:1, and the length of the shear wall shall not be less than 610mm (2').

In order to verify the applicability of this allowance, the proposed nominal shear resistances of high aspect ratio walls listed in Table 3.24 were multiplied by 2w/h as required by the AISI S400 (2015) and compared with the results obtained from the testing program of the

high aspect ratio walls (W3, W4, W5 and W6). The shear resistances listed in Table 3.24 were taken from Tables 3.1, 3.2 and 3.3 and were reduced based on thickness and tensile stress as listed in Table 3.21 As shown in Table 3.26, the test-based-resistances of the high aspect ratio walls calibrated for thickness and tensile stress resulted in higher shear strength values than the nominal resistance value modified according to the recommendation of the AISI S400. As listed in Tables 2.3, 2.4 and 2.5, the high aspect ratio walls had to be pushed to large displacement in order to reach those load levels.

Figures 3.10 and 3.11 illustrate a comparison of the drifts  $\Delta_d$  between the 610mm (2') long wall (W5-M) and the 1830mm (6') long walls (W9-M). The drift  $\Delta_d$  is determined as the displacement reached at the equivalent resistance level for the 610mm (2') and 1830mm (6') long walls. As shown in Table 3.27, the drifts  $\Delta_d$  for the high aspect ratio walls are less or equivalent to the drifts for the 1830mm (6') walls. Based on these results, it is adequate to judge that the reduction factor of 2w/h listed in the AISI S400 is applicable, because if the high aspect ratio walls reach the modified resistance level, they would reach similar drifts as the longer walls and thus perform adequately.

Table 3.26 Verification of Shear Resistance Reduction for High Aspect Ratio Walls (CANADA)

Group	Framing mm:mils	Sheathing mm:mils	Fastener Spacing mm:in	Test	S <sub>y</sub> (kN/m)	S <sub>y,red</sub> (kN/m)	$S_{y,red,avg} \atop (kN/m)$	S <sub>y</sub> nominal (kN/m)	S <sub>y</sub> ×2w/h (kN/m)
3			50:2	W3-M	32.020	24.463	24.897	25.040	12.520
			50.2	W3-C	33.157	25.332	2	25.0.0	12.020
4			75:3	W4-M	27.520	21.025	20.385	20.170	10.085
	1.37:54	0.76:30	75.5	W4-C	25.844	19.745		20.170	10.005
5	1.37.31	0.70.50	100:4	W5-M	22.460	17.159	17.597	17.740	8.870
3			100.4	W5-C	23.605	18.034	17.377	17.740	0.070
6			150:6	W6-M	17.670	13.500	13.496	13.490	6.745
			150.0	W6-C	17.660	13.492	13.470	13.470	0.743

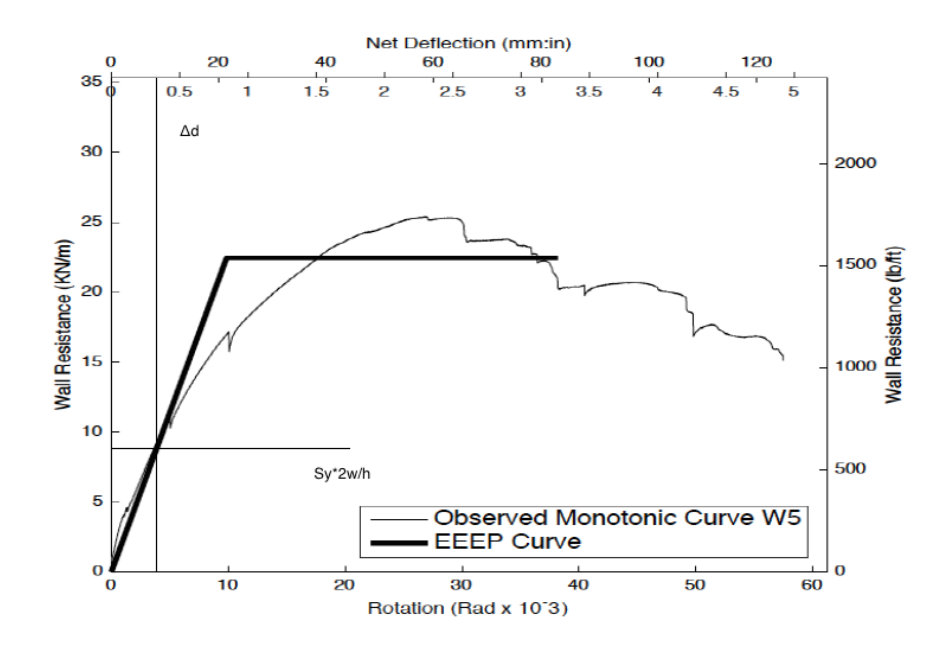


Figure 3.10 Drift,  $\Delta_d$  , for Short Wall at Reduced Resistance

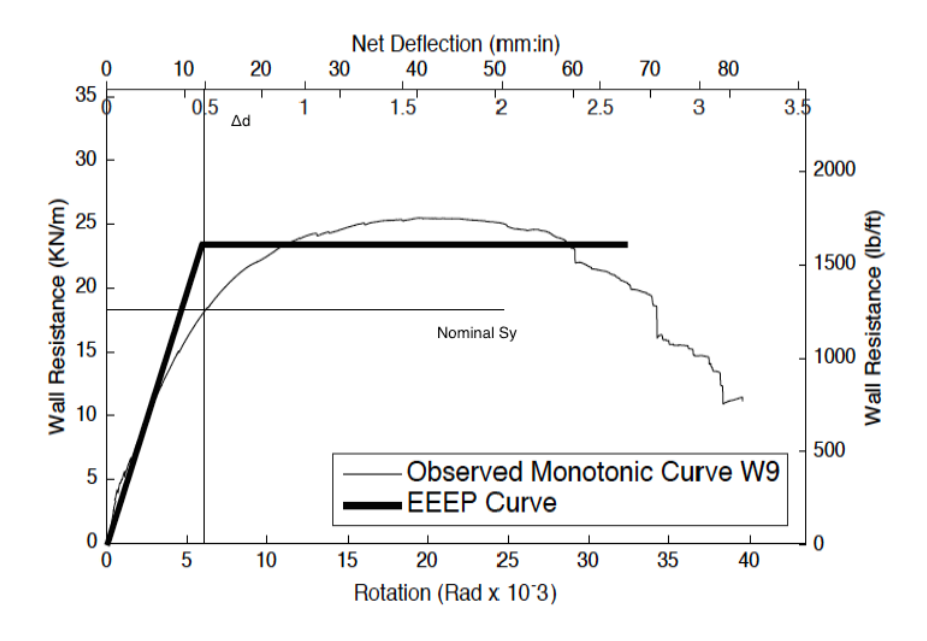


Figure 3.11 Drift,  $\Delta d$ , for 1830mm (6') Long Wall at Nominal Resistance

111

Table 3.27 Average Drift Values,  $\Delta_d$ 

Group	Framing (mm:mils)	Sheathing (mm:mils)	Fastener Spacing (mm:in)	Average Drift, $\Delta_d$ , for 610mm Long Walls (mm)	$\begin{array}{c} Average \\ Drift,  \Delta_d, \\ For  1830mm \\ Long \\ Walls  (mm) \end{array}$
3		0.76:30	50:2	14.4	13.4
4	1.37:54		75:3	10.6	16.2
5	1.57.51	0.70.50	100:4	8.0	12.0
6			150:6	10.4	12.8

## 3.5.6 VERIFICATION OF SHEAR RESISTANCE REDUCTION FOR HIGH ASPECT RATIO WALLS FOR THE USA & MEXICO

As recommended by the AISI S400 (2015), the same approach used for Canada for the verification of the shear resistance reduction for high aspect ratio walls is used in the United States of America and Mexico.

Figures 3.12 and 3.13 illustrate a comparison of the drifts  $\Delta_d$  between the 610mm (2') long wall (W5-M) and the 1830mm (6') long walls (W9-M). The drift  $\Delta_d$  is determined as the displacement reached at the equivalent resistance level for the 610mm (2') and 1830mm (6') long walls. As shown in Table 3.29, the drifts  $\Delta_d$  for the high aspect ratio walls are less or equivalent to the drifts for the 1830mm (6') walls. Based on these results, it is adequate to judge that the reduction factor of 2w/h listed in the AISI S400 is applicable, because if the high aspect ratio walls reach the modified resistance level, they would reach similar drifts as the longer walls and thus perform adequately.

Table 3.28 Verification of Shear Resistance Reduction for High Aspect Ratio Walls (USA & MEXICO)

Group	Framing mm:mils	Sheathing mm:mils	Fastener Spacing mm:in	Test	S <sub>u</sub> (lb/ft/m)	$S_{u,red} \\ (lb/ft)$	$S_{u,red,avg} \atop (lb/ft)$	S <sub>u</sub> nominal <sup>1</sup> (lb/ft)	$S_u \!\!\times\! 2w/h \\ (lb/ft)$
3			50:2	W3-M	2423	1851	1904	1921	960.5
			30.2	W3-C	2561	1956	1704	1)21	700.5
4			75:3	W4-M	2056	1571	1527	1512	756
	1.37:54	0.76:30	75.5	W4-C	1940	1482			
5	1.37.34	0.70.30	100:4	W5-M	1743	1331	1361	1371	685.5
			100.4	W5-C	1820	1390	1301	13/1	083.3
6			150:6	W6-M	1381	1055	1045	1042	521
0			150.0	W6-C	1356	1036	1043		321

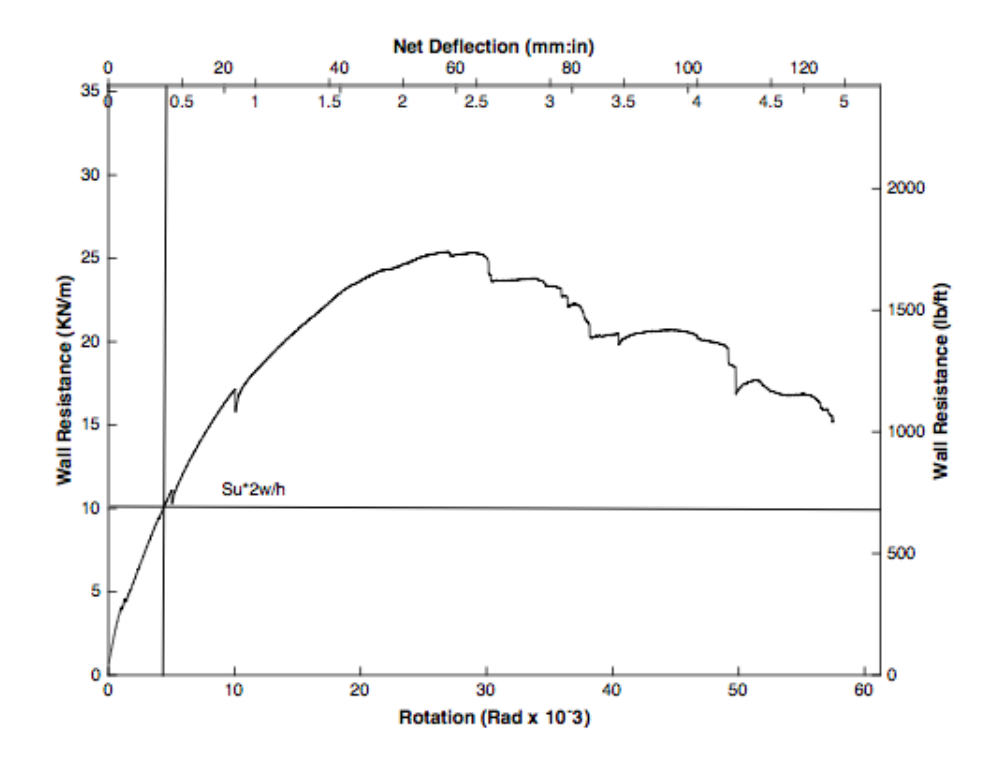


Figure 3.12 Drift,  $\Delta_d$ , for Short Wall at Reduced Resistance (W5-M)

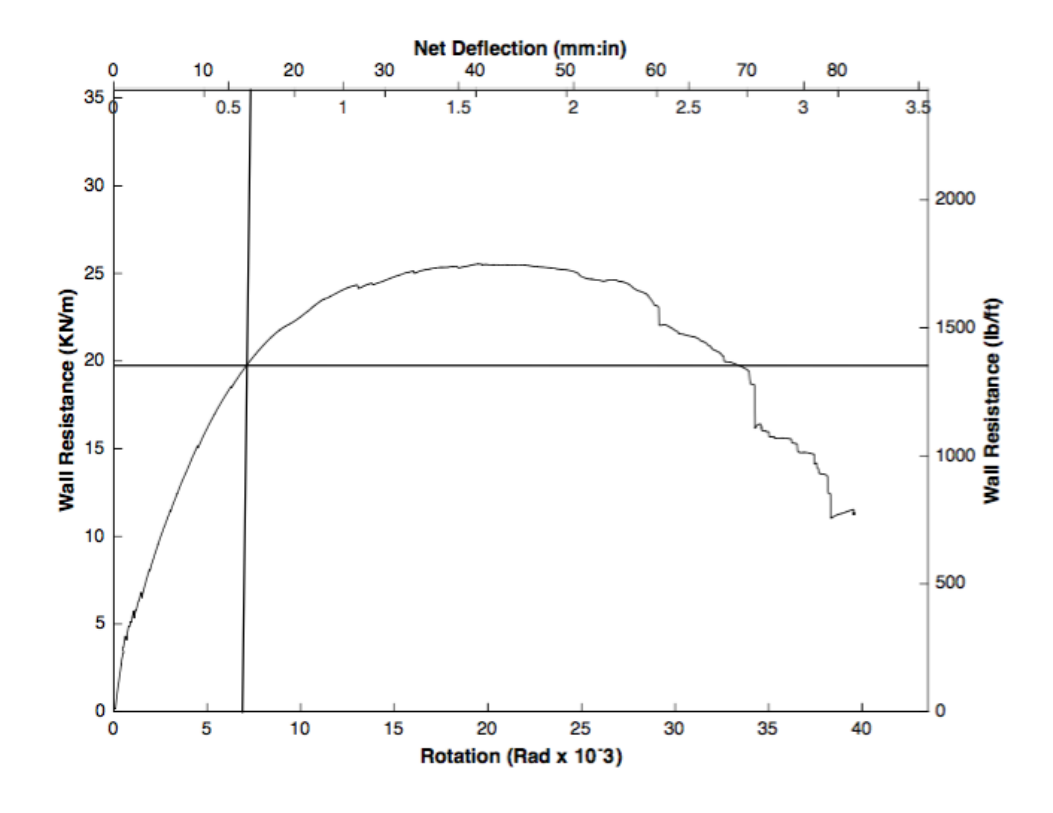


Figure 3.13 Drift,  $\Delta_d$  , for 1830mm (6') Long Wall at Nominal Resistance (W9-M)

Table 3.29 Average Drift Values,  $\Delta_d$ 

Group	Framing (mm:mils)	Sheathing (mm:mils)	Fastener Spacing (mm:in)	Average Drift, $\Delta_d$ , for 610mm Long Walls (in)	$\begin{array}{c} Average \\ Drift,  \Delta_d, \\ For  1830mm \\ Long \\ Walls  (in) \end{array}$
3			50:2	0.7	0.5
4	1.37:54	0.76:30	75:3	0.5	0.7
5	1.37.34	0.70.30	100:4	0.4	0.6
6			150:6	0.5	0.7

## 3.5.7 FACTOR OF SAFETY, CANADA

The factor of safety is calculated according to Equation 3-18. Figure 3.14 illustrates the ratio of the ultimate shear resistance  $S_u$  to the factored resistance of a shear wall  $S_r = \phi S_y$ .

Factor of Safety = 
$$\frac{S_u}{S_r}$$
 (3-18)

Where,

 $S_u$ : Ultimate shear resistance of test specimen

 $S_r = \phi S_v$ : Factored wall shear resistance,  $\phi = 0.7$ 

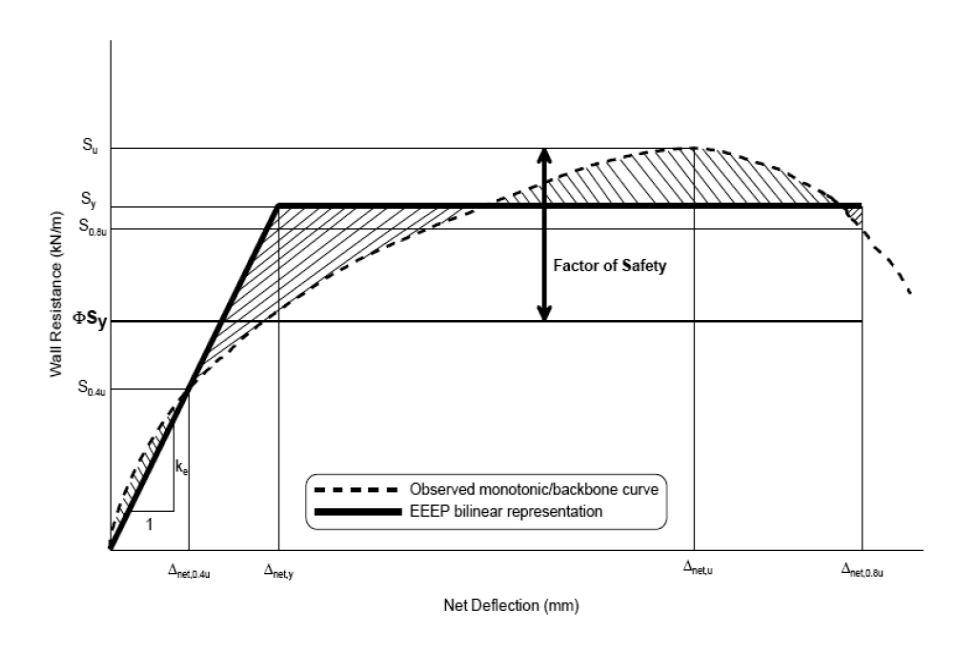


Figure 3.14 Factor of safety relationship with ultimate and factored resistances

In addition, for allowable strength design (ASD), the factor of safety is amplified by the load factor defined by the 2015 NBCC for wind loading of 1.4 (Equation 3-19).

Factor of Safety (ASD) = 1.4 
$$\frac{S_u}{S_r}$$
 (3-19)

Tables 3.30 and 3.31 list the factors of safety calculated for both monotonic and reversed-cyclic tests. The test values from the positive and negative cycles were combined since the data collected from the testing program indicates that the difference in the ultimate resistance of the shear walls in the positive and negative zones of the reversed cyclic tests was small and was negligible. Tables 3.30 and 3.31 list the average factor of safety, standard deviation and coefficient of variation calculated for LSD and ASD. The obtained factors of safety are in-line with the values obtained by Ong-Tone (2010), Balh (2010) and DaBreo (2012).

Table 3.30 Factor of safety for the monotonic test specimens

		Ultimate	Nominal	Factored	Factor of	Factor of
Configuration	Test	Resistance,	Resistance,	Resistance,	Safety	Safety
Configuration	Name	$S_{\mathrm{u}}$	$S_{y}$	$S_r (\phi = 0.7)$	(LSD)	(ASD)
		(kN/m)	(kN/m)	(kN/m)	$S_u/S_r$	$1.4 \times S_u/S_r$
1	W1-M	34.88	24.70	17.29	2.02	2.83
2	W2-M	39.13	27.30	19.11	2.05	2.87
3	W3-M	35.32	25.00	17.5	2.02	2.83
4	W4-M	29.97	20.20	14.14	2.12	2.97
5	W5-M	25.41	17.70	12.39	2.05	2.87
6	W6-M	20.13	13.50	9.45	2.13	2.98
7	W7-M	33.47	23.30	16.31	2.05	2.87
8	W8-M	27.92	19.90	13.93	2.00	2.81
9	W9-M	25.55	17.20	12.04	2.12	2.97
10	W10-M	18.94	13.30	9.31	2.04	2.85
11	W11-M	32.87	23.30	16.31	2.02	2.82
12	W12-M	28.81	19.90	13.93	2.07	2.90
13	W13-M	24.68	17.20	12.04	2.05	2.87
14	W14-M	19.51	13.30	9.31	2.10	2.93
		1	1	AVERAGE	2.059	2.88
				S.D	0.042	0.059

1 kN/m=75.547 lb/ft

Table 3.31 Factor of safety for the reversed-cyclic test specimens

	Test	Ultimate	Nominal	Factored	Factor of	Factor of
Configuration	Name	Resistance,	Resistance,	Resistance,	Safety	Safety
Configuration		$S_{\mathrm{u}}$	$S_{y}$	S <sub>r</sub> (\$\phi=0.7)	(LSD)	(ASD)
		(kN/m)	(kN/m)	(kN/m)	$S_u\!/S_r$	$1.4 \times S_u/S_r$
1	W1-C	35.96	24.70	17.29	2.08	2.91
2	W2-C	40.95	27.30	19.11	2.14	3.00
3	W3-C	37.34	25.00	17.50	2.13	2.99
4	W4-C	28.28	20.20	14.14	2.00	2.80
5	W5-C	26.53	17.70	12.39	2.14	3.00
6	W6-C	19.77	13.50	9.45	2.09	2.93
7	W7-C	30.79	23.30	16.31	1.89	2.64
8	W8-C	28.63	19.90	13.93	2.06	2.88
9	W9-C	25.00	17.20	12.04	2.08	2.91
10	W10-C	19.92	13.30	9.31	2.14	3.00
11	W11-C	33.67	23.30	16.31	2.06	2.89
12	W12-C	29.62	19.90	13.93	2.13	2.98
13	W13-C	24.28	17.20	12.04	2.02	2.82
14	W14-C	18.66	13.30	9.31	2.00	2.81
	L			AVERAGE	2.07	2.90
				S.D	0.073	0.102

1 kN/m=75.547 lb/ft

## 3.5.8 CAPACITY BASED DESIGN, CANADA

The design of structures for seismic resistance must follow the capacity based design method required by the AISI S400 Standard. This method consists of selecting a fuse element within the SFRS; that is, a ductile element that dissipates energy during inelastic deformations. The other elements in the SFRS, such as field and chord studs, holdowns, anchors, tracks and blockings, are designed to remain elastic and are expected to be able to resist the probable capacity of the "fuse" element and the corresponding principal and companion loads as defined by the 2015 NBCC. The energy dissipating element or fuse element in the case of CFS framed/steel sheathed shear walls is the connection between the sheathing and framing. The ductile energy dissipation is provided through bearing

deformation at the sheathing connections. The shear wall is expected to reach its ultimate capacity when pushed to the inelastic range during a design level earthquake. In order to approximate the probable capacity of the shear wall, an overstrength factor is used and is applied in the design of the other structural component in the SFRS to ensure that they do not themselves exhibit inelastic behaviour. Equation 3-20 is used to calculate the overstrength factor.

$$overstrength = \frac{S_u}{S_y} \tag{3-20}$$

Where,

 $S_u$ : Ultimate shear resistance of test specimen

 $S_v$ : Nominal yield wall resistance

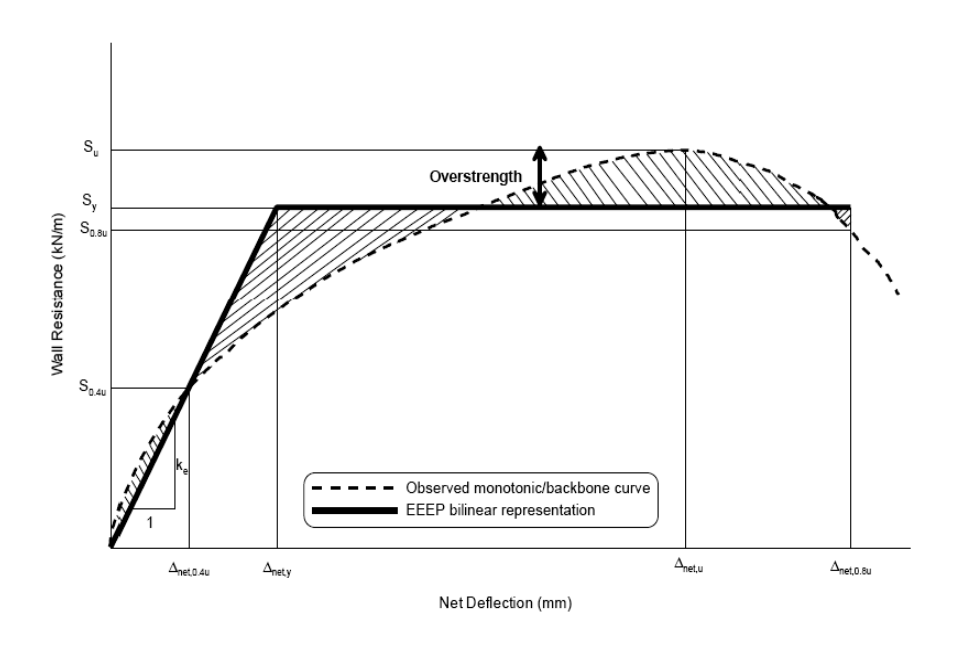


Figure 3.15 Overstrength relationship with ultimate and nominal shear resistance

Tables 3.32 and 3.33 list the overstrength factors and their corresponding standard deviation for the monotonic and reversed-cyclic tests, respectively. The computed mean overstrength factor for the monotonic tests is equal to 1.44 and for the reversed-cyclic tests is equal to 1.45. The average overstrength factor is then equal to 1.445. The overstrength values recommended by Balh (2010) Ong-Tone (2010) and DaBreo (2012) were respectively 1.4, 1.35 and 1.37. The average overstrength value of the blocked specimen tested by Rizk (2017) and DaBreo (2012) is 1.4. It is then recommended to use a value 1.4 for the design of structural elements within the steel sheathed blocked cold-formed shear walls. This is consistent with the AISI S400 Standard, which recommends to use a value of 1.4 in Canada for walls with steel sheathing.

Table 3.32 Overstrength design values for monotonic tests (Canada)

Configuration	Test Name	Ultimate Resistance, Su (kN/m)	Nominal Resistance, S <sub>y</sub> (kN/m)	Overstrength $S_u/S_y$
1	W1-M	34.88	24.70	1.41
2	W2-M	39.13	27.30	1.43
3	W3-M	35.32	25.00	1.41
4	W4-M	29.97	20.20	1.48
5	W5-M	25.41	17.70	1.44
6	W6-M	20.13	13.50	1.49
7	W7-M	33.46	23.30	1.44
8	W8-M	27.92	19.90	1.40
9	W9-M	25.55	17.20	1.49
10	W10-M	18.94	13.30	1.42
11	W11-M	32.87	23.30	1.41
12	W12-M	28.81	19.90	1.45
13	W13-M	24.68	17.20	1.44
14	W14-M	19.51	13.30	1.47
			AVERAGE	1.44
			S.D	0.03

1 kN/m=75.547 lb/ft

Table 3.33 Overstrength design values for reversed-cyclic tests (Canada)

	Test	Ultimate	Nominal	Overstrength
Configuration	Name	Resistance,	Resistance,	$S_u/S_y$
		S <sub>u</sub> (kN/m)	S <sub>y</sub> (kN/m)	
1	W1-C	35.96	24.70	1.46
2	W2-C	40.94	27.30	1.50
3	W3-C	37.34	25.00	1.49
4	W4-C	28.28	20.20	1.40
5	W5-C	26.53	17.70	1.50
6	W6-C	19.77	13.50	1.46
7	W7-C	30.79	23.30	1.32
8	W8-C	28.63	19.90	1.44
9	W9-C	25.00	17.20	1.45
10	W10-C	19.92	13.30	1.50
11	W11-C	33.67	23.30	1.45
12	W12-C	29.62	19.90	1.49
13	W13-C	24.28	17.20	1.41
14	W14-C	18.66	13.30	1.40
		I	AVERAGE	1.45
			S.D	0.051

1 kN/m=75.547 lb/ft

### 3.5.9 CAPACITY BASED DESIGN FOR THE USA AND MEXICO

According to the AISI S400 (2015), in the United States of America and Mexico, specific research on the expected strength of the cold-formed shear steel frame shear walls with steel sheathing based on energy dissipation at the connection between the studs and the sheathing has not been completed. For this reason, a conservative estimate based on the recommendation of the ASCE 7 (2010) is adopted. Thus, the overstrength factor  $\Omega_0$  is equal to 3.0 for bearing wall systems.

#### 3.5.10 TEST-BASED SEISMIC FORCE MODIFICATION FACTORS FOR CANADA

The base shear force V, used for seismic design as specified by the equivalent static force method in Clause 4.1.8.11 of the 2015 NBCC (NRCC 2015), is calculated using Equation 3-21.

$$V = \frac{S(T_a)M_v I_e W}{R_d R_o} \tag{3-21}$$

Where,

 $S(T_a)$ : Design spectral acceleration

 $T_a$ : Fundamental lateral period of vibration of the building

 $M_v$ : Factor accounting for higher mode effects

 $I_e$ : Earthquake importance factor of the structure

W: Weight of the structure (dead load plus 25% snow load)

 $R_d$ : Ductility-related force modification factor

 $R_o: Overstrength\mbox{-related force modification factor}$ 

Two factors are related to seismic design. The ductility-related force modification factor,  $R_d$ , and the overstrength-related force modification factor,  $R_o$ . Referring to the AISI S400 Standard (2015), the seismic force modification factors,  $R_dR_o$  are generally listed in the NBCC. However, since cold-formed steel frame shear walls with steel sheathing is a relatively new system for Canada, the seismic force modification factors  $R_dR_o$  have not been adopted yet by the NBCC. The AISI S400 suggests an  $R_dR_o$  value of 2.6 ( $R_d$ =2.0,  $R_o$ =1.3) for screw-connected shear walls with steel sheathing.

# 3.5.11 TEST-BASED DUCTILITY-RELATED FORCE MODIFICATION FACTOR, $R_d$

The ductility-related force modification factor  $R_d$  measures the ability of the fuse element to dissipate energy through inelastic deformation. Equations 3-22, 3-23, and 3-24 represent the relationship between ductility and the ductility-related force modification factor,  $R_d$ , derived by Newmark and Hall (1982) and based on the natural period of the structure.

$$R_d = \mu$$
, for T> 0.5 s (3-22)

$$R_d = \sqrt{2\mu - 1}$$
, for  $0.1$ s < T <  $0.5$ s (3-23)

$$R_d = 1.0$$
, for T < 0.03 s (3-24)

Where,

 $R_d$ : Ductility-related force modification factor

 $\mu$ : Ductility of shear wall

T: Natural period of structure

As suggested by Boudreault (2005), the natural period of many light-framed structures is between 0.03 to 0.5 seconds. Therefore, and in order to determine the  $R_d$  value of the steel sheathed shear walls, Equation 3-19 was used. Tables 3.34 and 3.35 list, respectively, the test-based  $R_d$  values obtained of the monotonic and reversed-cyclic tests. The average value of the ductility-related force modification factor is equal to 2.73. This result is in line with the values computed in previous research programs. DaBreo (2012) found an  $R_d$  value of 2.93, Balh (2010) recommended a value of 2.5. This value is higher than the  $R_d$  value listed in the AISI S400 (2015) by 35%.

Table 3.34 Ductility and test-based Rd values for monotonic tests

Configuration	Test Name	Ductility (μ)	Ductility- Related Force Modification Factor (R <sub>d</sub> )
1	W1-M	3.14	2.30
2	W2-M	4.05	2.67
3	W3-M	2.64	2.07
4	W4-M	3.30	2.37
5	W5-M	3.87	2.60
6	W6-M	2.91	2.20
7	W7-M	6.64	3.50
8	W8-M	3.19	2.32
9	W9-M	5.45	3.15
10	W10-M	4.23	2.73
11	W11-M	8.05	3.89
12	W12-M	3.59	2.49
13	W13-M	4.73	2.91
14	W14-M	6.10	3.35
		AVG.	2.75
		S.D	0.54

Table 3.35 Ductility and test-based Rd values for reversed-cyclic tests

Configuration	Test Name	Ductility (μ)	Ductility- Related Force Modification Factor (R <sub>d</sub> )
1	W1-C	2.94	2.21
2	W2-C	3.26	2.35
3	W3-C	2.75	2.12
4	W4-C	3.02	2.25
5	W5-C	4.20	2.72
6	W6-C	4.50	2.83
7	W7-C	6.44	3.45
8	W8-C	4.91	2.97
9	W9-C	4.11	2.69
10	W10-C	5.79	3.25
11	W11-C	6.10	3.35
12	W12-C	4.36	2.78
13	W13-C	3.43	2.42
14	W14-C	4.21	2.72
		AVG.	2.721
		S.D	0.425

NOTE: The ductility values for the reversed cyclic test were computed by taking the average value of ductility of the positive and negative cycles.

# 3.5.12 TEST-BASED OVERSTRENGTH-RELATED FORCE MODIFICATION FACTOR, $R_{\circ}$

As stated for limit states design, it is required that the factored resistance must be greater or equal to the factored loads, computed based on the critical load cases listed in the 2015 NBCC (NRCC 2015). In order to achieve conservative values for design, the factored loads are often overestimated. In contrast, in capacity-based design, the probable forces within the seismic force resisting system must not be overestimated in order for adequate inelastic deformation of the chosen energy dissipating element or "fuse" element. Therefore, the overstrength factor  $R_{o}$  is used in seismic design and is calculated using Equation 3-25 proposed by Mitchell et al. (2003).

$$R_o = R_{\text{Size}} R_{\phi} R_{vield} R_{sh} R_{mech} \tag{3-25}$$

Where,

 $R_{size}$ : overstrength due to restricted choices for sizes of components

 $R_{\phi}: 1/\phi, (\phi=0.7)$ 

 $R_{yield}$ : ratio of test yield strength to minimum specified yield strength

 $R_{sh}$ : overstrength due to development of strain hardening

 $R_{mech}$ : overstrength due to collapse mechanism

The overstrength related force modification factor,  $R_o$ , as indicated by Equation 3-25, is a function of five overstrength factors. First, the size factor,  $R_{\rm size}$ , is used to take into consideration the limitations of component sizes available for structural engineers in their designs. Second,  $R_{\phi}$ , computed as the inverse of the resistance factor,  $\phi$ , is applied to consider nominal load values and not the factored loads as given in limit states design. The third factor  $R_{\rm yield}$  is computed by taking the average overstrength values listed in Tables 3.32 and 3.33 for monotonic and reversed cyclic tests. The last two factors  $R_{\rm sh}$  and  $R_{\rm mech}$ , are considered to be equal to unity because the cold-formed steel shear walls are not affected by the steel's ability to undergo strain hardening, and, the collapse mechanism for

cold-formed steel sheathed shear walls has not been established yet. Table 3.36 lists a summary of the overstrength factors.

Table 3.36 Overstrength factors for calculating the test-based overstrength-related force modification factor,  $R_0$ 

	$R_{size}$	$R_{\phi}$	$R_{yield}$	$R_{sh}$	R <sub>mech</sub>	$R_{o}$
All Groups	1.05	1.43	1.45	1.00	1.00	2.18

As indicated in Table 3.36, the value of the calculated  $R_o$  factor is 2.18. DaBreo (2012), Balh (2010) and Ong-Tone (2009) obtained respectively 2.01, 2.10 and 2.00 and recommended to use an  $R_o$  of 1.7, a value consistent with the  $R_o$  value for wood sheathed shear walls given in the 2015 NBCC). The AISI S400 Standard for CFS framed / steel sheathed shear walls suggests an  $R_o$  value of 1.3.

# 3.5.13 TEST BASED SEISMIC FORCE MODIFICATION FACTORS FOR THE UNITED STATES OF AMERICA

According to the AISI S400 Standard (2015), the seismic response modification coefficient, R for light-framed walls sheathed with steel sheets for the USA and Mexico is equal to 6.5.

### 3.5.14 INELASTIC DRIFT LIMIT

The inelastic drift limit is set to be equal to 2.5% of the storey height by the 2015 NBCC. The results presented in Tables 3.37 and 3.38 indicate that the specimens tested under monotonic loading exhibited higher drifts than the walls tested under reversed-cyclic loading. Only walls with a length of 1220mm (4') or longer were considered. The short, 610x2440mm (2'x8'), shear walls were excluded because they had high drift values due to their high aspect ratio. Based on the results listed in Tables 3.37 and 3.38 an average drift of 2.45% was computed based on the post-peak  $\Delta_{0.8u}$ . This average drift is lower than the 2.5% limit specified by the 2015 NBCC. The stronger wall specimens produced drifts higher than the 2.5% limit set by the 2015 NBCC. But as demonstrated previously, the

ductility of the blocked walls was lower than their unblocked counterparts, which witnessed lower rates of strength degradation. For these reasons, it is suggested to set an inelastic drift limit for seismic design of 2%, as proposed by DaBreo (2012) for blocked shear walls and by Balh (2010) for ordinary steel sheathed shear walls.

Table 3.37 Drifts at  $\Delta_{0.8u}$  of monotonic tests

Configuration	Test Name	Δ <sub>0.8u</sub> (mm)	% Drift
1	W1-M	83.7	0.034
2	W2-M	85.9	0.035
7	W7-M	75.5	0.031
8	W8-M	59.4	0.024
9	W9-M	67.0	0.027
10	W10-M	50.0	0.021
11	W11-M	86.8	0.036
12	W12-M	54.0	0.022
13	W13-M	42.4	0.017
14	W14-M	42.8	0.018
		AVG.	0.027
		S.D	0.007

1 mm = 0.0394 in

Table 3.38 Drifts at  $\Delta_{0.8u}$  of reversed-cyclic tests

Configuration	Test	$\Delta_{0.8u}$	% Drift
	Name	(mm)	
1	W1-C	63.6	0.026
2	W2-C	60.7	0.025
7	W7-C	81.8	0.034
8	W8-C	56.2	0.023
9	W9-C	47.9	0.020
10	W10-C	46.9	0.019
11	W11-C	64.3	0.026
12	W12-C	44.5	0.018
13	W13-C	39.5	0.016
14	W14-C	36.2	0.015
		AVG.	0.022
		S.D	0.006

NOTE: The drift values for the reversed-cyclic tests were computed by taking the average value of drifts of the positive and negative cycles.

1 mm = 0.0394 in

# 4 CHAPTER 4 – COMPONENT EQUIVALENCY METHODOLOGY

#### 4.1 INTRODUCTION

The Component Equivalency Methodology of FEMA P-795 (2011) is an adaptation of the FEMA P-695 General Methodology, Quantification of Building Seismic Performance Factors (FEMA, 2009). Similar to the general methodology in FEMA P-695, the goal of the FEMA P-795 is to ensure that code designed buildings have adequate resistance to earthquake-induced collapse. The Component Methodology is a statistically based procedure for evaluating the seismic performance equivalency of new structural components proposed as substitutes for reference components. Reference Components are listed in ASCE/SEI 7-10 Minimum Design Load for Building and Other Structures (ASCE, 2010). For clarity, it is important to mention that the term "component" in ASCE/SEI 7-10 is used to refer to non-structural components, whereas in the Component Methodology the term "component" is used to refer to structural elements that are part of the SFRS. Throughout this chapter, the FEMA P 795 methodology will be applied to determine if the cold-formed shear walls designed with full frame blocking and thick Sheathing / Framing Members is equivalent to line A.16 in Table 12.2-1 of ASCE/SEI (2010), which reads "Light-Frame (cold-formed steel) walls sheathed with wood structural panels rated for shear resistance of steel sheets."

Several requirements need to be met in order to apply the Component Methodology to the proposed component. A detailed explanation of the required criteria is provided in Subsection 2.3 of FEMA P-795 (2011), and is presented in Section 4.3 of this document. Once the applicability of the method is judged satisfactory, test data are classified into component performance groups. Structuring the component performance groups is subjective. As a default, proposed and reference component data are respectively compiled into one performance group. In order to adequately capture different behavioural characteristics associated with major differences in the design of the components, it is recommend that the test data be complied into separate performance groups. The

equivalency of proposed components and reference components for each performance group is measured by comparing key performance parameters, e.g. Strength, stiffness, effective ductility and deformation capacity, determined from a statistical evaluation of test data compiled from monotonic and reversed cyclic tests.

According to FEMA P-795, the Component Methodology provides a practical and rational process for evaluating component equivalency. The component methodology has been previously applied to evaluate the equivalency for substitution of:

- 1. Buckling restrained braces for special steel concentric braces.
- 2. Stapled wood shear walls components for nailed wood shear wall components.
- 3. Pre-fabricated shear walls products for use in wood light-frame construction.
- 4. Pre-fabricated Bamboo walls for conventional Timber Shear walls

The reference component data set is based on Yu et al. (2007, 2009), El-Saloussy (2010), Balh (2010) and Ong-Tone (2009). These cold-formed steel framed shear walls with steel sheathing were tested at the University of North Texas and McGill University under monotonic and reversed cyclic loading.

The proposed component data set is based on the tests by DaBreo (2012) and the tests from the shear wall laboratory research program completed by the author; described herein. Specimens were tested under monotonic and reversed cyclic loading at McGill University.

A more detailed description of the reference component and proposed component is provided in Sections 4.4 and 4.5, respectively.

### 4.2 COMPONENT TESTING REQUIREMENT

The general requirements for component testing of both reference and proposed components are provided in this section.

4.2.1 GENERAL REQUIREMENTS FOR COMPONENT TESTING

Various criteria must be taken into consideration during the development of the proposed

component testing program and when the quality of existing data obtained from previous

testing program is evaluated.

Size effects:

FEMA P-795 (2011) requires the following:

"Tests should be performed on full-size components unless it can be shown by theory

or experimentation that testing of reduced scale specimens will not significantly affect

behavior".

Proposed component : <u>OK</u>

Reference component :  $\underline{OK}$ 

Boundary conditions:

FEMA P-795 (2011) requires the following:

"The boundary conditions of component tests should be:

1. Representative of constraints that a component would experience in a typical

structural system.

2. Sufficiently general so that the results can be applied to boundary conditions

that might be experienced in other system configurations. Boundary conditions

should not impose beneficial effects on seismic behavior that would".

Proposed component : <u>OK</u>

Reference component : OK

Load application:

FEMA P-795 (2011) requires the following:

"Loads should be applied to test specimens in a manner that replicates the transfer of load to the component as it would occur in common system configurations, and tests should generally be conducted using displacement control unless the component under investigation requires load control testing."

Proposed component : <u>OK</u>

Reference component : OK

Test specimen construction:

FEMA P-795 (2011) requires the following:

"Specimens should be constructed in a setting that simulates commonly encountered field conditions".

Proposed component : OK

Reference component :  $\underline{OK}$ 

Quality of test specimen construction:

FEMA P-795 (2011) requires the following:

"The component should be of a construction quality that is equivalent to what will be commonly implemented in the field".

Proposed component : <u>OK</u>

Reference component :  $\underline{OK}$ 

Testing of materials:

FEMA P-795 (2011) requires the following:

"Material testing should be conducted when such data are needed to develop properties

for component design requirements".

Proposed component : OK

Reference component : OK

Laboratory accreditation:

FEMA P-795 (2011) requires the following:

"Testing laboratories used to conduct an experimental investigation program should

generally comply with national or international accreditation criteria, such as the

ISO/IEC 17025 General Requirements for the Competence of Testing and Calibration

Laboratories (ISO, 2005)".

Proposed component : <u>OK</u>

Reference component :  $\underline{OK}$ 

Instrumentation:

FEMA P-795 (2011) requires the following:

"Instrumentation should be installed to permit reliable measurement of all required

strength, stiffness, and deformation quantities. Where necessary, deformation

measurements should be corrected to remove rigid body displacement effects, inertial

effects, or deformations due to the flexibility of the test apparatus".

Proposed component : <u>OK</u>

Reference component : OK

The general requirements for component testing listed are fulfilled by the reference

component and proposed component.

4.2.2 CYCLIC LOAD TESTING

The proposed and referenced components were tested according to the CUREE reverse

cyclic loading protocol. The CUREE protocol, described in-depth by Krawinkler et al.

(2000) and ASTM E2126 (2007), represents the demand expected during a design level

earthquake with a 2% in 50 year return period. A more detailed description of the

procedures used during the testing of the proposed specimens under reversed cyclic loading

are provided in Section 2.4 of this document, and in Section 2.5 of the thesis of DaBreo

(2012).

Referring to Section 2.2.2 of FEMA P-795 (2011), cyclic load testing should be performed

in accordance with the following protocol:

"Proposed components and reference components should be tested with load histories

that are equivalently damaging, quantified in terms of accumulated deformation

imposed on the test specimen".

Proposed component : OK

Reference component : <u>OK</u>

"The number of cycles should be sufficient to measure possible degradation of strength,

stiffness, or energy dissipation capacity of the component under repeated cycles of

loading".

Proposed component : <u>OK</u>

Reference component : OK

"The deformation history should be described in terms of a well-defined quantity (e.g.,

displacement, story drift, rotation) and should consist of essentially symmetric

deformation cycles of step-wise increasing amplitude. Cycles of smaller amplitudes

between cycles of increasing amplitudes (trailing cycles) should only be included in

the deformation history if they affect the cyclic response of the component".

Proposed component : <u>OK</u>

Reference component :  $\underline{OK}$ 

"Proposed and reference component specimens should be tested to deformations large

enough to achieve a 20% reduction in applied load, and therefore reach the ultimate

deformation,  $\Delta_U$ , in at least one direction of loading"

Proposed component : OK

Reference component :  $\underline{OK}$ 

As shown in Figure 4.1, several parameters must be determined from both positive and

negative portions of the envelope curve.

 $Q_M$ : Ultimate load

 $\Delta_{U^+}$ : Ultimate deformation at 0.8  $Q_M$ 

 $K_I$ : Initial stiffness based on force and deformation at 0.4  $Q_M$ 

 $\Delta_{Y,eff}$ : Effective yield deformation,  $\Delta_{Y,eff} = Q_M/K_I$ 

 $\mu_{eff}$ : Effective ductility capacity,  $\mu_{eff} = \Delta_U/\Delta_{Y,eff}$ 

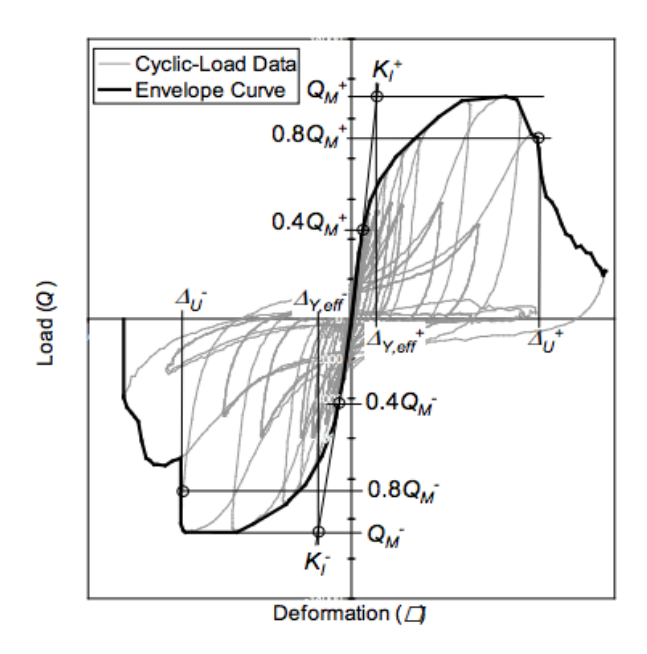


Figure 4.1 Reversed cyclic load test data, envelope cure and performance parameters, (FEMA P-795, 2011)

#### 4.3 MONOTONIC LOAD TESTING

Referring to Section 2.2.3 of FEMA P-795 (2011), monotonic load testing should be performed in accordance with the following protocol:

- "Component test specimens should be tested in both directions for components that have significant asymmetric behavior".
- "Component test specimens should be tested to deformations large enough to achieve a 20% reduction in applied load, and therefore reach the ultimate deformation,  $\Delta_{UM}$ ".

Proposed component : <u>OK</u>

Reference component : OK

A more detailed description of the procedures used during the testing of the proposed specimens under monotonic loading are provided in Section 2.4 of this document, and in Section 2.5 of the thesis of DaBreo (2012).

As shown in Figure 4.2, several parameters must be determined from the monotonic-load testing curve.

 $Q_{MM}$ : Ultimate load

 $\Delta_{UM}$ : Ultimate deformation at 0.8  $Q_{MM}$ 

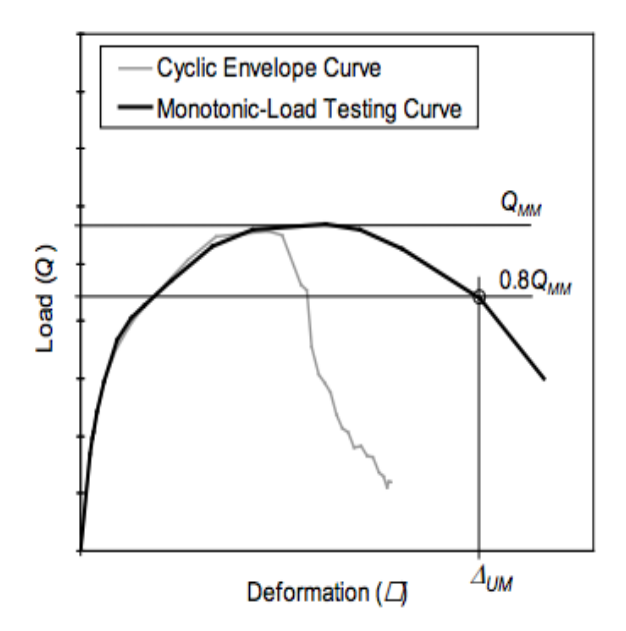


Figure 4.2 Monotonic load test data and performance parameters, (FEMA P-795, 2011)

#### 4.4 EVALUATION OF APPLICABILITY CRITERIA

In order to use the Component Methodology, the proposed component must meet the criteria described in this section. Various parameters must be addressed to evaluate the applicability of the component methodology:

- The suitability of the reference SFRS.
- The adequacy of the reference component design criteria and test data.
- The adequacy of the proposed component design criteria and test data.
- The characteristics of the proposed component.

## 4.4.1 REFERENCE SEISMIC-FORCE-RESISTING SYSTEM: COLLAPSE PERFORMANCE CRITERIA

The collapse performance criteria established in the FEMA P-695 Methodology must be met by the reference seismic-force-resisting system. For the purposes of the Component Equivalency Methodology, the SFRS listed in ASCE/SEI 7-10 are assumed to meet these criteria.

This requirement is fulfilled by the cold-formed steel frame shear walls designed with steel sheathing used as reference component. The reference components used correspond to line A.16 in Table 12.2-1 of ASCE/SEI (2010), which reads "Light-Frame (cold-formed steel) walls sheathed with wood structural panels rated for shear resistance of steel sheets."

#### 4.4.2 QUALITY RATING CRITERIA

In order to ensure that the data used in this report is robust enough for the application of the Component Methodology, FEMA P-795 imposes a minimum quality rating for the reference and proposed component test data and design requirements.

Referring to Section 2.3.3 of FEMA P-795 (2011):

- The quality rating of design requirements and test data should be Good or Superior for the reference component.
- The quality rating of design requirements and test data should be Fair, Good or Superior for the proposed components.

Referring to Section 4.7 of this document, these criteria were met by the reference components and the proposed components.

#### 4.4.3 GENERAL CRITERIA

In order to apply the Component Methodology, FEMA P-795 (2011) requires that the proposed components and the reference components be unambiguously defined with a clear definition of the component boundary.



Figure 4.3 Illustration of Proposed component boundaries (Courtesy of RJC Ltd)

REFERENCE COMPONENT TEST DATA

REFERENCE COMPONENT DESIGN SPACE 4.5.1

The reference components are defined as cold-formed steel framed shear walls sheathed

with steel sheathing. With the purpose to represent a wide variation of configurations, the

selected reference components are characterized by a variation in system geometry,

component sections, material properties and detailing.

The general characteristics are listed below and a more detailed description of each

configuration of the reference component is provided in Tables 4.1, 4.2 and 4.3.

Wall Dimensions (height and length (mm:ft)):  $1240 \times 2440$  (4×8) to  $2440 \times 2440$  (8×8).

Aspect ratio (height/length): 2:1 to 1:1 (aspect ratios above 2:1 are not included in the

design space).

Openings: No opening are considered.

Sheathing thickness (mm:in): 0.46 (0.018) to 0.84 (0.033).

Framing thickness (mm:in): 0.084 (0.033) to 1.37 (0.054)

Sheathing screws spacing (mm:in) (on-centre):

Edge spacing: 50 (2) to 150 (6),

Field spacing:300 (12)

Tables 4.1, 4.2 and 4.3 list various configurations of the reference components analysed

respectively by El-Saloussy (2010), Balh (2010) and Ong-Tone (2009). Specimens were

tested under both monotonic and reversed cyclic loading.

Table 4.1 Summary of cold-formed steel framed shear walls with steel sheathing configurations in the Reference Component Data by Yu et al. (2007) Phase 1

	Phase 1 Main Group Test Matrix (Yu et al., 2007)										
Test Label	Wall Dimensions (mm:ft)	Framing thickness (mm:in.)	Steel Sheet thickness (mm:in.)	Fastener spacing Perimeter/Field (mm/mm) (in./in.)	Number of monotonic tests	Number of cyclic tests	Fastener Size (No.)				
8ft×4ft×43 mil	1220×2440 (4×8)	1.09 (0.043)	0.84 (0.033)	50/300 (2/12)	2	2	8				
8ft×4ft×43 mil	1220×2440 (4×8)	1.09 (0.043)	0.84 (0.033)	50/300 (2/12)	2	2	8				
8ft×4ft×43 mil	1220×2440 (4×8)	1.09 (0.043)	0.76 (0.03)	50/300 (2/12)	2	2	8				
8ft×4ft×43 mil	1220×2440 (4×8)	1.09 (0.043)	0.76 (0.03)	50/300 (2/12)	2	2	8				
8ft×4ft×43 mil	1220×2440 (4×8)	1.09 (0.043)	0.76 (0.03)	50/300 (2/12)	2	2	8				
8ft×4ft×43 mil	1220×2440 (4×8)	1.09 (0.043)	0.76 (0.03)	50/300 (2/12)	2	2	8				
8ft×4ft×33 mil	1220×2440 (4×8)	1.09 (0.043)	0.69 (0.027)	50/300 (2/12)	2	2	8				
8ft×4ft×33 mil	1220×2440 (4×8)	1.09 (0.043)	0.69 (0.027)	50/300 (2/12)	2	2	8				
8ft×4ft×33 mil	1220×2440 (4×8)	1.09 (0.043)	0.69 (0.027)	50/300 (2/12)	2	2	8				

Table 4.2 Summary of cold-formed steel framed shear walls with steel sheathing configurations in the Reference Component Data by Yu et al. (2009) Phase 2

			Phase 2 (Yu	et al., 2009)				
Test Label	Wall Dimensions (mm:ft)	Framing thickness (mm:in.)	Steel Sheet thickness (mm:in.)	Fastener spacing Perimeter/Field (in./in.)	Number of monotonic tests	Number of cyclic tests	Fastener Size (No.)	
		Phase 2 Tasl	k 1 Group Tes	t Matrix (Yu et al.	., 2009)			
8×4×350- 33×18-6	1220×2440 (4×8)	1.09 (0.043)	0.46 (0.018)	150/300 (6/12)	2	2	8	
	Phase 2 Task 2 Group Test Matrix (Yu et al., 2009)							
8×6×350- 43×30-2- C1-A	1830×2440 (6×8)	1.09 (0.043)	0.76 (0.03)	50/300 (2/12)	0	1	8	
8×6×350- 43×30-2- C1-B	1830×2440 (6×8)	1.09 (0.043)	0.76 (0.03)	50/300 (2/12)	0	1	8	
8×6×350- 43×33-2- M1-C	1830×2440 (6×8)	1.09 (0.043)	0.84 (0.033)	50/300 (2/12)	1	0	10	
8×6×350- 43×33-2- C1-C	1830×2440 (6×8)	1.09 (0.043)	0.84 (0.033)	50/300 (2/12)	0	1	10	
8×6×350- 43×33-2- C2-C	1830×2440 (6×8)	1.09 (0.043)	0.84 (0.033)	50/300 (2/12)	0	1	10	
8×6×350- 43×30-2- M1-C	1830×2440 (6×8)	1.09 (0.043)	0.76 (0.03)	50/300 (2/12)	1	0	10	
8×6×350- 43×30-2- C1-C	1830×2440 (6×8)	1.09 (0.043)	0.76 (0.03)	50/300 (2/12)	0	1	10	
8×6×350- 43×30-2- C2-C	1830×2440 (6×8)	1.09 (0.043)	0.76 (0.03)	50/300 (2/12)	0	1	10	
8×6×600- 43×33-2- M1-C	1830×2440 (6×8)	1.09 (0.043)	0.84 (0.033)	50/300 (2/12)	1	0	10	
8×6×600- 43×33-2- C1-C	1830×2440 (6×8)	1.09 (0.043)	0.84 (0.033)	50/300 (2/12)	0	1	10	
8×6×600- 43×33-2- C2-C	1830×2440 (6×8)	1.09 (0.043)	0.84 (0.033)	50/300 (2/12)	0	1	10	
8×6×350- 54×33-2- M1-B	1830×2440 (6×8)	1.09 (0.043)	0.84 (0.033)	50/300 (2/12)	1	0	8	

	Phase	2 Task 2 Group Tes	st Matrix (	Yu et al., 20	009)		
8×6×350-54×33-	1830×2440	1.37	0.84	50/300	0	1	8
2-C1-B	(6×8)	(0.054)	(0.033)	(2/12)	U	1	0
8×6×350-54×33- 2-C2-B	1830×2440	1.37	0.84	50/300	0	1	8
	(6×8)	(0.054)	(0.033)	(2/12)			
8×6×350-43×27- 2-M1-D	1830×2440	1.09	0.69	50/300	1	0	10
	(6×8)	(0.043)	(0.027)	(2/12)			
8×6×350-43×27- 2-C1-D	1830×2440	1.09	0.69	50/300	0	1	10
	(6×8)	(0.043)	(0.027)	(2/12)			
8×6×350-54×33- 2-M1-C	1830×2440	1.37	0.84	50/300	1	0	10
	(6×8)	(0.054)	(0.033)	(2/12)			
8×6×350-54×33- 2-C1-C	1830×2440	1.37	0.84	50/300	0	1	10
	(6×8)	(0.054)	(0.033)	(2/12)			
8×6×350-54×33- 2-C2-C	1830×2440	1.37	0.84	50/300	0	1	10
	(6×8)	(0.054)	(0.033)	(2/12)			
8×4×350-43×33- 2-C1-C	1220×2440	1.09	0.84	50/300	0	1	10
	(4×8)	(0.043)	(0.033)	(2/12)			
8×4×350-43×33- 2-C2-C	1220×2440	1.09	0.84	50/300	0	1	10
	(4×8)	(0.043)	(0.033)	(2/12)			

Tables 4.1 and 4.2 list various configurations of the reference components analysed by El-Saloussy (2010).

Table 4.3 Summary of cold-formed steel framed shear walls with steel sheathing configurations in the Reference Component Data by Balh (2010) and Ong-Tone (2009)

Test Label	Wall Dimensions	Framing Thickness (mm:in.)	Steel Sheet Thickness (mm:in.)	Fastener spacing Perimeter/Field (mm/mm) : (in./in.)	Number of monotonic tests	Number of cyclic tests	Fastener Size (No.)
1	1220×2440 (4×8)	1.09 (0.043)	0.46 (0.018)	150/300 (6/12)	3	2	8
2	1220×2440 (4×8)	1.09 (0.043)	0.46 (0.018)	50/300 (2/12)	2	2	8
3	1220×2440 (4×8)	0.084 (0.033)	0.46 (0.018)	150/300 (6/12)	2	3	8
4	1220×2440 (4×8)	1.09 (0.043)	0.76 (0.03)	150/300 (6/12)	2	2	8
5	1220×2440 (4×8)	1.09 (0.043)	0.76 (0.03)	100/300 (4/12)	3	2	8
6	1220×2440 (4×8)	1.09 (0.043)	0.76 (0.03)	50/300 (2/12)	3	2	8
7	1220×2440 (4×8)	0.084 (0.033)	0.76 (0.03)	100/300 (4/12)	1	0	8
11	2440×2440 (4×8)	1.09 (0.043)	0.76 (0.03)	100/300 (4/12)	2	2	8
12	1830×2440 (4×8)	1.09 (0.043)	0.76 (0.03)	100/300 (4/12)	1	0	8
13	1830×2440 (4×8)	1.09 (0.043)	0.76 (0.03)	50/300 (2/12)	1	0	8

Tables 4.3 list various configurations of the reference components analysed by Balh (2010) and Ong-Tone (2010).

#### 4.5.2 REFERENCE COMPONENT PERFORMANCE GROUPS

According to Section 2.4.4 of FEMA P-795 (2011), the data collected from the testing programs of the various reference components should be compiled into a single performance group unless there are fundamental differences in behaviour among reference component data. In this case, the reference component data should be segmented in two or more performance groups in order to capture the changes in performance associated with the differences in the designs. When several performance groups are created, the acceptance criteria listed in Section 4.8 of this thesis to evaluate the component equivalency should be applied independently for each pair of proposed and reference performance groups.

Based on this, it was judged reasonable to segment the reference component data into a single performance group.

#### 4.5.3 TEST DATA & SUMMARY STATISTICS

The reference component test data are compiled into a single performance group. The reference component data set for monotonic and reversed cyclic loading are listed in Tables 4.6 and 4.7, respectively.

Figures 4.4 and 4.5 illustrate the typical monotonic and reversed cyclic response to lateral loading of cold-formed steel framed shear walls sheathed with steel sheathing

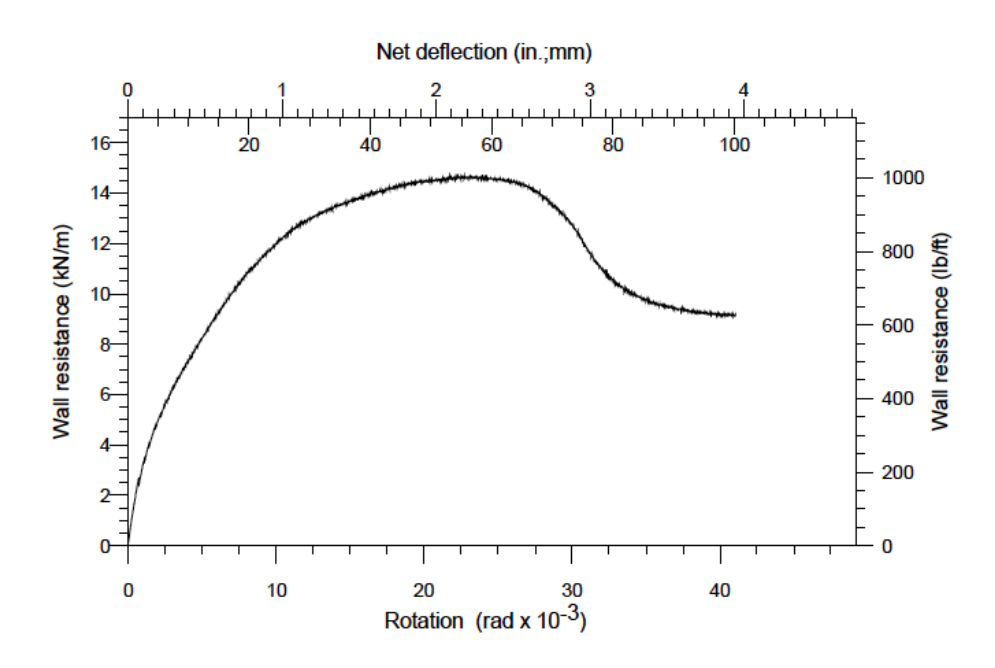


Figure 4.4 Illustration of Monotonic response of cold-formed steel shear walls sheathed with steel sheathing, data from Balh (2010)

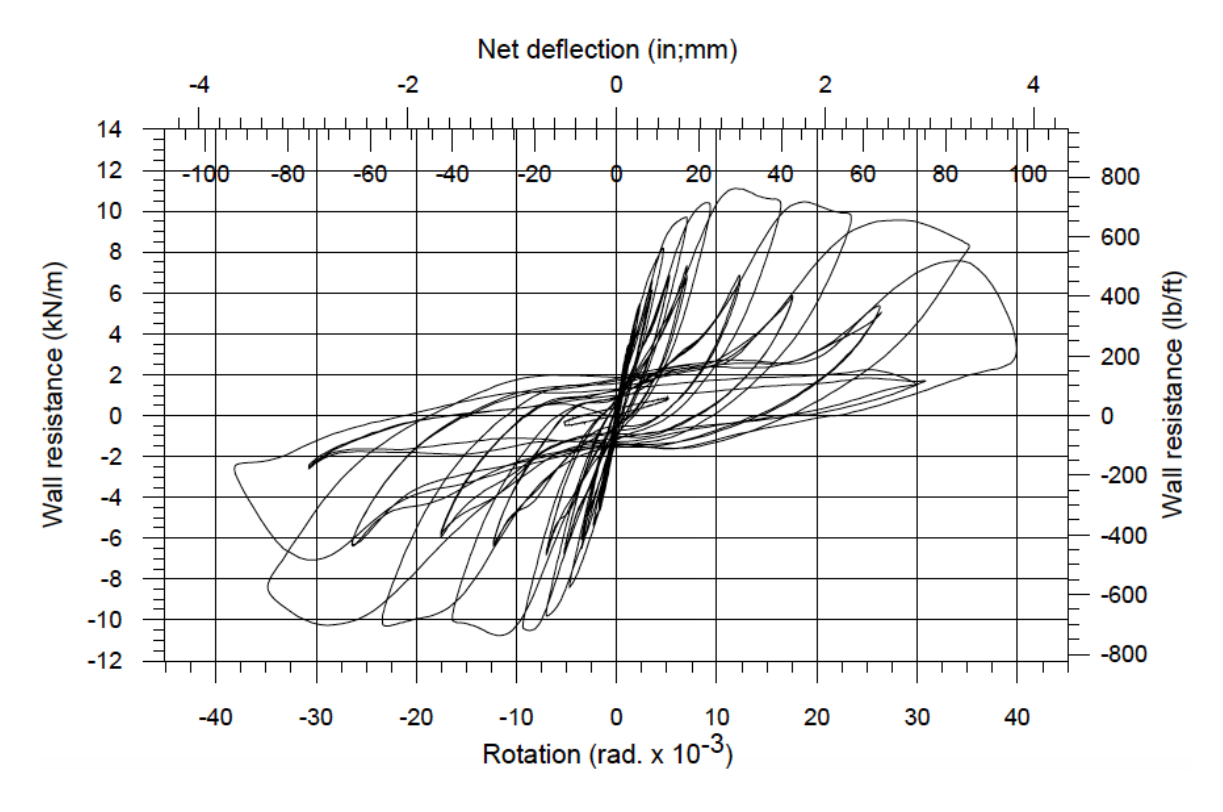


Figure 4.5 Illustration of cyclic response of cold-formed steel shear walls sheathed with steel sheathing, data from Balh (2010)

As shown in Tables 4.6 and 4.7, the displacement quantity was applied to the wall, and the force quantity was monitored during the testing

As recommended by FEMA P-795 (2011), the adopted design procedure to determine the design strength of the reference and proposed component (Load and Resistance Factor Design LRFD) was based on the recommendation of the AISI S400 Standard (2015).

The available strength [factored resistance] ( $\phi_v v_n$ ) for Load and Resistance Factor Design (LRFD) was determined using the appropriate nominal strength listed in Table 4.4 for the USA and Mexico and for Limit States Design (LSD) in Table 4.5 for Canada.

Table 4.4 Nominal Shear Strength [Resistance] (vn) per Unit Length for Seismic and Other In-Plane Loads for Shear Walls With Steel Sheet Sheathing On One Side of Wall (USA and Mexico) (AISI S400 2015)

	USA and MEXICO (lb/ft)									
	Max	Fasten	er Spacing (in		Edges	Stud	Designation Thickness of Stud,	Maximum		
Assembly Description	Aspect Ratio (h:w)	6	4	3	2	Blocking Required	Track and Stud Blocking (mils)	Sheathing screw size		
0.018" steel sheet	2:1	390	-	-	-	No	33 (min.)	8		
0.027" steel sheet	2:1	-	1000	1085	1170	No	43 (min.)	8		
0.027" steel sheet	2:1	647	710	778	845	No	33 (min.)	8		
0.030" steel sheet	2:1	910	1015	1040	1070	No	43 (min.)	8		
0.030" steel sheet	2:1				1355	Yes	43 (min.)	10		
0.033" steel sheet	2:1	1055	1170	1235	1305	No	43 (min.)	8		
0.033" steel sheet	2:1	-	-	-	1505	Yes	43 (min.)	10		
0.033" steel sheet	2:1	-	-	-	1870	No	54 (min.)	8		
0.033" steel sheet	2:1				2085	Yes	54 (min.)	10		

Table 4.5 Nominal Shear Strength [Resistance] (vn) per Unit Length for Seismic and Other In-Plane Loads for Shear Walls With Steel Sheet Sheathing on One Side of Wall (Canada) (AISI S400 2015)

	Canada (kN/m)									
Assembly	Max Aspect	Fasten	_	g at Panel	Edges	Stud	Designation Thickness of Stud, Track	Maximum		
Description	Ratio (h:w)	150	100	75	50	Blocking Required	and Stud Blocking (mils)	Sheathing screw size		
0.46 mm steel sheet	2:1	4.1	-	-	-	No	33 (min)	8		
0.46 mm steel sheet	2:1	4.5	6.0	6.8	7.5	No	43 (min)	8		
0.68 mm steel sheet	2:1	6.5	7.2	7.9	8.7	No	33 (min)	8		
0.76 mm steel sheet	4:1	8.9	10.6	11.6	12.5	No	43 (min)	8		
0.84 mm steel sheet	4:1	10.7	12.0	13.0	14.0	No	43 (min)	8		
0.46 mm steel sheet	2:1	7.4	9.7	11.6	13.5	Yes	43 (min)	8		
0.76 mm steel sheet	2:1	11.7	14.3	-	-	Yes	43 (min)	8		
0.76 mm steel sheet	2:1	-	-	19.9	23.3	Yes	54 Min)	8		

Table 4.6 Summary of Important Component Parameters for the Reference Component Data Set -Monotonic Test data by Yu et al. (2007) Phase 1

T I. I.	S	Strengtl	1	Stiffness	Duct	ility	Deformation Capacity
Test Label	Q <sub>M</sub> (kN)	Q <sub>D</sub> (kN)	$R_Q$	K <sub>I</sub> (kN /mm)	$\Delta_{ m Y,eff}$ (mm)	$\mu_{eff}$	Δ <sub>U</sub> (mm)
4×8×43×33-6/12-M1	18.2	11.3	1.62	0.62	29.4	1.98	58.1
4×8×43×33-6/12-M2	20.0	11.3	1.78	0.91	21.9	2.21	48.5
4×8×43×33-4/12-M1	20.9	12.5	1.67	0.94	22.2	2.66	59.0
4×8×43×33-4/12-M2	21.4	12.5	1.72	0.80	26.8	2.50	67.0
4×8×43×33-2/12-M1	23.4	13.9	1.68	0.72	32.5	2.18	71.0
4×8×43×33-2/12-M2	24.5	13.9	1.76	0.78	31.4	1.58	49.6
4×8×43×30-6/12-M1	14.3	9.72	1.47	0.44	32.4	2.45	79.3
4×8×43×30-6/12-M2	14.0	9.72	1.44	0.42	33.3	2.39	79.7
4×8×43×30-4/12-M1	16.7	10.8	1.54	0.50	33.4	2.17	72.4
4×8×43×30-4/12-M2	17.4	10.8	1.60	0.46	37.8	2.08	78.6
4×8×43×30-2/12-M1	19.2	11.4	1.68	0.52	36.9	2.80	103.5
4×8×43×30-2/12-M2	18.3	11.4	1.61	0.54	34.0	2.48	84.2
4×8×33×27-6/12-M1	11.5	6.91	1.66	0.46	24.9	2.33	58.0
4×8×33×27-6/12-M2	10.8	6.91	1.56	0.57	18.9	4.06	76.9
4×8×33×27-4/12-M1	12.2	7.58	1.61	0.60	20.3	2.66	54.0
4×8×33×27-4/12-M2	12.1	7.58	1.60	0.56	21.7	3.58	77.7
4×8×33×27-2/12-M1	15.2	9.02	1.69	0.68	22.4	2.80	62.7
4×8×33×27-2/12-M2	14.5	9.02	1.61	0.57	25.5	2.52	64.3
1M-a	7.93	3.29	2.41	0.96	8.23	8.87	73.0
1M-b	8.08	3.29	2.46	1.15	7.05	5.25	37.0
1M-c	7.82	3.29	2.37	1.52	5.13	6.97	35.7
2M-a	12.3	5.49	2.24	1.09	11.2	8.06	90.4
2M-b	12.0	5.49	2.18	1.37	8.76	11.4	100
3M-a	6.63	3.00	2.21	0.93	7.16	8.04	57.6
3M-b	6.80	3.00	2.27	0.87	7.86	7.66	60.2
4M-a	13.4	6.51	2.06	2.04	6.60	10.2	67.6

Table 4.7 Summary of Important Component Parameters for the Reference Component Data Set -Monotonic Test data by Yu et al. (2009) Phase 2

Total I de la	S	Strength	1	Stiffness	Duc	tility	Deformation Capacity
Test Label	Q <sub>M</sub> (kN)	Q <sub>D</sub> (kN)	$R_Q$	K <sub>I</sub> (kN/mm)	$\Delta_{ m Y,eff}$ (mm)	$\mu_{eff}$	Δ <sub>U</sub> (mm)
4M-b	13.4	6.51	2.06	2.17	6.17	10.2	63.0
5M-a	17.3	7.75	2.23	2.28	7.59	6.93	52.6
5M-b	16.3	7.75	2.10	2.16	7.57	8.52	64.5
5M-c	21.0	7.75	2.71	1.76	12.0	8.37	100
6M-a	20.6	11.4	1.81	1.84	11.2	8.92	100
6M-b	20.2	11.4	1.77	2.22	9.10	6.92	63.0
6М-с	23.3	11.4	2.04	2.22	10.5	5.55	58.2
8×6×350-43×33- 2-M1-C	32.4	20.9	1.55	3.27	9.91	5.72	56.7
8×6×350-43×30- 2-M1-C	33.5	17.1	1.95	2.72	12.3	3.98	49.0
8×6×600-43×33- 2-M1-C	36.1	20.9	1.73	1.28	28.2	2.71	76.4
8×6×350-54×33- 2-M1-B	45.3	29.9	1.51	2.38	19.0	3.06	58.3
8×6×350-43×27- 2-M1-D	36.9	18.7	1.97	2.63	14.0	4.39	61.5
8×6×350-54×33- 2-M1-C	53.1	29.9	1.77	2.19	24.2	3.17	76.8
11M-a	37.2	21.7	1.72	5.00	7.44	7.43	55.3
11M-b	37.6	21.7	1.73	4.08	9.23	5.52	51.0
12M-a	26.2	16.2	1.62	4.75	5.53	12.6	69.8
13M-a	33.9	17.1	1.98	3.69	9.18	6.39	58.7

Table 4.8 Summary of Important Component Parameters for the Reference Component Data Set –Reversed Cyclic Test data by Yu et al. (2007) Phase 1

T . I . I . I		Strength		Stiffness	Ducti	lity	Deformation Capacity
Test Label	Q <sub>M</sub> (kN)	Q <sub>D</sub> (kN)	RQ	K <sub>I</sub> (kN/mm)	$\Delta_{ m Y,eff} \ ( m mm)$	$\mu_{\mathrm{eff}}$	$\Delta_{ m U}$ (mm)
4×8×43×33- 6/12-C1	19.8	7.51	2.64	0.83	23.9	2.05	49.0
4×8×43×33- 6/12-C2	19.1	7.51	2.54	0.88	21.7	2.37	51.3
4×8×43×33- 4/12-C1	21.1	8.33	2.54	0.85	24.8	2.25	56.0
4×8×43×33- 4/12-C2	21.9	8.33	2.63	0.91	24.1	2.49	60.0
4×8×43×33- 2/12-C1	24.9	9.29	2.68	1.56	16.0	3.92	62.5
4×8×43×33- 2/12-C2	24.4	9.288	2.62	1.02	23.9	2.94	70.3
4×8×43×30- 6/12-C1	16.0	6.48	2.48	0.62	25.9	2.68	69.4
4×8×43×30- 6/12-C2	16.4	6.48	2.53	0.58	28.2	2.93	82.7
4×8×43×30- 4/12-C1	18.5	7.22	2.56	0.72	25.7	2.57	66.1
4×8×43×30- 2/12-C2	19.0	7.62	2.49	0.73	26.0	2.48	64.5
4×8×33×27- 6/12-C1	11.6	4.61	2.53	0.71	16.4	3.51	57.5
4×8×33×27- 6/12-C2	11.4	4.61	2.47	0.73	15.6	3.44	53.6
4×8×33×27- 4/12-C1	12.9	5.05	2.56	0.73	17.7	2.97	52.5
4×8×33×27- 4/12-C2	12.4	5.05	2.44	0.68	18.1	3.23	58.6
4×8×33×27- 2/12-C1	14.3	6.01	2.37	0.62	23.0	2.48	57.1
4×8×33×27- 2/12-C2	15.8	6.01	2.63	0.56	28.2	2.25	63.4
8×4×350- 33×18-6-C1	8.7	2.78	3.14	1.01	8.63	9.05	78.1
8×4×350- 33×18-6-C2	9.33	2.78	3.36	0.88	10.6	5.79	61.4
8×4×350- 43×33-2-C1- C	27.5	9.29	2.96	1.41	19.5	2.72	53.0
8×4×350- 43×33-2-C2- C	28.0	9.29	3.01	1.95	14.3	3.69	53.0
1C-a	7.71	2.20	3.51	1.06	7.26	6.31	45.8
1C-b	7.61	2.20	3.47	1.01	7.52	4.98	37.4

Table 4.9 Summary of Important Component Parameters for the Reference Component Data Set –Reversed Cyclic Test data by Yu et al. (2007) Phase 2

		Strength		Stiffness	Duct	ility	Deformation Capacity
Test Label	Q <sub>M</sub> (kN)	Q <sub>D</sub> (kN)	$R_Q$	K <sub>I</sub> (kN/mm)	$\Delta_{Y,eff}$ (mm	$\mu_{ m eff}$	Δ <sub>U</sub> (mm)
2C-a	13.3	3.66	3.65	1.27	10.5	7.89	83.0
2C-b	13.0	3.66	3.57	1.31	9.96	9.23	91.9
3C-a	7.05	2.00	3.52	0.88	8.03	7.82	62.8
3С-с	7.43	2.00	3.71	0.98	7.57	6.58	49.8
4C-a	14.4	4.34	3.33	1.90	7.61	6.71	51.1
4C-b	15.0	4.34	3.45	1.56	9.60	4.78	45.9
5C-a	17.6	5.17	3.41	1.93	9.16	5.87	53.8
5C-B	17.3	5.17	3.35	1.80	9.64	6.17	59.5
6C-a	20.9	7.62	2.74	1.84	11.4	6.98	79.3
6C-b	21.3	7.62	2.80	1.75	12.2	4.65	56.7
8×6×350-43×30-2- C1-A	27.9	11.4	2.44	2.62	10.7	5.43	57.9
8×6×350-43×30-2- C1-B	33.2	11.4	2.90	3.24	10.2	5.74	58.8
8×6×350-43×33-2- C1-C	40.8	13.9	2.93	2.94	13.9	3.72	51.6
8×6×350-43×33-2- C2-C	39.6	13.9	2.85	3.39	11.7	4.37	51.1
8×6×350-43×30-2- C1-C	35.8	11.4	3.13	3.17	11.3	3.99	45.0
8×6×350-43×30-2- C2-C	36.6	11.4	3.21	2.83	12.9	3.48	45.0
8×6×600-43×33-2- C1-C	40.0	13.9	2.87	1.70	23.5	2.29	53.8
8×6×600-43×33-2- C2-C	39.4	13.9	2.83	3.00	13.1	3.09	40.6
8×6×350-54×33-2- C1-B	49.2	19.9	2.47	2.97	16.6	3.23	53.5
8×6×350-54×33-2- C2-B	50.6	19.9	2.54	3.14	16.1	3.10	50.0
8×6×350-43×27-2- C1-D	39.1	12.4	3.13	2.90	13.5	4.10	55.4
8×6×350-54×33-2- C1-C	53.3	20.0	2.67	3.07	17.3	3.56	61.8

Table 4.10 Summary of Important Component Parameters for the Reference Component Data Set –Reversed Cyclic Test data by Balh (2010) and Ong-Tone (2009)

Test Label	S	Strength		Stiffness	Duct	tility	Deformation Capacity
Test Laber	Q <sub>M</sub> (kN)	Q <sub>D</sub> (kN)	$R_{Q}$	K <sub>I</sub> (kN/mm)	$\Delta_{Y,eff}$ (mm)	$\mu_{\mathrm{eff}}$	$\Delta_{ m U}$ (mm)
8×6×350- 54×33-2- C2-C	58.0	20.0	2.91	3.10	18.7	2.95	55.2
11C-a	39.4	14.4	2.73	2.29	17.2	3.26	56.1
11C-b	39.0	14.4	2.70	2.79	14.0	3.52	49.1
8×6×350- 43×27-2- C1-D	39.1	12.5	3.13	2.90	13.5	4.10	55.4
8×6×350- 54×33-2- C1-C	53.2	20.0	2.67	3.07	17.3	3.56	61.8
8×6×350- 54×33-2- C2-C	58.0	20.0	2.91	3.10	18.7	2.95	55.2
11C-a	39.4	14.4	2.73	2.29	17.2	3.26	56.1
11C-b	39.0	14.4	2.70	2.79	14.0	3.52	49.1

Assuming a lognormal distribution of the data collected from the testing programs of the reference components as described in FEMA P-795 (2011), the median and lognormal standard deviation values are computed for each of the component parameters:

 $Q_{M:}$  Maximum load applied to a component during cyclic-load testing, based on positive and negative cycles of loading

 $K_I$ : Effective value of initial stiffness of the component test specimen through the secant at 0.4QM, based on positive and negative cycles of loading

 $\Delta_U$ : Ultimate deformation of a component test specimen at 0.8QM based on positive and negative cycles of loading during cyclic load testing,

 $\Delta_{Y,eff}$ : Effective yield deformation of a component test specimen during cyclic-load testing based on positive and negative cycles of loading.

 $\mu_{eff}$ : Effective ductility capacity of a component test specimen, defined as the ultimate deformation,  $\Delta_U$ , divided by the effective yield deformation,  $\Delta_{Y,eff}$ .

 $Q_{MM}$ : Maximum load applied to a component during monotonic testing.

 $\Delta_{UM}$ : Ultimate deformation of a component test specimen at 0.8QMM based on monotonic-load testing.

 $Q_D$ : Load corresponding to the specified design strength of a component configuration, as derived from, or specified in, design requirements documentation.

 $K_D$ : Design stiffness of proposed or reference component configuration, as derived from, or specified in, design requirements documentation.

 $R_Q$ : Ratio of the maximum cyclic load, QM, to the design load, QD, of a component test specimen.

 $R_K$ : Ratio of initial stiffness, KI, to design stiffness, KD, for a component test specimen. The following steps should be followed to compute the reference component statistics for every component performance group (median and lognormal standard deviation values). The computation of  $\widetilde{\Delta}_{U,PC}$  is used as an example:

- 1. Calculate the natural logarithm of  $\Delta_{U,RC}$ , LN[ $\Delta_{U,RC}$ ], for each test.
- 2. Calculate the average of the LN[ $\Delta_{U,RC}$ ] values.
- 3. Calculate the exponent of the result obtained from step (2)  $e^{Mean(LN[\Delta U,RC])}$ . The result obtained from step (3) represent the fitted median value,  $\widetilde{\Delta}_{U,RC}$
- 4. Calculate the standard deviation of LN[ $\Delta_{U,RC}$ ] values. The result obtained from step (4) represent the fitted logarithmic standard deviation value,  $\sigma_{\Delta U,RC}$

Table 4.11 Summary Statistics for Reference Component Parameters- Monotonic Tests (43 specimens)

Performance Group	Summary Statistics	$R_Q = V_M / V_D$	$\mu_{e\!f\!f}$	$arDelta_U$
	Median	$\tilde{R}_{\mathcal{Q}}$ =1.831	$\widetilde{\mu}_{Eff}$ =4.365	$\widetilde{\Delta}_{U}$ =65.155
1	Variability	$\sigma_{\tilde{R}Q}$ =0.158	$\sigma_{\widetilde{\mu}eff}$ =0.594	$\sigma_{\widetilde{A}U} = 0.240$

Table 4.12 Summary Statistics for Reference Component Parameters- Reversed Cyclic Tests (53 specimens)

Performance Group	Summary Statistics	$R_Q = V_M/V_D$	$\mu_{e\!f\!f}$	$\Delta_U$
	Median	$\tilde{R}_{Q}=2.869$	$\widetilde{\mu}_{Eff}$ =3.896	$\widetilde{\Delta}_{U} = 56.923$
1	Variability	$\sigma_{\tilde{R}Q}=0.131$	$\sigma_{\widetilde{\mu}eff}$ =0.409	$\sigma_{\widetilde{\Delta}U} = 0.183$

PROPOSED COMPONENT TEST DATA

PROPOSED COMPONENT DESIGN SPACE

The proposed components are defined as cold-formed steel framed shear walls with steel

sheathing designed with full frame blocking and thick sheathing / framing members. With

the purpose to represent a wide variation of configurations, the tested proposed component

are characterized by a variation in system geometry, component sections, material

properties and detailing. The general characteristics are listed below and a more detailed

description of each configuration of the proposed components is provided in Tables 4.10

and 4.11.

Wall Dimensions (height and length (mm:ft)):1240x2440 (4x8) to 2440x2440 (8x8).

Aspect ratio (height/length): 2:1 to 1:1 (aspect ratios above 2:1 are not included in the

design space).

Openings: No opening are considered.

Sheathing thickness (mm:in): 0.46 (0.018) to 0.76 (0.03).

Framing thickness (mm:in): 1.09 (0.046) to 2,49 (0.098)

Edge spacing: 50 (2) to 150 (6),

Field spacing: 300 (12)

Sheathing screws spacing (mm:in) (on-center):

Tables 4.10 and 4.11 list the various configurations of the proposed components analyzed

respectively by DaBreo (2012) and the author of this document, respectively. The shear

wall specimens were tested under both monotonic and reversed cyclic loading.

Table 4.13 Summary of cold-formed steel framed steel sheathed shear walls designed with full frame blocking and thick sheathing / framing members (DaBreo (2012)).

Test Label	Wall Dimensions	Framing Thickness (in:mm)	Steel Sheet Thickness (mm:in.)	Fastener spacing Perimeter/Field (in./in.): (mm/mm)	Number of monotonic tests	Number of cyclic tests	Fastener Size (No.)
B1	1220×2440 (4×8)	0.054:1. 37	0.03:0.76	2/12 : 5/300	1	1	8
B2	1220×2440 (4×8)	0.043:1. 09	0.018 : 0.46	2/12 : 50/300	1	1	8
В3	1220×2440 (4×8)	0.043:1. 09	0.03:0.76	4/12 :100/300	1	1	8
B4	1220×2440 (4×8)	0.043:1. 09	0.03:0.76	6/12 :150/300	1	1	8
В5	1220×2440 (4×8)	0.043:1. 09	0.018 : 0.46	4/12 :100/300	1	1	8
В6	1220×2440 (4×8)	0.043:1. 09	0.018 : 0.46	6/12 :150/300	1	1	8
В7	1220×2440 (4×8)	0.054:1. 37	0.03:0.76	3/12:75/300	1	1	8

Table 4.14 Summary of cold formed steel framed steel sheathed shear walls designed with full frame blocking and thick sheathing / framing members (Rizk (2017)).

Test Label	Wall Dimensions	Framing Thickness (in:mm)	Steel Sheet Thickness (mm:in.)	Fastener spacing Perimeter/Field (in./in.): (mm/mm))	Number of monotonic tests	Number of cyclic tests	Fastener Size (No.)
W1	1220×2440 (4×8)	0.068:1.73	0.03:0.76	2/12 : 51/305	1	1	8
W2	1220×2440 (4×8)	0.097:2.46	0.03:0.76	2/12 : 51/305	1	1	8
W3	610×2440 (2×8)	0.054:1. 37	0.03:0.76	2/12 : 51/305	1	1	8
W4	610×2440 (2×8)	0.054:1. 37	0.03:0.76	3/12 : 76/305	1	1	8
W5	610×2440 (2×8)	0.054:1. 37	0.03:0.76	4/12 : 102/305	1	1	8
W6	610×2440 (2×8)	0.054:1. 37	0.03:0.76	6/12 : 152/305	1	1	8
W7	1830×2440 (6×8)	0.054:1. 37	0.03:0.76	2/12: 51/305	1	1	8
W8	1830×2440 (6×8)	0.054:1. 37	0.03:0.76	3/12 : 76/305	1	1	8
W9	1830×2440 (6×8)	0.054:1. 37	0.03:0.76	4/12 : 102/305	1	1	8
W10	1830×2440 (6×8)	0.054:1. 37	0.03:0.76	6/12 : 152/305	1	1	8
W11	2440×2440 (8×8)	0.054:1. 37	0.03:0.76	2/12: 51/305	1	1	8
W12	2440×2440 (8×8)	0.054:1. 37	0.03:0.76	3/12 : 76/305	1	1	8
W13	2440×2440 (8×8)	0.054:1. 37	0.03:0.76	4/12 : 102/305	1	1	8
W14	2440×2440 (8×8)	0.054:1. 37	0.03:0.76	6/12 : 152/305	1	1	8

#### 4.6.2 PROPOSED COMPONENT PERFORMANCE GROUPS

Referring to Section 2.6.5 of FEMA P-795 (2011), and consistent with the approach taken for the reference component data set, the proposed component data were compiled in a single performance group.

#### 4.6.3 TEST DATA & SUMMARY STATISTICS

The proposed component test data are compiled into a single performance group. The proposed component data set for monotonic and reversed cyclic loading are listed in Tables 4.12 and 4.13, respectively.

Table 4.15 Summary of Important Component Parameters for the Proposed

Test	S	Strength		Stiffness	Ductility		Deformation Capacity
Label	Q <sub>M</sub> (kN)	Q <sub>D</sub> (kN)	$R_{Q}$	K <sub>I</sub> (kN /mm)	$\Delta_{ m Y,eff}$ (mm)	$\mu_{eff}$	$\Delta_{ m U}$ (mm)
B1-M	41.4	17.0	2.43	1.93	21.5	3.46	74.3
B2-M	20.6	9.88	2.09	1.10	18.8	3.64	68.3
В3-М	23.7	10.5	2.26	1.11	21.3	2.40	51.2
B4-M	20.5	8.56	2.40	1.67	12.3	4.39	54.0
B5-M	14.6	7.1	2.06	0.85	17.2	3.25	55.9
В6-М	11.4	5.41	2.10	1.19	9.54	6.92	66.0
B7-M	34.2	14.6	2.35	1.65	20.7	3.08	63.8
W1-M	42.5	17.0	2.50	1.49	28.54	2.93	83.7
W2-M	47.7	17.0	2.81	1.98	24.1	3.56	85.9
W7-M	61.2	25.6	2.39	4.71	13.00	5.81	75.5
W8-M	51.1	21.8	2.34	2.56	20.0	2.98	59.4
W9-M	46.7	15.7	2.98	3.49	13.4	5.01	67.0
W10-M	34.7	12.8	2.70	2.64	13.1	3.81	50.0
W11-M	80.2	34.1	2.35	6.70	12.0	7.25	86.8
W12-M	70.2	29.1	2.41	4.34	16.2	3.34	54.0
W13-M	60.2	20.9	2.88	6.06	9.93	4.27	42.4
W14-M	47.6	17.1	2.780	6.050	7.860	5.440	42.8

Table 4.16 Summary of Important Component Parameters for the Proposed

Test	S	Strength		Stiffness	Ductil	ity	Deformation Capacity
Label	Q <sub>M</sub> (kN)	Q <sub>D</sub> (kN)	$R_Q$	K <sub>I</sub> (kN /mm)	$\Delta_{ m Y,eff}$ (mm)	$\mu_{ m eff}$	Δ <sub>U</sub> (mm)
B1-R	38.2	17.0	2.24	1.87	20.5	3.43	70.1
B2-R	20.5	9.88	2.08	1.52	13.5	5.21	70.4
B3-R	25.3	10.5	2.41	1.95	13.0	3.46	45.0
B4-R	20.1	8.56	2.35	2.12	9.49	4.49	42.6
B5-R	15.1	7.10	2.13	1.43	10.6	3.88	41.2
B6-R	11.6	5.41	2.14	1.21	9.53	3.61	34.4
W1-C	43.9	17.0	2.57	1.81	24.22	2.62	63.6
W2-C	49.9	17.0	2.93	2.37	21.1	2.88	60.7
W7-C	56.3	25.6	2.20	4.08	13.8	5.92	81.8
W8-C	52.4	21.8	2.40	4.14	12.7	4.44	56.2
W9-C	45.7	15.7	2.91	3.49	13.1	3.66	47.9
W10-C	36.4	12.8	2.84	4.09	8.92	5.26	46.9
W11-C	82.1	34.1	2.41	6.97	11.8	5.46	64.3
W12-C	72.2	29.1	2.48	6.50	11.1	4.01	44.5
W13-C	59.2	20.9	2.83	4.70	12.6	3.13	39.5
W14-C	45.5	17.1	2.66	4.86	9.4	3.86	36.2

Assuming a lognormal distribution of the data collected from the testing programs of the proposed components as described in FEMA P-795 (2011), the median and lognormal standard deviation values are computed for each of the component parameters:

 $Q_{M:}$  Maximum load applied to a component during cyclic-load testing, based on positive and negative cycles of loading

 $K_I$ : Effective value of initial stiffness of the component test specimen through the secant at 0.4QM, based on positive and negative cycles of loading

 $\Delta_U$ : Ultimate deformation of a component test specimen at 0.8QM based on positive and negative cycles of loading during cyclicload testing,

 $\Delta_{Y,eff}$ : Effective yield deformation of a component test specimen during cyclic-load testing based on positive and negative cycles of loading.

 $\mu_{eff}$ : Effective ductility capacity of a component test specimen, defined as the ultimate

deformation,  $\Delta_U$ , divided by the effective yield deformation,  $\Delta_{Y,eff}$ .

 $Q_{MM}$ : Maximum load applied to a component during monotonic testing.

 $\Delta_{UM}$ : Ultimate deformation of a component test specimen at 0.8QMM based on monotonic-load testing.

 $Q_D$ : Load corresponding to the specified design strength of a component configuration, as derived from, or specified in, design requirements documentation.

 $K_D$ : Design stiffness of proposed or reference component configuration, as derived from, or specified in, design requirements documentation.

 $R_Q$ : Ratio of the maximum cyclic load, QM, to the design load, QD, of a component test specimen.

 $R_K$ : Ratio of initial stiffness, KI, to design stiffness, KD, for a component test specimen.

The following steps should be followed to compute the reference component statistics for every component performance group (median and lognormal standard deviation values). The computation of  $\widetilde{\Delta}_{U,PC}$  is used as an example:

- 1. Calculate the natural logarithm of  $\Delta_{U,RC}$ , LN[ $\Delta_{U,RC}$ ], for each test.
- 2. Calculate the average of the LN[ $\Delta_{U,RC}$ ] values.
- 3. Calculate the exponent of the result obtained from step (2)  $e^{Mean(LN[\Delta U,RC])}$ . The result obtained from step (3) represent the fitted median value,  $\widetilde{\Delta}_{U,RC}$
- 4. Calculate the standard deviation of LN[ $\Delta_{U,RC}$ ] values. The result obtained from step (4) represent the fitted logarithmic standard deviation value,  $\sigma_{\Delta U,RC}$

Table 4.17 Summary Statistics for Proposed Component Parameters- Monotonic Tests, (17 specimens)

Performance Group	Summary Statistics	$R_Q = V_M / V_D$	$\mu_{e\!f\!f}$	$arDelta_U$
	Median	$\tilde{R}_{Q}$ =2.445	$\widetilde{\mu}_{Eff}$ =4.009	$\tilde{\Delta}_{U}$ =62.089
1	Variability	$\sigma_{\tilde{R}Q}$ =0.112	$\sigma_{\widetilde{\mu}eff}$ =0.315	$\sigma_{\widetilde{\Delta}U} = 0.226$

Table 4.18 Summary Statistics for Proposed Component Parameters- Reversed Cyclic Tests, (16 specimens)

Performance Group	Summary Statistics	$R_Q = V_M/V_D$	$\mu_{e\!f\!f}$	$\Delta_U$
	Median	$\tilde{R}_{Q}$ =2.458	$\widetilde{\mu}_{Eff}$ =3.978	$\widetilde{\Delta}_U$ =51.127
1	Variability	$\sigma_{\tilde{R}Q}$ =0.115	$\sigma_{\widetilde{\mu}eff}$ =0.235	$\sigma_{\widetilde{\Delta}U}$ =0.262

#### 4.7 EVALUATE QUALITY RATINGS

#### 4.7.1 QUALITY RATING OF TEST DATA

Referring to Section 3.7.1 of FEMA P-795 (2011), quality ratings are assigned because the quality of the test data on which the collapse prediction is based affects the uncertainty in the collapse capacity of a structural system.

Table 4.16 should be used in order to rate the test data for the reference component and the proposed component. Two factors should be taken into consideration to evaluate the quality rating of the test data:

- Completeness and robustness of the overall testing program.
- The confidence in the test results.

According to Section 2.3.3 of FEMA P-795 (2011), the quality rating of design requirements and test data should be Good or Superior for the reference components, and should be Fair, Good or Superior for the proposed components.

Table 4.19 Quality Rating of Test Data, (FEMA P-795, 2011)

Completeness and Robustness of Tests	Confidence in Test Results			
Completeness and Robustness of Tests	High	Medium	Low	
High. Material, component, and connection behavior well understood and accounted for. All, or nearly all, important testing issues addressed.	Superior	Good	Fair	
Medium. Material, component, and connection behavior generally understood and accounted for. Most important testing issues addressed.	Good	Fair	Not Permitted	
Low. Material, component, and connection behavior fairly understood and accounted for. Several important testing issues not addressed.	Fair	Not Permitted	Not Permitted	

Various factors listed in Section 2.7 of FEMA P-795 must be taken into consideration in

order to evaluate the completeness and robustness of the testing program and the

confidence in test results of the reference and proposed components.

The reference components were tested in the structures laboratories of McGill University

and the University of North Texas. Multiple researchers were involved in completing the

testing programs and a large number of tests were performed on various specimen

configurations. In addition, all important testing issues were properly addressed and all

important failure modes were uncovered in the testing programs. For these reasons, and

referring to Table 4.16, the data compiled from the reference component testing program

is rated Superior. This rating results from

• High rating for confidence in Test Results

• High rating for completeness and robustness of tests.

Reference component :  $\underline{OK}$ 

The proposed components were tested in the structures laboratory of McGill University.

Multiple researchers were involved in completing the testing programs and a large number

of tests were performed on various specimen configurations. In addition, all important

testing issues were properly addressed and all important failure modes were uncovered in

the testing. For these reasons, and referring to Table 4.16, the data compiled from the

reference component testing program is rated Superior. This rating results from

High rating for confidence in Test Results

High rating for completeness and robustness of tests.

Proposed component :  $\underline{OK}$ 

163

#### 4.7.2 QUALITY RATING OF DESIGN REQUIREMENTS

Referring to Section 3.7.2 of FEMA P-795 (2011), quality ratings are assigned because the uncertainty in the overall collapse performance of the structural system is affected by the quality of the design requirements. Table 4.17 should be used in order to rate the design requirements for the reference component. Two factors should be taken into consideration to evaluate the quality rating of design requirements.

- Completeness and Robustness of Design Requirements
- Confidence in Design requirements

Table 4.20 Quality Rating of Design Requirements, (FEMA P-795, 2011)

Completeness and Robustness of	Confidence in Design Requirements		
Design Requirements	High	Medium	Low
High. Extensive safeguards against unanticipated failure modes. All important design and quality assurance issues are addressed.	Superior	Good	Fair
Medium. Reasonable safeguards against unanticipated failure modes. Most of the important design and quality assurance issues are addressed.	Good	Fair	Not Permitted
Low. Questionable safeguards against unanticipated failure modes. Many important design and quality assurance issues are not addressed.	Fair	Not Permitted	Not Permitted

The reference components were constructed in a controlled laboratory environment at McGill University and the University of North Texas, with rigorous quality control and according to clear construction requirements. In addition, multiple research programs were conducted in various academic institutions allowing a good understanding of the component behaviour.

For these reasons, and referring to Table 4.17, the reference component design requirements is rated Superior. This rating results from

High rating for confidence in Design Requirements.

• High rating for completeness and robustness of Design Requirements.

Reference component :  $\underline{\underline{OK}}$ 

The proposed components were constructed in a controlled laboratory environment at

McGill University, with rigorous quality control and according to clear construction

requirements. In addition, the research programs conducted at McGill University consisted

of testing a large number of specimen, allowing a good understanding of the component

behavior.

For these reasons, and referring to Table 4.17, the proposed component design

requirements is rated Superior. This rating results from

• High rating for confidence in Design Requirements.

• High rating for completeness and robustness of Design Requirements.

Reference component :  $\underline{OK}$ 

EVALUATE COMPONENT EQUIVALENCY

4.8.1 **OVERVIEW** 

The equivalency between the proposed and reference components is evaluated in this section

based on several acceptance criteria. The acceptance criteria listed in Tables 4.18 and 4.19

are based on the summary statistics of the proposed and reference component performance

parameters in each component performance group computed in Sections 4.4 and 4.5

according to the requirements of FEMA P-795 (2011). In order to consider the proposed

components equivalent to the reference components, the comparison of summary statistics

must comply with the acceptance criteria listed in Tables 4.18 and 4.19 across all

performance groups.

165

Table 4.21 Summary of Acceptance Criteria (Cyclic-Load Test Data), (FEMA P-795, 2011)

Requirements Based on Cyclic-Load Test Data			
Ultimate Deformation Capacity (performance	$\widetilde{\Delta}_{U,PC} \geq \widetilde{\Delta}_{U,RC} P_U P_Q$		
group)	_		
Ultimate Deformation Capacity (individual	$\widetilde{\Delta}_{Uj,PC} \ge (1-1.5\widetilde{\sigma}_{\Delta RC})(\widetilde{\Delta}_{U,RC}) P_U P_Q$		
configurations)	2,1.0,7, 2		
Initial Stiffness Ratio	$0.75 \le \tilde{R}_{K,PC} / \tilde{R}_{K,RC} \le 1.33$		
Effective Ductility Capacity	$\widetilde{\mu}_{Eff,PC} \geq 0.5 \ \widetilde{\mu}_{Eff,RC}$		

Table 4.22 Summary of Acceptance Criteria (Monotonic-Load Test Data), (FEMA P-795, 2011)

Requirements Based on Monotonic-Load Test Data		
Ultimate Deformation Capacity (Option 1)	$\widetilde{\Delta}_{UM,PC} \geq \widetilde{\Delta}_{UM,RC} P_U P_Q$	
Ultimate Deformation Capacity (Option 2)	$\widetilde{\Delta}_{UM,PC} \geq 1,2 \ \widetilde{D}_C \widetilde{\Delta}_{UM,RC} P_U P_Q$	

# 4.8.2 REQUIREMENTS BASED ON CYCLIC-LOAD TEST DATA: STRENGTH AND ULTIMATE DEFORMATION

Requirements for Component Performance Groups.

Referring to Equation 4.1, the median value of the ultimate deformation  $\widetilde{\Delta}_{U,PC}$  for each proposed component performance group should be compared with the median value of ultimate deformation capacity for the associated reference component performance group  $\widetilde{\Delta}_{U,RC}$ .

$$\widetilde{\Delta}_{U,PC} \ge \widetilde{\Delta}_{U,RC} P_U P_Q$$
 (4.1)

Referring to Tables 4.9 and 4.15, the median ultimate deformations of the reference and proposed component data set,  $\widetilde{\Delta}_{U,RC}$  and  $\widetilde{\Delta}_{U,RC}$  are 56.9 and 51.1 mm respectively.

As shown in Table 4.20, the uncertainty factor  $P_U$  is based on the quality rating of the proposed component test data and the relative quality ratings of the proposed and reference component design requirements.

Table 4.23 Penalty Factor to Account for Uncertainty,

Penalty Factor for Uncertainty (P <sub>U</sub> )			
Quality Rating of	Quality Rating of Proposed Component Design Requirements Relative to		
Proposed Component	Reference Component Design Requirements		
Test Data	Higher	Same	Lower
Superior	0.95	1.00	1.15
Good	1.00	1.05	1.25
Fair	1.15	1.25	1.40

Referring to Section 4.7, the quality Rating of both proposed and reference Component Test Data is superior. Based on Table 4.20, the penalty factor  $P_U$ =1.00.

As shown in Table 4.21, the load penalty factor  $P_Q$  is based on the strength ratio  $\tilde{R}_{Q,PC}/\tilde{R}_{Q,RC}$ . Referring to Tables 4.9 and 4.15

$$\frac{\tilde{R}_{Q,PC}}{\tilde{R}_{Q,RC}} = \frac{2.458}{2.869} = 0.895$$

**Table 4.24 Penalty Factor to Account for Differences in Load (Strength)** 

Penalty Factor for Differences in Strength (PQ)			
$ ilde{R}_{Q,PC}/ ilde{R}_{Q,RC}$	$P_Q$	$ ilde{R}_{Q,PC}/ ilde{R}_{Q,RC}$	$P_Q$
0.50	1.88	1.10	1.00
0.60	1.55	1.20	1.00
0.70	1.31	1.30	1.04
0.80	1.14	1.40	1.09
0.90	1.00	1.50	1.13
1.00	1.00	1.60	1.24
1.10	1.00	1.70	1.32

Table 4.21 shows the strength penalty factor  $P_Q$ =1.00.

Incorporating these values indicate that the median ultimate deformation value of the proposed component does not meet the requirement of Equation 4.1.

$$51.127 \leq 56.923 \times 1.00 \times 1.00 \rightarrow \underline{NOT\ OK}$$

Requirements for Individual Component Configurations:

Referring to Equation 4.2, the median value of ultimate deformation for each configuration j,  $\widetilde{\Delta}_{Uj,PC}$ , should be compared with the median value the ultimate deformation capacity for the associated reference component performance group,  $\widetilde{\Delta}_{U,RC}$ 

$$\widetilde{\Delta}_{Uj,PC} \ge (1-1.5\widetilde{\sigma}_{\Delta U,RC})(\widetilde{\Delta}_{U,RC})P_{U}P_{Q}$$
 (4.2)

If  $\widetilde{\sigma}_{\Delta U,RC} > 0.3$  , then 0.3 should be used in Equation 4.2.

According to Table 4.9, the variability in ultimate deformation  $\tilde{\sigma}_{\Delta U,RC}$  Is 0.183 for the reference component data.

$$\widetilde{\Delta}_{Uj,PC} \ge (1-1.5(0.183))(56.923)(1.00)(1.00)$$

$$\widetilde{\Delta}_{Uj,PC} \ge 41.298$$

Table 4.25 Evaluation of Equivalency Acceptance Criteria for Individual Component Configurations

	Deformation Capacity	Acceptance Check	
Test Label	$\Delta_U \ (mm)$	Acceptance Criteria (mm)	Pass/Fail
B1-R	70.1	41.3	Pass
B2-R	70.4	41.3	Pass
B3-R	45.0	41.3	Pass
B4-R	42.6	41.3	Pass
B5-R	41.2	41.3	Fail
B6-R	34.4	41.3	Fail
W1-C	63.6	41.3	Pass
W2-C	60.7	41.3	Pass
W7-C	81.8	41.3	Pass
W8-C	56.2	41.3	Pass
W9-C	47.9	41.3	Pass
W10-C	46.9	41.3	Pass
W11-C	64.3	41.3	Pass
W12-C	44.5	41.3	Pass
W13-C	39.5	41.3	Fail
W14-C	36.2	41.3	Fail

As shown in Table 4.22 configuration B5-R, B6-R, W13-C and W14-C do not meet the criteria listed in section 2.7 of the FEMA P-795 (2011).

$$\widetilde{\Delta}_{Uj,PC} \geq (1\text{-}1.5\widetilde{\sigma}_{\Delta U,RC})(\widetilde{\Delta}_{U,RC})\,P_{U}P_{Q} \to \underline{NOT~OK}$$

# 4.8.3 REQUIREMENTS BASED ON CYCLIC-LOAD TEST DATA: EFFECTIVE DUCTILITY CAPACITY

Referring to Equation 4.4, the median value of the effective ductility capacity of the proposed component should be greater or equal to 50% of the median value of the effective ductility capacity of the reference component. This requirement ensures approximate parity between the post-yield deformation capacities of the proposed and reference components.

$$\widetilde{\mu}_{Eff,PC} \ge 0.5 \ \widetilde{\mu}_{Eff,RC}$$
 (4.3)

Referring to Tables 4.9 and 4.15,

$$3.978 \ge 0.5(3.896) = 1.948 \rightarrow \underline{OK}$$

# 4.8.4 REQUIREMENTS BASED ON CYCLIC-LOAD TEST DATA: EFFECTIVE INITIAL STIFFNESS

Referring to Equation 4.4, the median value of the proposed component initial stiffness ratio  $\tilde{R}_{K,PC}$  Should be comprised within the range

$$0.75 \le \tilde{R}_{K,PC} \le 1.33.$$
 (4.4)

# 4.8.5 REQUIREMENTS BASED ON MONOTONIC-LOAD TEST DATA: ULTIMATE DEFORMATION

The median value of the proposed component ultimate deformation for each component performance group  $\widetilde{\Delta}_{UM,PC}$ , should satisfy the requirement of either Equation 4.5 or 4.6.

$$\widetilde{\Delta}_{UM,PC} \ge \widetilde{\Delta}_{UM,RC} P_U P_Q$$
 (4.5)

$$\widetilde{\Delta}_{UM,PC} \ge 1.2 \, \widetilde{D}_C \widetilde{\Delta}_{UM,RC} P_U P_Q$$
 (4.6)

The cyclic-load ultimate deformation  $\widetilde{\Delta}_{U,PC}$  may be used in lieu of the monotonic load ultimate deformation  $\widetilde{\Delta}_{UM,PC}$  in equation 4.6.

Referring to Tables 4.8 and 4.14,  $\widetilde{\Delta}_{UM,PC}$  is equal to 62.089mm and  $\widetilde{\Delta}_{UM,RC}$  is equal to 65.155mm.

Referring to section 4.7, the quality Rating of both proposed and reference Component Test Data is superior. Based on Table 4.20, the penalty factor  $P_U$ =1.00.

As shown in Table 4.21, the load penalty factor  $P_Q$  is based on the strength ratio  $\tilde{R}_{Q,PC}/\tilde{R}_{Q,RC}$ . Referring to tables 4.8 and 4.14

$$\frac{\tilde{R}_{Q,PC}}{\tilde{R}_{O,RC}} = \frac{2.445}{1.831} = 1.33$$

Table 4.21 shows the strength penalty factor  $P_Q$ =1.04.

Incorporating these values indicate that the median ultimate deformation value of the proposed component does not meet the requirement of equation 4.5.

$$62.89 \le 65.155(1.0)(1.03) \le 67.11 \to \underline{NOT\ OK}$$

#### 4.9 CONCLUSION

Based on the analysis conducted with respect to the requirements listed in the FEMA P-795 (2011), it was found that cold-formed steel framed steel sheathed shear walls designed with full frame blocking and thick sheathing / framing members is not equivalent to Light-Frame (cold-formed steel) walls sheathed with steel panels. It is important to mention that the data available to conduct such an analysis was not large enough. The results indicate that the proposed components have a higher overstrength than the reference components, requirements based on ductility capacity were satisfied but a slightly lower median deformation capacity than the reference components. In order for shear walls designed with full frame blocking and thick Sheathing / Framing Members to be found equivalent, it is suggested to generate additional test data. In addition, the available data for the reference component did not include two component test specimens per shear wall configuration as suggested by the FEMA P-795 (2011). It is then reasonable to say that the application of the FEMA P795 was not entirely conclusive. It is recommended to apply the FEMA P-695 methodology, in which R values are evaluated using a non-linear response history dynamic analyses of representative structures, whose load-deformation response is modelled after the results of the shear wall tests.

### 5 CHAPTER 5- CONCLUSIONS AND

#### RECOMMENDATIONS

#### 5.1 CONCLUSIONS

The current North American Standards, AISI S240 (2015) & AISI S400 (2015), provide design information for steel sheathed shear walls having a maximum sheathing thickness of 0.84mm (0.33") and a 1.37mm (0.54") thick frame (Balh et al. 2014, DaBreo et al. 2014, Yu 2010, Yu & Chen 2011). The specimens tested as part of past research programs composed of these members developed a shear resistance close to 30 kN/m (2058lb/ft) (#10 screws @ 50 mm (2") o.c.). There is a demand to be able to design all-steel shear walls that are capable of developing lateral resistance beyond 100 kN/m (6860lb/ft) to bridge the gap between cold-formed steel and hot-rolled steel lateral framing shear wall systems. DaBreo (2012) showed that full blocking of the stud members increased the resistance of the shear walls by up to 25%. In addition, the results showed that the quarter point blocking members were effective in reducing the twisting deformations and local buckling of the chord studs. The first objective of the current research project was to analyze the influence of the wall length for shear walls designed and built with quarter point blocking members. The second objective was to determine the influence of the framing thickness on the performance of the shear walls.

The testing program executed in the winter of 2016 consisted of 28 (14 configurations) fully blocked cold-formed shear walls. The walls were designed and built with a single sided cold-formed steel sheathing having a nominal thickness of 0.76mm (0.03") connected to a cold-formed steel frame. Specimens were designed having different wall length, framing thickness (wall studs, blockings and tracks), and fastener spacing. Every configuration was tested according to the monotonic and CUREE reversed-cyclic loading protocols. As predicted prior to testing, the dominant mode of failure was in most cases was located at the screw connections between the sheathing and the cold-formed steel frame, i.e. Bearing sheathing failure, tilting of sheathing screw, pull-out failure of sheathing screw, pull-through sheathing and tear-out of sheathing. The short walls (4:1 aspect ratio (610×2440mm) (2'×8')) tested as part of this research program suffered from a high level of in-plane rotation, as anticipated.

The flat sheathing panels experienced tear out at the bottom corner fastener locations. In addition, the chord studs suffered from local buckling caused by a combination of axial compression and bending, a mode of failure that was dominant in the case of slender walls. Walls having an aspect ratio of 2:1 (1220×2440mm (4'×8')), constructed with heavier frames suffered from flange and lip distortion of the chord studs at the top and bottom corners, caused by the torsion load applied to these members due to the placement of the sheathing. Further, tear out of the sheathing at the bottom corners was observed. In addition, the pull through sheathing failure mode occurred along the field studs, and deformations of the upper tracks and uplift of the bottom tracks were observed. Walls of size 1830×2440mm (6'×8') and 2440×2440mm (8'×8') suffered from different modes of failures. The field stud of the walls designed with closely spaced sheathing fasteners did suffer from damage caused by the overall out-of-plane bending of the walls. The full blocking did not restrict effectively this deformation mode for the longer walls.

For Canada, the data analysis was conducted using the Equivalent Energy Elastic Plastic (EEEP) methodology, which consists of modeling the energy dissipated by the shear wall specimen subjected to monotonic or reversed-cyclic loading using a bi-linear curve. The EEEP curve illustrates the behaviour of a perfectly elastic/plastic shear wall. Several design parameters were obtained from the EEEP curve, such as shear resistance values, lateral displacement values, elastic stiffness, ductility and energy dissipation. The equivalent parameters were also obtained for the United States of America and Mexico.

The data collected from the tests indicates that a wall's shear resistance is inversely proportional to the sheathing fastener spacing. This was expected, because sheathing fastener configurations with a smaller screw spacing behave as a group in resisting the shear forces applied to a wall. Each individual fastener in the configurations having a denser screw spacing has to resist forces of smaller magnitude compared to the connectors of the configurations designed with larger fastener spacing. Second, data shows that the shear resistance (normalized to length) is not affected by the wall length for walls having an aspect ratio (h:w) less than (2:1). Third, as predicted, the shear resistance of the walls is proportional to the framing thickness. Lastly, the analysis of the effect of frame blocking indicated that the blocked walls developed higher ultimate shear resistances, Su, and yield shear resistances,

S<sub>y</sub>, compared to their conventional (unblocked) counterparts. The quarter point blocking reinforcement reduced the distortion of the chord studs and allowed for higher in-plane lateral loads to be carried by the wall. A significant increase in energy dissipation and a general decrease in ductility of the blocked walls compared to their conventional (unblocked) counterparts, were also observed.

The thickness and tensile stress modification factors obtained from the ancillary tests of the steel sheathing were used to compute the nominal shear resistance values for each shear wall configuration for Canada, the USA and Mexico. The recommended Canadian limits states design resistance factor  $\phi$  for shear walls with blocking reinforcement designed to carry lateral wind loads is 0.7. For the USA and Mexico a resistance factor  $\phi = 0.6$  was recommended. Further, the reduction factor of 2w/h listed in the AISI S400 Standard for high aspect ratio walls is applicable for the design of blocked shear walls. The recommended factors of safety, calculated for limit states design (LSD) and allowable strength design (ASD) are respectively 2.06 and 2.88. For Canada, an overstrength value of 1.4 was recommended for the blocked specimens. Finally, for Canada, as recommended by DaBreo (2012) and the AISI S400 Standard for CFS framed / steel sheathed shear walls, the measured "test based" seismic force modification factors for ductility are  $R_d$ =2.0 and for overstrength,  $R_o$ =1.3.

The FEMA P795 methodology was applied in order to determine if the cold formed shear walls designed with full frame blocking and thick Sheathing / Framing Members is equivalent to line A.16 in Table 12.2-1 of ASCE/SEI (2010), which reads « Light-Frame (cold-formed steel) walls sheathed with wood structural panels rated for shear resistance of steel sheets. ». The results obtained from the analysis were not conclusive, some of the requirements listed by the FEMA P-795 to confirm the equivalency were not met.

#### 5.2 RECOMMENDATIONS FOR FUTURE STUDY

First, the specimens designed and built with closely spaced sheathing fasteners suffered from twisting of the chord studs, mainly due to the asymmetry of the walls and resulting torsional forces. The specimens were designed with a sheathing panel placed on one side of the wall,

leading to bending effects about the loading axis and resulting in twisting of the chord studs. It is recommended to test shear wall specimens designed with sheathing panels placed on both sides of the walls, or positioned at the centre of mass of the specimen in order to achieve a symmetry in the application of load. Second, the top and bottom tracks of the specimens having closely spaced sheathing connectors suffered from uplift deformations during the testing of the walls. These configurations experienced the development of a high level of tension field action within the sheathing. The vertical component of this force is the main reason that uplift deformations occurred in the track members. It is recommended to investigate the impact of increasing the thickness of the tracks and better fastening them to their supporting members. The data collected from this research program shows that, the full frame blocking did not restrict effectively the overall out-of-plane deformation of the long walls. It is recommended to analyze the influence of the blocking element thickness on the performance of these long walls. The application of the FEMA P795 was not entirely conclusive. It is recommended to apply the FEMA P-695 methodology, in which R values are evaluated using a non-linear response history dynamic analyses of representative structures, whose load-deformation response is modelled after the results of the shear wall tests.

#### REFERENCES

American Iron and Steel Institute (AISI). 2007. "AISI S213-07, North American Standard for Cold-Formed Steel Framing-Lateral Design". Washington, DC, USA.

American Iron and Steel Institute (AISI). 2015. "AISI S230-15, North American Standard for Cold-Formed Steel Framing- Prescriptive Method for One and Two Family Dwelling 2007 Edition". Washington, DC, USA.

American Iron and Steel Institute (AISI). 2015. "AISI S240-15, North American Standard for Cold-Formed Steel Structural Framing". Washington, DC, USA.

American Iron and Steel Institute (AISI). 2015. "AISI S400-15, North American Standard for Cold-Formed Steel Structural Systems". Washington, DC, USA.

American Iron and Steel Institute (AISI). 2016. "AISI S100-16, North American Specification for the Design of Cold-Formed Steel Structural Members". Washington, DC, USA.

American Society for Testing and Materials, A193. 2016. "Standard Specification for Alloy-Steel and Stainless Steel Bolting Materials for High Temperature or High Pressure Service and Other Special Purpose Applications". West Conshohocken, PA, USA.

American Society for Testing and Materials, A370. 2014. "Standard test Methods and Definitions for Mechanical Testing of Steel Products". West Conshohocken,PA, USA.

Balh, N. 2010. "Development of Canadian Seismic Design Provisions for Steel Sheathed Shear Walls". M.Eng. thesis. Department of Civil Engineering and Applied Mechanics, McGill University. Montreal, QC.

Boudreault, F.A. 2005. "Seismic Analysis of Steel Frame/ Wood Panel Shear Boudreault, F.A. 2005. "Seismic Analysis of Steel Frame/ Wood Panel Shear McGill University. Montreal, QC, Canada.

Branston, A.E. 2004. "Development of a Design Methodology for Steel Frame/Wood Panel Shear Walls". M.Eng. thesis. Department of Civil Engineering and Applied Mechanics, McGill University. Montreal, QC.

Consortium of Universities for Research in Earthquake Engineering (CUREE).2004a. "Recommendations for Earthquake Resistance in Design and Construction of Wood frame Buildings- Part 1: Recommendations". CUREEPublication No. W-30b, Richmond, CA, USA.

El-Saloussy, K. 2010. "Additional Cold-Formed Steel Frame/Steel Sheathed Shear Wall Design Values for Canada". Project Report, Department of Civil Engineering and Applied Mechanics, McGill University. Montreal, QC.

Morello, D. 2009. "Seismic Force Modification Factors for the Proposed 2005 Edition of the National Building Code of Canada". M.Eng. thesis. Department of Civil Engineering and Applied Mechanics, McGill University. Montreal, QC.

Newmark, N.M., Hall, W.J., 1982. "Earthquake Spectra and Design". EngineeringMonograph, Earthquake engineering Research Institute. Berkeley, CA, USA.

Foliente, G.C. 1996. "Issues in Siesmic Performance Testing and Evaluation of Timber Structural Systems". Proc., International Wood Engineering Conference. New Orleans, LA, USA, Vol. 1, 29-36.

Ong-Tone, C. 2009. "Tests and Evaluation of Cold-Formed Steel Framing/Steel Sheathed Shear Walls". Project Report, Department of Civil Engineering and Applied Mechanics, McGill University. Montreal, QC.

Park, R. 1989. "Evaluation of Ductility of Structures and Structural Assemblages from Laboratory Testing". Bulletin of the New Zealand National Society for Earthquake Engineering, Vol.22, No.3, 155-166.

Serrette, R. 1997. "Behaviour of Cyclically Loaded Light Gauge Steel Framed Shear Walls". Building to Last: Proc., Fifteenth Structures Congress.Portland, OR, USA.

Shamim, I. 2012. "Seismic Design of Lateral Resisting Cold-Formed Steel Framed(CFS) Structures". Ph.D thesis. Department of Civil Engineering and Applied Mechanics, McGill University. Montreal, QC.

Simpson Strong-Tie Co., Inc. 2008. "S/HDS & S/HDB Holdowns Specification". Catalog C-CFS06, Pleasanton, CA, USA. 23.

Yu, C., Chen, Y. 2009. "Steel Sheet Sheathing Options for Cold-Formed Steel Framed Shear Wall Assemblies Providing Shear Resistance- Phase 2". Report No.UNT-G70752, American Iron and Steel Institute, Department of Engineering Technology, University of North Texas, Denton, Texas, USA.

Yu, C., Vora, H., Dainard, T., Tucker, J., Veetvkuri, P. 2007. "Steel Sheet Sheathing Options for Cold-Formed Steel Framed Shear Wall Assemblies Providing ShearResistance". Report No. UNT-G76234, American Iron and Steel Institute, Department of Engineering Technology, University of North Texas, Denton, Texas, USA.

Zhao, Y. 2002. "Cyclic Performance of Cold-Formed Steel Stud Shear Walls".M.Eng. thesis, Department of Civil Engineering and Applied Mechanics,McGill University. Montreal, QC, Canada.

### APPENDIX A TEST CONFIGURATION

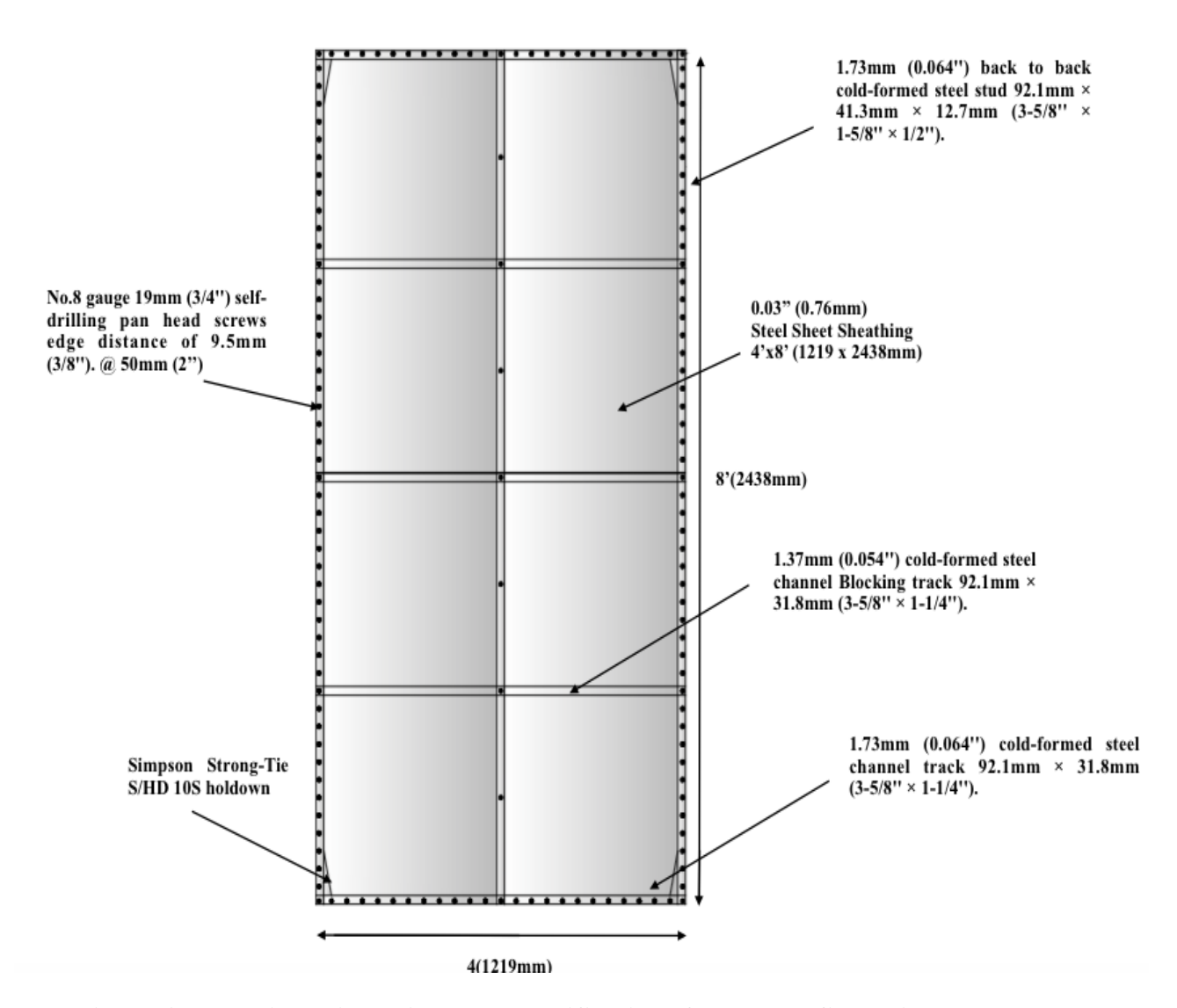


Figure A.1 Nominal dimensions and specifications for test configuration W1

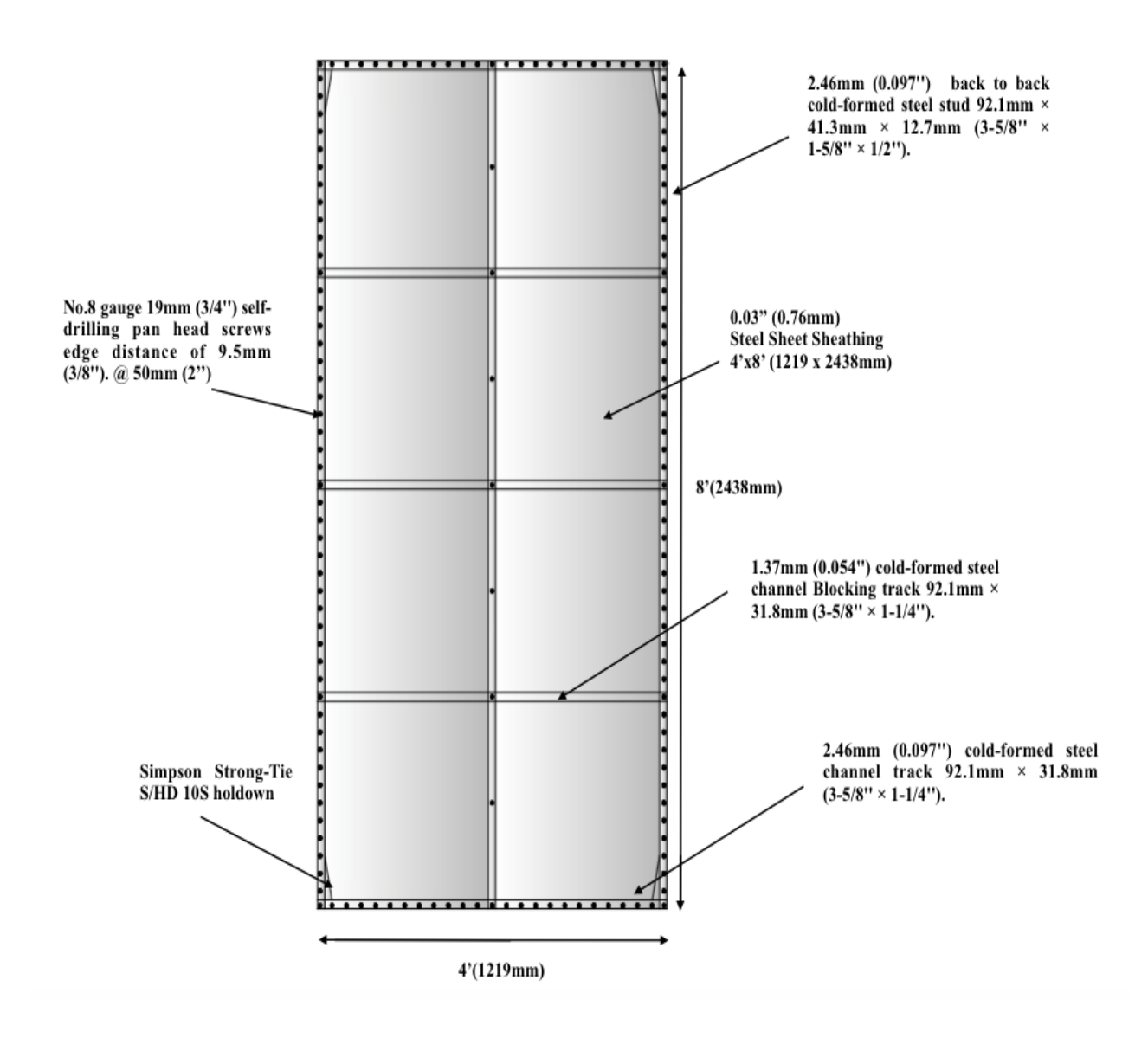


Figure A.2 Nominal dimensions and specifications for test configuration W2

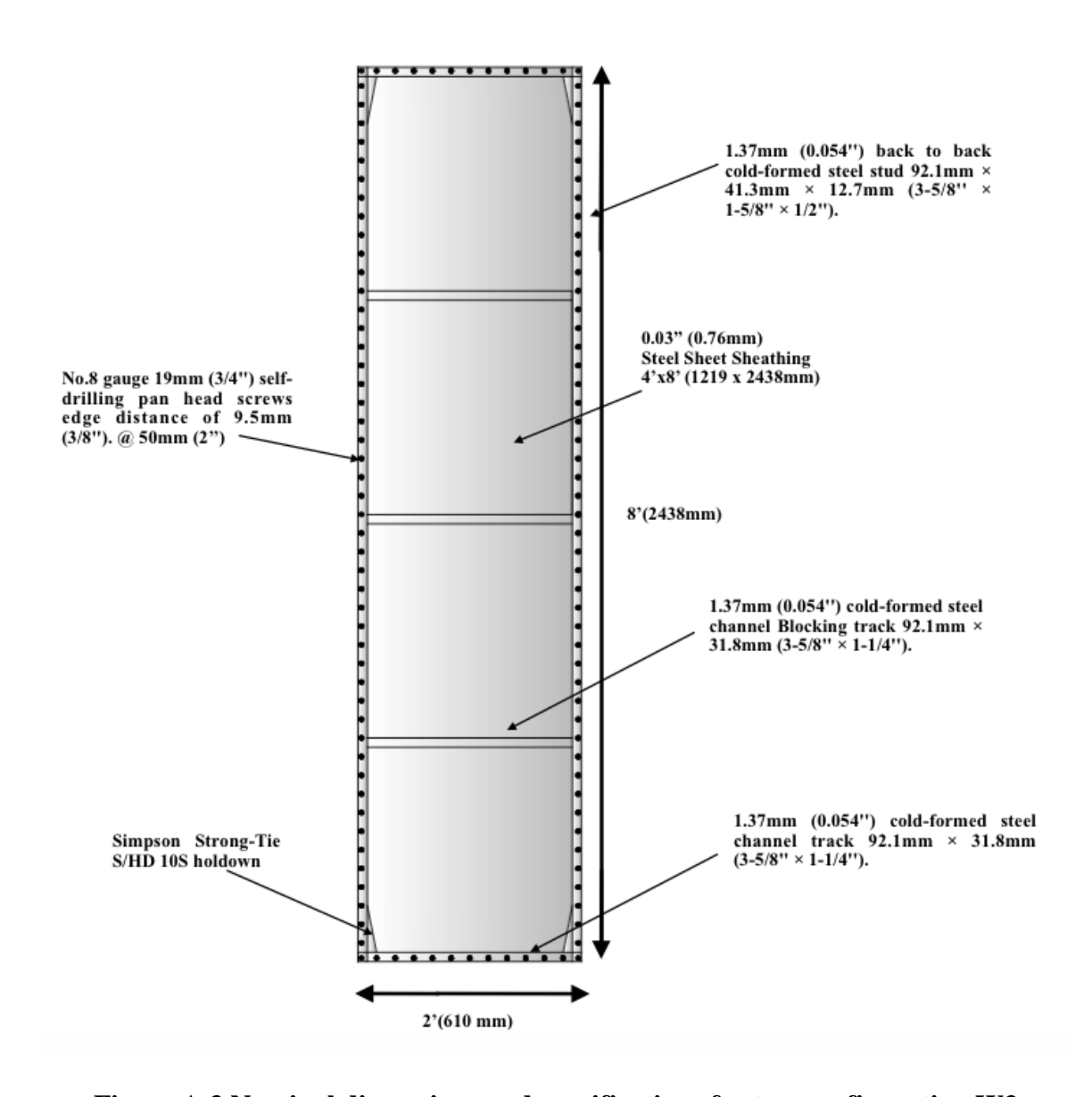


Figure A.3 Nominal dimensions and specifications for test configuration W3

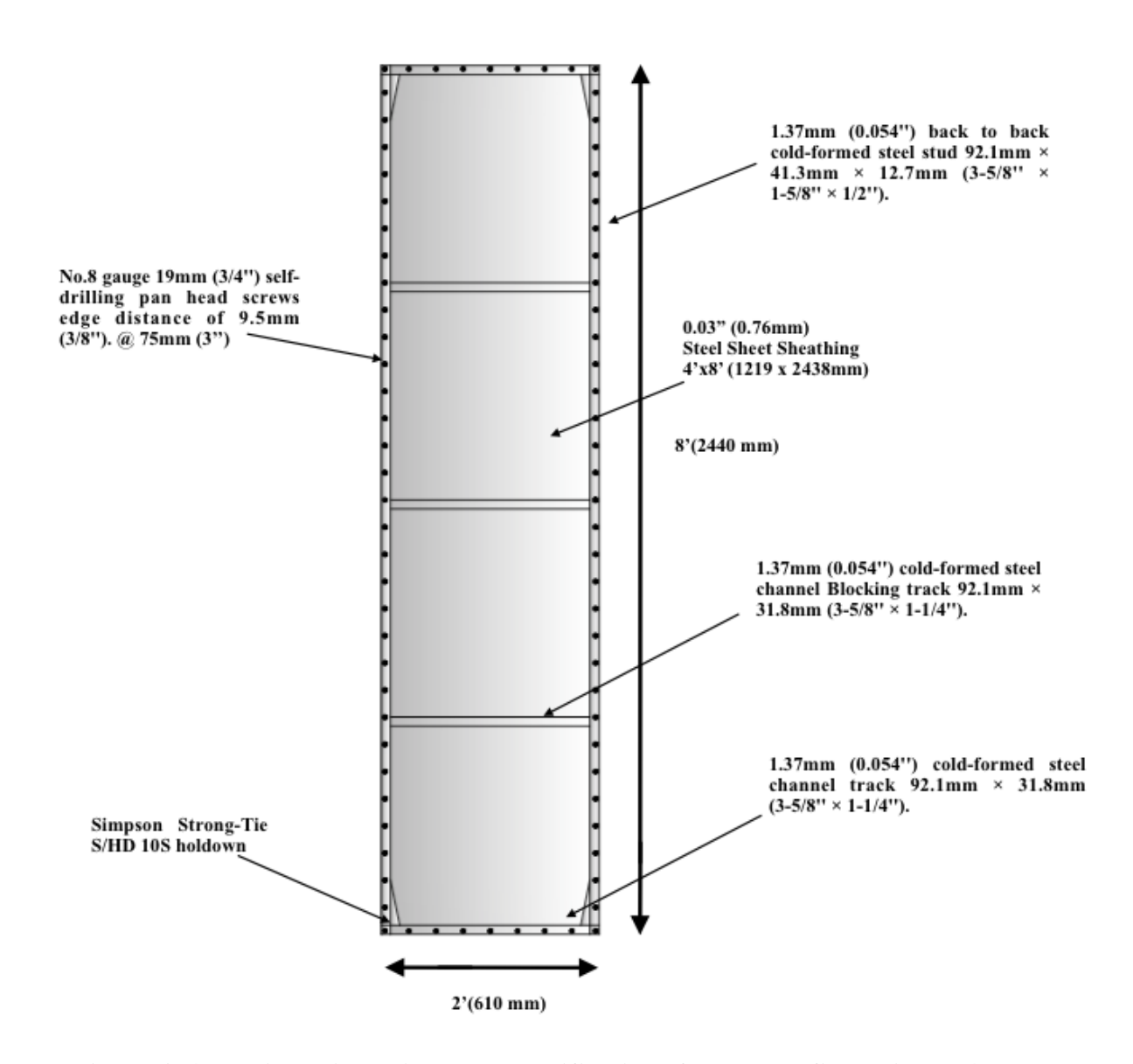


Figure A.4 Nominal dimensions and specifications for test configuration W4

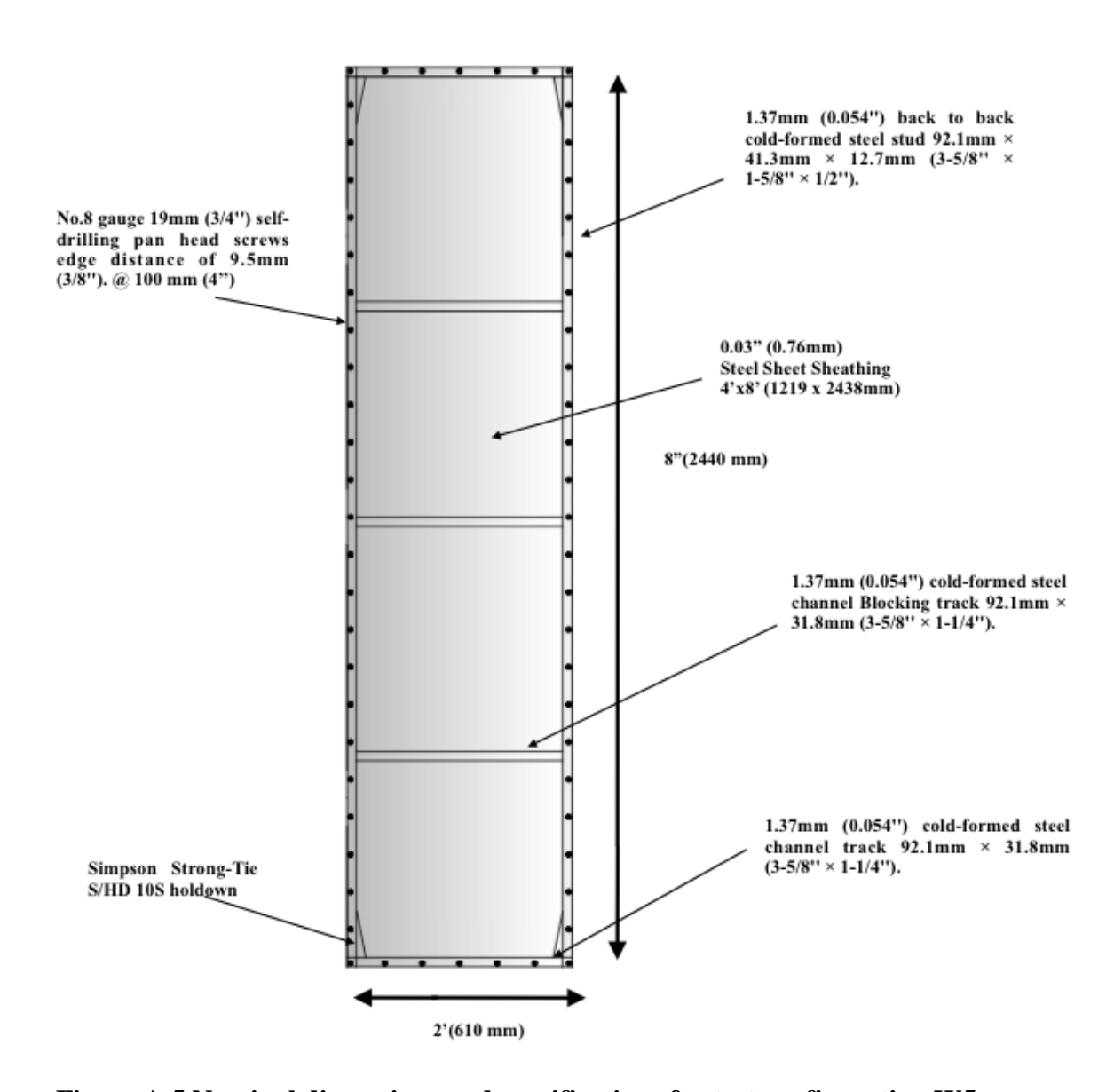


Figure A.5 Nominal dimensions and specifications for test configuration W5

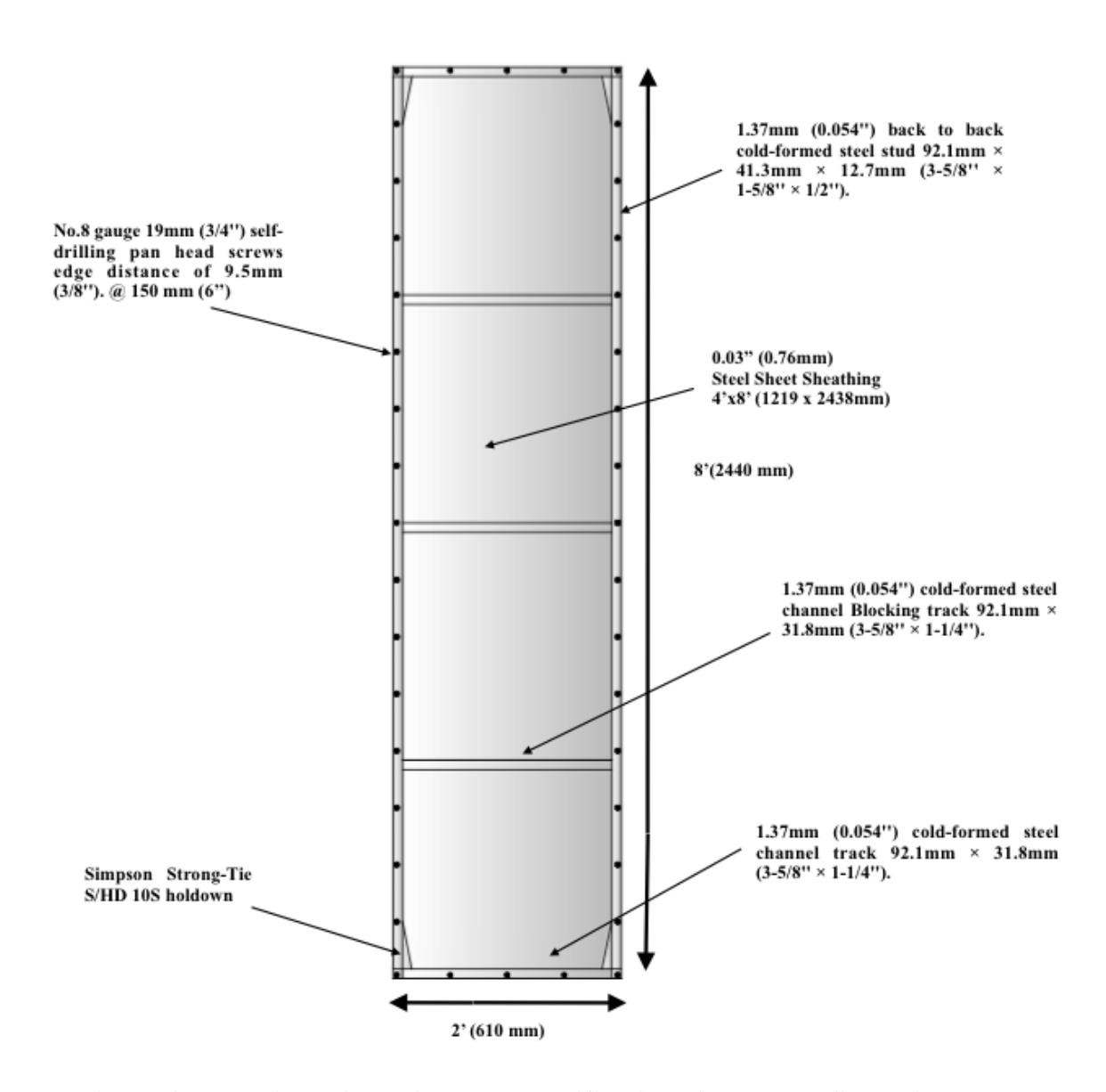


Figure A.6 Nominal dimensions and specifications for test configuration W6

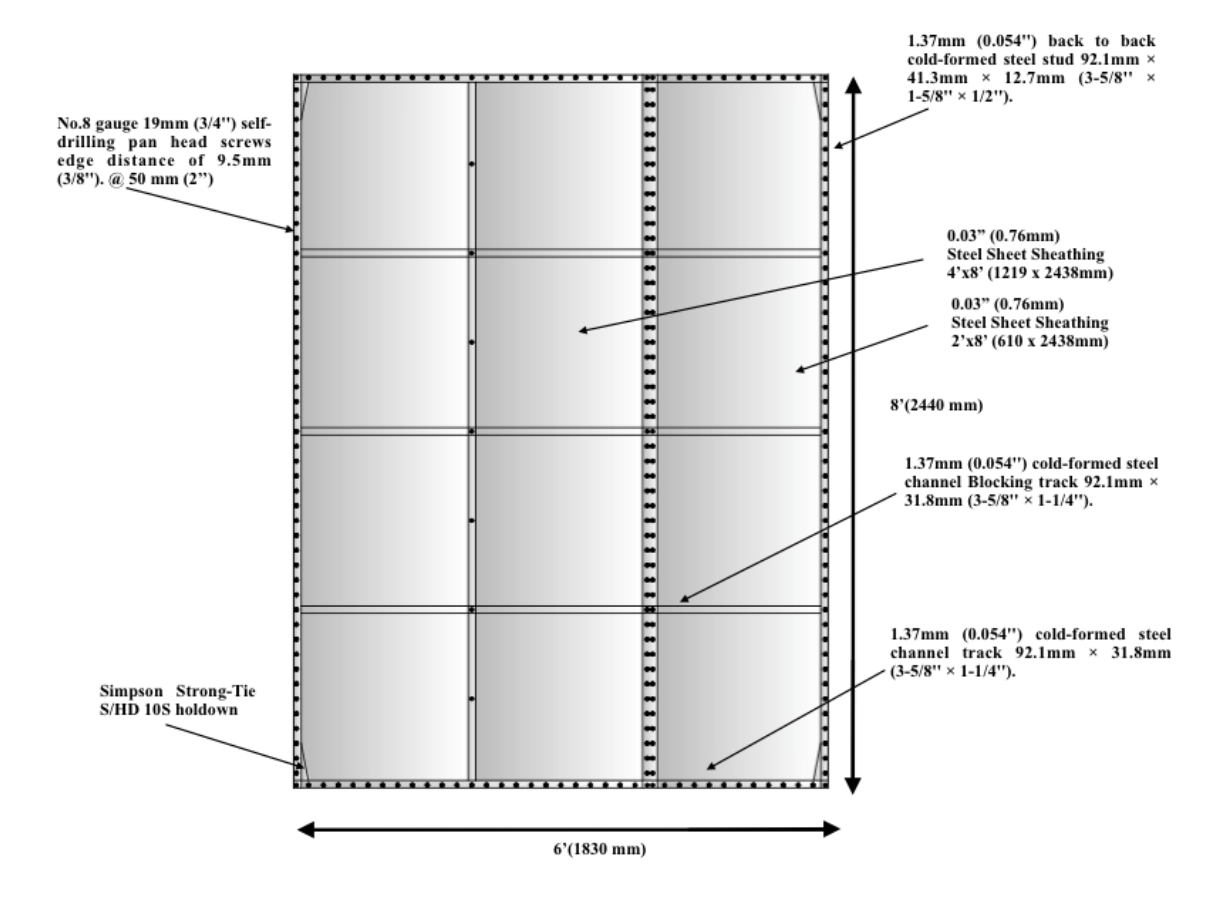


Figure A.7 Nominal dimensions and specifications for test configuration W7

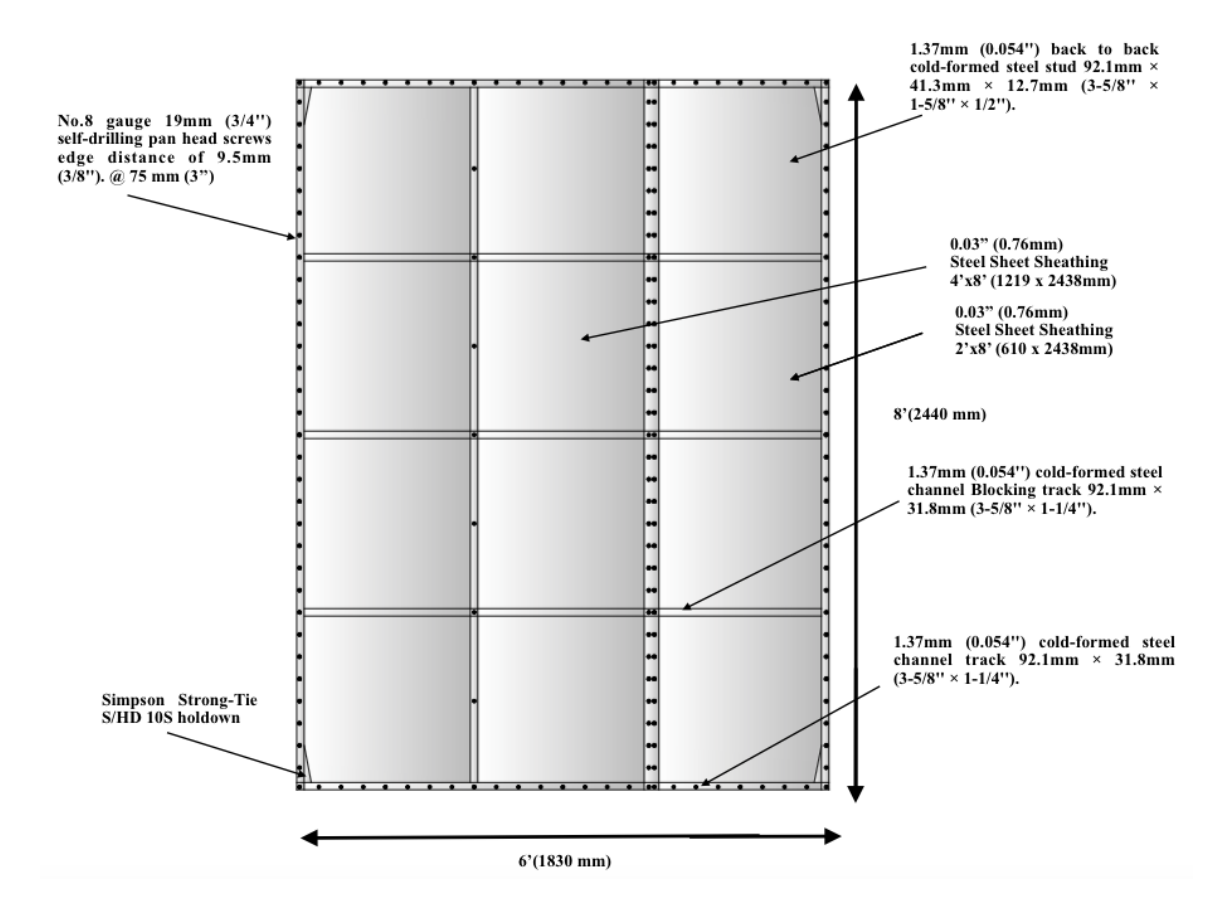


Figure A.8 Nominal dimensions and specifications for test configuration W8

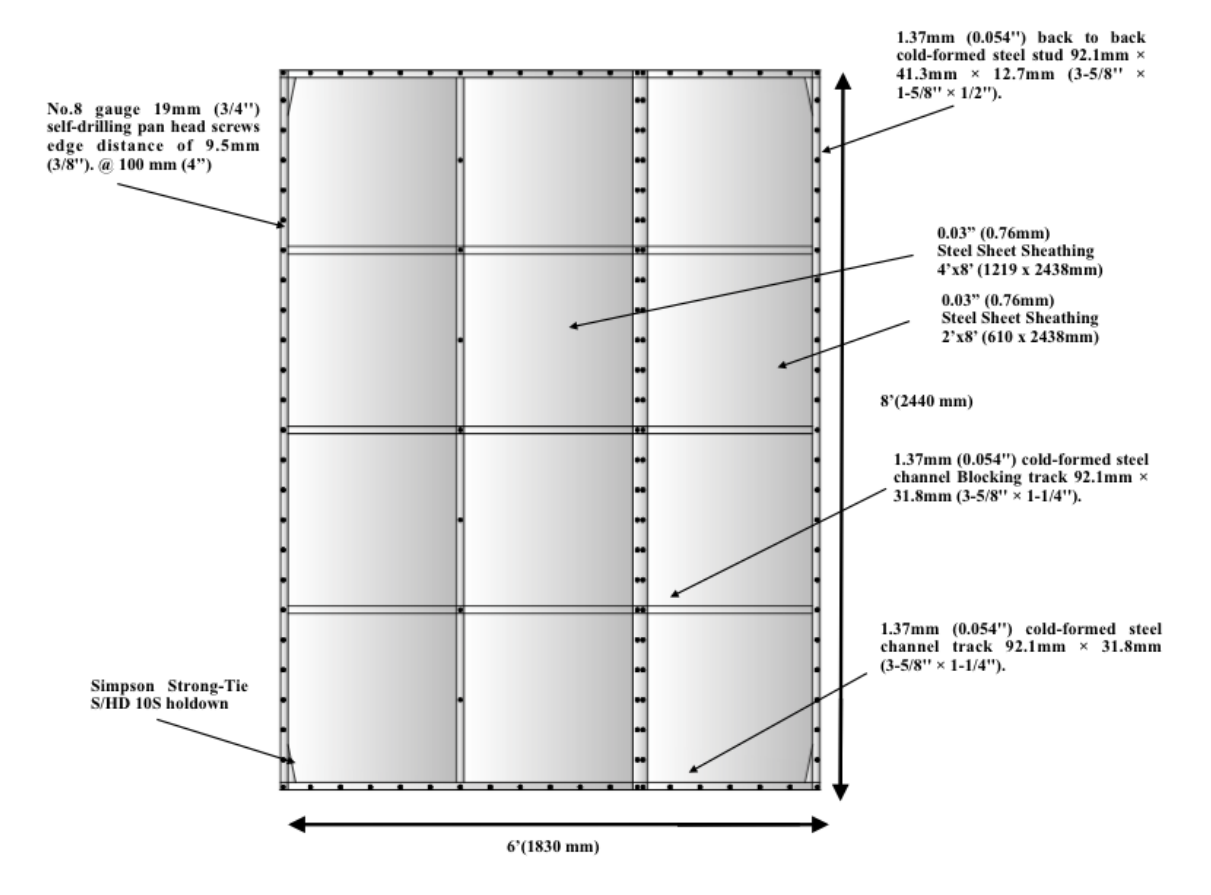


Figure A.9 Nominal dimensions and specifications for test configuration W9

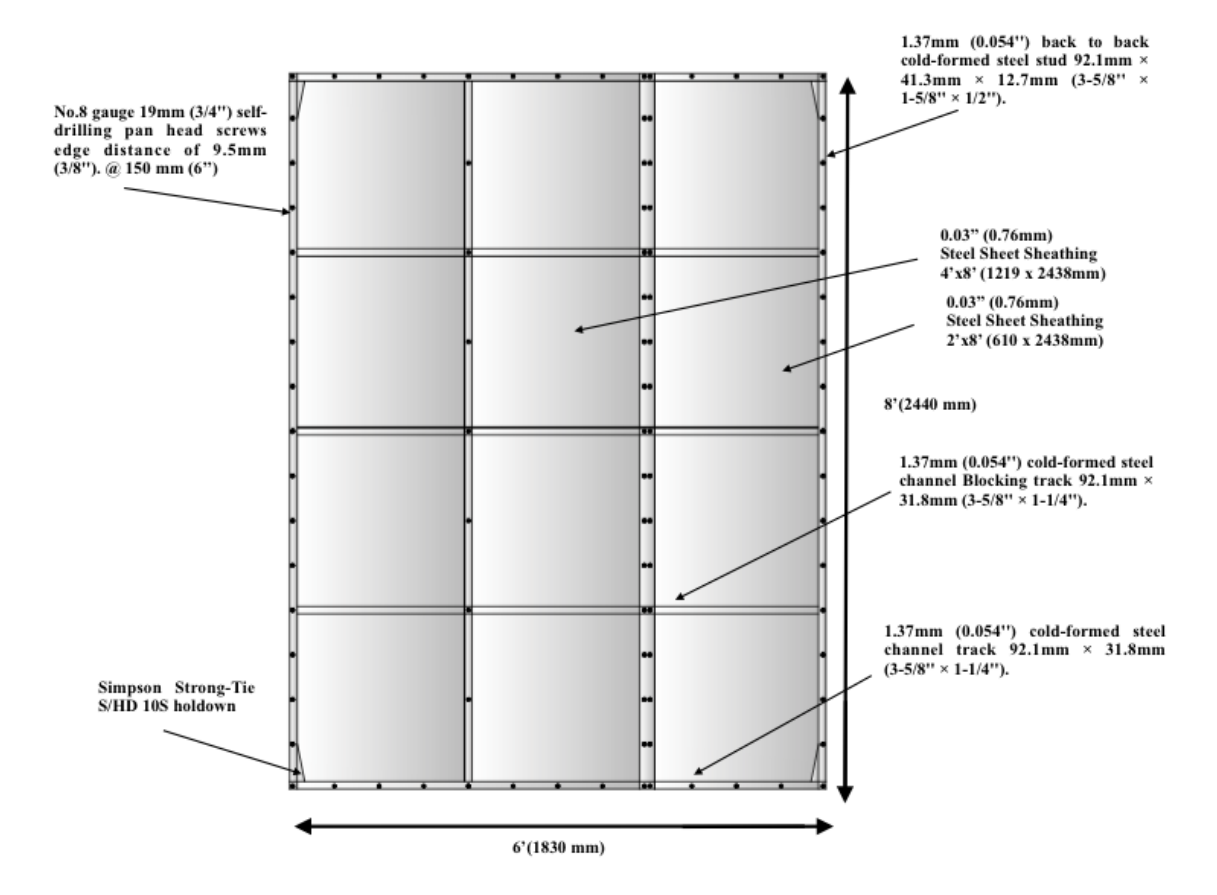


Figure A.10 Nominal dimensions and specifications for test configuration W10

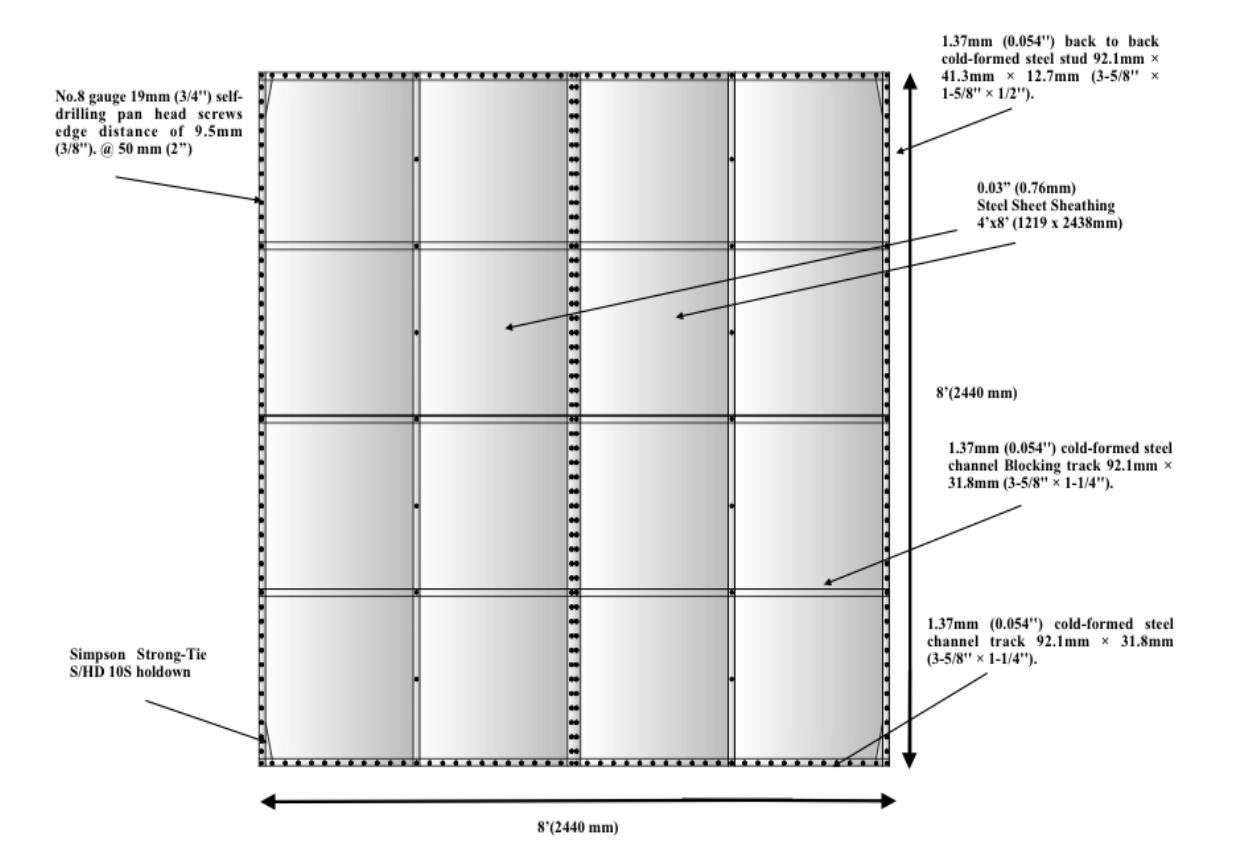


Figure A.11 Nominal dimensions and specifications for test configuration W11

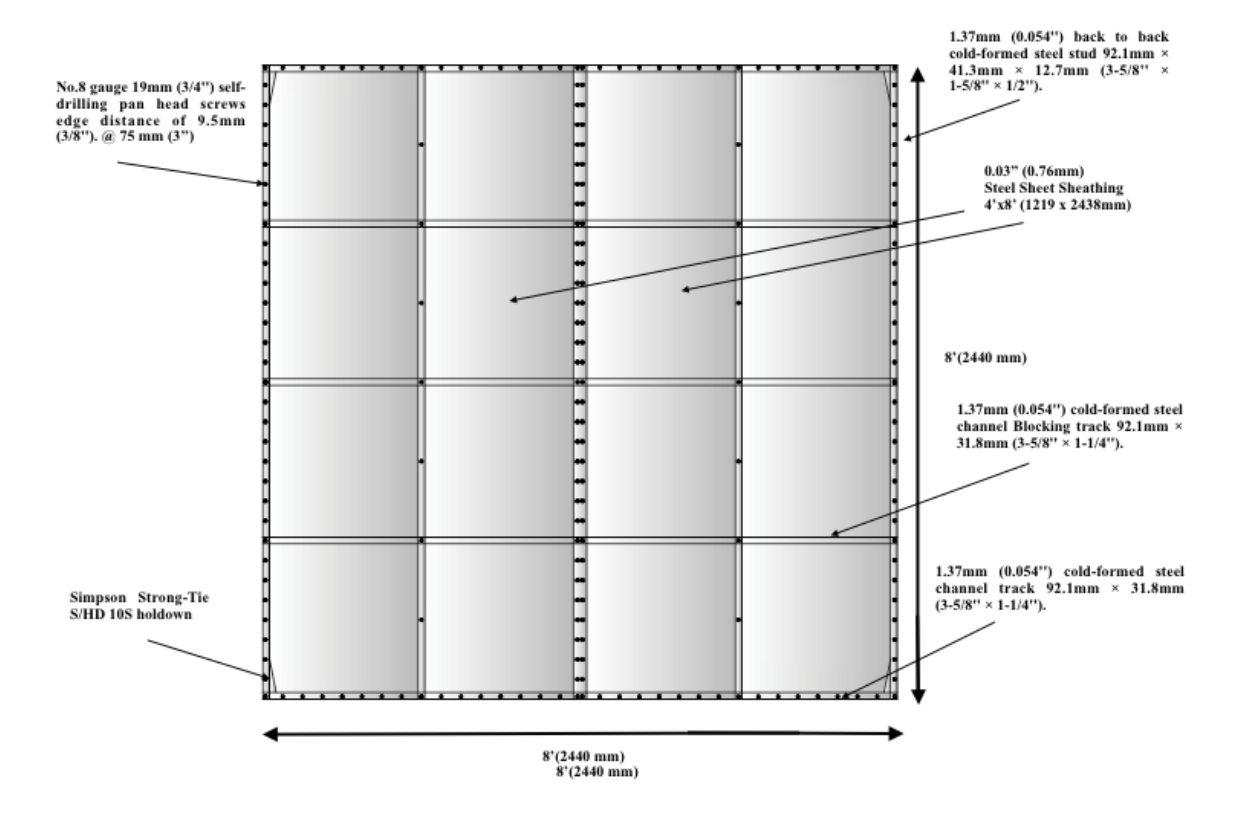


Figure A.12 Nominal dimensions and specifications for test configuration W12

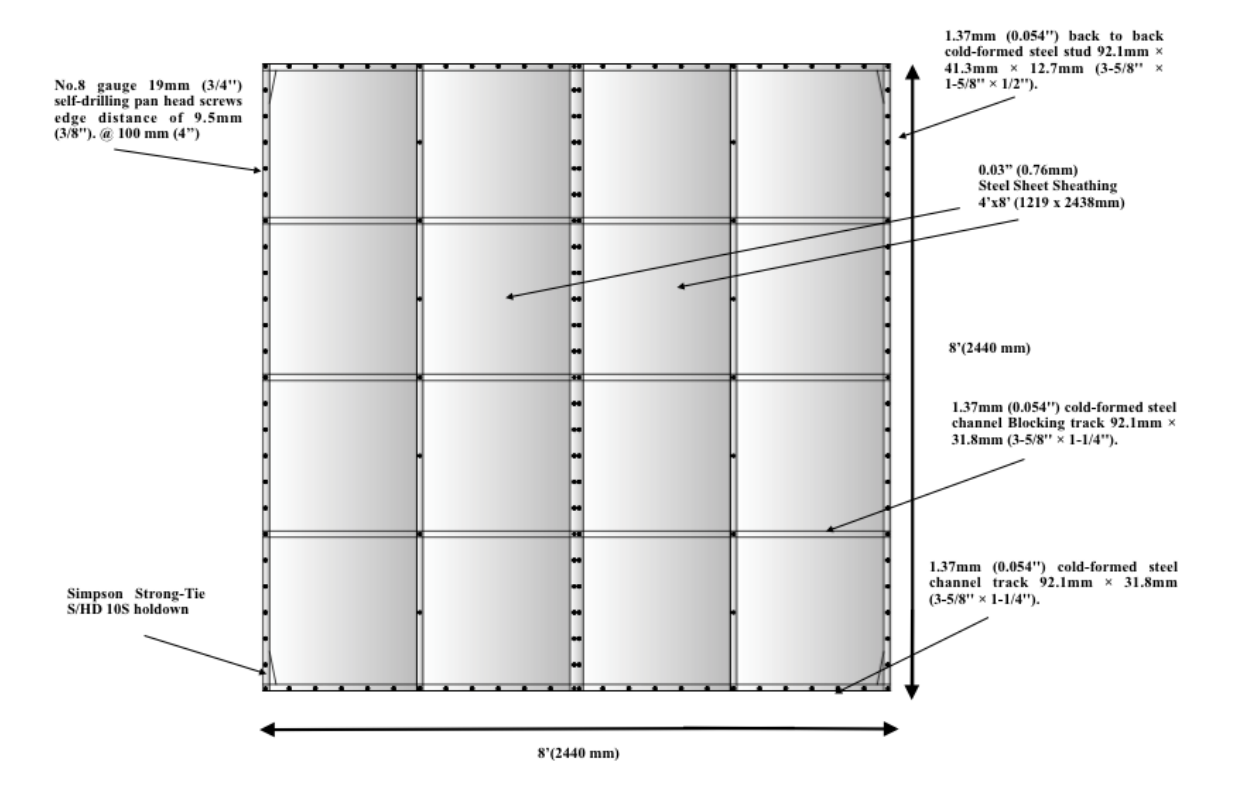


Figure A.13 Nominal dimensions and specifications for test configuration W13

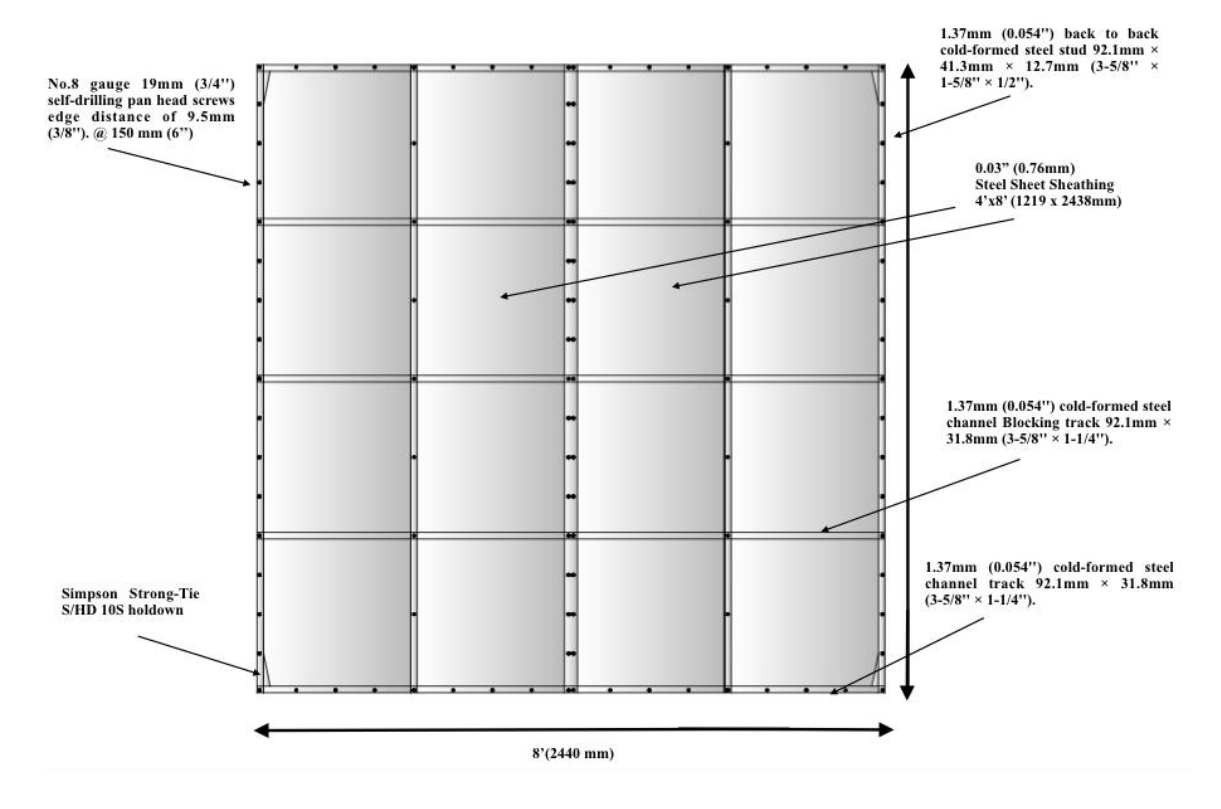


Figure A.14 Nominal dimensions and specifications for test configuration W14

### APPENDIX B DATA ANALYSIS

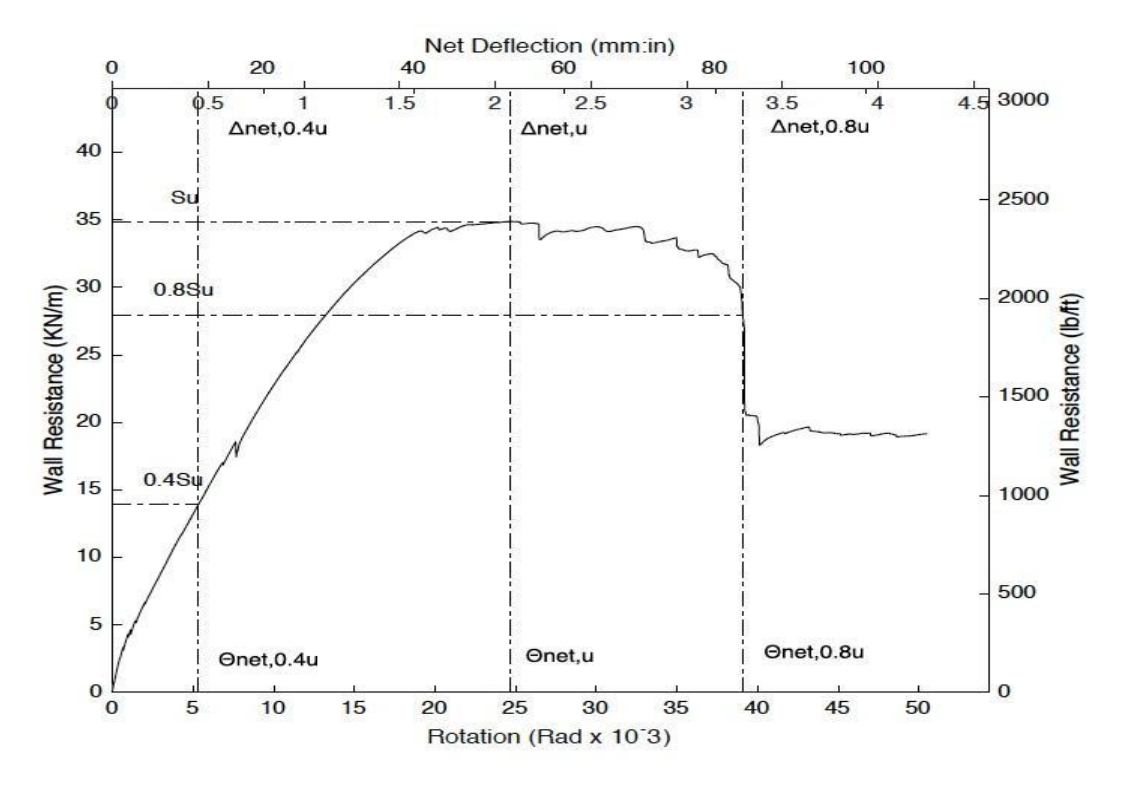


Figure B1 - Parameters of Monotonic Test W1-M

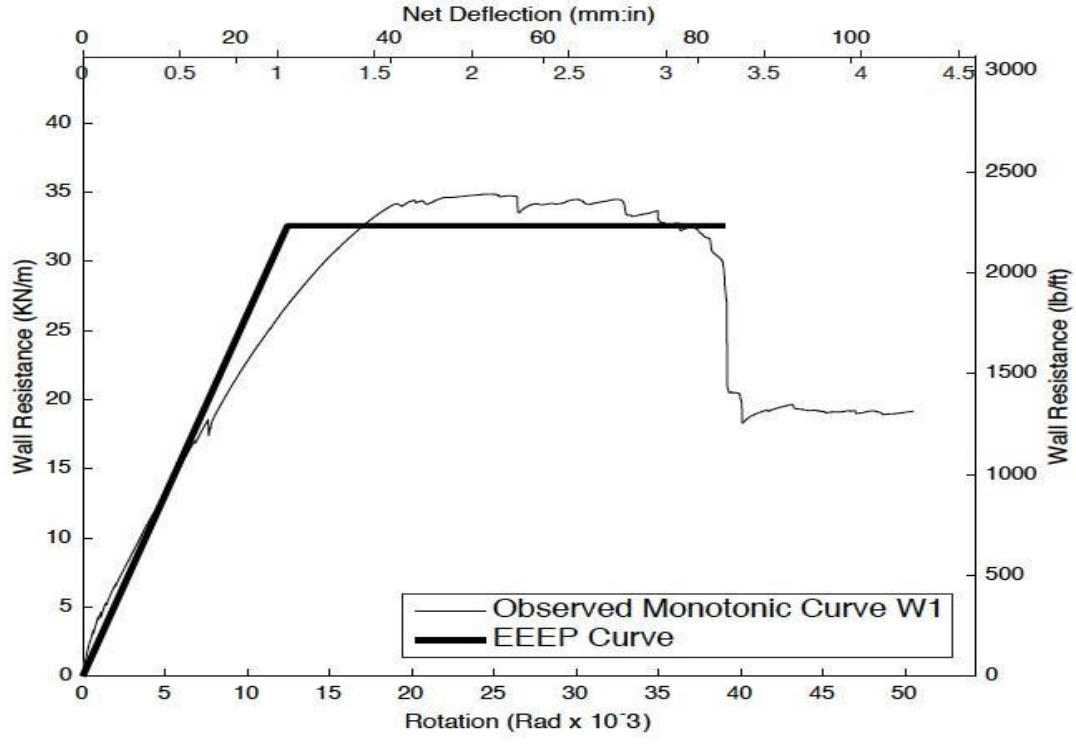


Figure B2 - Observation and EEEP Curves for Test W1-M

Parameters		Units
Fu	42,53	kN
Fu_80	34,02	kN
Fu40	17,01	kN
Fy	39,73	kN
Ke	1,49	kN/m m
μ	3,14	
Δnet,y	26,67	mm
Δnet,u	52,76	mm
Δnet,0.8u	83,65	mm
Δnet,0.4u	11,42	mm
Area Backbone	2 793,95	J
Area EEEP	2 793,95	J
Rd	2,30	
Sy	32,59	kN/m

Table B1 - Results for test W1-M

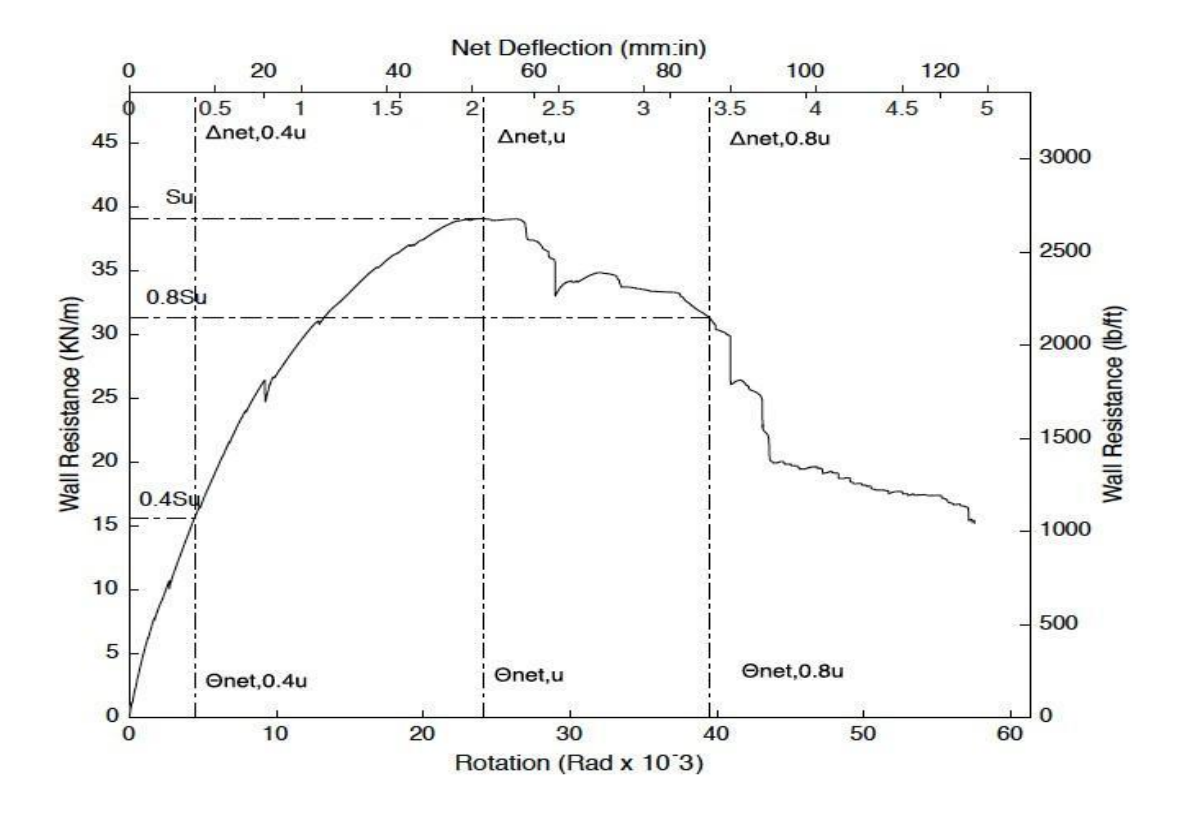


Figure B3 - Parameters of Monotonic Test W2-M

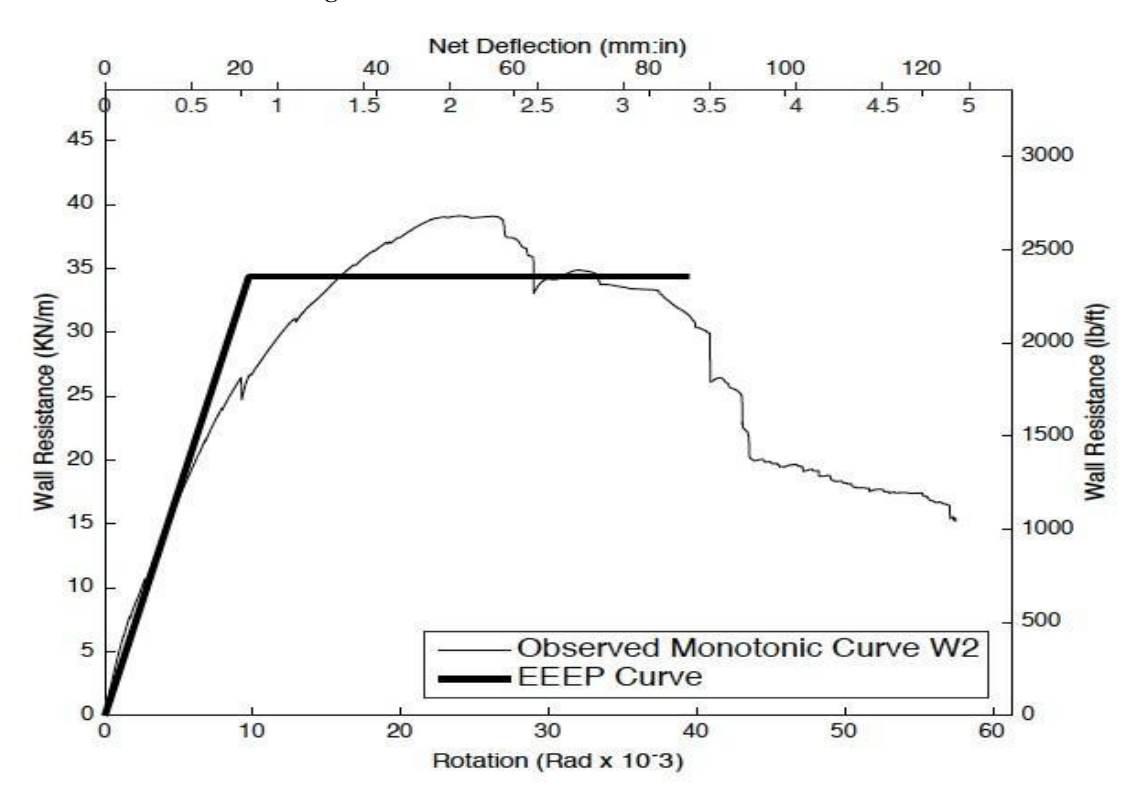


Figure B4 - Observation and EEEP Curves for Test W2-M

Parameters		Units
Fu	47,71	kN
Fu_80	38,16	kN
Fu40	19,08	kN
Fy	41,91	kN
Ke	1,98	kN/m m
μ	4,05	
Δnet,y	21,18	mm
Δnet,u	52,38	mm
Δnet,0.8u	85,87	mm
Δnet,0.4u	9,64	mm
Area Backbone	3 154,97	J
Area EEEP	3 154,97	J
Rd	2,67	
Sy	34,37	kN/m

Table B2 - Results for test W2-M

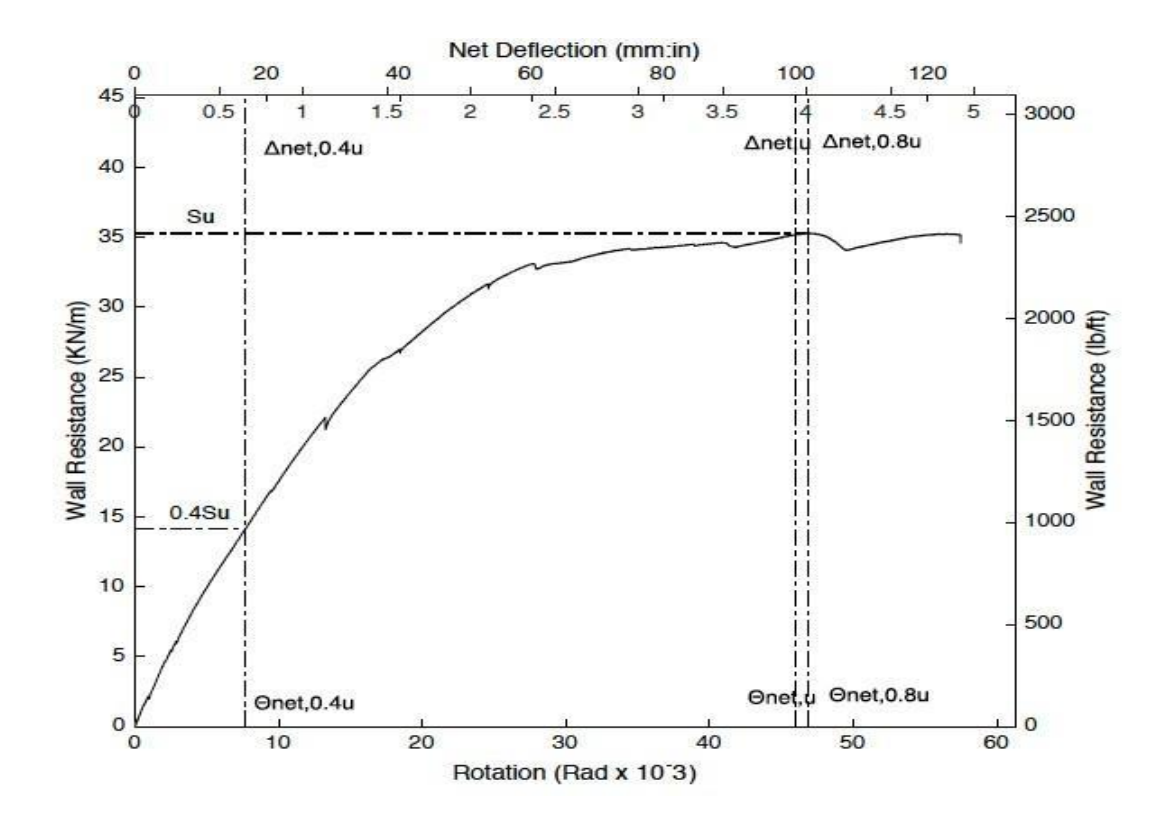


Figure B5 - Parameters of Monotonic Test W3-M

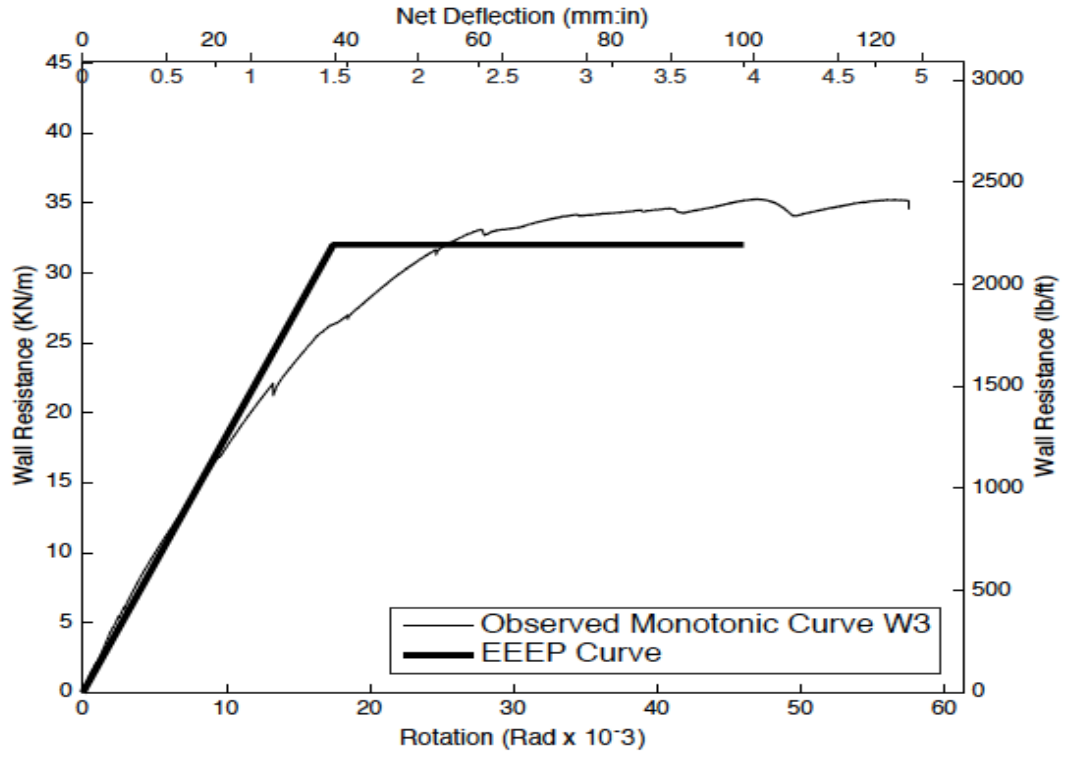


Figure B6 - Observation and EEEP Curves for Test W3-M

Parameters		Units
Fu	21,53	kN
Fu_80	21,45	kN
Fu40	8,61	kN
Fy	19,52	kN
Ke	0,52	kN/m m
μ	2,64	
Δnet,y	37,86	mm
Δnet,u	101,87	mm
Δnet,0.8u	100,00	mm
Δnet,0.4u	16,70	mm
Area Backbone	1 582,48	J
Area EEEP	1 582,48	J
Rd	2,07	
Sy	32,02	kN/m

Table B3 - Results for test W3-M

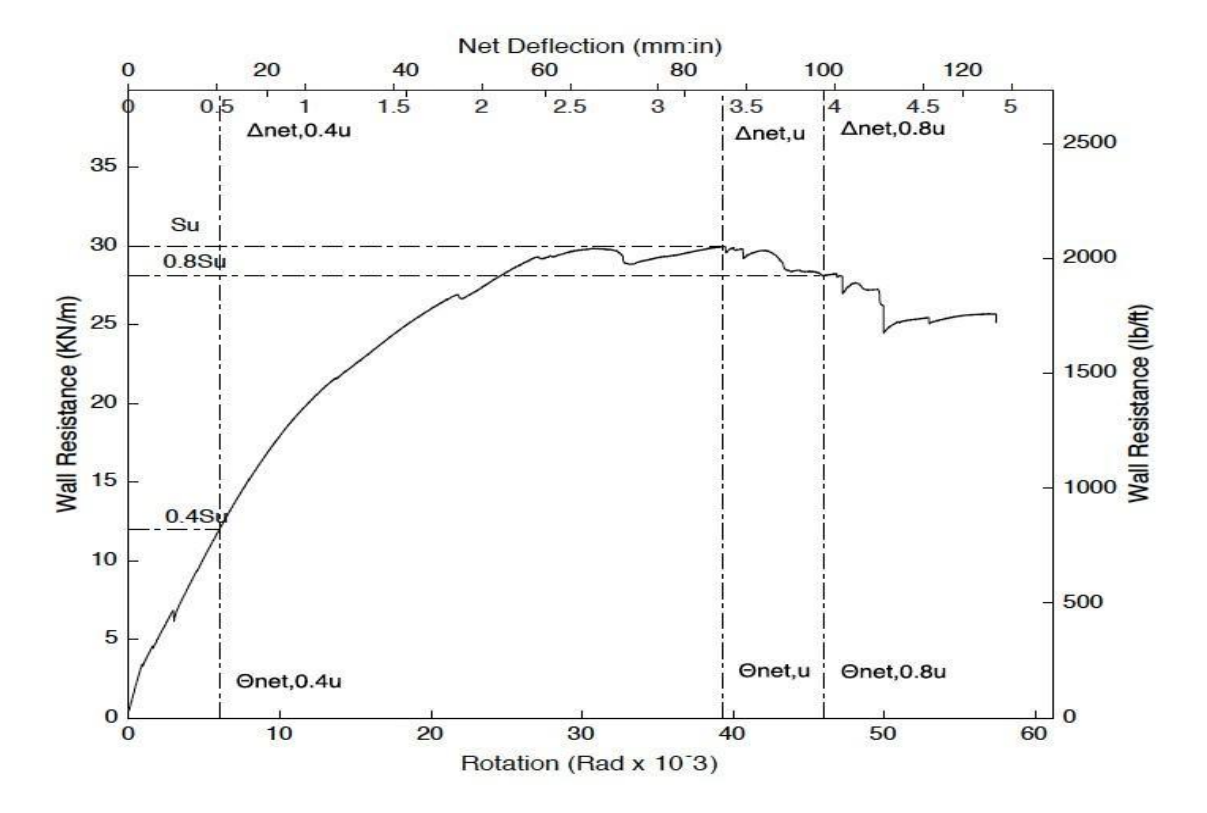


Figure B7 - Parameters of Monotonic Test W4-M

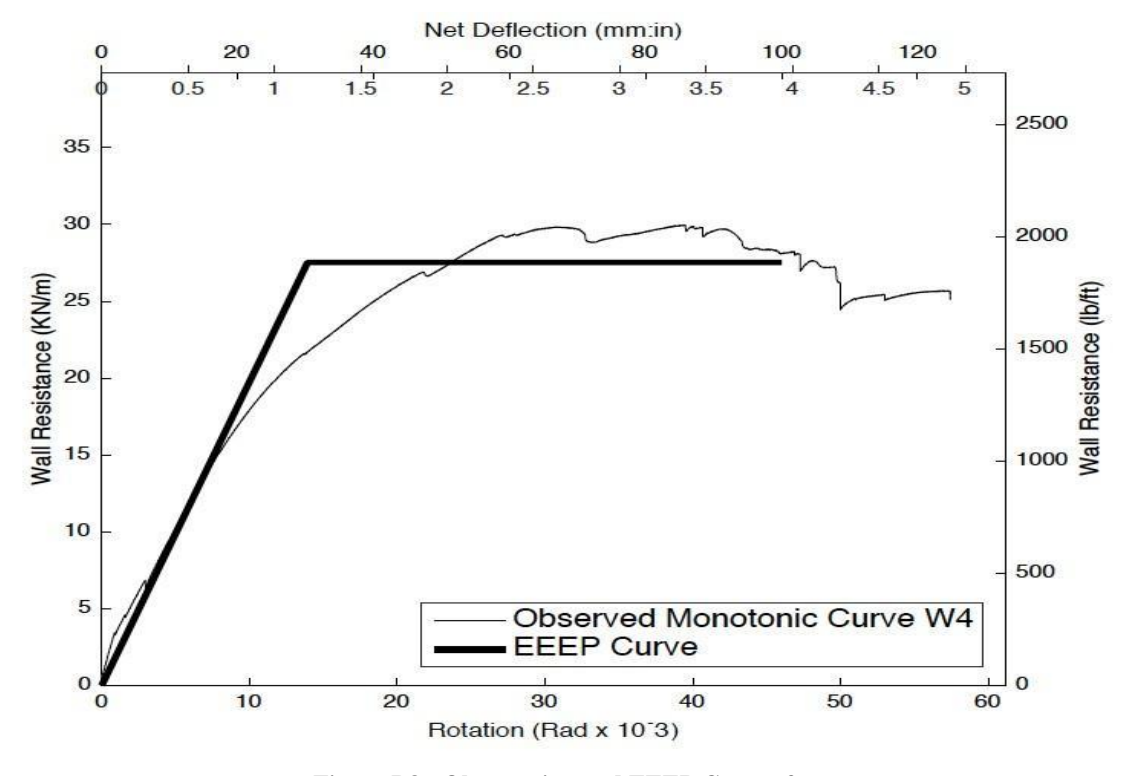


Figure B8 - Observation and EEEP Curves for Test W4-M

Parameters		Units
Fu	18,27	kN
Fu_80	17,13	kN
Fu40	7,31	kN
Fy	16,78	kN
Ke	0,55	kN/m m
μ	3,30	
Δnet,y	30,27	mm
Δnet,u	85,56	mm
Δnet,0.8u	100,00	mm
Δnet,0.4u	13,18	mm
Area Backbone	1 423,98	J
Area EEEP	1 423,98	J
Rd	2,37	
Sy	27,52	kN/m

Table B4 - Results for test W4-M

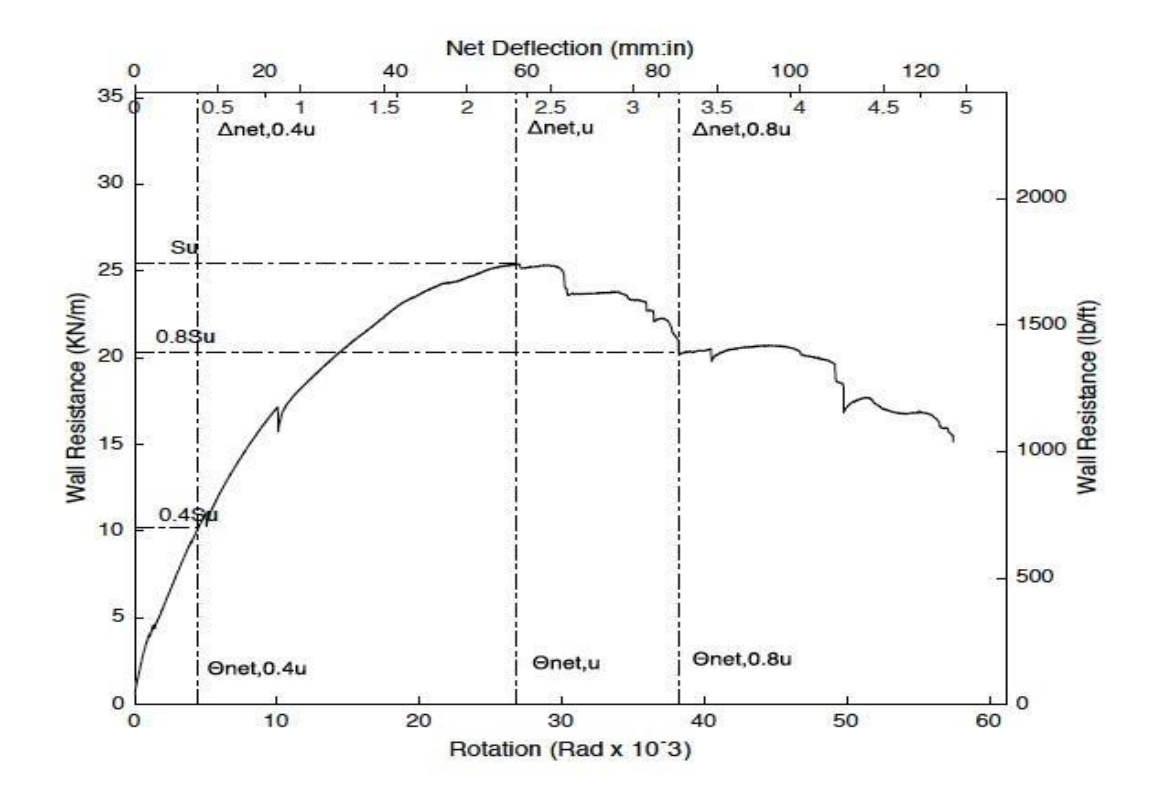


Figure B9 - Parameters of Monotonic Test W5-M

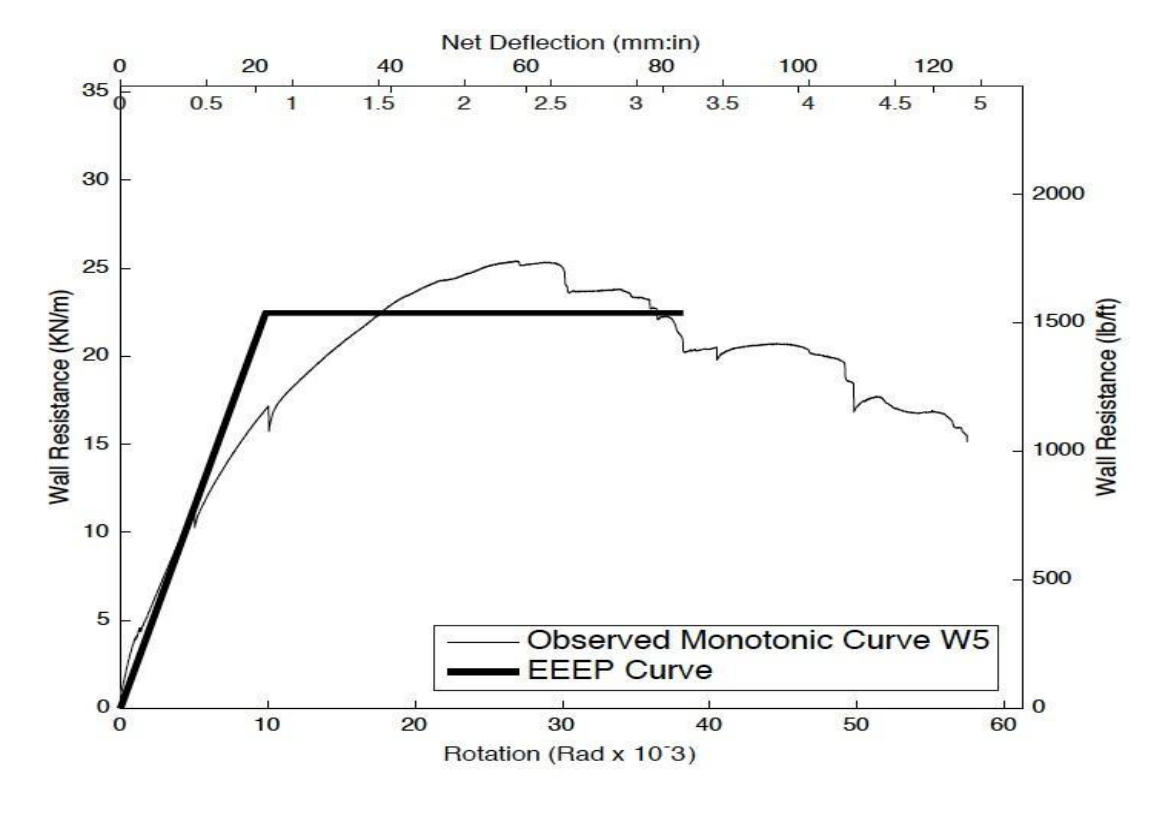


Figure B10 - Observation and EEEP Curves for Test W5-M

Parameters		Units
Fu	15,49	kN
Fu_80	12,39	kN
Fu40	6,20	kN
Fy	13,69	kN
Ke	0,64	kN/m m
μ	3,87	
Δnet,y	21,44	mm
Δnet,u	58,14	mm
Δnet,0.8u	83,03	mm
Δnet,0.4u	9,71	mm
Area Backbone	989,9 5	J
Area EEEP	989,9 5	J
Rd	2,60	
Sy	22,46	kN/m

Table B5 - Results for test W5-M

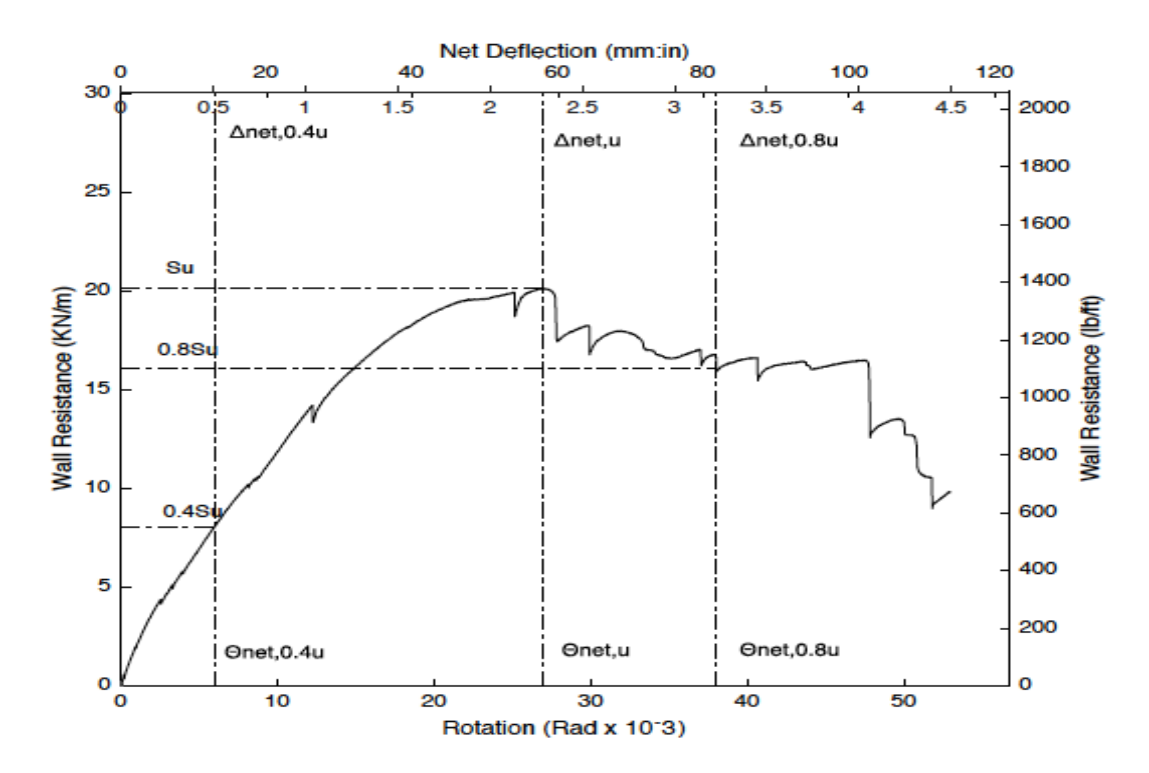


Figure B11 - Parameters of Monotonic Test W6-M

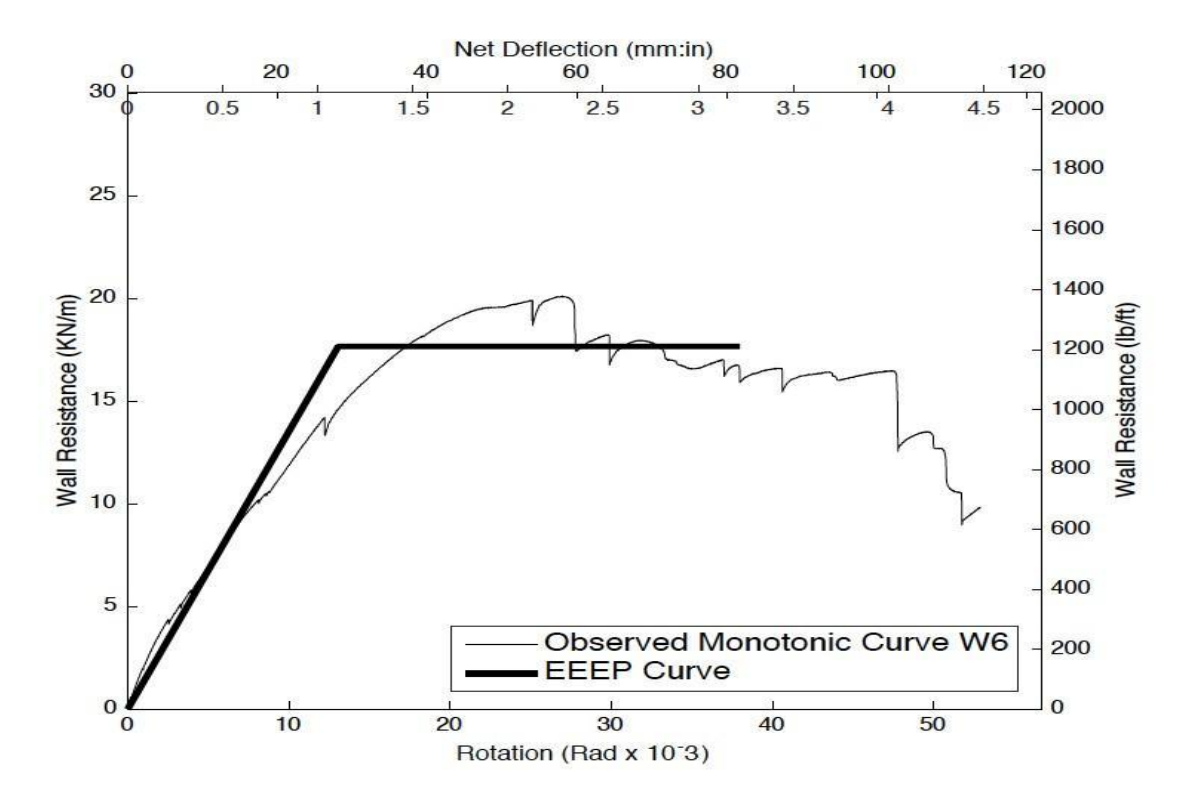


Figure B12 - Observation and EEEP Curves for Test W6-M

Parameters		Units
Fu	Fu 12,27	
Fu_80	9,82	kN
Fu40	4,91	kN
Fy	10,77	kN
Ke	0,38	kN/m m
μ	2,91	•
Δnet,y	28,12	mm
Δnet,u	58,03	mm
Δnet,0.8u	81,73	mm
Δnet,0.4u	12,81	mm
Area Backbone	729,0 1	J
Area EEEP	729,0 1	J
Rd	2,19	•
Sy	17,67	kN/m

Table B6 - Results for test W6-M

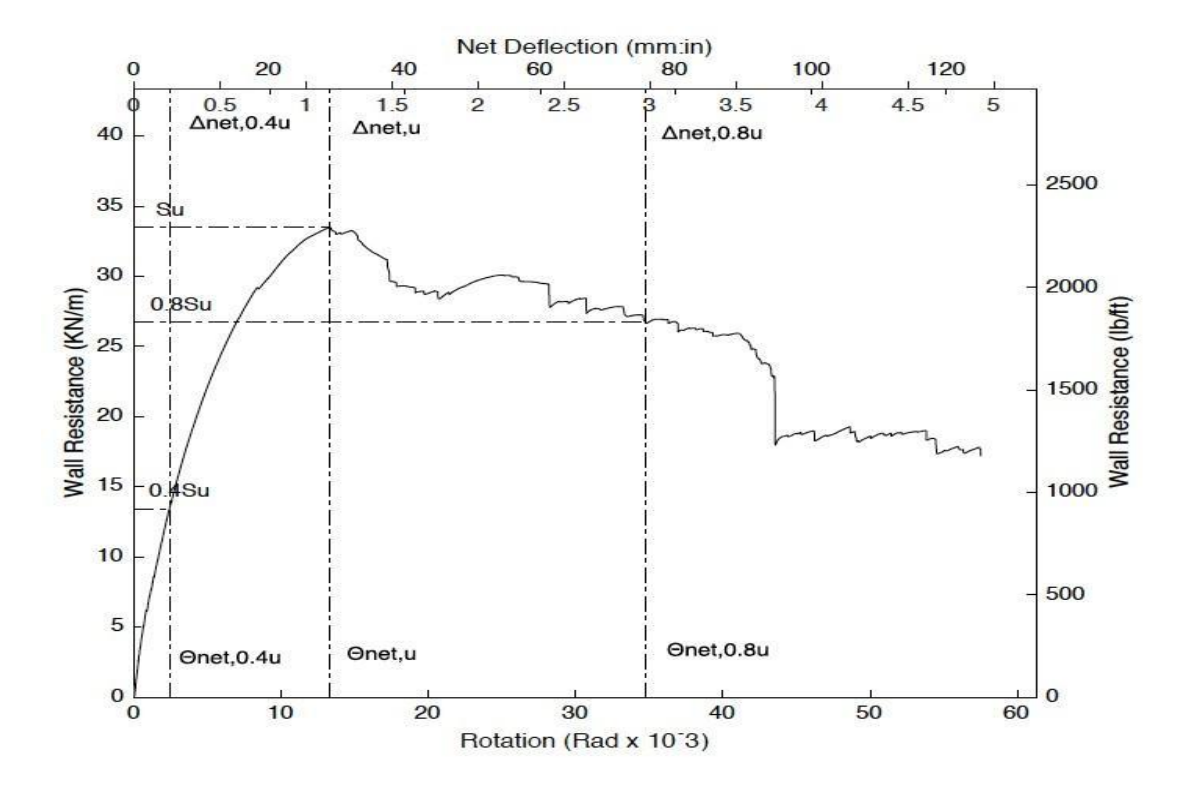


Figure B13 - Parameters of Monotonic Test W7-M

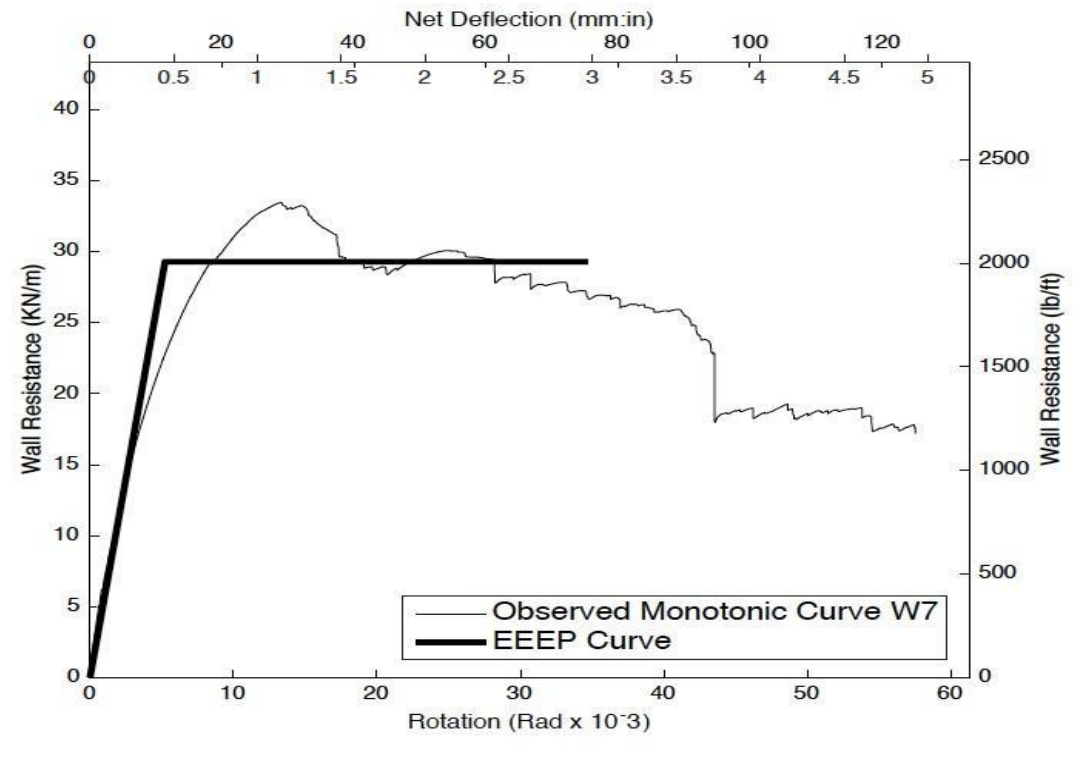


Figure B14 - Observation and EEEP Curves for Test W7-M

Parameters		Units
Fu	61,20	kN
Fu_80	48,96	kN
Fu40	24,48	kN
Fy	53,56	kN
Ke	4,71	kN/m m
μ	6,64	
Δnet,y	11,37	mm
Δnet,u	28,80	mm
Δnet,0.8u	75,48	mm
Δnet,0.4u	5,20	mm
Area Backbone	3 738,51	J
Area EEEP	3 738,51	J
Rd	3,50	
Sy	29,29	kN/m

Table B7 - Results for test W7-M

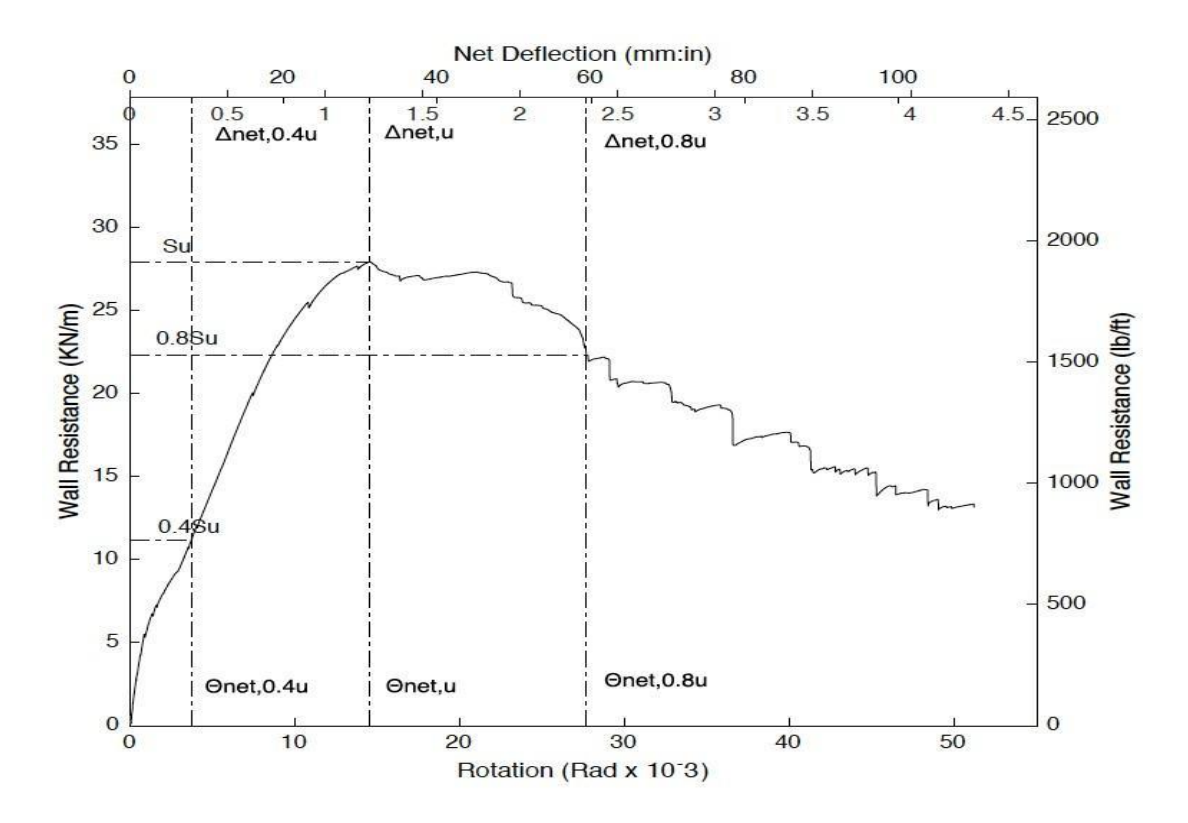


Figure B15 - Parameters of Monotonic Test W8-M

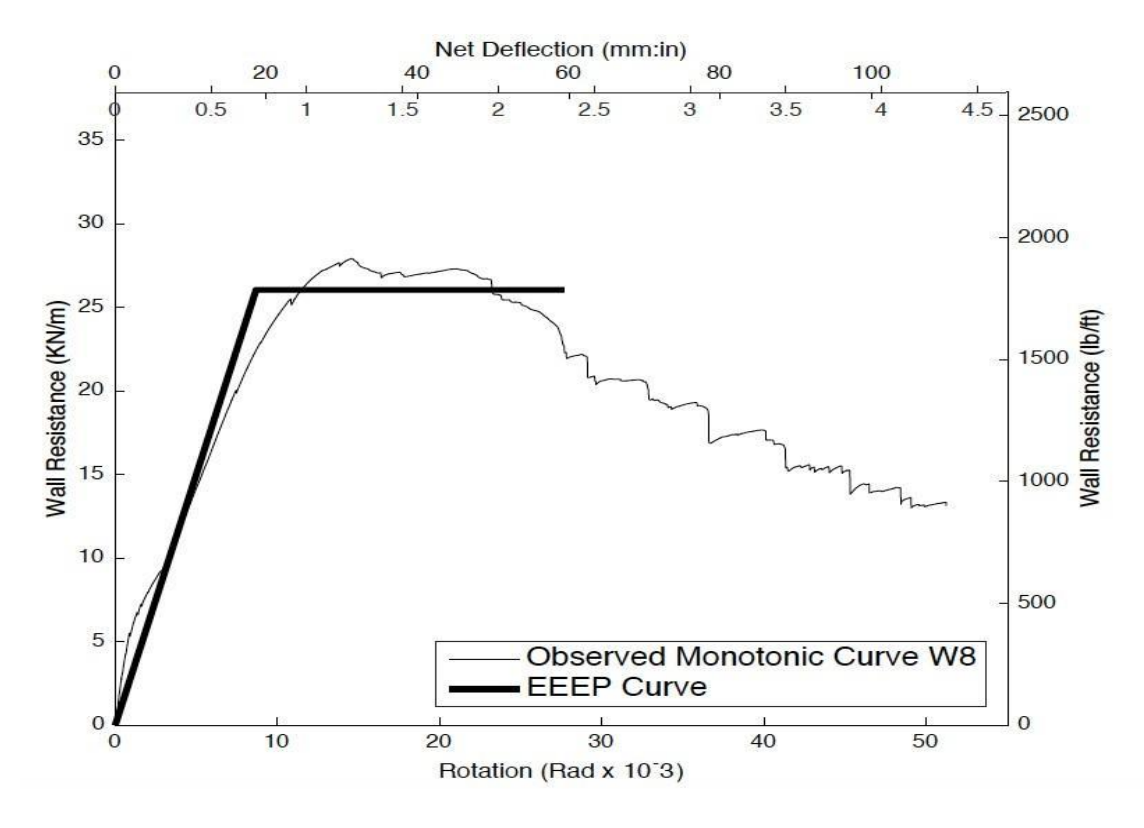


Figure B16 - Observation and EEEP Curves for Test W8-M

Parameters		Units
Fu	51,06	kN
Fu_80	40,85	kN
Fu40	20,42	kN
Fy	47,64	kN
Ke	2,56	kN/m m
μ	3,19	
Δnet,y	18,63	mm
Δnet,u	31,25	mm
Δnet,0.8u	59,38	mm
Δnet,0.4u	7,99	mm
Area Backbone	2 385,36	J
Area EEEP	2 385,36	J
Rd	2,32	
Sy	26,05	kN/m

Table B8 - Results for test W8-M

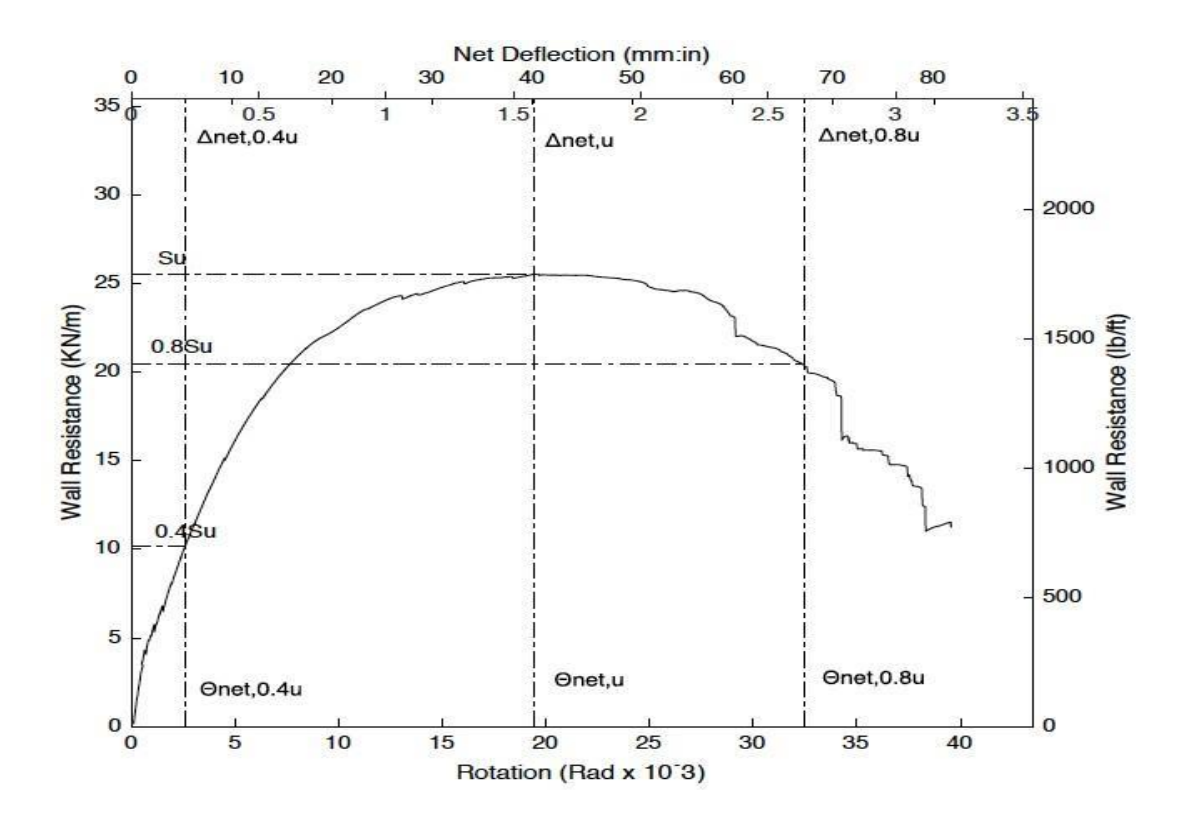


Figure B17 - Parameters of Monotonic Test W9-M

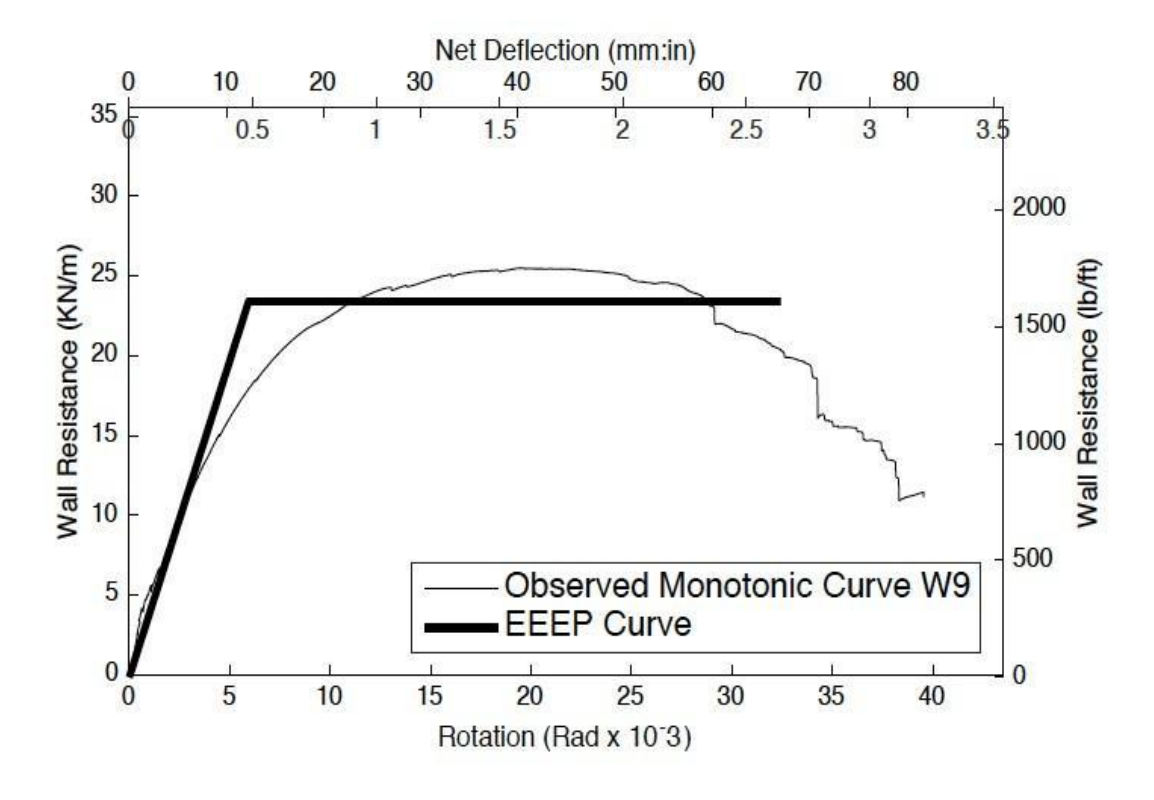


Figure B18 - Observation and EEEP Curves for Test W9-M

Parameters		Units
Fu	46,72	kN
Fu_80	37,38	kN
Fu40	18,69	kN
Fy	42,90	kN
Ke	3,49	kN/m m
μ	5,45	
Δnet,y	12,29	mm
Δnet,u	40,19	mm
Δnet,0.8u	67,04	mm
Δnet,0.4u	5,35	mm
Area Backbone	2 612,03	J
Area EEEP	2 612,03	J
Rd	3,15	
Sy	23,46	kN/m

Table B9 - Results for test W9-M

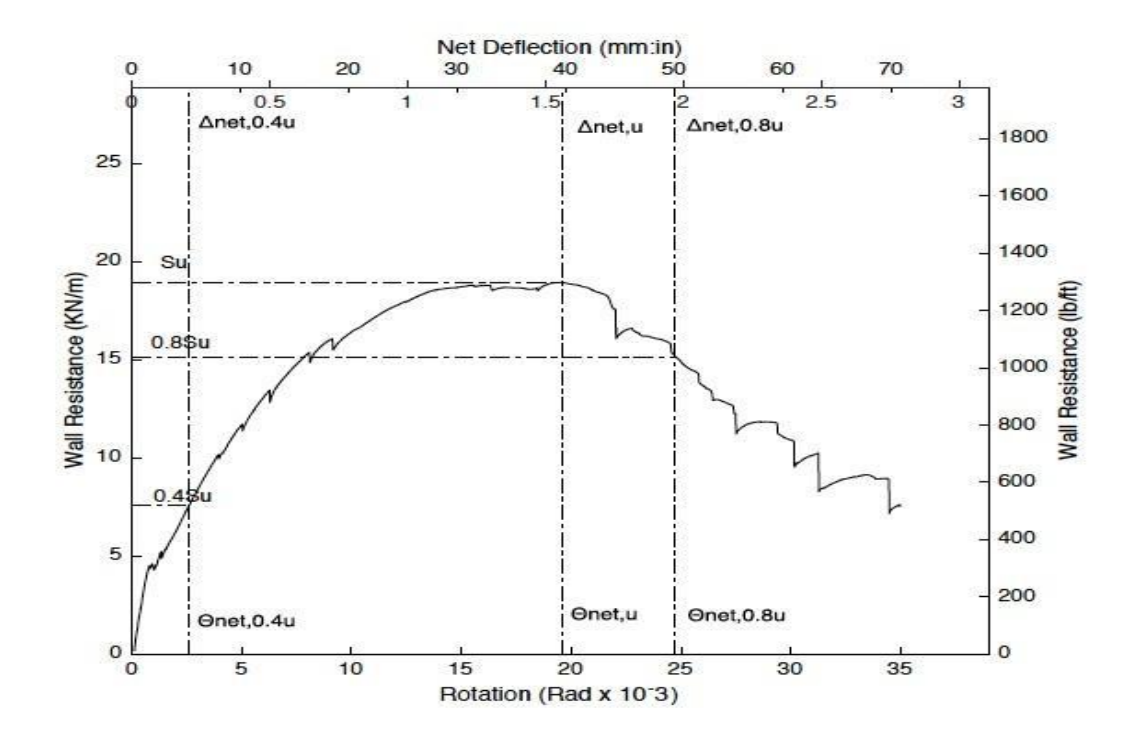


Figure B19 - Parameters of Monotonic Test W10-  $$\rm M$$ 

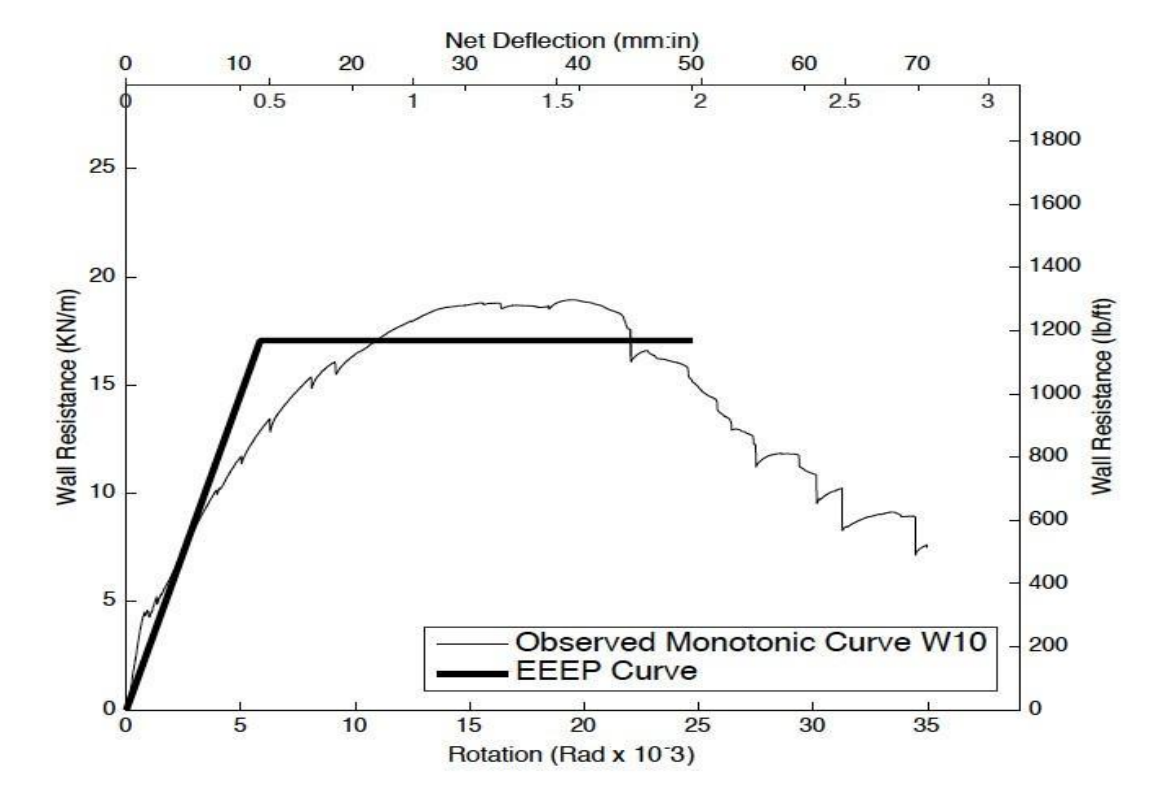


Figure B20 - Observation and EEEP Curves for Test W10-M

Parameters		Units
Fu	34,64	kN
Fu_80	27,71	kN
Fu40	13,86	kN
Fy	31,19	kN
Ke	2,64	kN/m m
μ	4,23	
Δnet,y	11,84	mm
Δnet,u	39,59	mm
Δnet,0.8u	50,04	mm
Δnet,0.4u	5,26	mm
Area Backbone	1 376,30	J
Area EEEP	1 376,30	J
Rd	2,73	
Sy	17,06	kN/m

Table B10 - Results for test W10-M

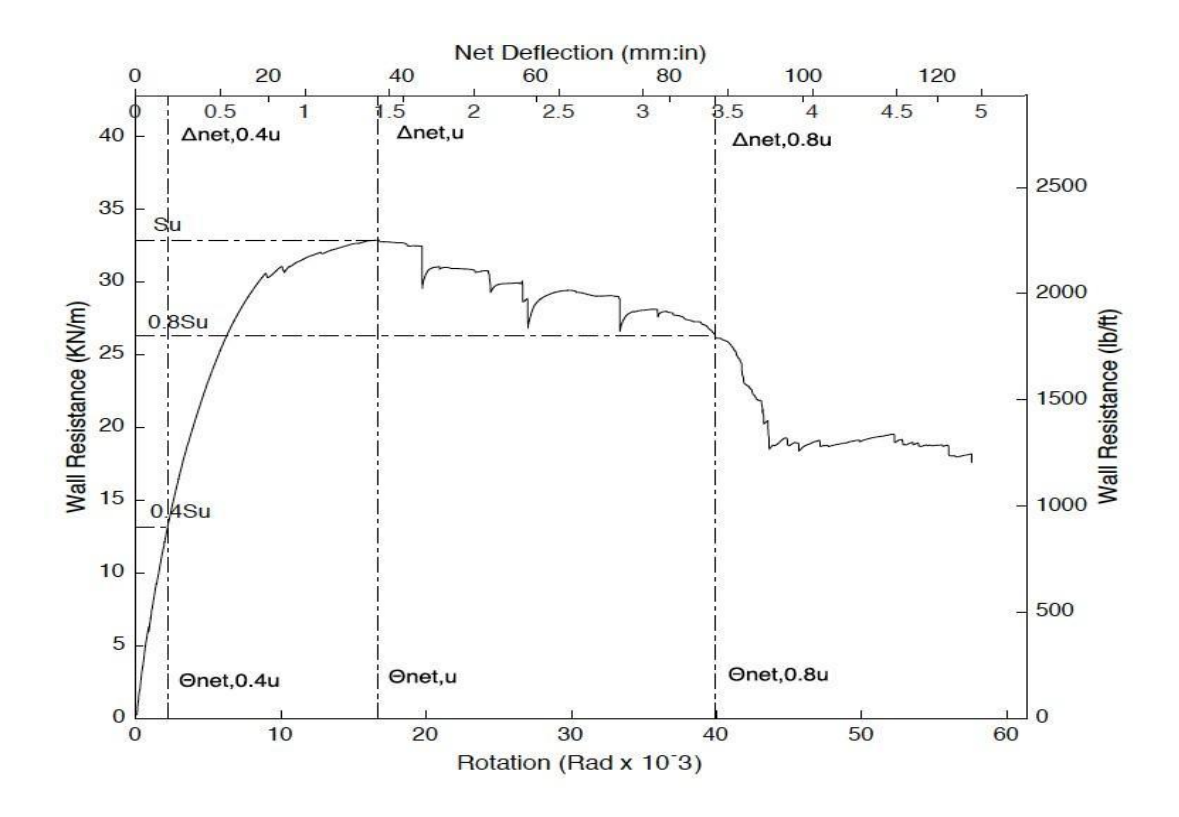


Figure B21 - Parameters of Monotonic Test W11-  $$\rm M$$ 

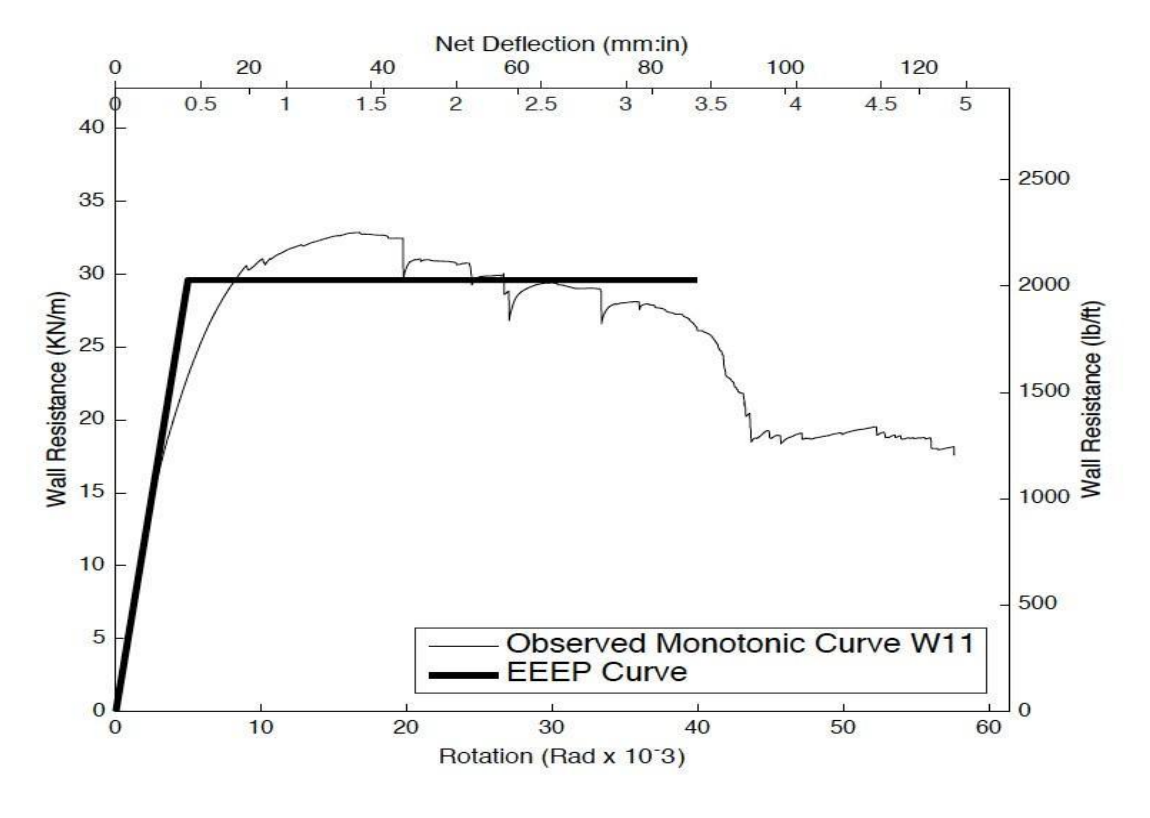


Figure B22 - Observation and EEEP Curves for Test W11-M

Parameters		Units
Fu	80,16	kN
Fu_80	64,13	kN
Fu40	32,07	kN
Fy	72,18	kN
Ke	6,70	kN/m m
μ	8,05	
Δnet,y	10,78	mm
Δnet,u	36,31	mm
Δnet,0.8u	86,77	mm
Δnet,0.4u	4,79	mm
Area Backbone	5 874,12	J
Area EEEP	5 874,12	J
Rd	3,89	
Sy	29,60	kN/m

Table B11 - Results for test W11-M

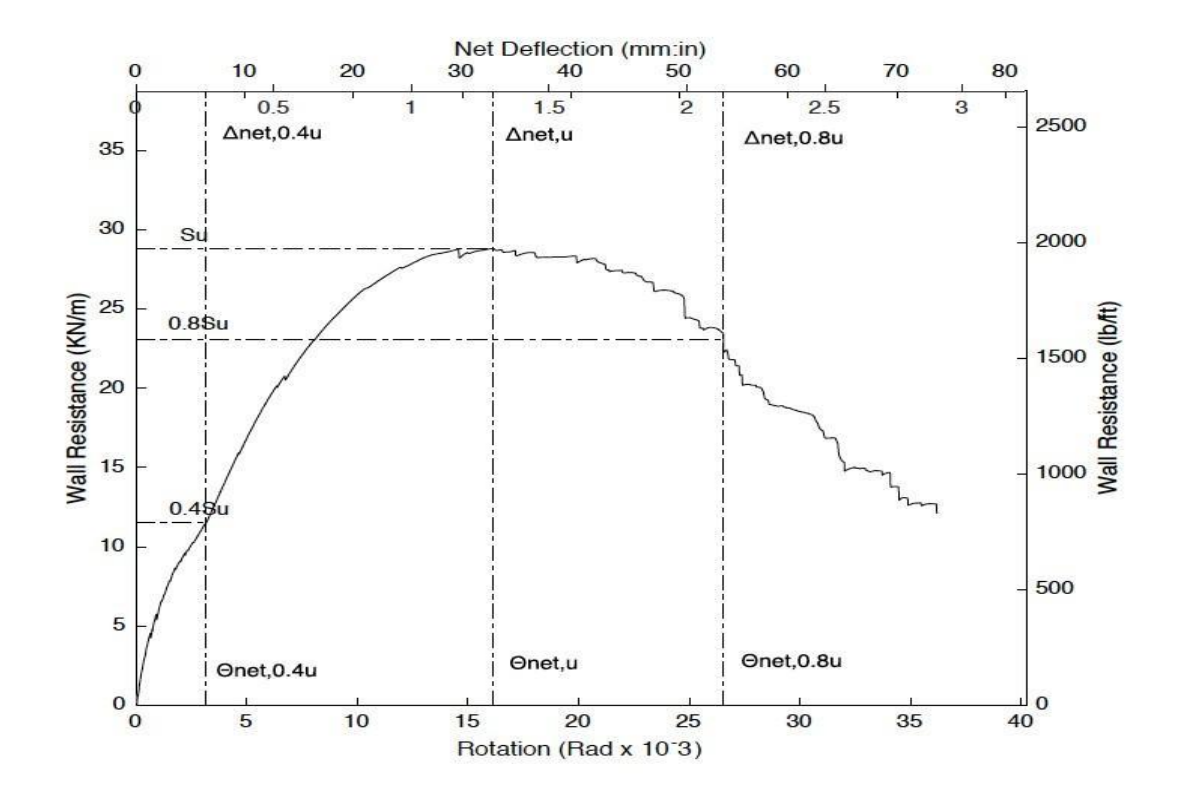


Figure B23 - Parameters of Monotonic Test W12-  $$\rm M$$ 

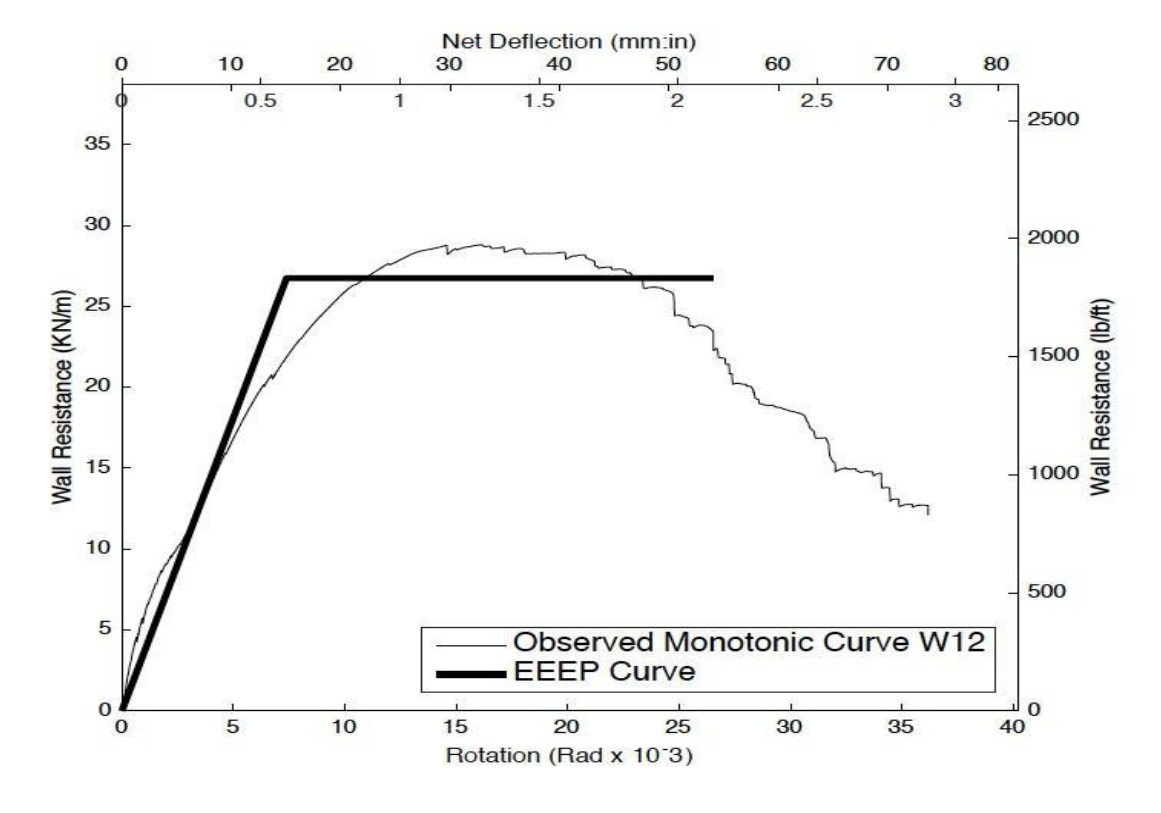


Figure B24 - Observation and EEEP Curves for Test W12-M

Parameters		Units
Fu	70,24	kN
Fu_80	56,19	kN
Fu40	28,09	kN
Fy	65,22	kN
Ke	4,34	kN/m m
μ	3,59	
Δnet,y	15,04	mm
Δnet,u	32,83	mm
Δnet,0.8u	54,03	mm
Δnet,0.4u	6,48	mm
Area Backbone	3 033,36	J
Area EEEP	3 033,36	J
Rd	2,49	
Sy	26,75	kN/m

Table B12 - Results for test W12-M

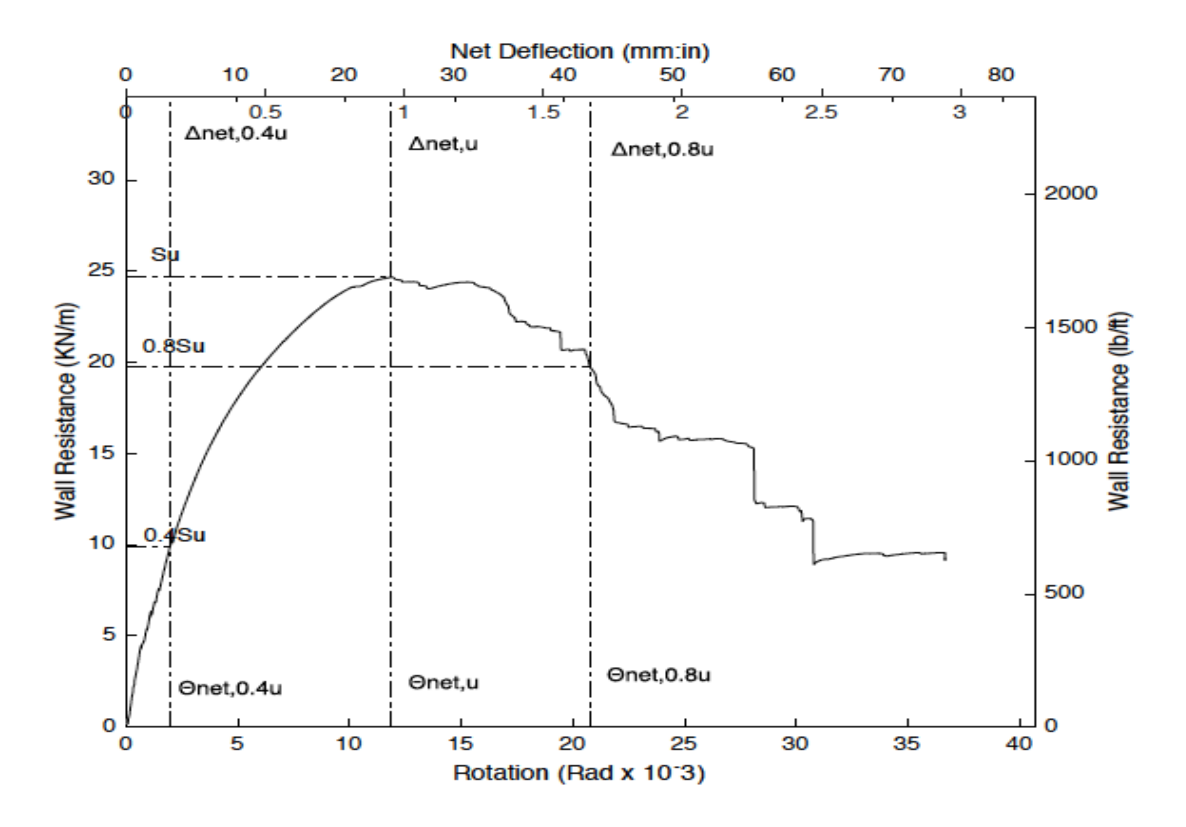


Figure B25 - Parameters of Monotonic Test W13-M

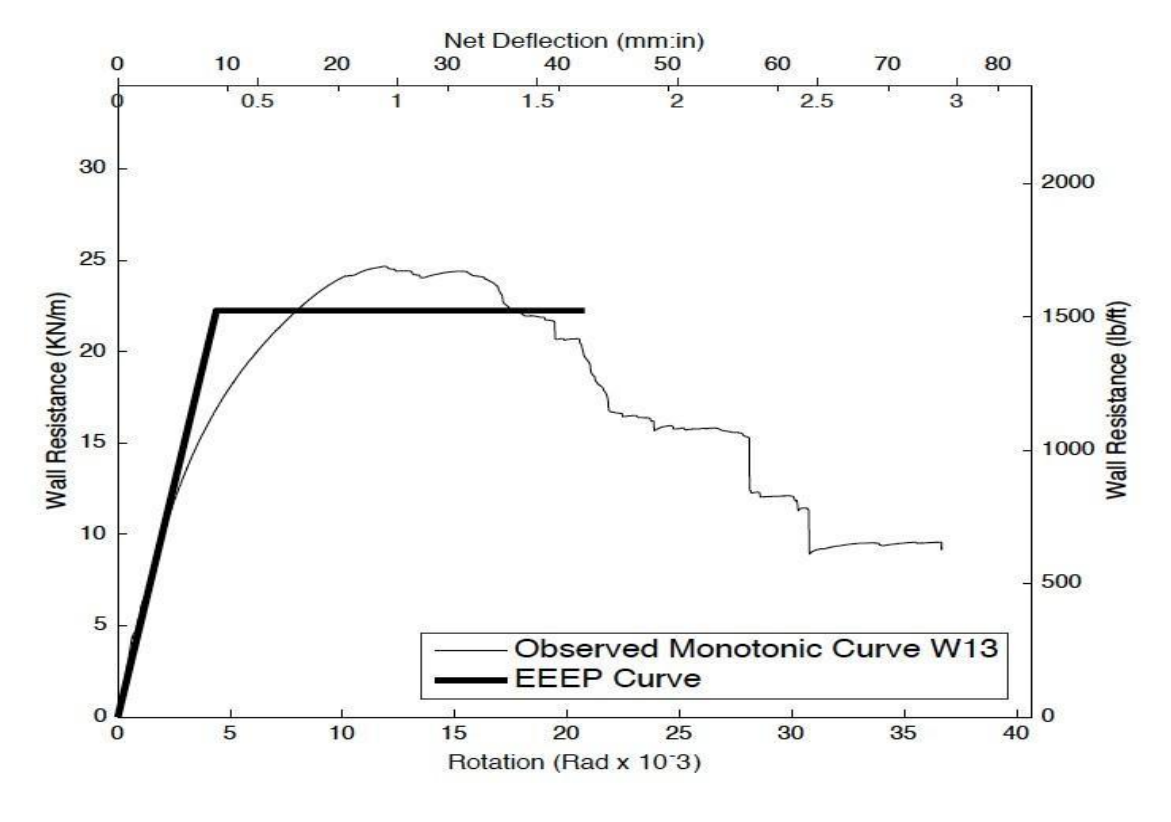


Figure B26 - Observation and EEEP Curves for Test W13-M

Parameters		Units
Fu	60,18	kN
Fu_80	48,14	kN
Fu40	24,07	kN
Fy	54,26	kN
Ke	6,06	kN/m m
μ	4,73	
Δnet,y	8,95	mm
Δnet,u	24,20	mm
Δnet,0.8u	42,37	mm
Δnet,0.4u	3,97	mm
Area Backbone	2 056,51	J
Area EEEP	2 056,51	J
Rd	2,91	
Sy	22,25	kN/m

Table B13 - Results for test W13-M

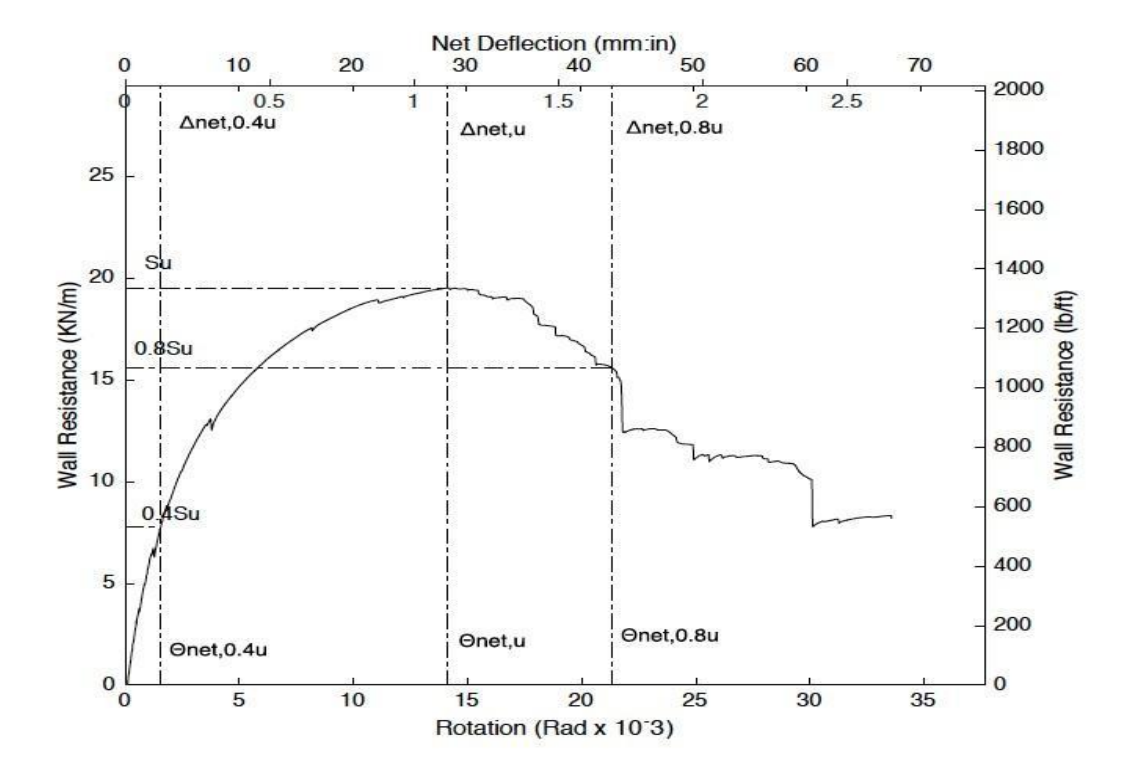


Figure B27 - Parameters of Monotonic Test W14-M

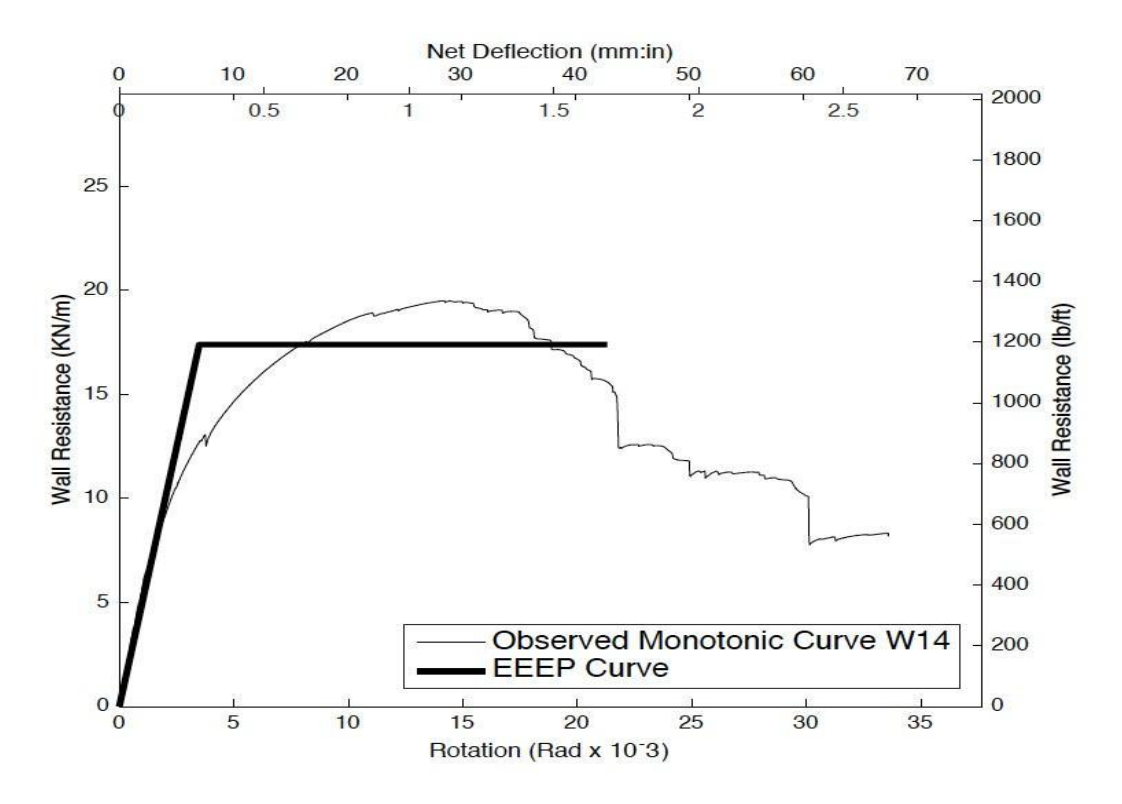


Figure B28 - Observation and EEEP Curves for Test W14-M

219

Parameters		Units
Fu	47,56	kN
Fu_80	38,05	kN
Fu40	19,02	kN
Fy	42,42	kN
Ke	6,05	kN/m m
μ	6,10	
Δnet,y	7,01	mm
Δnet,u	28,35	mm
Δnet,0.8u	42,77	mm
Δnet,0.4u	3,14	mm
Area Backbone	1 665,30	J
Area EEEP	1 665,30	J
Rd	3,35	
Sy	17,39	kN/m

Table B14 - Results for test W14-M

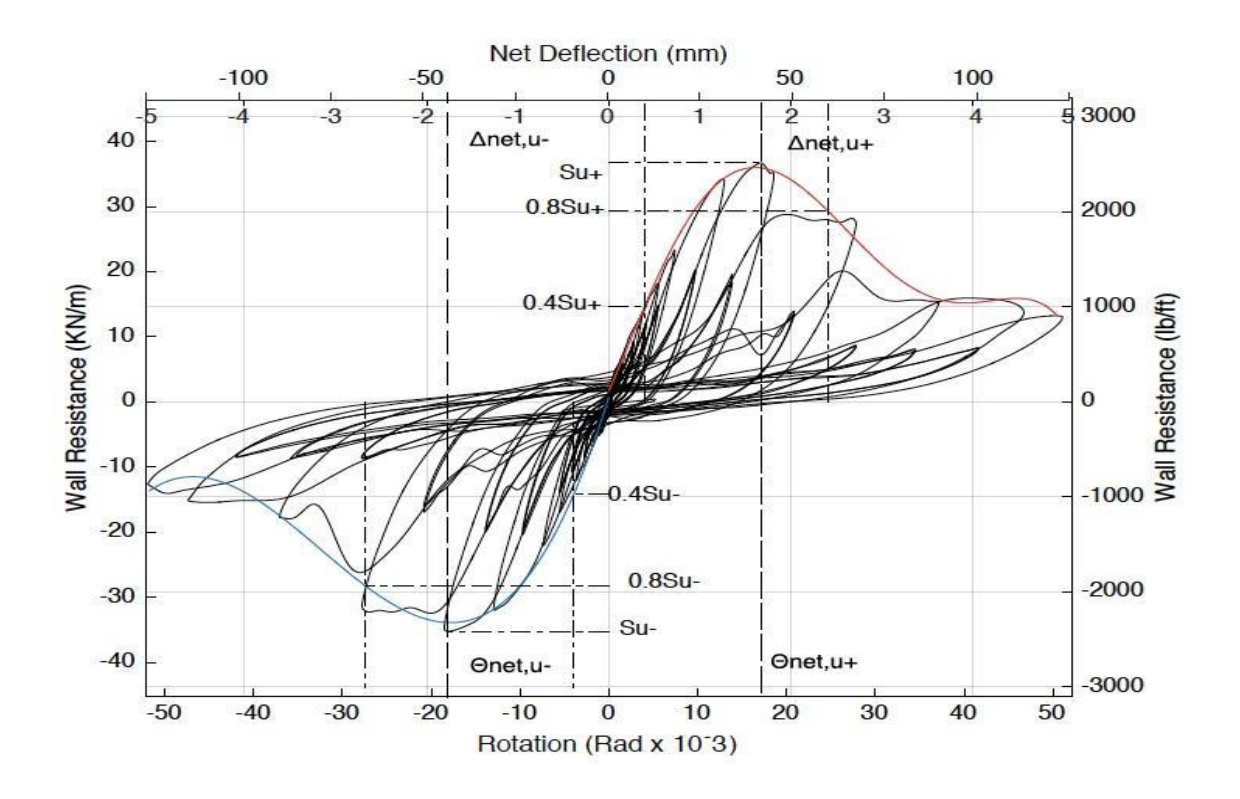


Figure B29 - Parameters of Reversed Cyclic Test W1-C

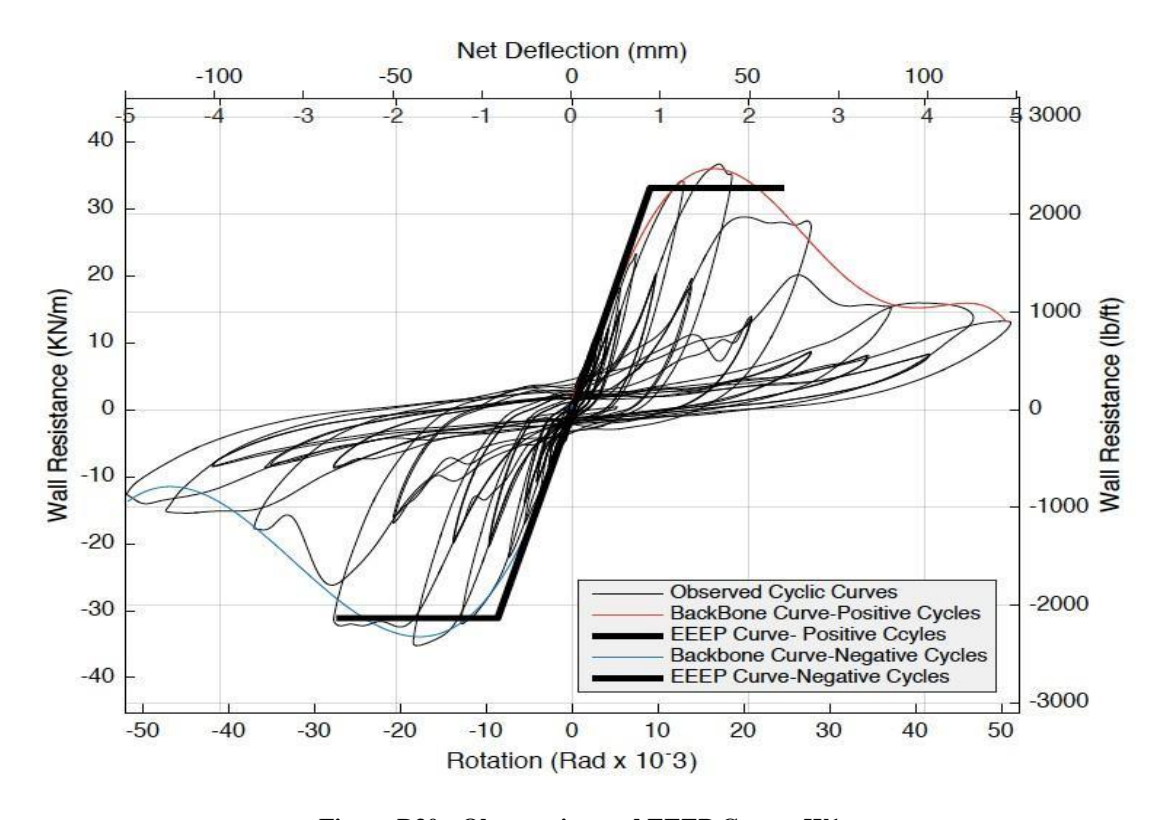


Figure B30 - Observation and EEEP Curves W1-

Parameters			Unit s
	Positive	Negative	
Fu	44,75	42,94	kN
Fu_80	35,80	34,35	kN
Fu40	17,90	17,18	kN
Fy	40,38	37,93	kN
Ke	1,83	1,79	kN/ mm
μ	2,72	3,16	
Δnet,y	22,11	21,20	mm
Δnet,u	41,68	44,16	mm
Δnet,0.8u	60,10	67,00	mm
Δnet,0.4u	9,80	9,60	mm
Area EEEP	1980,67	2139,45	J
Area Backbone	1980,67	2139,45	J
Rd	2,11	2,31	
Sy	33,12	31,11	kN/ m

Table B15 - Results for test W1-C

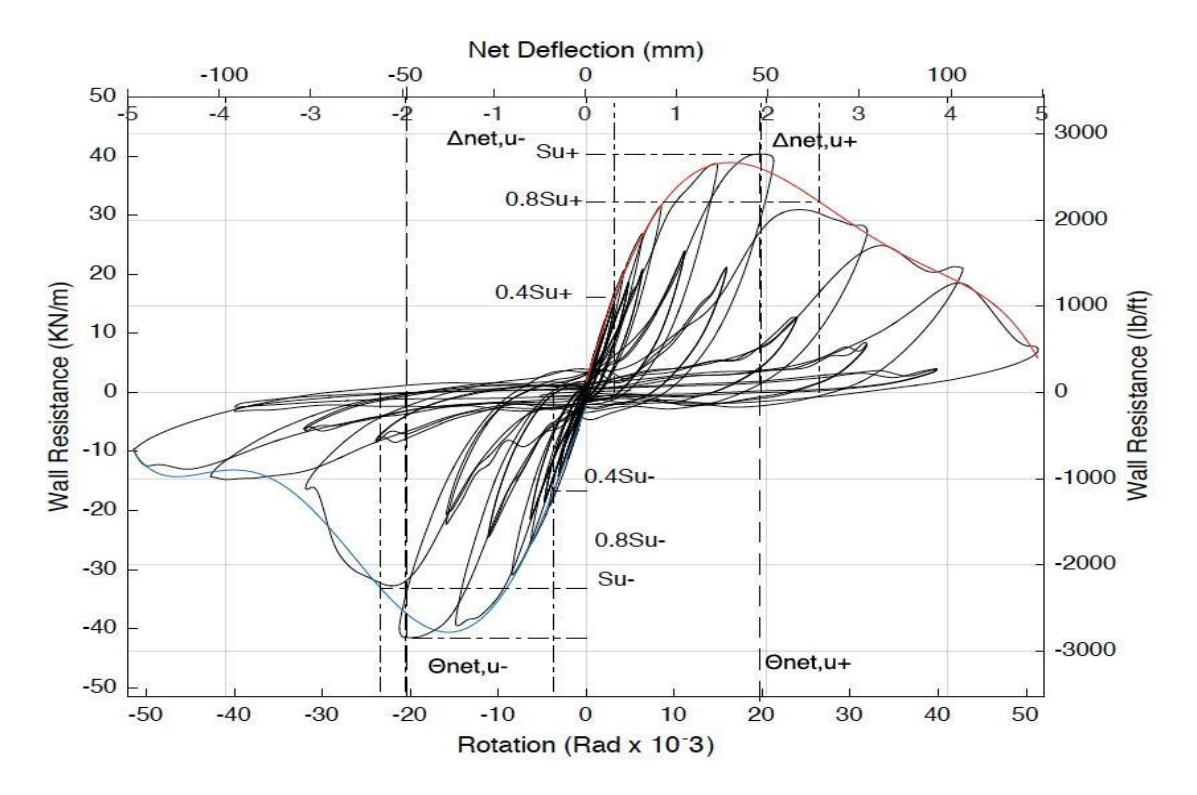


Figure B31 - Parameters of Reversed Cyclic Test W2-C

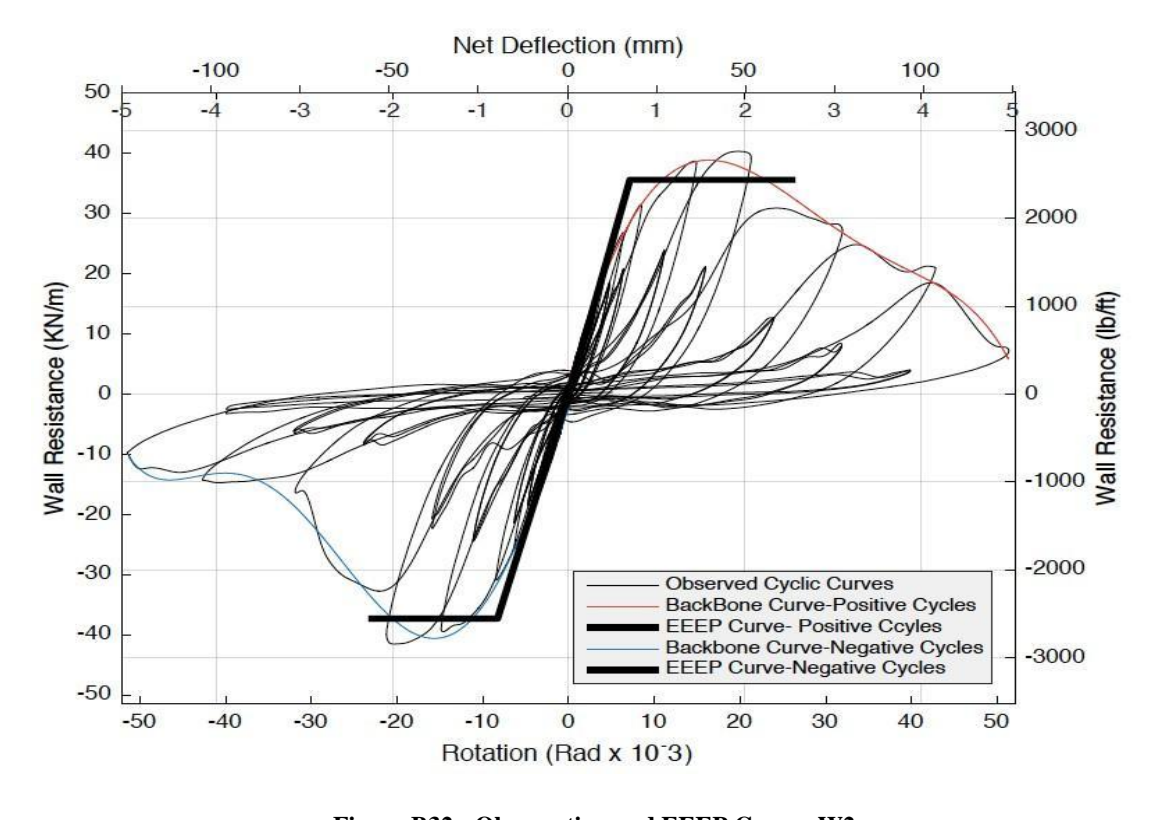


Figure B32 - Observation and EEEP Curves W2-

Parameters			Unit s
	Positiv e	Negative	
Fu	49,19	50,65	kN
Fu_80	39,35	40,52	kN
Fu40	19,68	20,26	kN
Fy	43,43	45,50	kN
Ke	2,49	2,25	kN/ mm
μ	3,70	2,82	
Δnet,y	17,44	20,21	mm
Δnet,u	48,29	49,97	mm
Δnet,0.8u	64,50	56,90	mm
Δnet,0.4u	7,90	9,00	mm
Area EEEP	2422,8 4	2129,07	J
Area Backbone	2422,8 4	2129,07	J
Rd	2,53	2,15	
Sy	35,63	37,32	kN/ m

Table B16 - Results for test W2-C

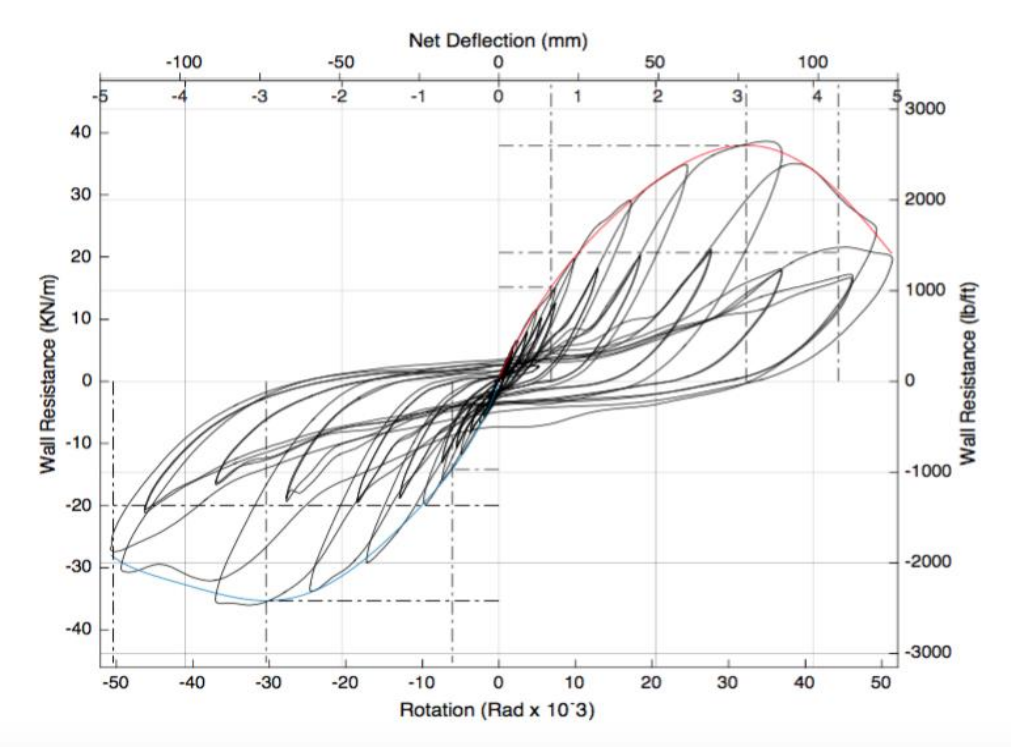


Figure B33 - Parameters of Reversed Cyclic Test W3-C

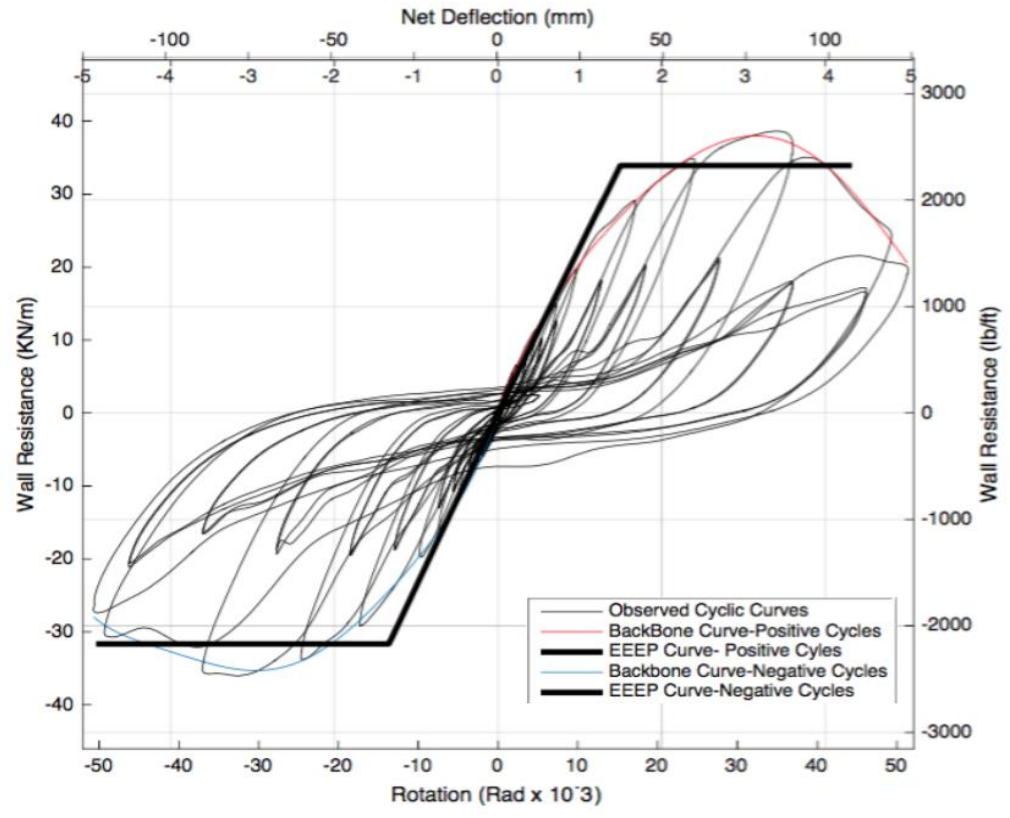


Figure B34 - Observation and EEEP Curves W3-

Parameters			Unit s
	Positive	Negative	
Fu	23.56	-21.96	kN
Fu_80	20.69	-19.53	kN
Fu40	9.42	-8.78	kN
Fy	20.85	19.58	kN
Ke	0.54	0.57	kN/ mm
μ	2.61	2.89	
Δnet,y	38.27	34.55	mm
Δnet,u	85.80	-79.80	mm
Δnet,0.8u	100.00	100.00	mm
∆net,0.4u	17.30	15.50	mm
Area EEEP	1,685.79	1,619.63	J
Area Backbone	1,685.79	1,619.63	J
Rd	2.06	2.19	
Sy	34.20	32.12	kN/ m

Table B17 - Results for test W3-C

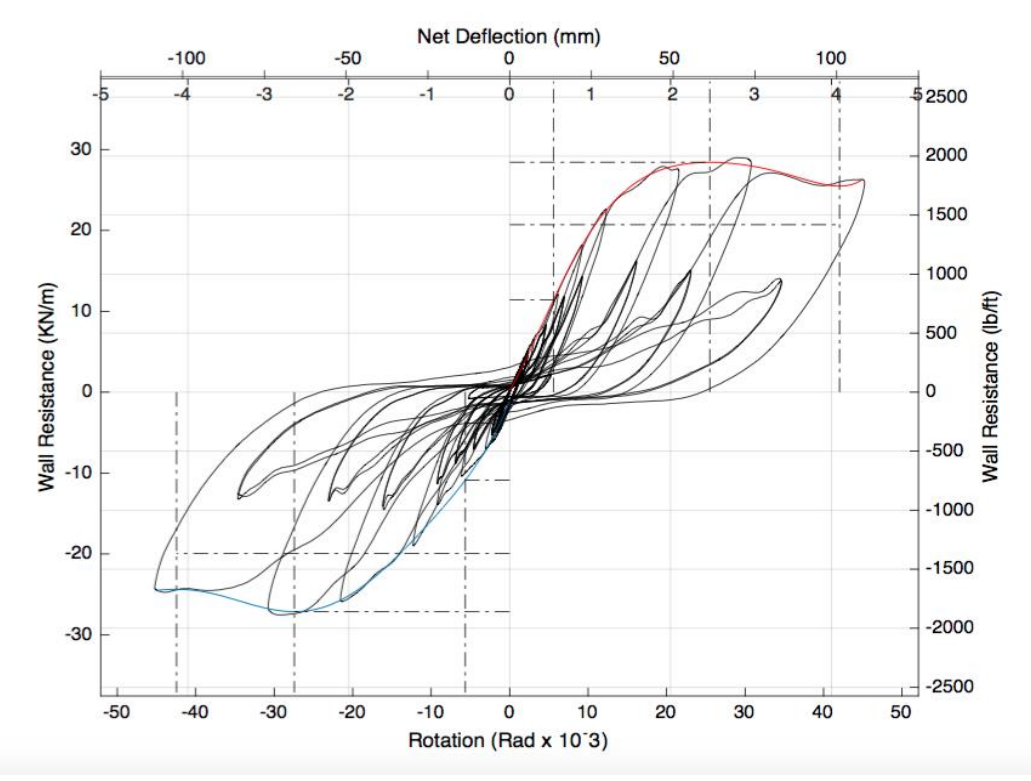


Figure B35 - Parameters of Reversed Cyclic Test W4-C

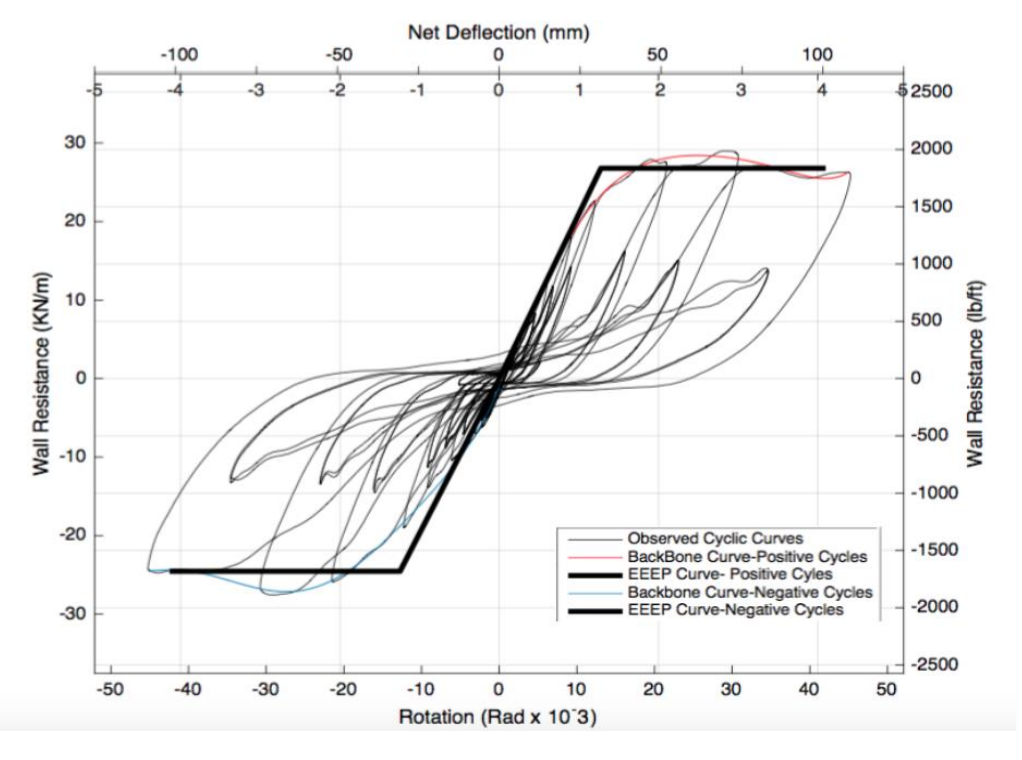


Figure B36 - Observation and EEEP Curves W4- C

Parameters			Units
	Positive	Negative	
Fu	17.68	-16.80	kN
Fu_80	15.54	-14.80	kN
Fu40	7.07	-6.72	kN
Fy	16.49	15.02	kN
Ke	0.51	0.45	kN/m m
μ	3.06	2.98	
Δnet,y	32.64	33.53	mm
Δnet,u	70.79	-71.12	mm
∆net,0.8u	100.00	100.00	mm
Δnet,0.4u	14.00	15.00	mm
Area EEEP	1379.58	1250.43	J
Area Backbone	1379.58	1250.43	J
Rd	2.26	2.23	
Sy	27.04	24.64	kN/m

Table B18 - Results for test W4-C

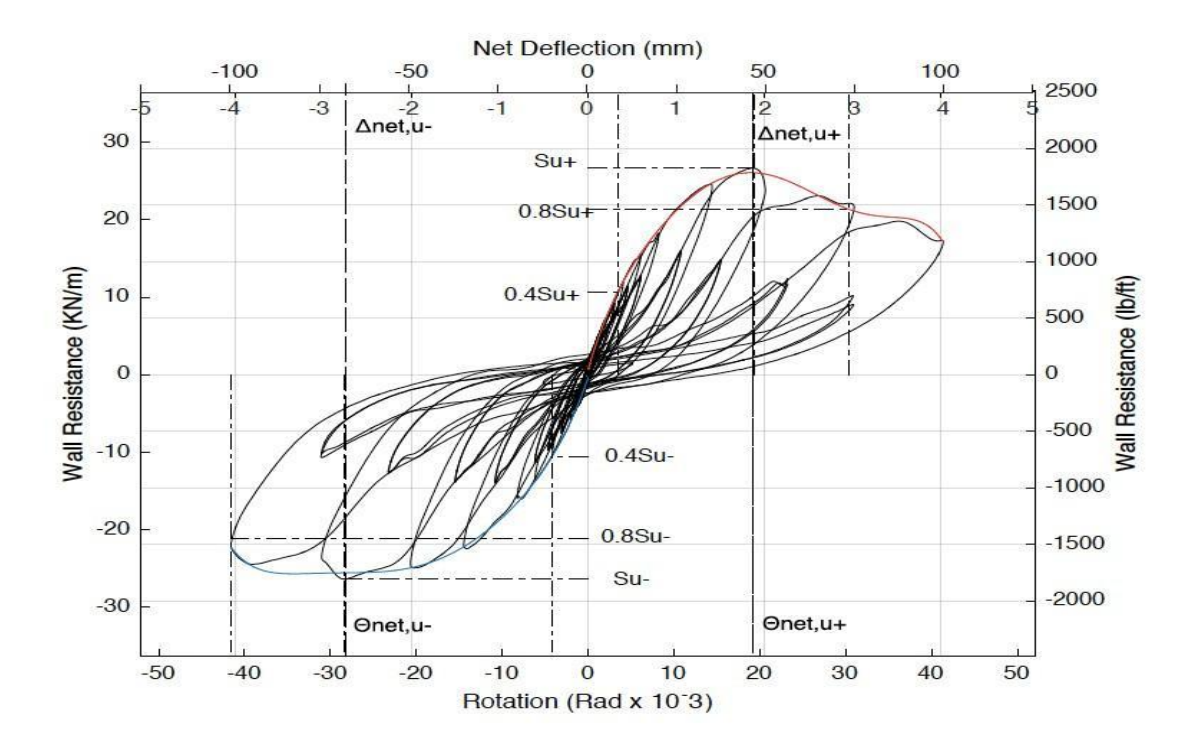


Figure B37 - Parameters of Reversed Cyclic Test W5-C

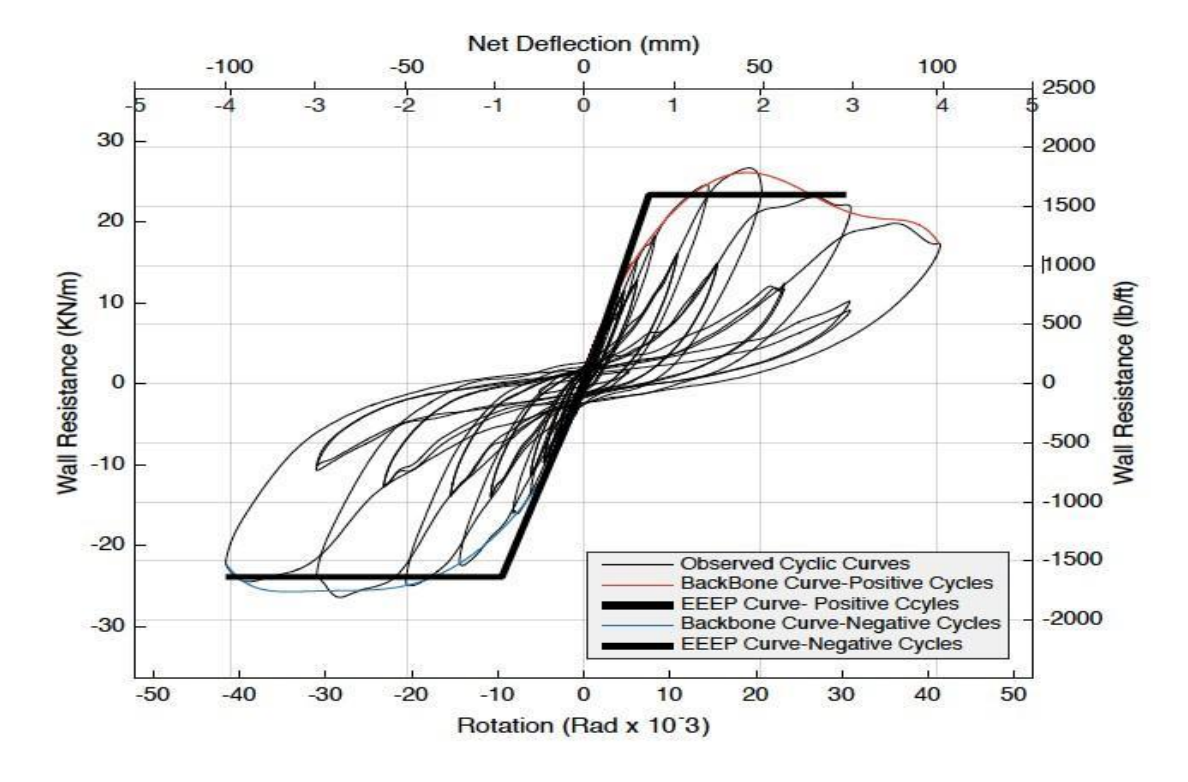


Figure B38 - Observation and EEEP Curves W5-

Parameters			Unit s
	Positiv e	Negative	
Fu	16,26	-16,09	kN
Fu_80	13,01	-12,87	kN
Fu40	6,50	-6,43	kN
Fy	14,23	-14,54	kN
Ke	0,77	0,62	kN/ mm
μ	4,04	4,35	
Δnet,y	18,38	23,28	mm
Δnet,u	47,13	-69,21	mm
Δnet,0.8u	74,20	-101,40	mm
Δnet,0.4u	8,40	-10,30	mm
Area EEEP	925,21	1305,48	J
Area Backbone	925,21	1305,48	J
Rd	2,66	2,78	
Sy	23,35	-23,86	kN/ m

Table B19 - Results for test W5-C

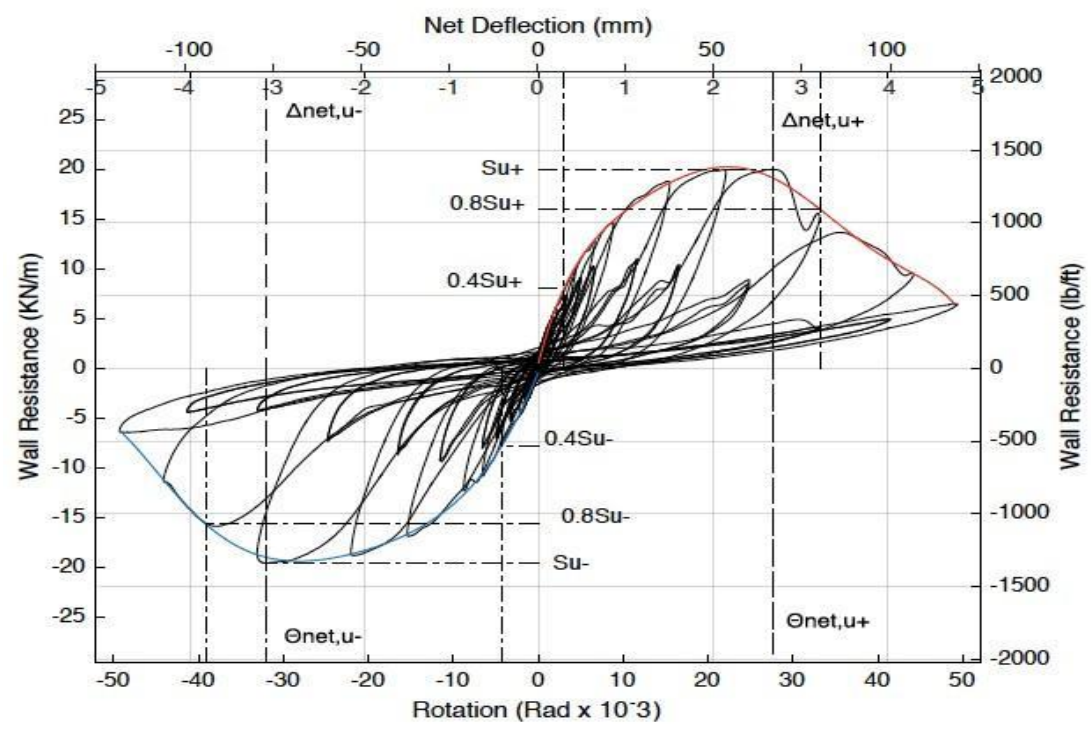


Figure B39 - Parameters of Reversed Cyclic Test W6-C

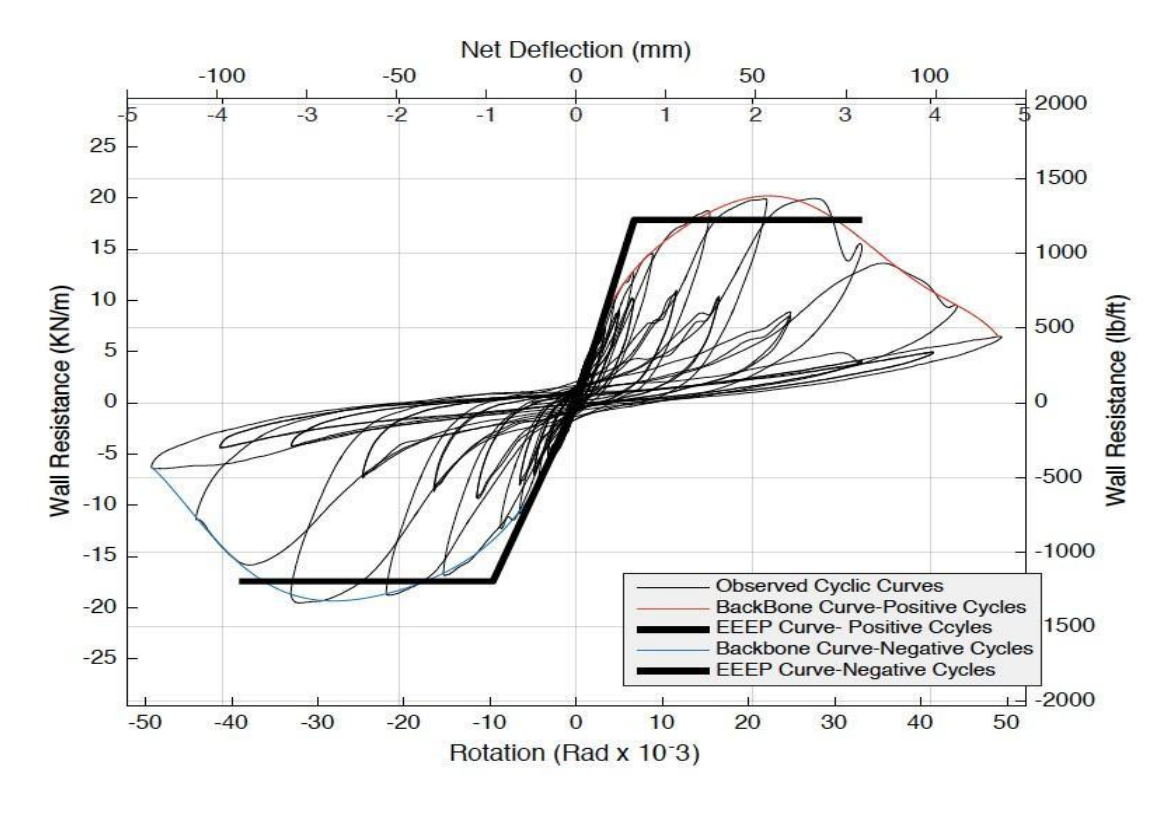


Figure B40 - Observation and EEEP Curves W6-

Parameters			Units
	Positive	Negative	
Fu	12,18	-11,92	kN
Fu_80	9,74	-9,54	kN
Fu40	4,87	-4,77	kN
Fy	10,90	-10,63	kN
Ke	0,67	0,45	kN/m m
μ	4,95	4,04	
Δnet,y	16,34	-23,64	mm
Δnet,u	67,27	-78,40	mm
Δnet,0.8u	80,80	-95,40	mm
Δnet,0.4u	7,30	-10,60	mm
Area EEEP	791,84	888,58	J
Area Backbone	791,84	888,58	J
Rd	2,98	2,66	
Sy	17,88	17,44	kN/m

Table B20 - Results for test W6-C

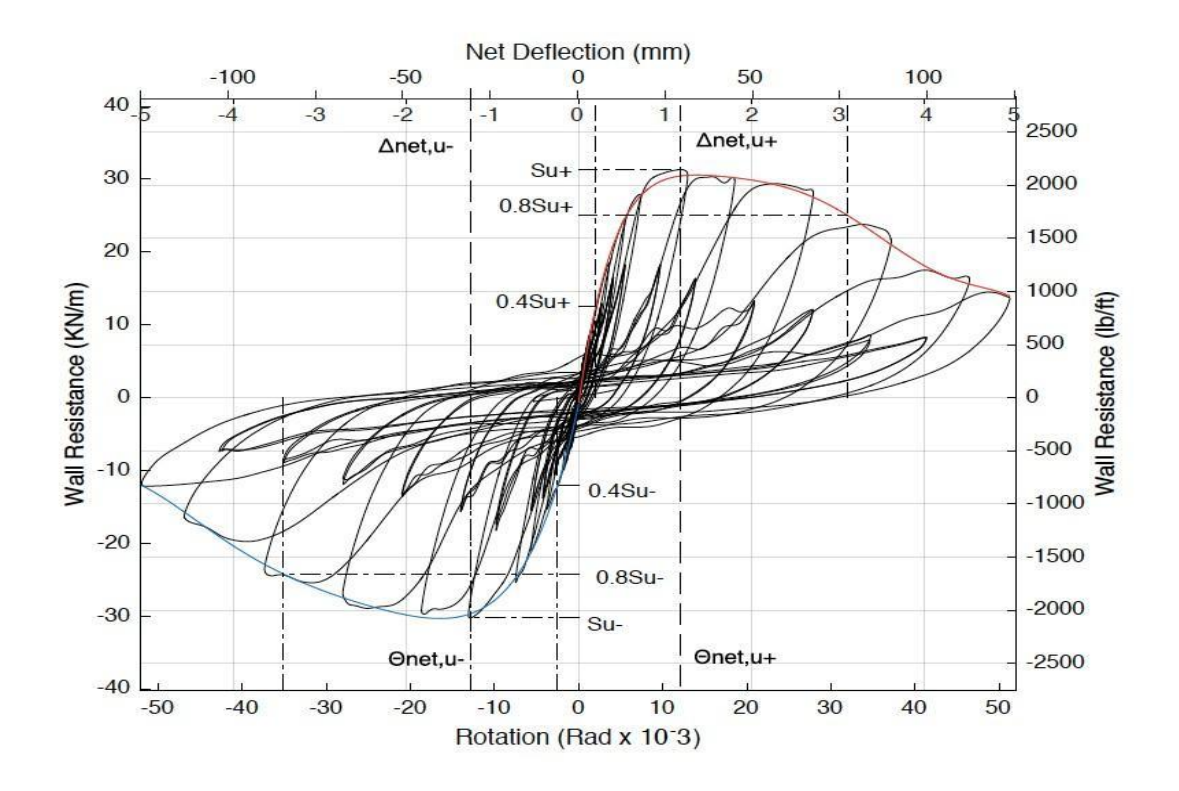


Figure B41 - Parameters of Reversed Cyclic Test W7-C

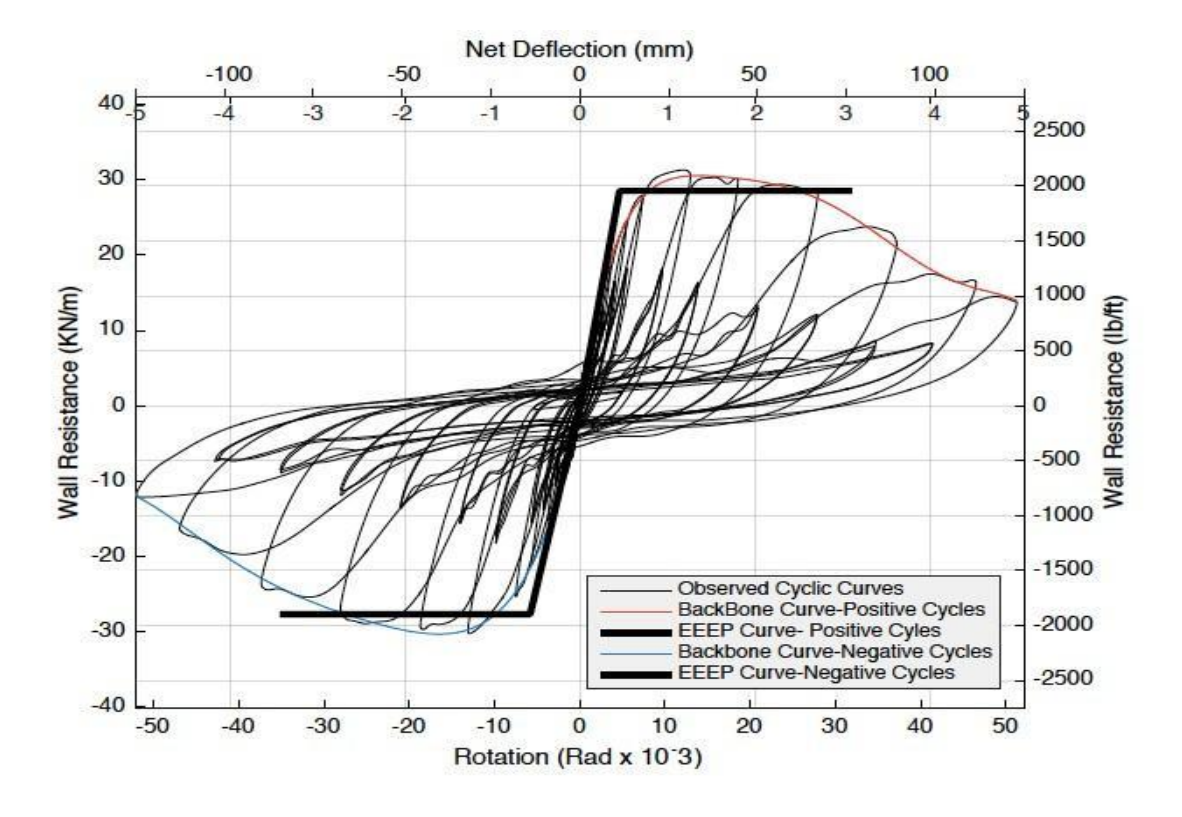


Figure B42 - Observation and EEEP Curves W7- C

Parameters			Units
	Positive	Negative	
Fu	57,31	55,31	kN
Fu_80	45,85	44,25	kN
Fu40	22,92	22,12	kN
Fy	52,18	50,65	kN
Ke	4,58	3,57	kN/m m
μ	6,84	6,04	
Δnet,y	11,38	14,19	mm
Δnet,u	29,54	31,42	mm
Δnet,0.8u	77,80	85,70	mm
Δnet,0.4u	5,00	6,20	mm
Area EEEP	3762,75	3980,96	J
Area Backbone			
	3762,75	3980,96	J
Rd	3,56	3,33	
Sy	28,53	27,69	kN/m

Table B21 - Results for test W7-C

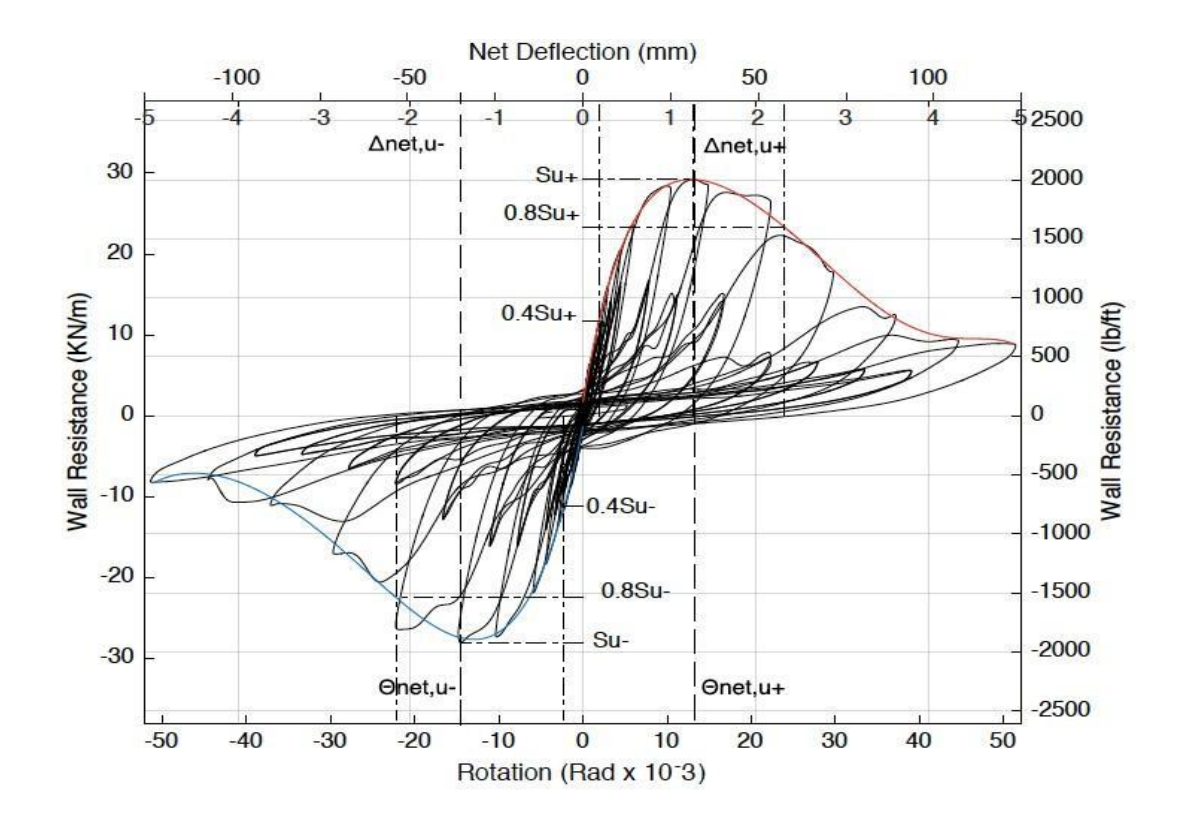


Figure B43 - Parameters of Reversed Cyclic Test W8-C

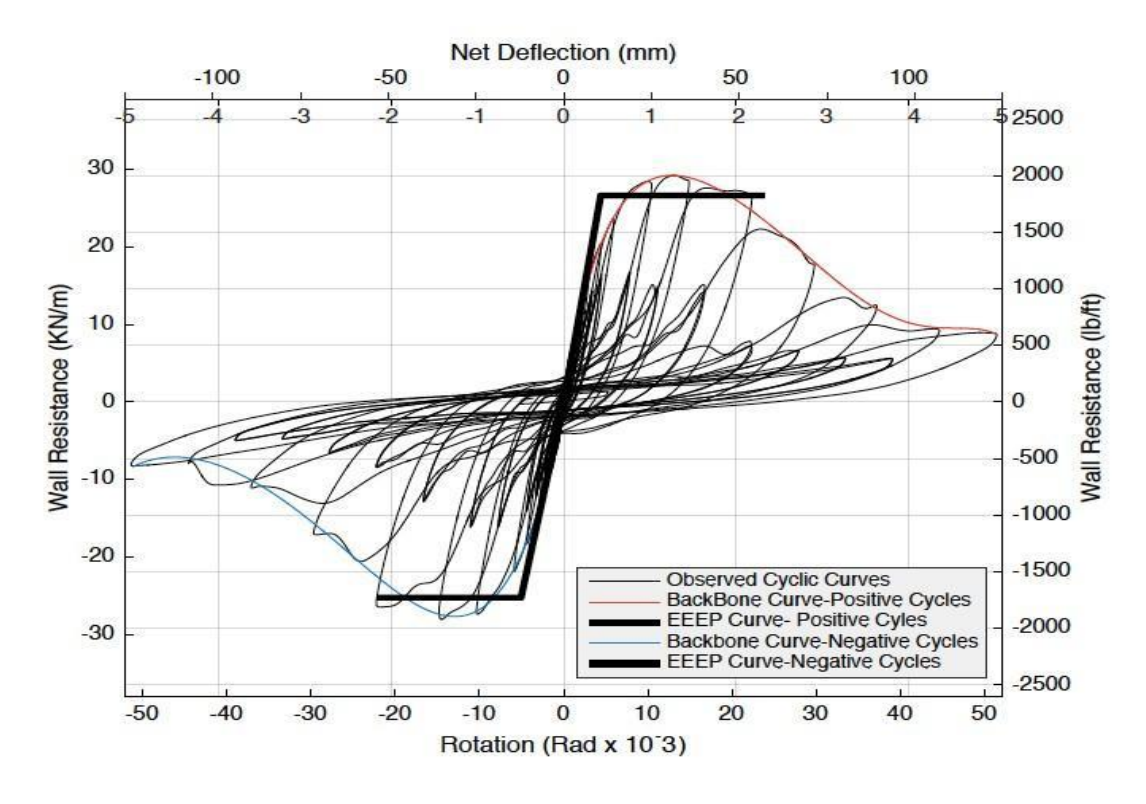


Figure B44 - Observation and EEEP Curves W8-C

Parameters	Parameters		
	Positive	Negative	
Fu	53,44	51,28	kN
Fu_80	42,75	41,02	kN
Fu40	21,38	20,51	kN
Fy	48,70	46,11	kN
Ke	4,55	3,73	kN/m m
μ	5,44	4,38	
Δnet,y	10,71	12,37	mm
Δnet,u	31,92	35,41	mm
Δnet,0.8u	58,20	54,20	mm
Δnet,0.4u	4,70	5,50	mm
Area EEEP	2573,53	2214,21	J
Area Backbone			
	2573,53	2214,21	J
Rd	3,14	2,79	
Sy	26,63	25,21	kN/m

Table B22 - Results for test W8-C

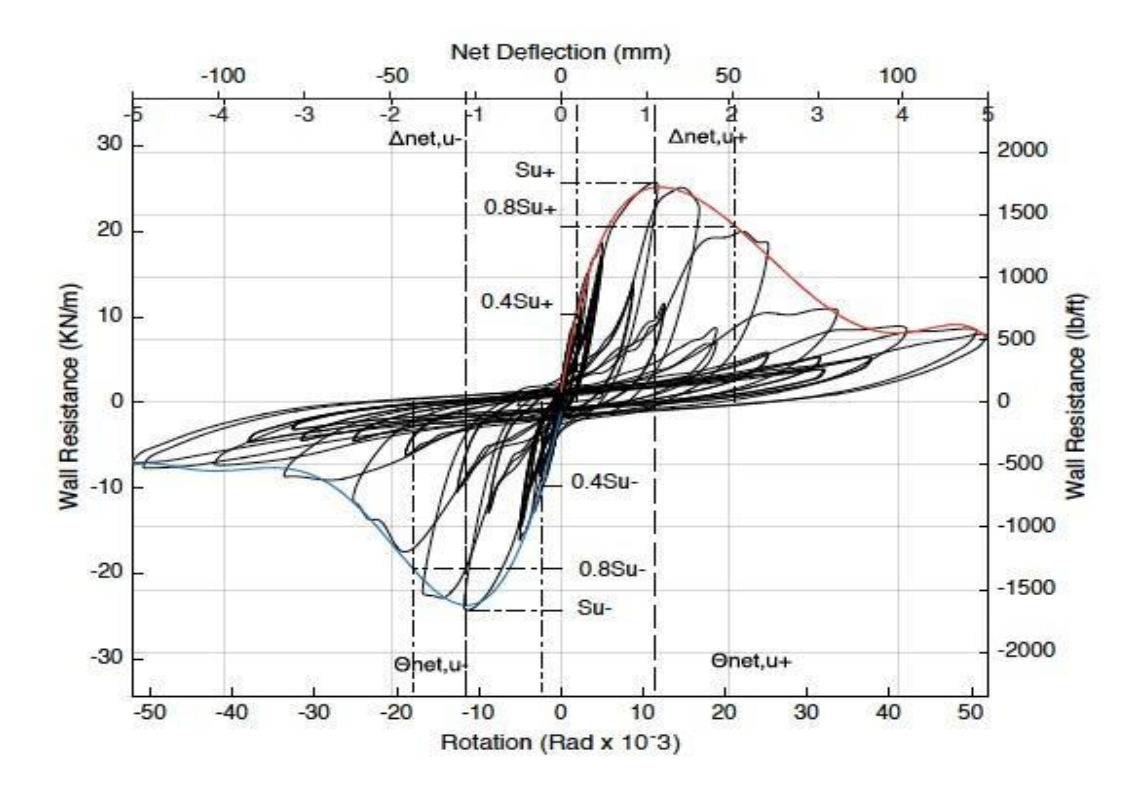


Figure B45 - Parameters of Reversed Cyclic Test W9-C

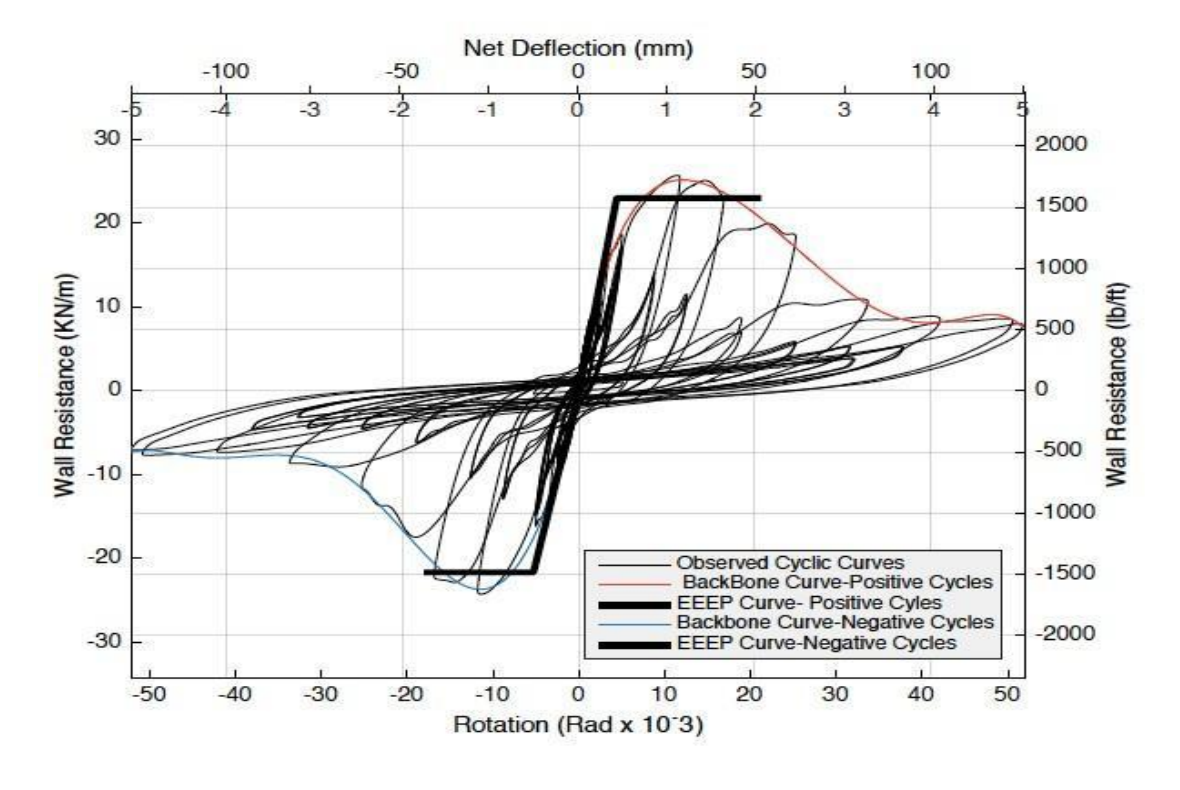


Figure B46 - Observation and EEEP Curves W9-

Parameters			Units
	Positive	Negativ e	
Fu	47,01	44,42	kN
Fu_80	37,61	35,54	kN
Fu40	18,80	17,77	kN
Fy	42,10	39,65	kN
Ke	3,92	3,06	kN/m m
μ	4,82	3,40	
Δnet,y	10,75	12,94	mm
Δnet,u	27,89	27,97	mm
Δnet,0.8u	51,80	44,00	mm
Δnet,0.4u	4,80	5,80	mm
Area EEEP	1954,58	1487,88	J
Area Backbone	1954,58	1487,88	J
Rd	2,94	2,41	
Sy	23,02	21,68	kN/m

Table B23 - Results for test W9-C

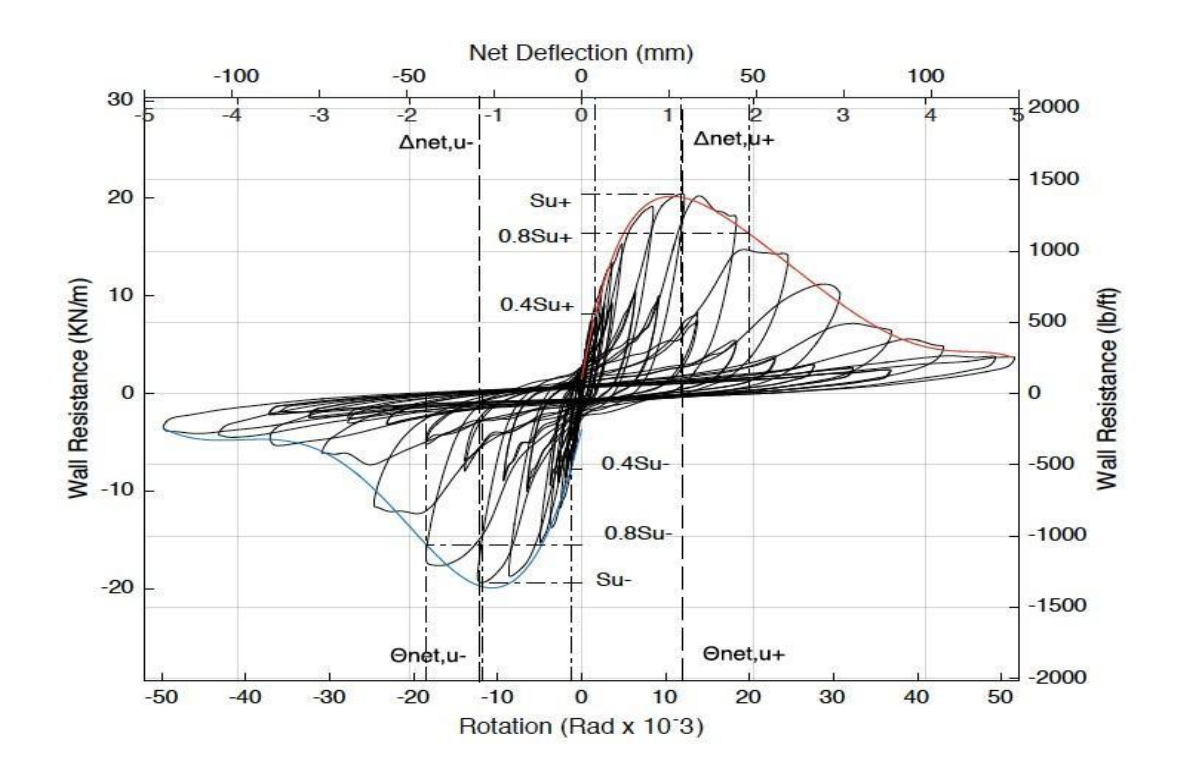


Figure B47 - Parameters of Reversed Cyclic Test W10-C

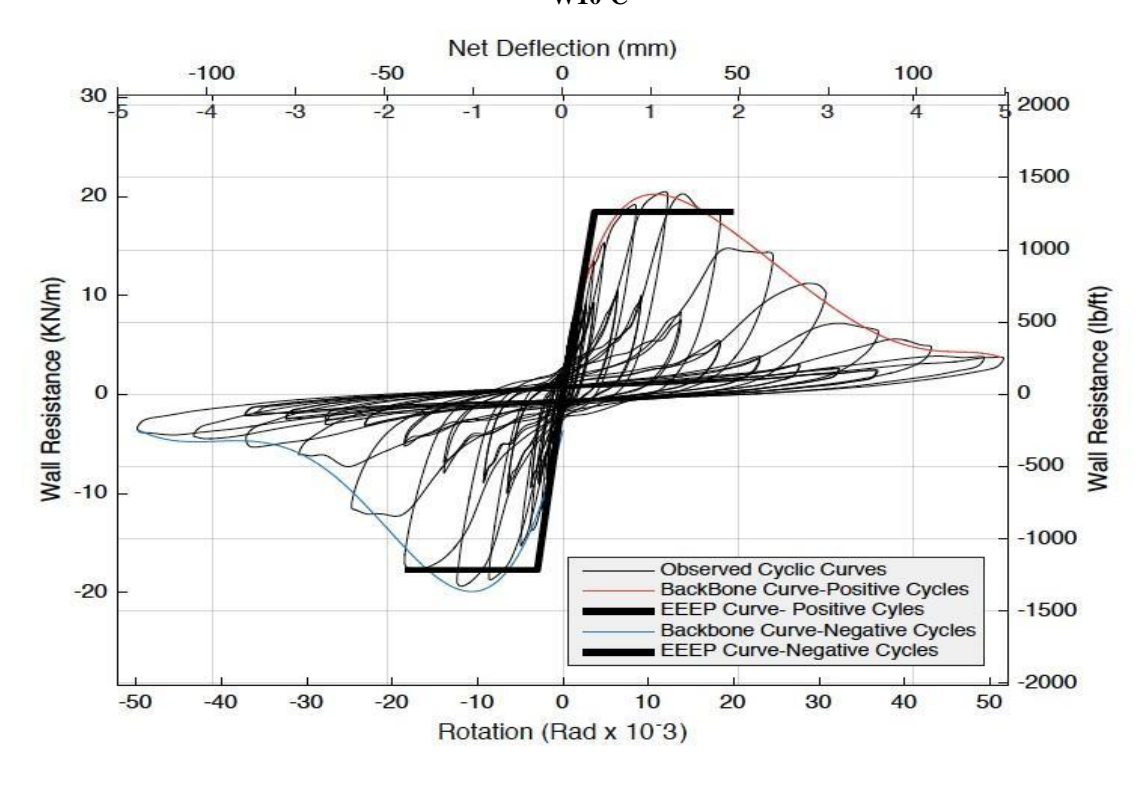


Figure B48 - Observation and EEEP Curves W10- C

Parameters	Parameters		
	Positive	Negative	
Fu	37,44	35,41	kN
Fu_80	29,95	28,33	kN
Fu40	14,98	14,16	kN
Fy	33,69	32,41	kN
Ke	3,74	4,43	kN/m m
μ	5,41	6,16	
Δnet,y	9,00	7,32	mm
Δnet,u	29,05	29,05	mm
Δnet,0.8u	48,70	45,10	mm
Δnet,0.4u	4,00	3,20	mm
Area EEEP	1489,24	1343,14	J
Area Backbone			
	1489,24	1343,14	J
Rd	3,13	3,36	
Sy	18,42	17,72	kN/m

Table B24 - Results for test W10-C

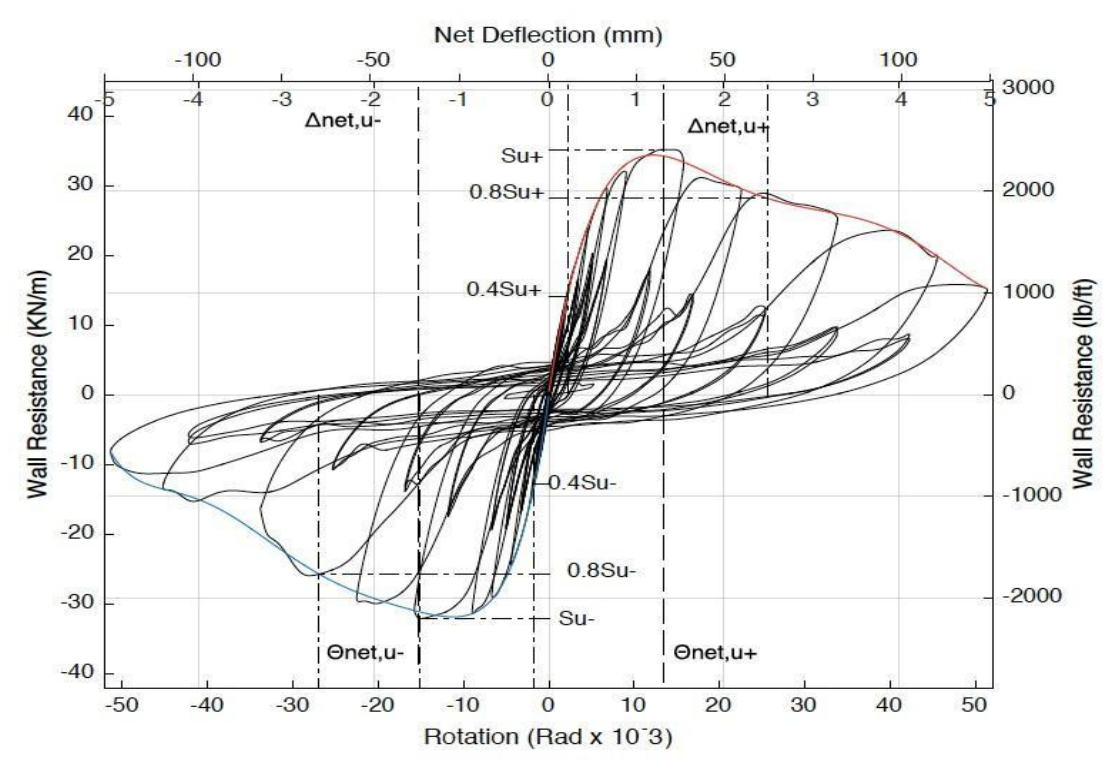


Figure B49 - Parameters of Reversed Cyclic Test W11-C

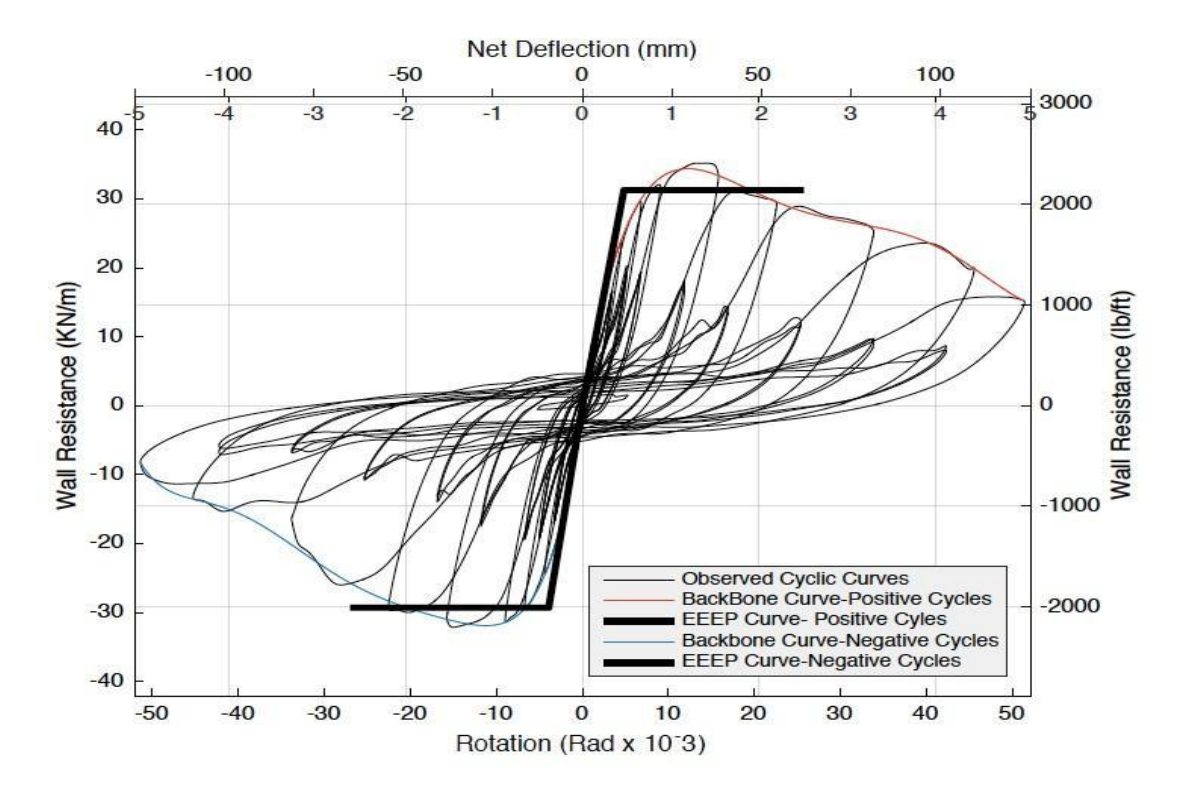


Figure B50 - Observation and EEEP Curves W11-  $\ensuremath{\text{C}}$ 

Parameters	Parameters		
	Positive	Negative	
Fu	85,82	78,38	kN
Fu_80	68,65	62,70	kN
Fu40	34,33	31,35	kN
Fy	76,31	71,46	kN
Ke	6,48	7,46	kN/m m
μ	5,32	6,87	
Δnet,y	11,78	9,57	mm
Δnet,u	32,66	36,77	mm
Δnet,0.8u	62,70	65,80	mm
Δnet,0.4u	5,30	4,20	mm
Area EEEP	4335,08	4359,82	J
Area Backbone			
	4335,08	4359,82	J
Rd	3,11	3,57	
Sy	31,29	29,30	kN/m

Table B25 - Results for test W11-C

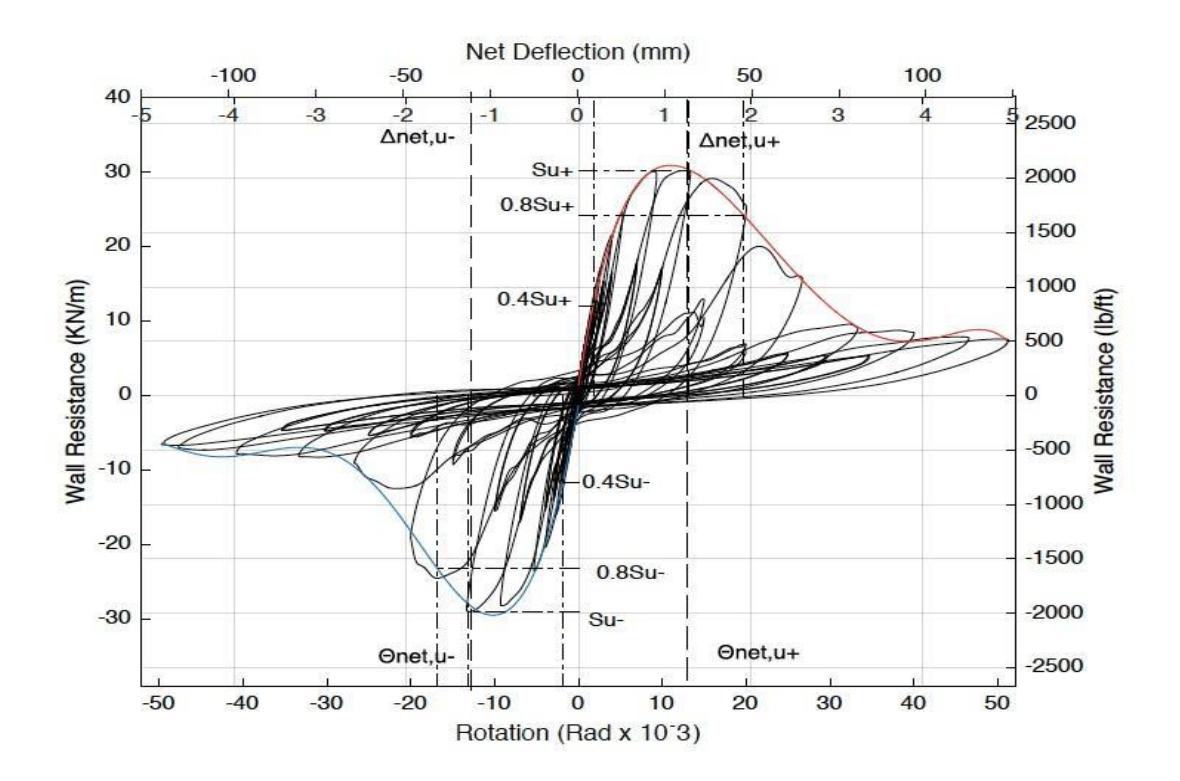


Figure B51 - Parameters of Reversed Cyclic Test W12-C

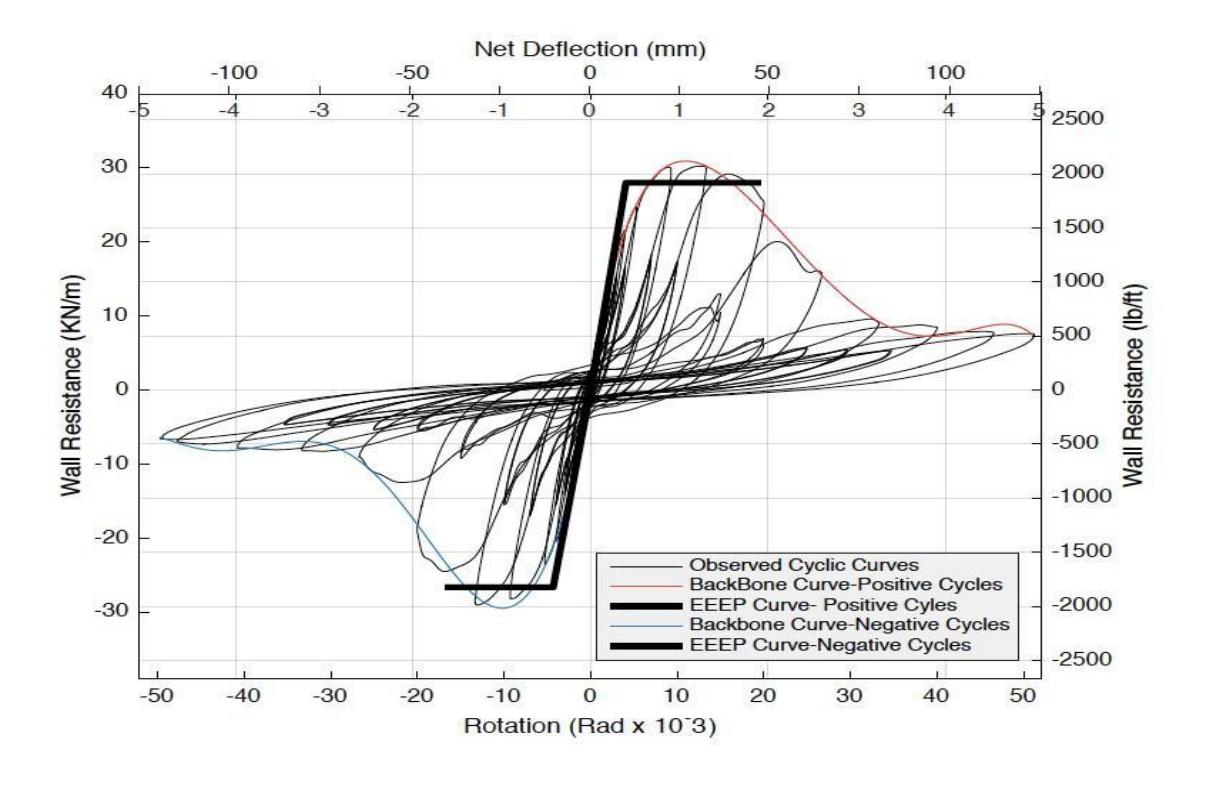


Figure B52 - Observation and EEEP Curves W12-

Parameters	Parameters		
	Positive	Negativ e	
Fu	73,69	70,77	kN
Fu_80	58,95	56,62	kN
Fu40	29,47	28,31	kN
Fy	68,18	64,95	kN
Ke	6,85	6,15	kN/m m
μ	4,83	3,88	
Δnet,y	9,95	10,55	mm
Δnet,u	31,90	31,92	mm
Δnet,0.8u	48,00	41,00	mm
Δnet,0.4u	4,30	4,60	mm
Area EEEP	2933,51	2320,16	J
Area Backbone	2933,51	2320,16	J
Rd	2,94	2,60	
Sy	27,96	26,64	kN/m

Table B26 - Results for test W12-C

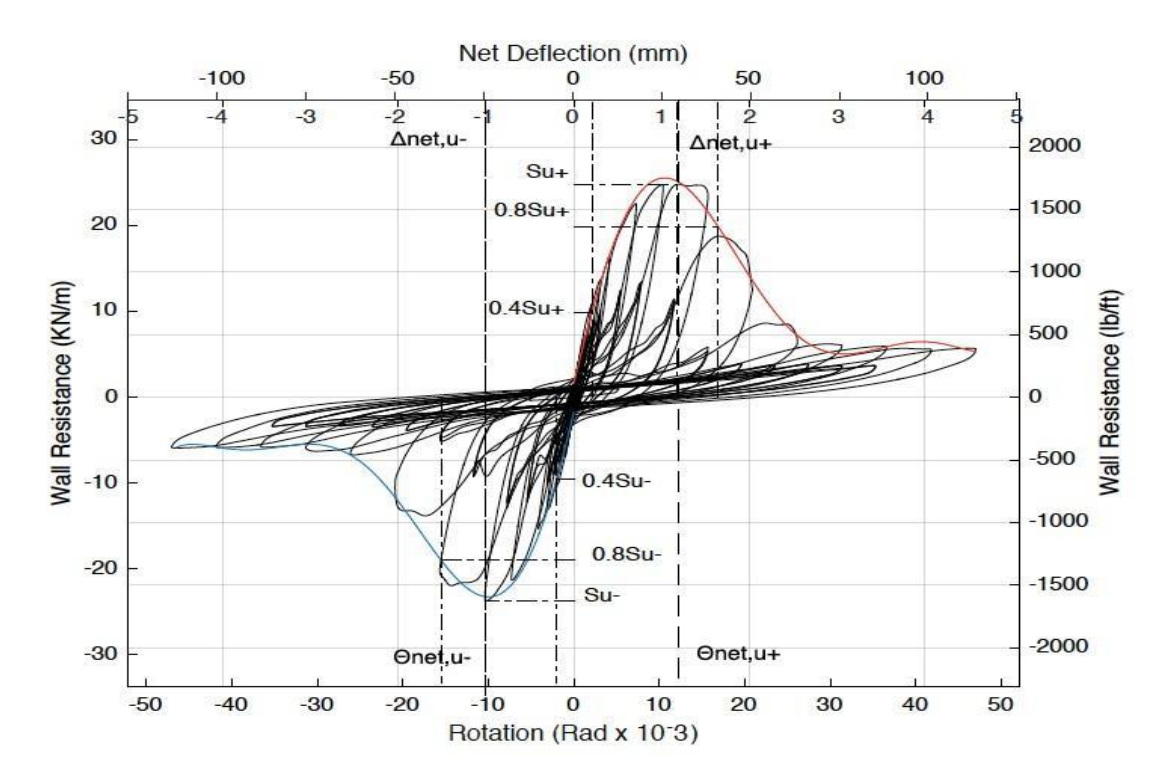


Figure B53 - Parameters of Reversed Cyclic Test W13-C

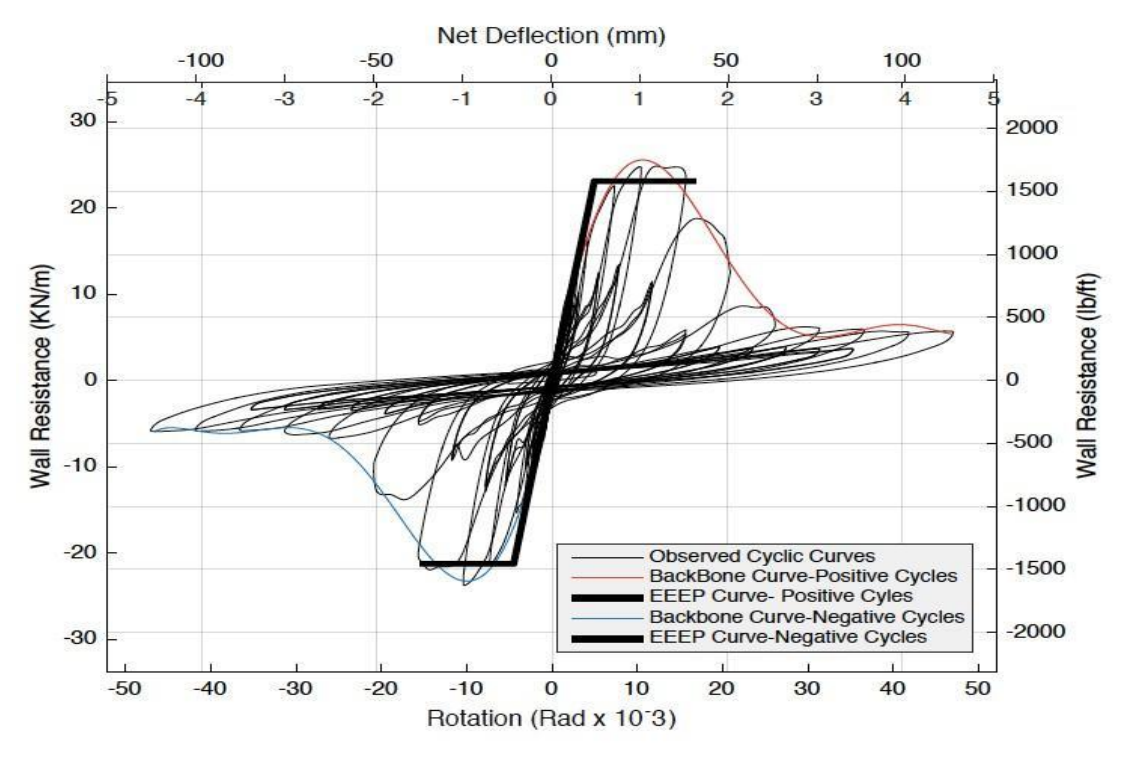


Figure B54 - Observation and EEEP Curves W13-  $\,$  C

Parameters			Units
	Positive	Negative	
Fu	60,52	57,90	kN
Fu_80	48,42	46,32	kN
Fu40	24,21	23,16	kN
Fy	56,31	51,76	kN
Ke	4,66	4,73	kN/m m
μ	3,41	3,45	
Δnet,y	12,09	10,95	mm
Δnet,u	29,57	25,14	mm
Δnet,0.8u	41,20	37,80	mm
Δnet,0.4u	5,20	4,90	mm
Area EEEP	1979,40	1673,12	J
Area Backbone			
	1979,40	1673,12	J
Rd	2,41	2,43	
Sy	23,09	21,23	kN/m

Table B27 - Results for test W13-C

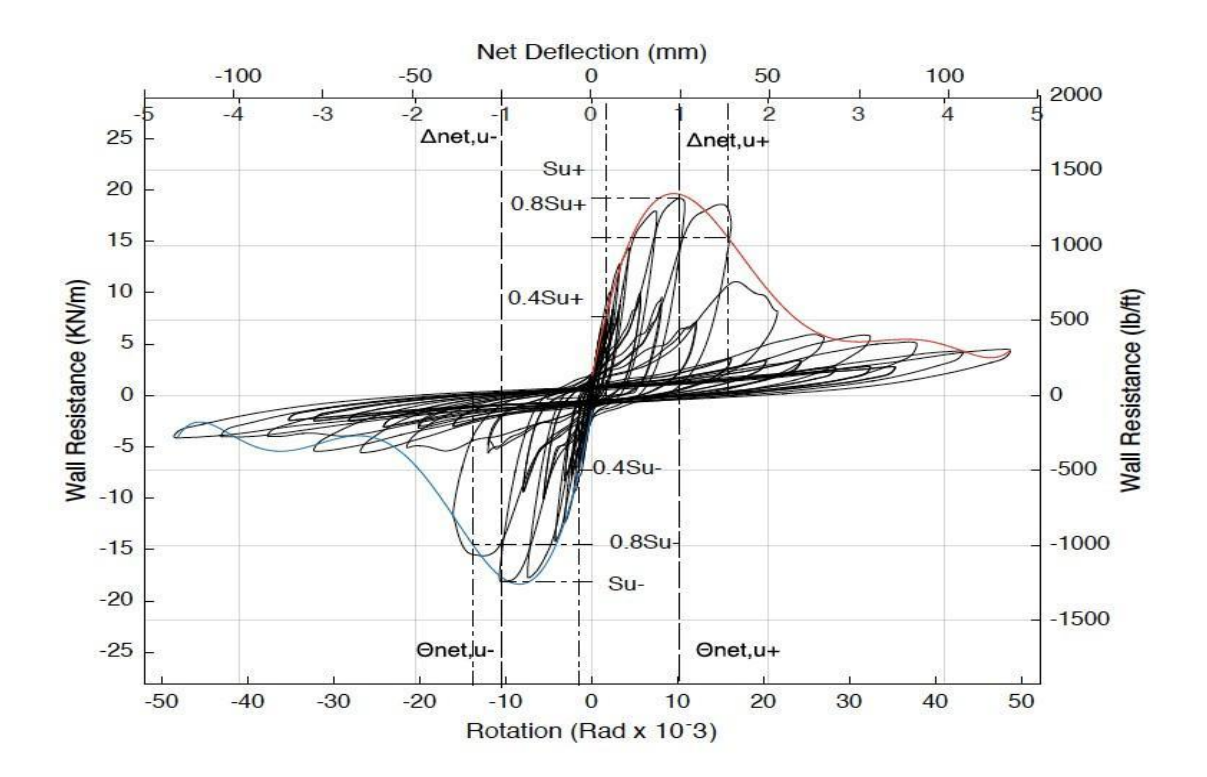


Figure B55 - Parameters of Reversed Cyclic Test W14-C

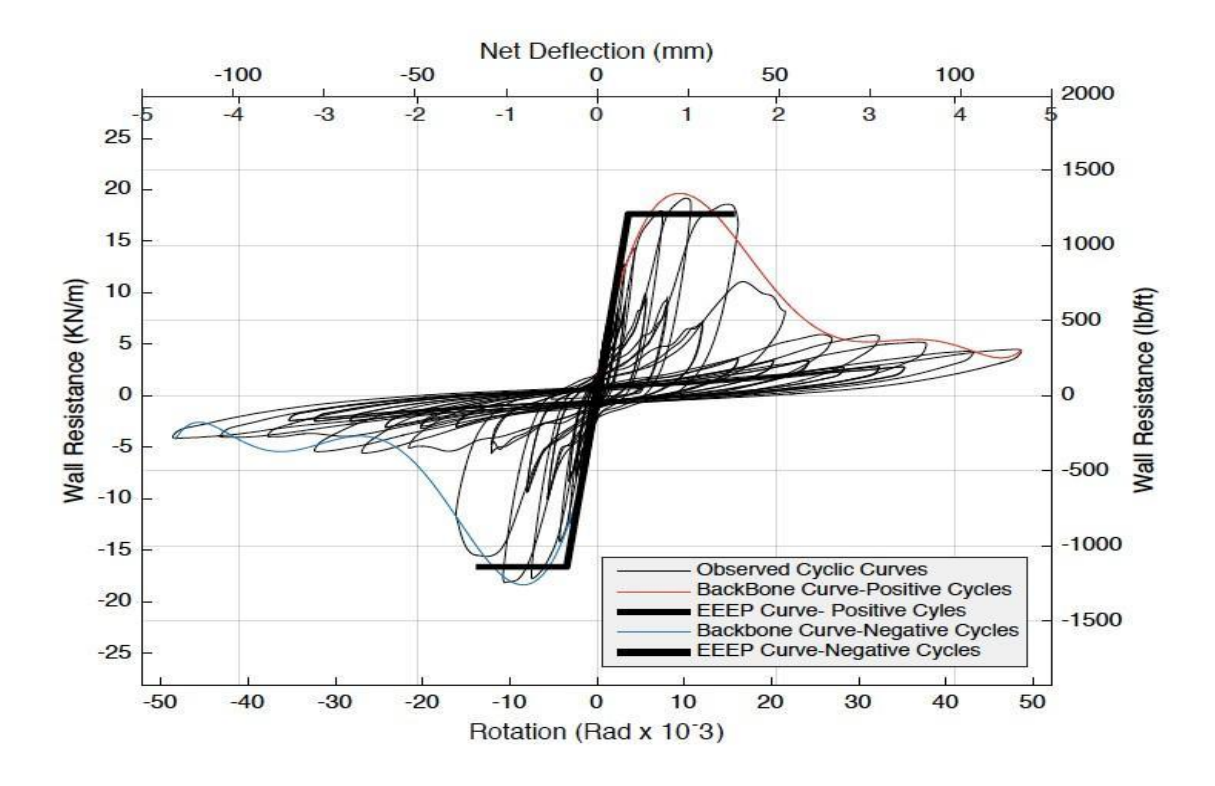


Figure B56 - Observation and EEEP Curves W14-  $\,$  C

Parameters			Units
	Positive	Negative	
Fu	46,79	44,20	kN
Fu_80	37,43	35,36	kN
Fu40	18,72	17,68	kN
Fy	43,04	40,51	kN
Ke	4,93	4,78	kN/m m
μ	4,41	4,00	
Δnet,y	8,74	8,48	mm
Δnet,u	24,64	25,62	mm
Δnet,0.8u	38,50	33,90	mm
Δnet,0.4u	3,80	3,70	mm
Area EEEP	1468,94	1201,59	J
Area Backbone	1468,94	1201,59	J
Rd	2,79	2,65	
Sy	17,65	16,61	kN/m

Table B28 - Results for test W14-C

## APPENDIX C LOADING PROTOCOL

Wall Configuration:	W1	l	
Screw Pattern:	2"/12"		
Δm	75.13mm		
Δ=0.6 Δm	45.088mm		
Displacement	Actuator Input (mm)	Number of Cycles	Cycle Type
0.05	2.254	6	Initiation
0.075	3.382	1	Primary
0.056	2.525	6	Trailing
0.1	4.509	1	Primary
0.075	3.382	6	Trailing
0.2	9.018	1	Primary
0.15	6.763	3	Trailing
0.3	13.526	1	Primary
0.225	10.145	3	Trailing
0.4	18.035	1	Primary
0.3	13.526	2	Trailing
0.7	31.561	1	Primary
0.525	23.671	2	Trailing
1	45.088	1	Primary
0.75	33.816	2	Trailing
1.5	67.632	1	Primary
1.125	50.724	2	Trailing
2	90.176	1	Primary
1.5	67.632	2	Trailing
2.5	112.72	1	Primary
1.875	84.54	2	Trailing
3	125	1	Primary
2.25	101.448	2	Trailing

Table C1 - CUREE protocol input displacements for test W1

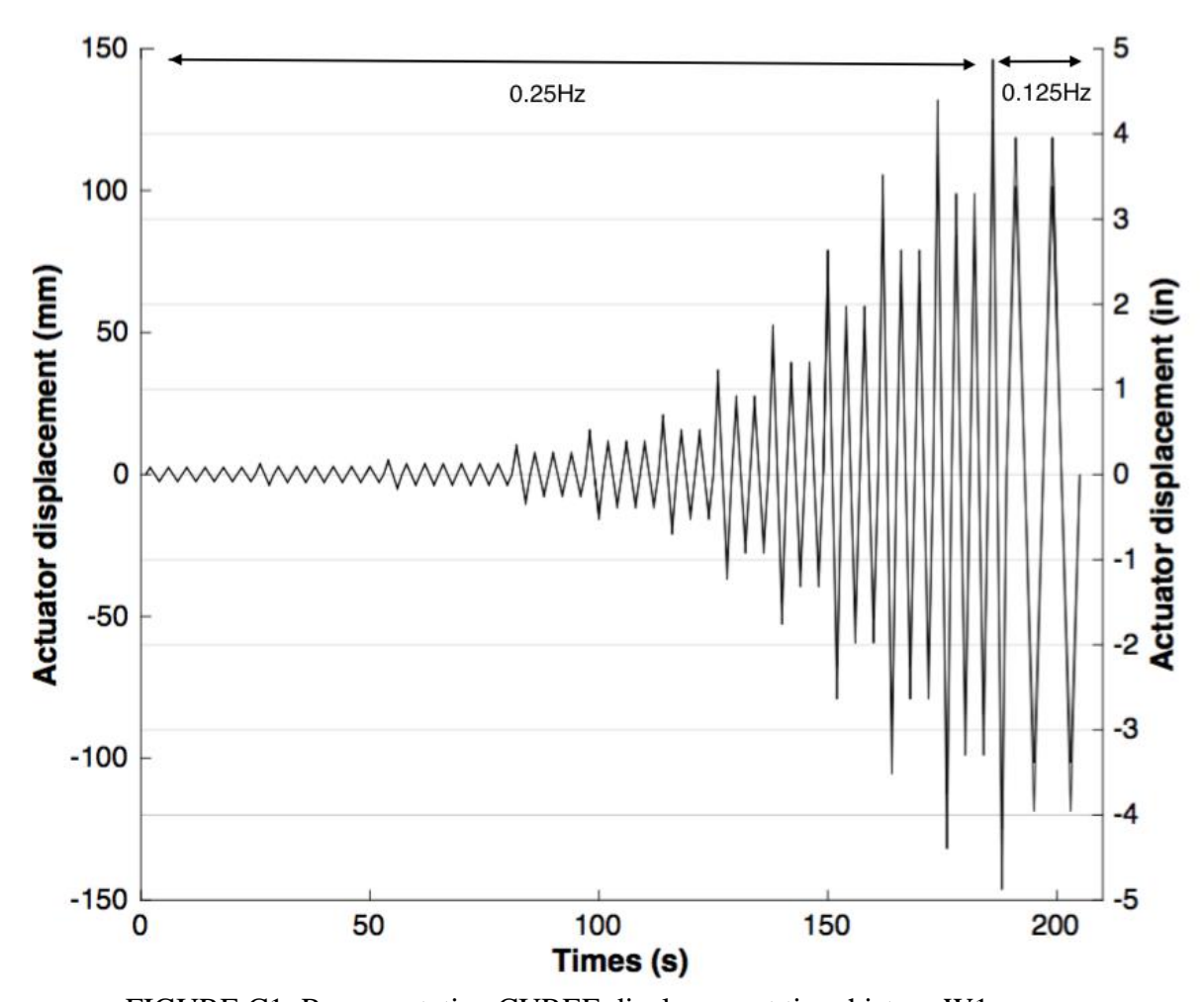


FIGURE C1 :Representative CUREE displacement time history W1

Wall Configuration:	W2		
Screw Pattern:	2"/12"		
Δm	86.20mm		
Δ=0.6 Δm	51.724mm		
Displacement	Actuator Input (mm)	Number of Cycles	Cycle Type
0.05	2.586	6	Initiation
0.075	3.879	1	Primary
0.056	2.897	6	Trailing
0.1	5.172	1	Primary
0.075	3.879	6	Trailing
0.2	10.345	1	Primary
0.15	7.759	3	Trailing
0.3	15.517	1	Primary
0.225	11.638	3	Trailing
0.4	20.69	1	Primary
0.3	15.517	2	Trailing
0.7	36.207	1	Primary
0.525	27.155	2	Trailing
1	51.724	1	Primary
0.75	38.793	2	Trailing
1.5	77.586	1	Primary
1.125	58.19	2	Trailing
2	103.448	1	Primary
1.5	77.586	2	Trailing
2.5	125	1	Primary
1.875	96.983	2	Trailing

Table C2 - CUREE protocol input displacements for test W2

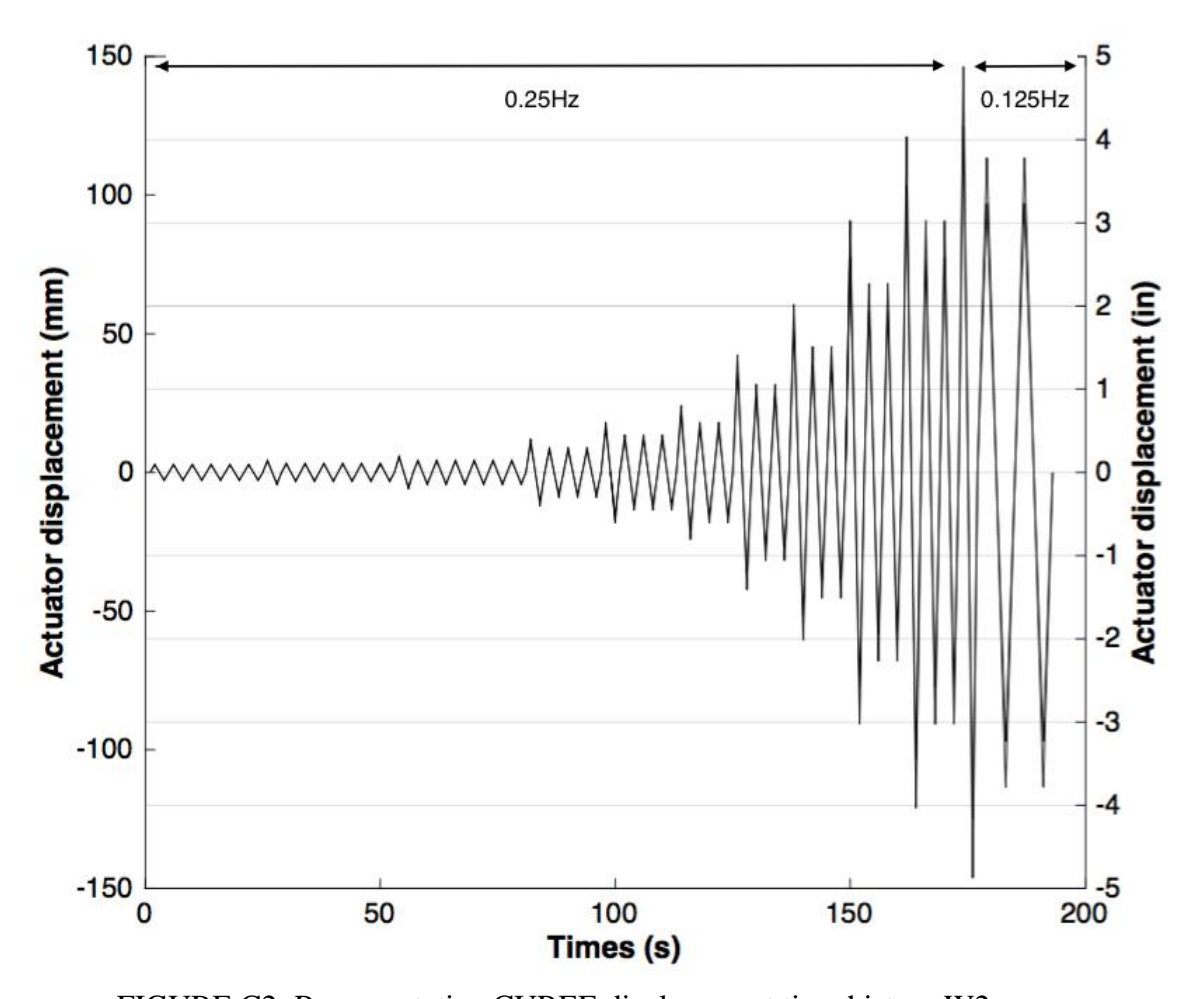


FIGURE C2 :Representative CUREE displacement time history W2

Wall Configuration:	W3		
Screw Pattern:	2"/12"		
Δm	100mm		
Δ=0.6 Δm	60mm		
Displacement	Actuator Input (mm)	Number of Cycles	Cycle Type
0.05	3	6	Initiation
0.075	4.5	1	Primary
0.056	3.36	6	Trailing
0.1	6	1	Primary
0.075	4.5	6	Trailing
0.2	12	1	Primary
0.15	9	3	Trailing
0.3	18	1	Primary
0.225	13.5	3	Trailing
0.4	24	1	Primary
0.3	18	2	Trailing
0.7	42	1	Primary
0.525	31.5	2	Trailing
1	60	1	Primary
0.75	45	2	Trailing
1.5	90	1	Primary
1.125	67.5	2	Trailing
2	120	1	Primary
1.5	90	2	Trailing
2.5	125	1	Primary
1.875	112.5	2	Trailing

Table C3 - CUREE protocol input displacements for test W3

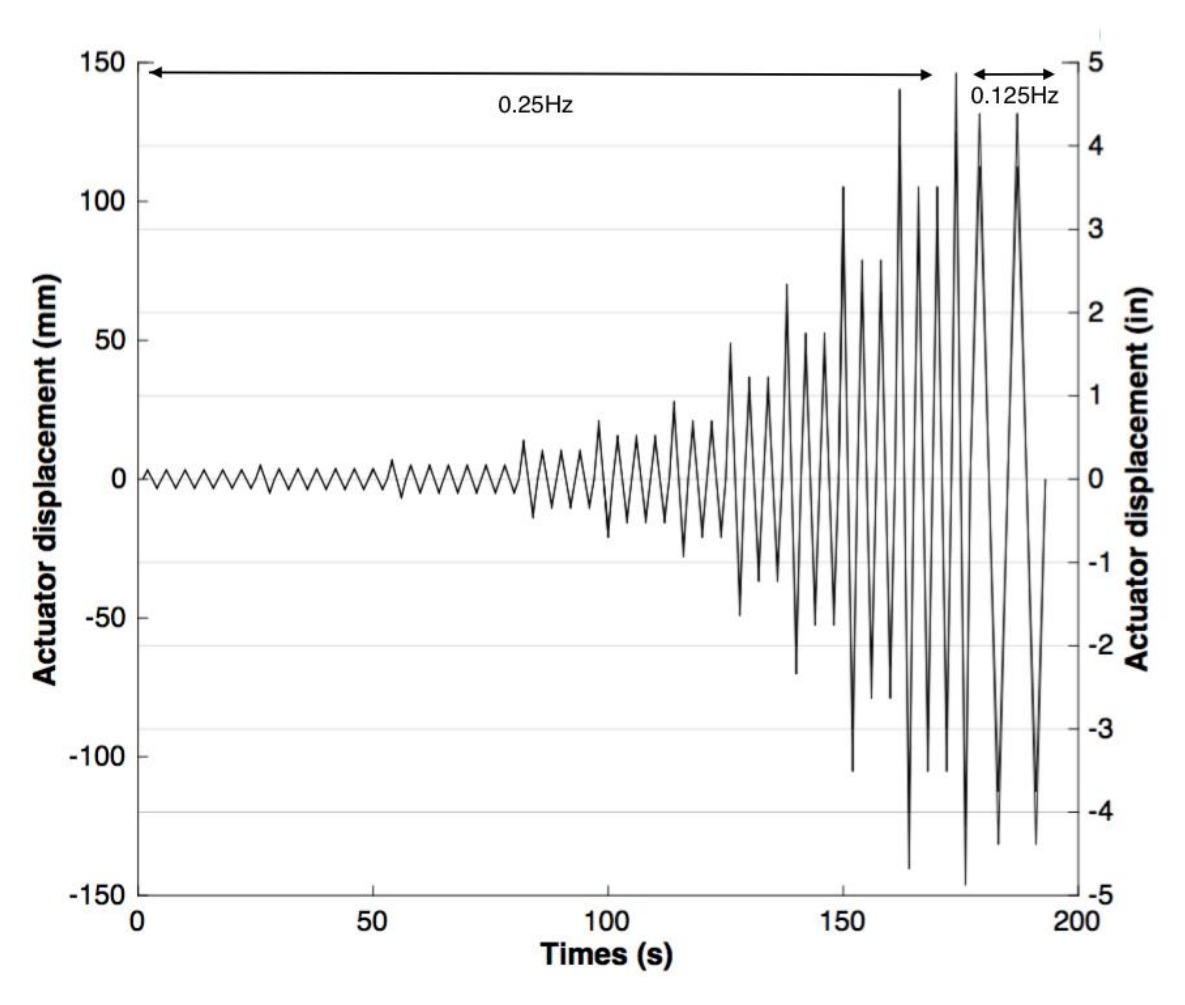


FIGURE C3 :Representative CUREE displacement time history W3

Wall Configuration:	W4		
Screw Pattern:	3"/12"		
Δm	124.786mm		
Δ=0.6 Δm	74.872mm		
Displacement	Actuator Input (mm)	Number of Cycles	Cycle Type
0.05	3.743	6	Initiation
0.075	5.615	1	Primary
0.056	4.193	6	Trailing
0.1	7.487	1	Primary
0.075	5.615	6	Trailing
0.2	14.974	1	Primary
0.15	11.231	3	Trailing
0.3	22.462	1	Primary
0.225	16.846	3	Trailing
0.4	29.949	1	Primary
0.3	22.462	2	Trailing
0.7	52.41	1	Primary
0.525	39.308	2	Trailing
1	74.872	1	Primary
0.75	56.154	2	Trailing
1.5	112.308	1	Primary
1.125	84.231	2	Trailing
2	125	1	Primary
1.5	112.308	2	Trailing

Table C4 - CUREE protocol input displacements for test W4

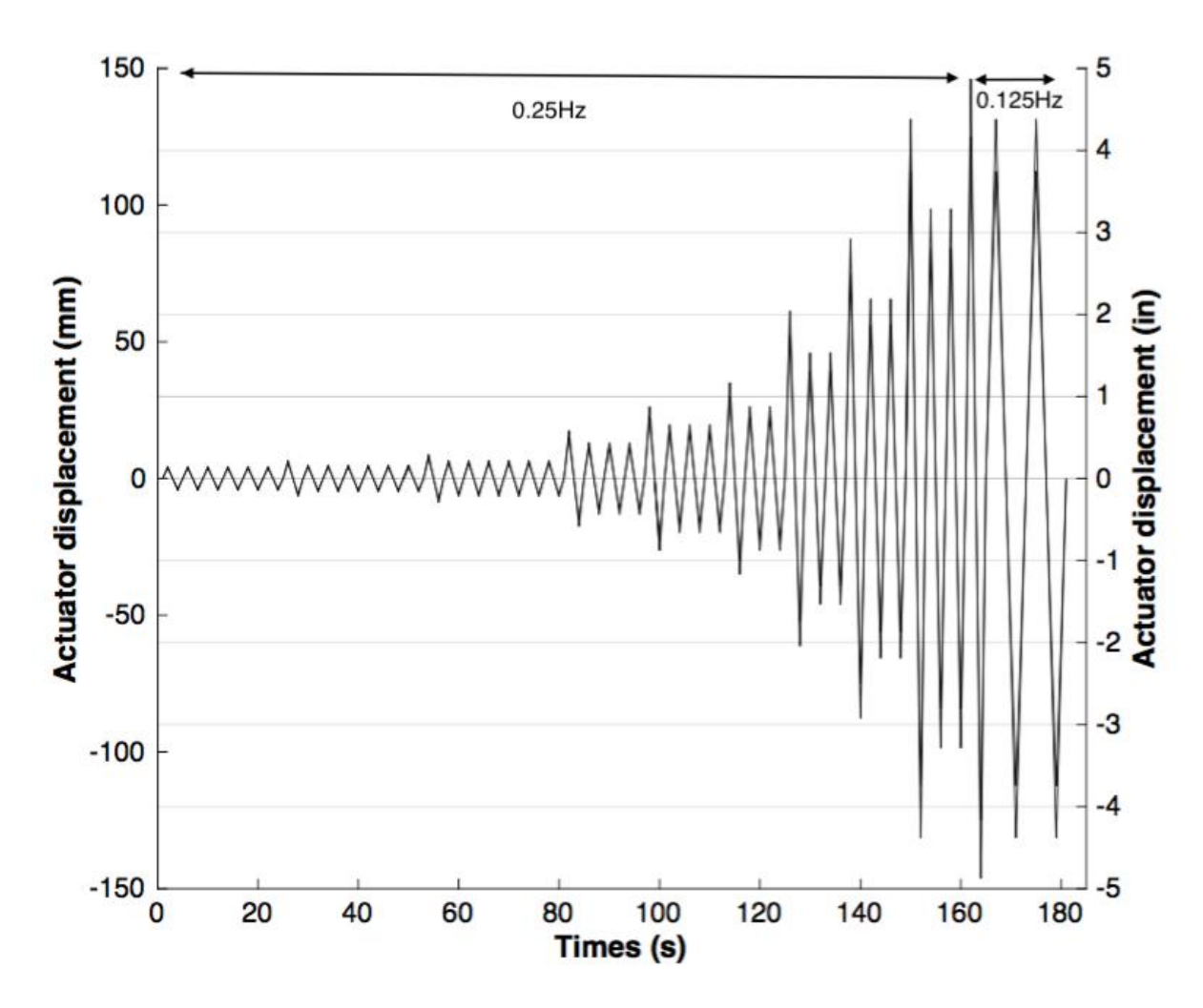


FIGURE C4 :Representative CUREE displacement time history W4

Wall Configuration:	W5		
Screw Pattern:	4"/12"		
Δm	83.773mm		
Δ=0.6 Δm	50.264mm		
Displacement	Actuator Input (mm)	Number of Cycles	Cycle Type
0.05	2.513	6	Initiation
0.075	3.77	1	Primary
0.056	2.815	6	Trailing
0.1	5.026	1	Primary
0.075	3.77	6	Trailing
0.2	10.053	1	Primary
0.15	7.54	3	Trailing
0.3	15.08	1	Primary
0.225	11.309	3	Trailing
0.4	20.106	1	Primary
0.3	15.08	2	Trailing
0.7	35.185	1	Primary
0.525	26.389	2	Trailing
1	50.264	1	Primary
0.75	37.698	2	Trailing
1.5	75.396	1	Primary
1.125	56.547	2	Trailing
2	100.528	1	Primary
1.5	75.396	2	Trailing

Table C5 - CUREE protocol input displacements for test W5

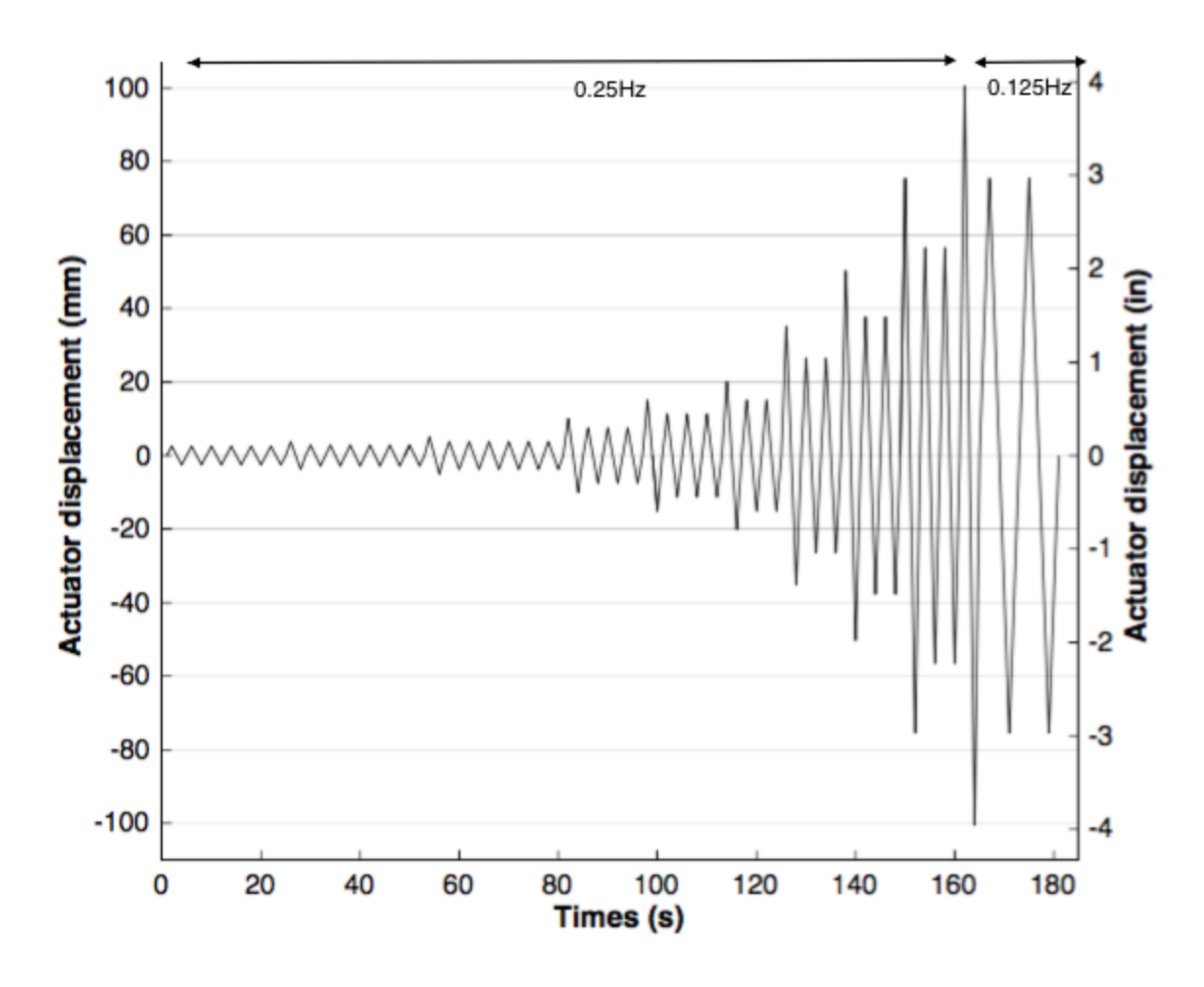


FIGURE C5 :Representative CUREE displacement time history W5

Wall Configuration:	W6		
Screw Pattern:	6"/12"		
Δm	89.488mm		
Δ=0.6 Δm	53.693mm		
Displacement	Actuator Input (mm)	Number of Cycles	Cycle Type
0.05	2.684	6	Initiation
0.075	4.027	1	Primary
0.056	3.007	6	Trailing
0.1	5.369	1	Primary
0.075	4.027	6	Trailing
0.2	10.739	1	Primary
0.15	8.054	3	Trailing
0.3	16.108	1	Primary
0.225	12.081	3	Trailing
0.4	21.477	1	Primary
0.3	16.108	2	Trailing
0.7	37.585	1	Primary
0.525	28.189	2	Trailing
1	53.693	1	Primary
0.75	40.269	2	Trailing
1.5	80.539	1	Primary
1.125	60.404	2	Trailing
2	107.386	1	Primary
1.5	80.539	2	Trailing
2.5	125	1	Primary
1.875	100.674	2	Trailing

Table C6 - CUREE protocol input displacements for test W6

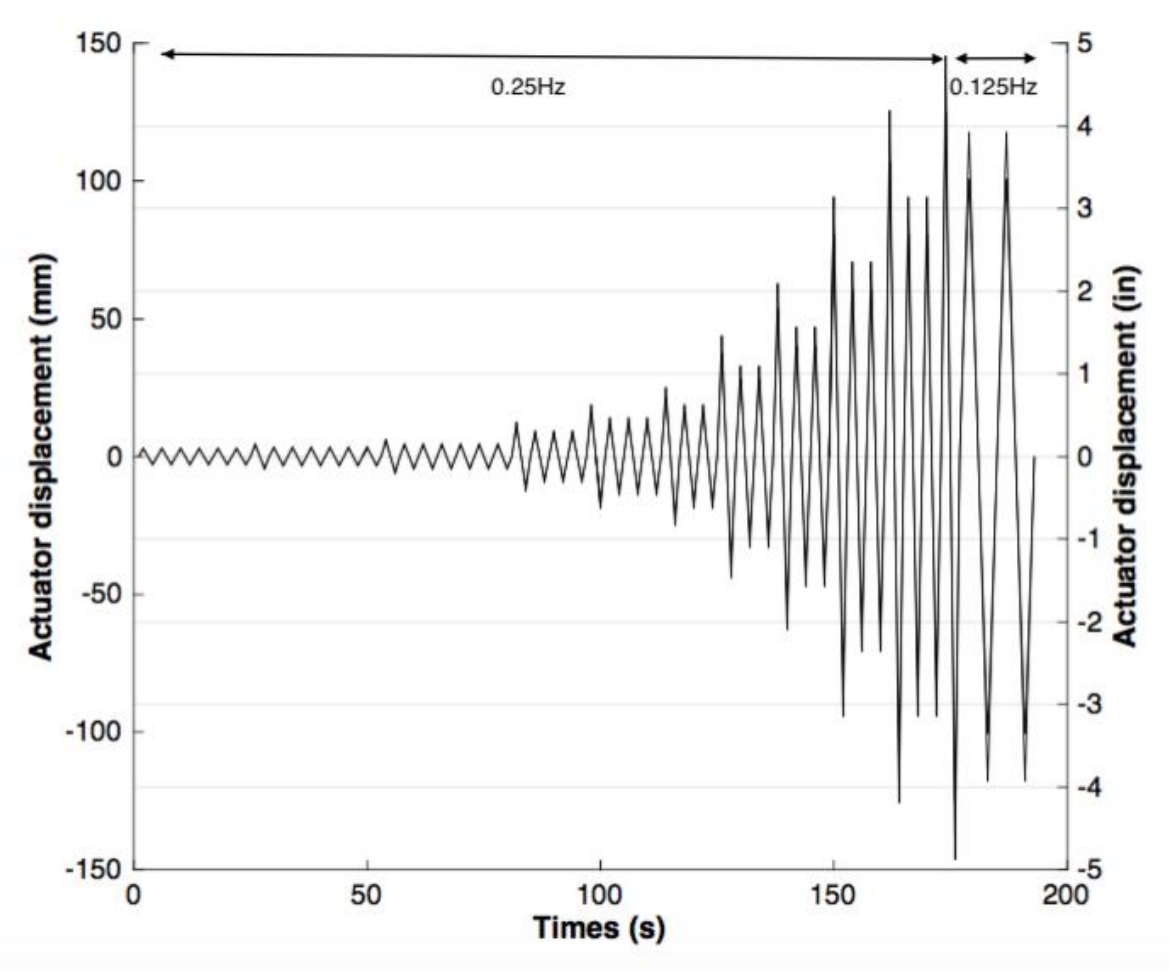


FIGURE C6 :Representative CUREE displacement time history W6

Wall Configuration:	W7		
Screw Pattern:	3"/12"		
Δm	75.481mm		
Δ=0.6 Δm	45.289 mm		
Displacement	Actuator Input (mm)	Number of Cycles	Cycle Type
0.05	2.264	6	Initiation
0.075	3.397	1	Primary
0.056	2.536	6	Trailing
0.1	4.529	1	Primary
0.075	3.397	6	Trailing
0.2	9.058	1	Primary
0.15	6.793	3	Trailing
0.3	13.587	1	Primary
0.225	10.189	3	Trailing
0.4	18.115	1	Primary
0.3	13.587	2	Trailing
0.7	31.702	1	Primary
0.525	23.777	2	Trailing
1	45.289	1	Primary
0.75	33.967	2	Trailing
1.5	67.934	1	Primary
1.125	50.95	2	Trailing
2	90.578	1	Primary
1.5	67.934	2	Trailing
2.5	113.223	1	Primary
1.875	84.917	2	Trailing
3	125	1	Primary
2.25	101.9	2	Trailing

Table C7 - CUREE protocol input displacements for test W7

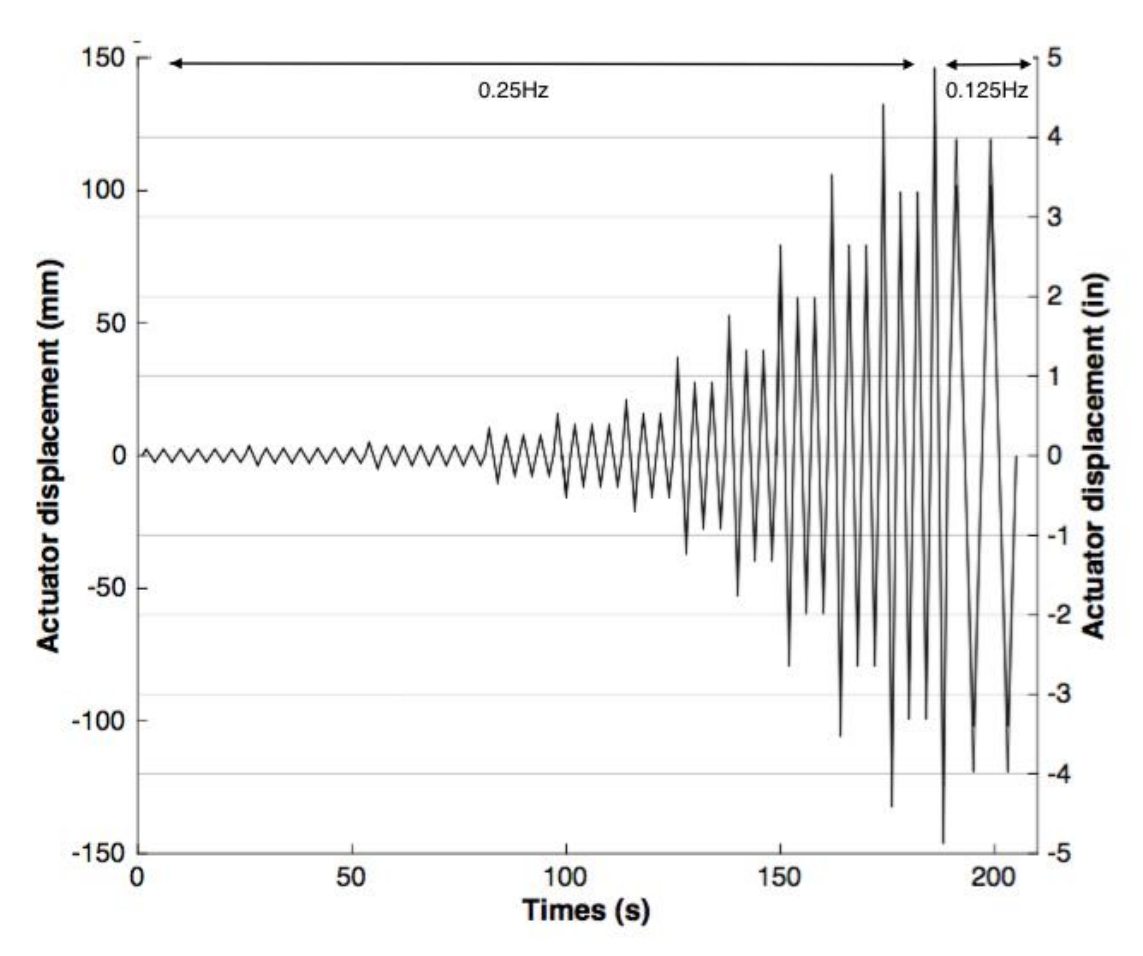


FIGURE C7 :Representative CUREE displacement time history W7

	W8		
Screw Pattern:	3"/12"		
$\Delta_{ m m}$	60.230mm		
Δ=0.6 Δ <sub>m</sub>	36.13mm		
Dianlacement	Actuator	Number of	Cycle Type
Displacement	Input (mm)	Cycles	Cycle Type
0.05 Δ	1.807	6	Initiation
0.075 Δ	2.710	1	Primary
0.056 Δ	2.014	6	Trailing
0.1 Δ	3.614	1	Primary
0.075 Δ	2.710	6	Trailing
0.2 Δ	7.228	1	Primary
0.15 Δ	5.421	3	Trailing
0.3 Δ	10.841	1	Primary
0.225 Δ	8.131	3	Trailing
0.4 Δ	14.455	1	Primary
0.3 Δ	10.841	2	Trailing
0.7 Δ	25.30	1	Primary
0.525 Δ	18.972	2	Trailing
1.0 Δ	36.138	1	Primary
0.75 Δ	27.104	2	Trailing
1.5 Δ	54.207	1	Primary
1.125 Δ	40.655	2	Trailing
2.0 Δ	72.726	1	Primary
1.5 Δ	54.207	2	Trailing
2.5 Δ	90.345	1	Primary
1.875 Δ	67.759	2	Trailing
3.0 Δ	108.414	1	Primary
2.250 Δ	81.301	2	Trailing
3.5 Δ	125	1	Primary
2.625 Δ	94.862	2	Trailing

Table C8 - CUREE protocol input displacements for test W8

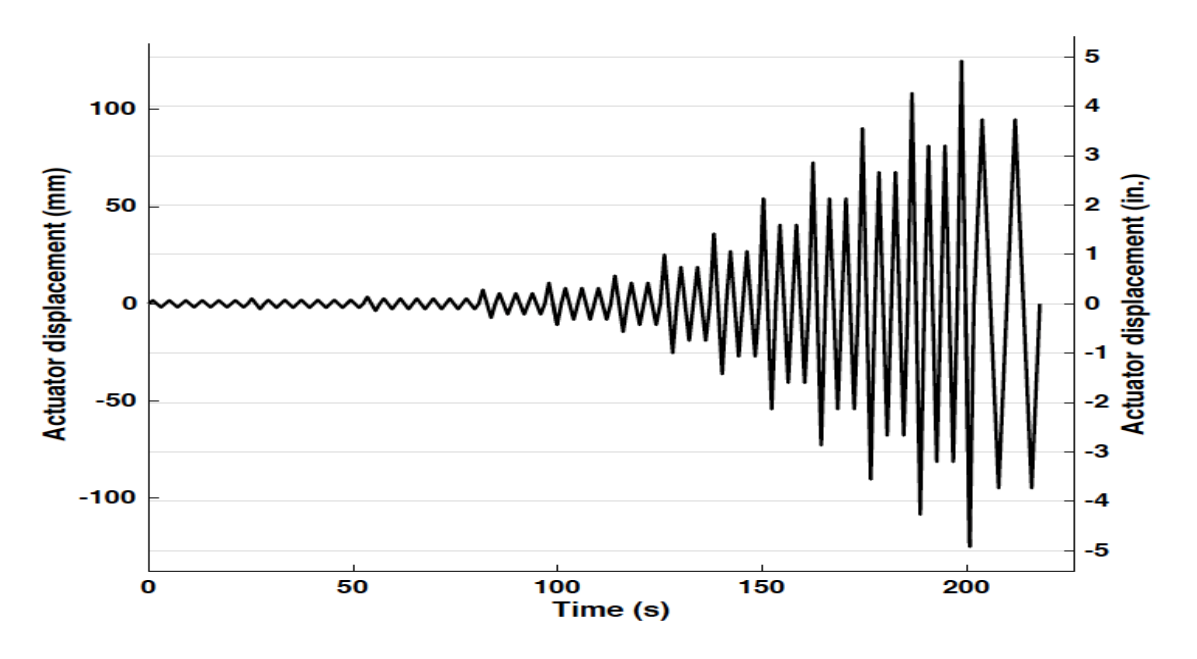


FIGURE C8 :Representative CUREE displacement time history W8

Wall Configuration:	W9		
Screw Pattern:	4"/12"		
Δm	68.319mm		
Δ=0.6 Δm	40.991mm		
Displacement	Actuator Input (mm)	Number of Cycles	Cycle Type
0.05	2.049	6	Initiation
0.075	3.074	1	Primary
0.056	2.295	6	Trailing
0.1	4.099	1	Primary
0.075	3.074	6	Trailing
0.2	8.198	1	Primary
0.15	6.148	3	Trailing
0.3	12.297	1	Primary
0.225	9.223	3	Trailing
0.4	12.011	1	Primary
0.3	12.297	2	Trailing
0.7	28.694	1	Primary
0.525	21.52	2	Trailing
1	40.991	1	Primary
0.75	30.743	2	Trailing
1.5	61.487	1	Primary
1.125	46.115	2	Trailing
2	81.982	1	Primary
1.5	61.487	2	Trailing
2.5	102.478	1	Primary
1.875	76.858	2	Trailing
3	122.973	1	Primary
2.25	92.229	2	Trailing
3.5	125	1	Primary
2.625	78.819	2	Trailing

Table C9 - CUREE protocol input displacements for test W9

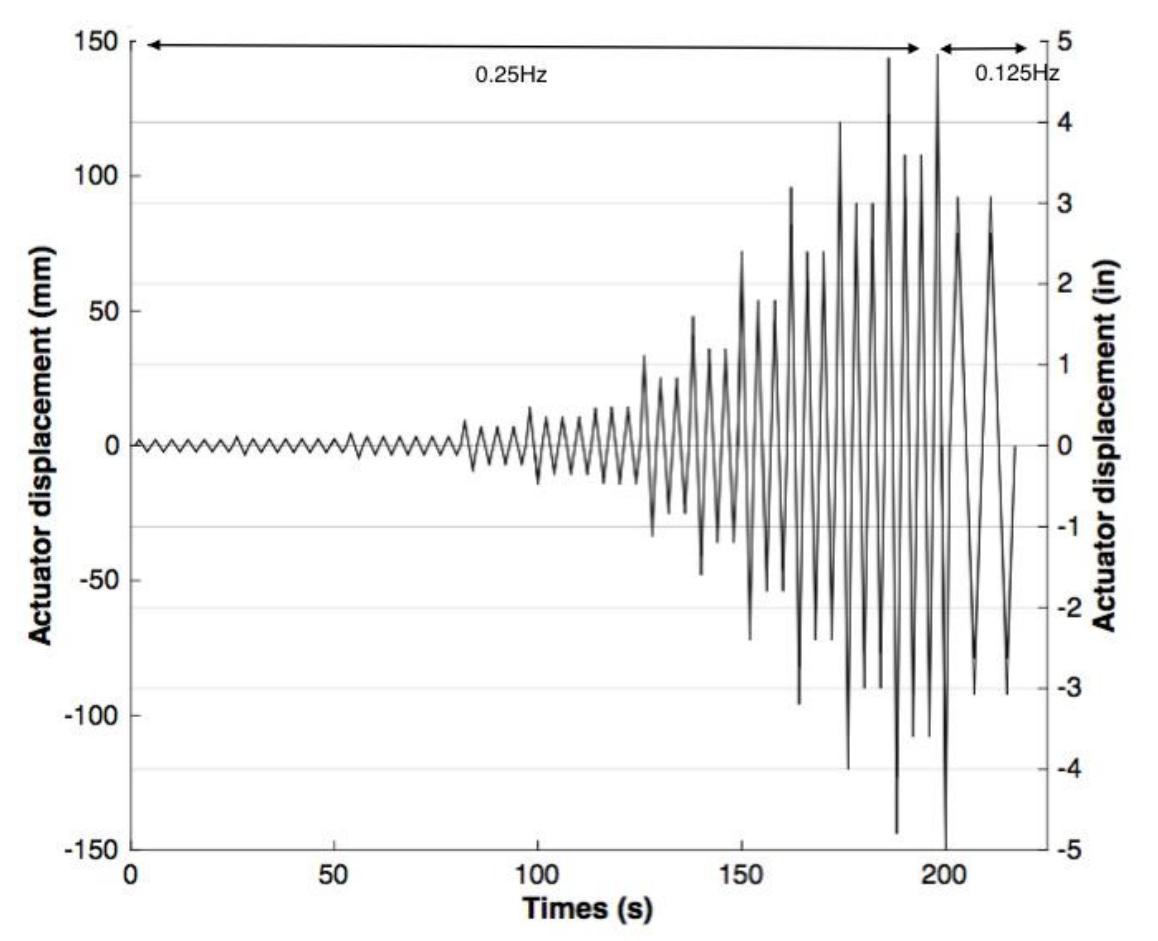


FIGURE C9 :Representative CUREE displacement time history W9

Wall Configuration:	W10		
Screw Pattern:	6"/12"		
Δm	50.044mm		
Δ=0.6 Δm	30.026 mm		
Displacement	Actuator Input (mm)	Number of Cycles	Cycle Type
0.05	1.501	6	Initiation
0.075	2.252	1	Primary
0.056	1.68	6	Trailing
0.1	3.026	1	Primary
0.075	2.252	6	Trailing
0.2	6.005	1	Primary
0.15	4.504	3	Trailing
0.3	9.008	1	Primary
0.225	6.756	3	Trailing
0.4	12.011	1	Primary
0.3	9.008	2	Trailing
0.7	21.019	1	Primary
0.525	15.764	2	Trailing
1	30.026	1	Primary
0.75	22.519	2	Trailing
1.5	45.039	1	Primary
1.125	33.779	2	Trailing
2	60.053	1	Primary
1.5	45.039	2	Trailing
2.5	75.066	1	Primary
1.875	56.299	2	Trailing
3	90.079	1	Primary
2.25	67.559	2	Trailing
3.5	105.093	1	Primary
2.625	78.819	2	Trailing
4.5	125	1	Primary

Table C10 - CUREE protocol input displacements for test W10

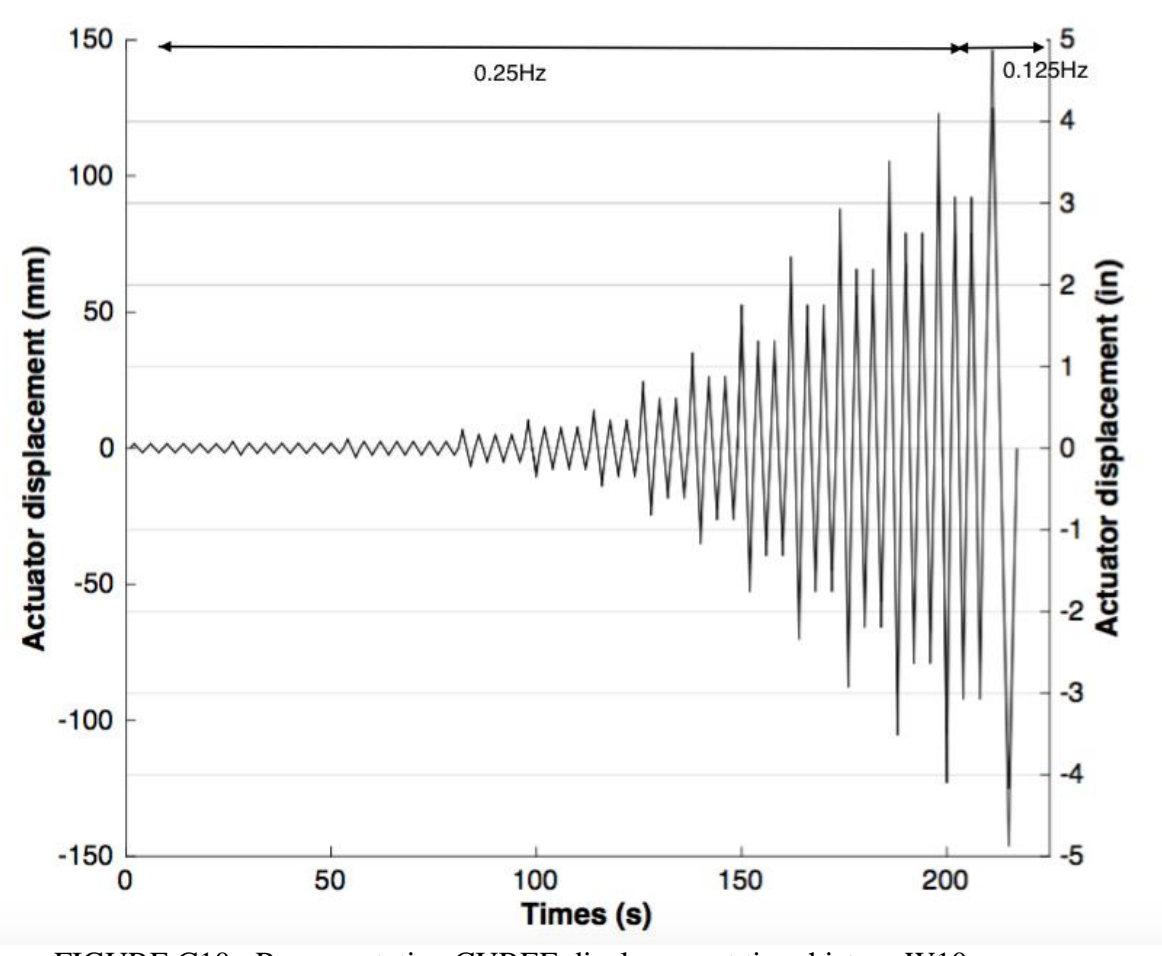


FIGURE C10 : Representative CUREE displacement time history W10

Wall Configuration:	W11		
Screw Pattern:	2"/12"		
Δm	91.419mm		
Δ=0.6 Δm	54.851mm		
Displacement	Actuator Input (mm)	Number of Cycles	Cycle Type
0.05	2.743	6	Initiation
0.075	4.114	1	Primary
0.056	3.072	6	Trailing
0.1	5.485	1	Primary
0.075	3.904	6	Trailing
0.2	10.97	1	Primary
0.15	8.227	3	Trailing
0.3	16.455	1	Primary
0.225	12.341	3	Trailing
0.4	21.94	1	Primary
0.3	16.455	2	Trailing
0.7	38.395	1	Primary
0.525	28.796	2	Trailing
1	54.851	1	Primary
0.75	41.138	2	Trailing
1.5	82.276	1	Primary
1.125	61.707	2	Trailing
2	109.97	1	Primary
1.5	82.276	2	Trailing
2.5	125	1	Primary
1.875	102.845	2	Trailing

Table C11 - CUREE protocol input displacements for test W11

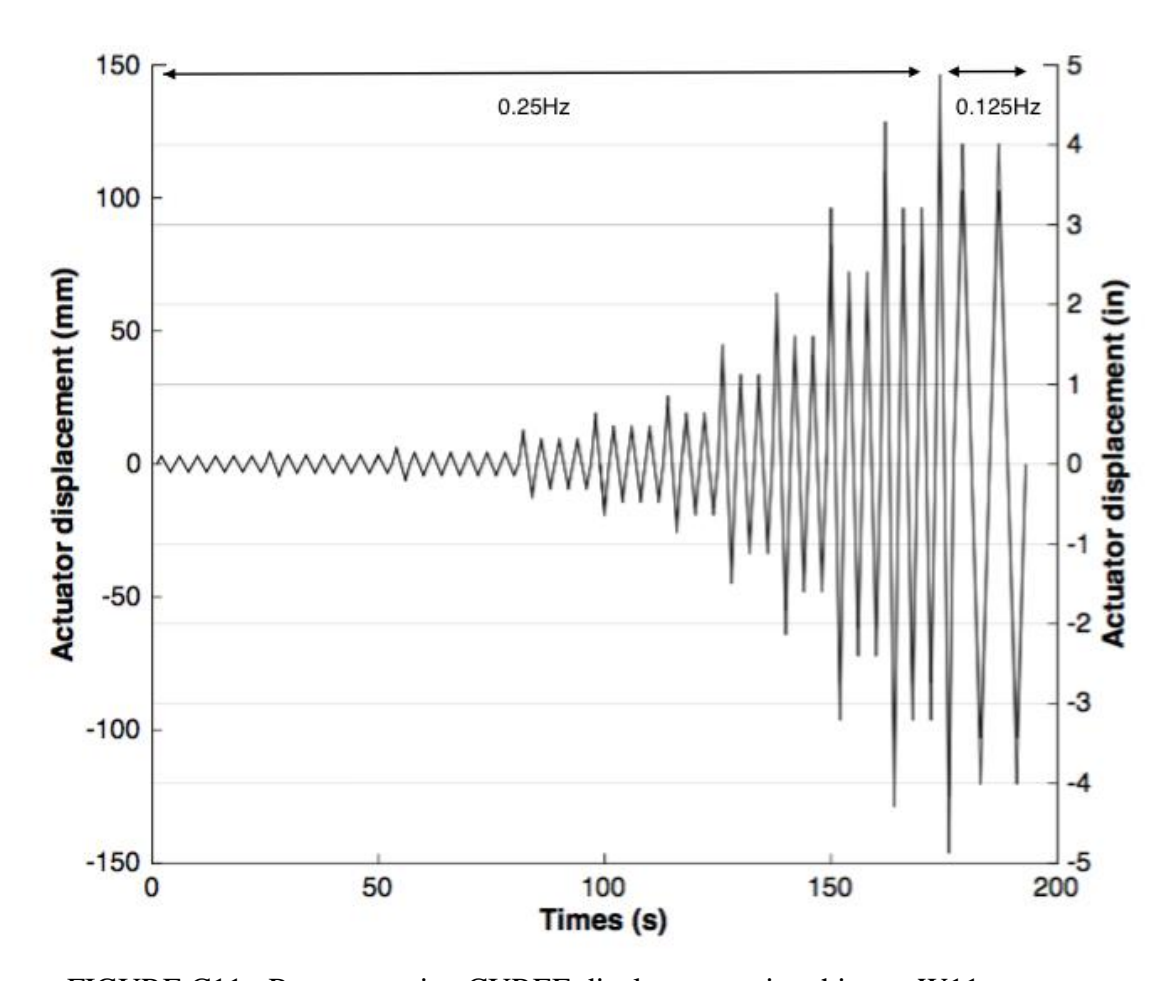


FIGURE C11 : Representative CUREE displacement time history W11

Wall Configuration:	W12		
Screw Pattern:	3"/12"		
Δm	54.031mm		
Δ=0.6 Δm	32.419 mm		
Displacement	Actuator Input (mm)	Number of Cycles	Cycle Type
0.05	1.621	6	Initiation
0.075	2.431	1	Primary
0.056	1.815	6	Trailing
0.1	3.242	1	Primary
0.075	2.431	6	Trailing
0.2	6.484	1	Primary
0.15	4.863	3	Trailing
0.3	9.726	1	Primary
0.225	7.294	3	Trailing
0.4	12.968	1	Primary
0.3	9.726	2	Trailing
0.7	22.693	1	Primary
0.525	17.02	2	Trailing
1	32.419	1	Primary
0.75	24.314	2	Trailing
1.5	48.629	1	Primary
1.125	36.471	2	Trailing
2	64.838	1	Primary
1.5	48.629	2	Trailing
2.5	81.048	1	Primary
1.875	60.786	2	Trailing
3	97.257	1	Primary
2.25	79.943	2	Trailing
3.5	113.467	1	Primary
2.625	85.099	2	Trailing

Table C12 - CUREE protocol input displacements for test W12  $\,$ 

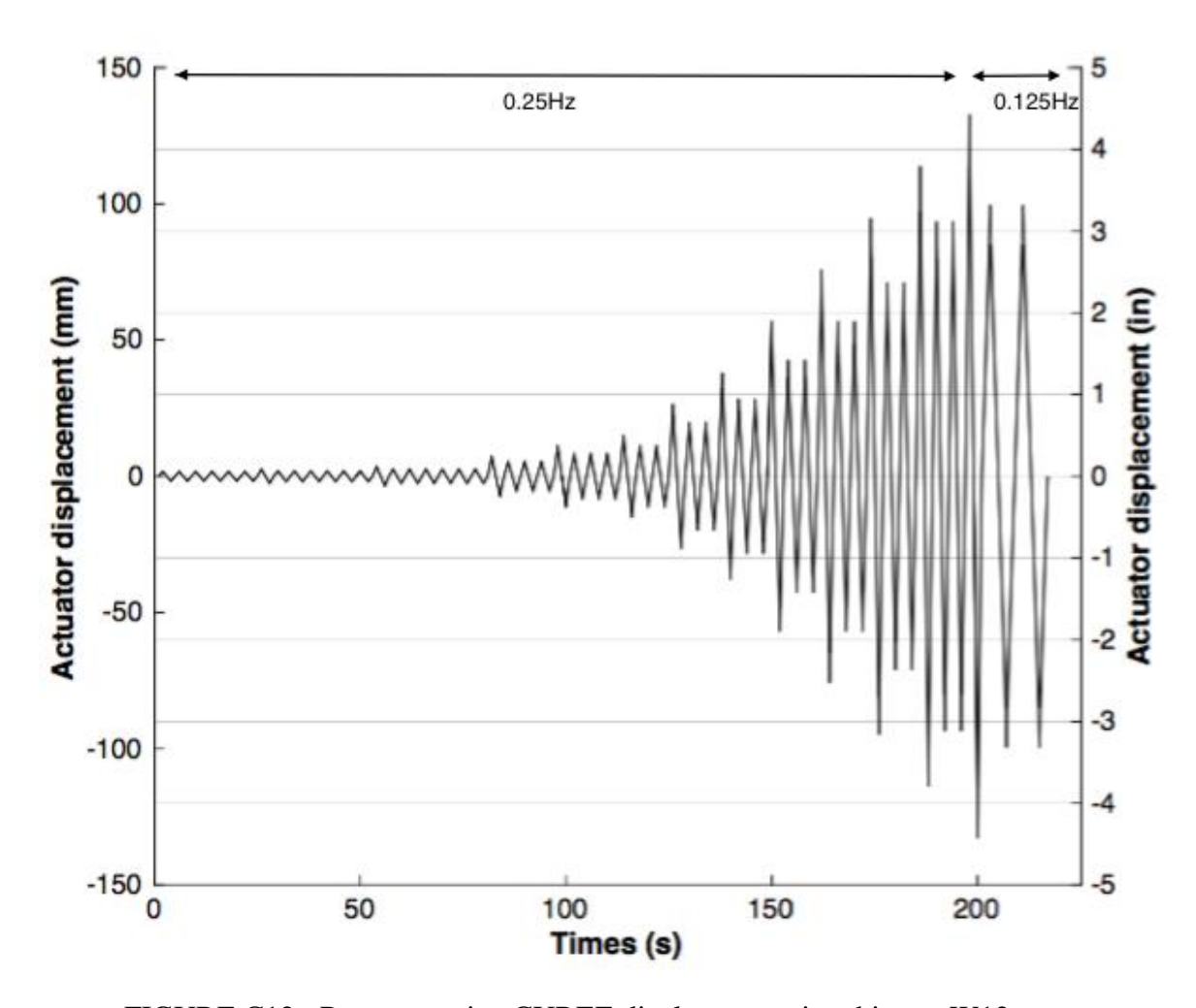


FIGURE C12: Representative CUREE displacement time history W12

Wall Configuration:	W13		
Screw Pattern:	4"/12"		
Δm	42.894mm		
Δ=0.6 Δm	25.425mm		
Displacement	Actuator Input (mm)	Number of Cycles	Cycle Type
0.05	1.271	6	Initiation
0.075	1.907	1	Primary
0.056	1.424	6	Trailing
0.1	2.543	1	Primary
0.075	1.907	6	Trailing
0.2	5.085	1	Primary
0.15	3.814	3	Trailing
0.3	7.628	1	Primary
0.225	5.721	3	Trailing
0.4	10.17	1	Primary
0.3	7.628	2	Trailing
0.7	17.798	1	Primary
0.525	13.348	2	Trailing
1	25.425	1	Primary
0.75	19.069	2	Trailing
1.5	38.138	1	Primary
1.125	28.603	2	Trailing
2	50.85	1	Primary
1.5	38.138	2	Trailing
2.5	63.563	1	Primary
1.875	47.672	2	Trailing
3	76.275	1	Primary
2.25	57.206	2	Trailing
3.5	88.988	1	Primary
2.625	66.741	2	Trailing
4	101.7	1	Primary

Table C13 - CUREE protocol input displacements for test W13

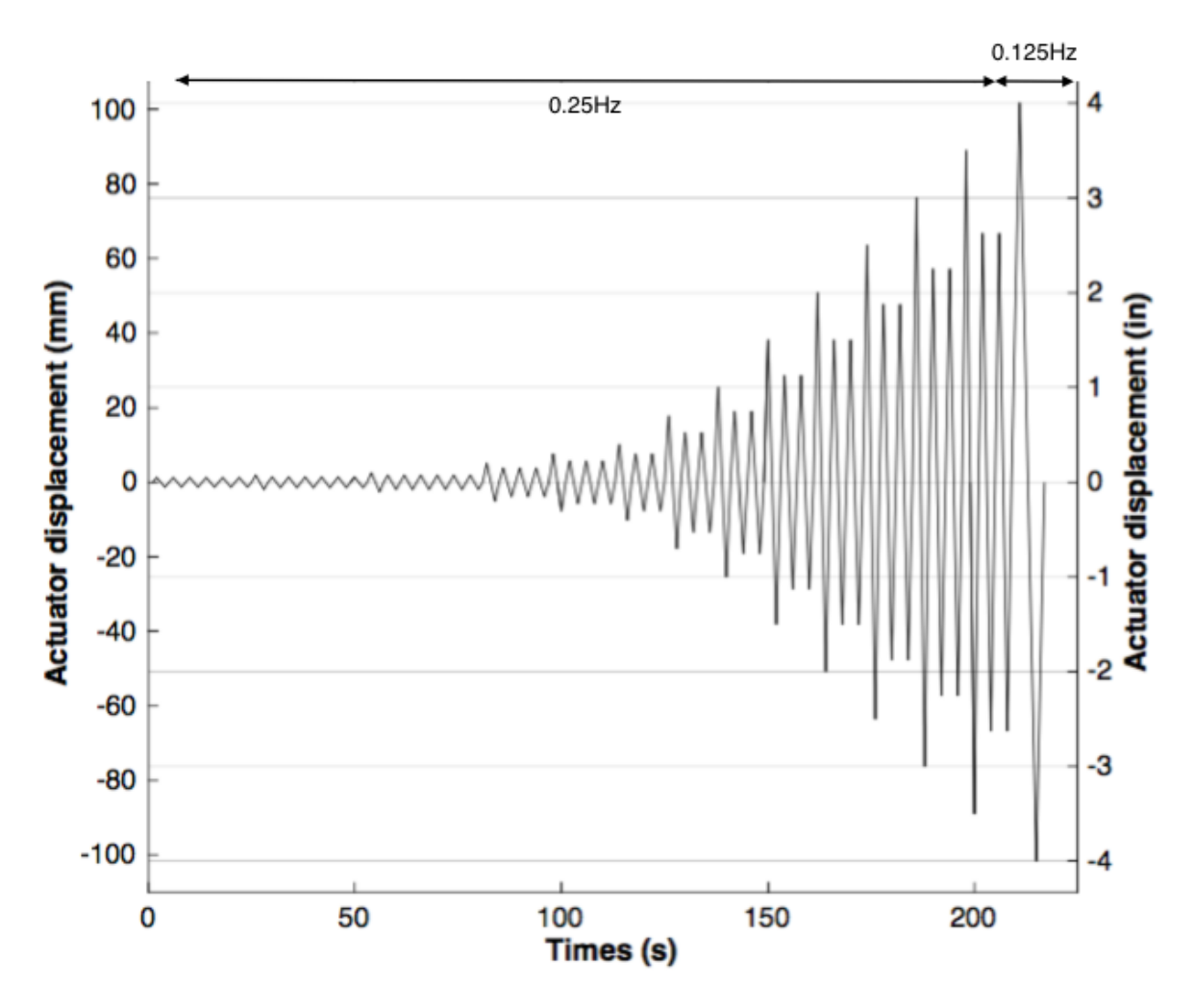


FIGURE C13 : Representative CUREE displacement time history W13

Wall Configuration:	W14		
Screw Pattern:	6"/12"		
Δm	43.722mm		
Δ=0.6 Δm	26.233mm		
Displacement	Actuator Input (mm)	Number of Cycles	Cycle Type
0.05	1.312	6	Initiation
0.075	1.967	1	Primary
0.056	1.469	6	Trailing
0.1	2.623	1	Primary
0.075	1.967	6	Trailing
0.2	5.247	1	Primary
0.15	3.935	3	Trailing
0.3	7.87	1	Primary
0.225	5.902	3	Trailing
0.4	10.493	1	Primary
0.3	7.87	2	Trailing
0.7	18.363	1	Primary
0.525	13.772	2	Trailing
1	26.233	1	Primary
0.75	19.675	2	Trailing
1.5	39.35	1	Primary
1.125	29.512	2	Trailing
2	52.466	1	Primary
1.5	39.35	2	Trailing
2.5	65.583	1	Primary
1.875	49.187	2	Trailing
3	78.7	1	Primary
2.25	59.024	2	Trailing
3.5	91.816	1	Primary
2.625	68.862	2	Trailing
4	104.932	1	Primary

Table C14 - CUREE protocol input displacements for test W14

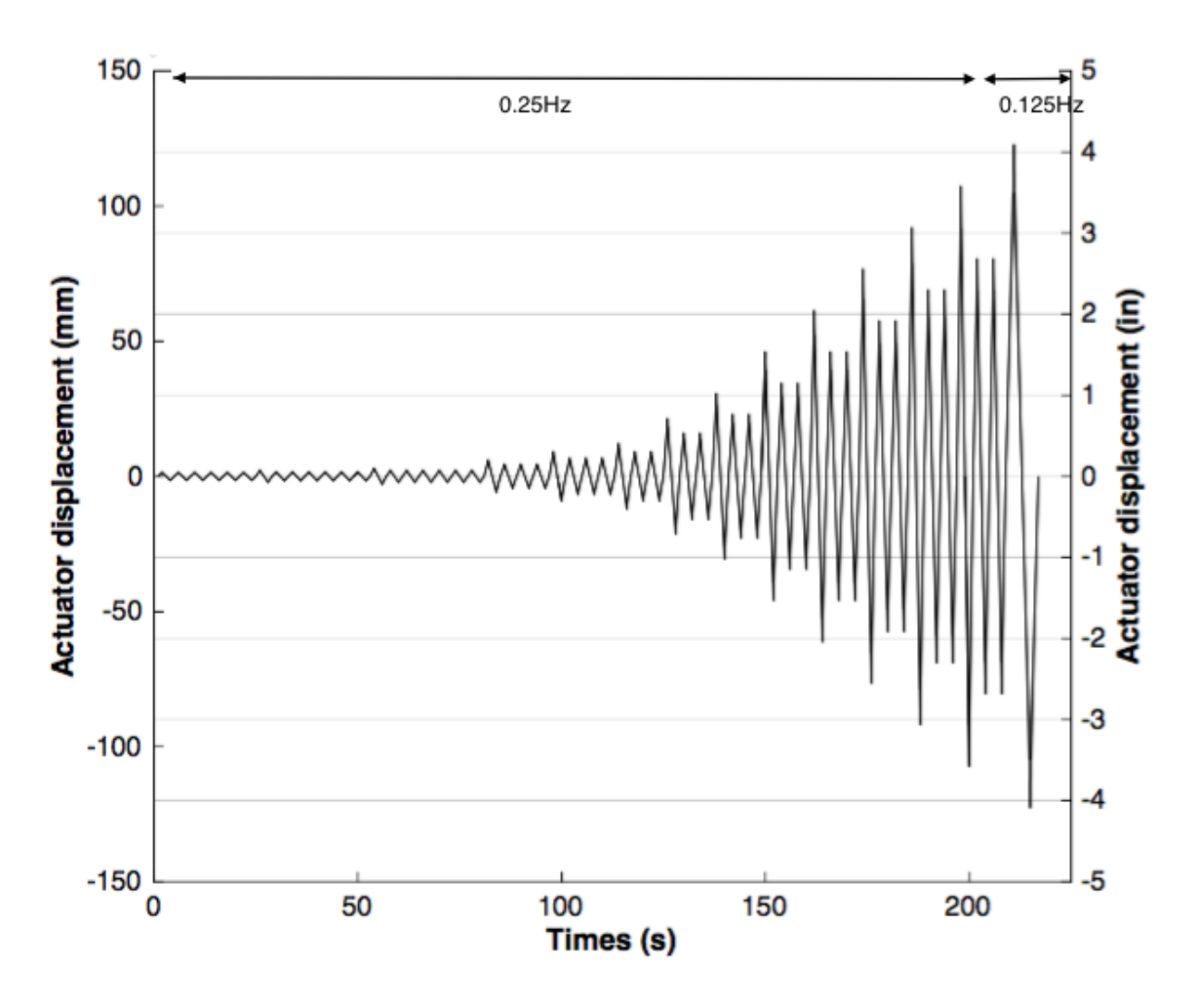
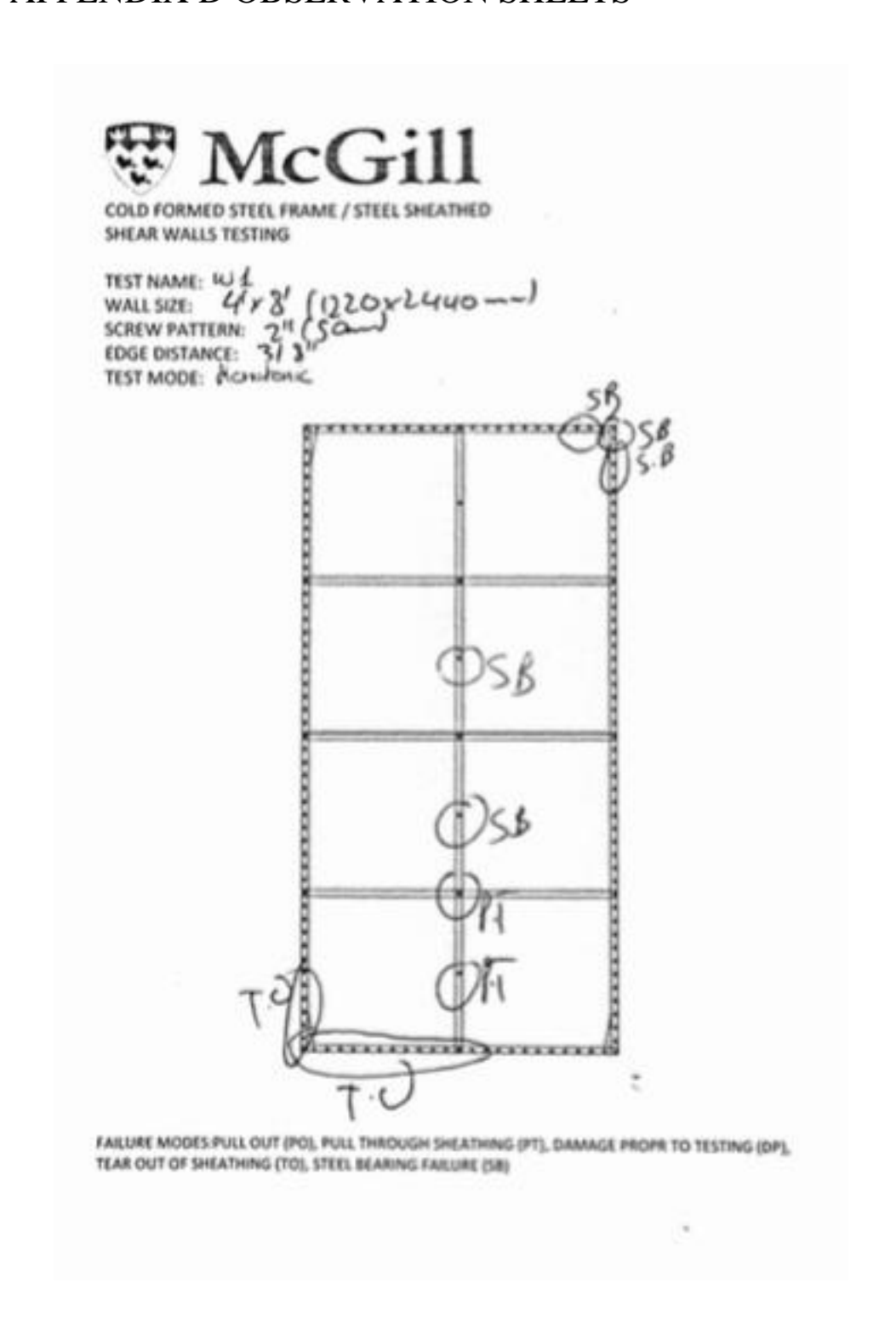


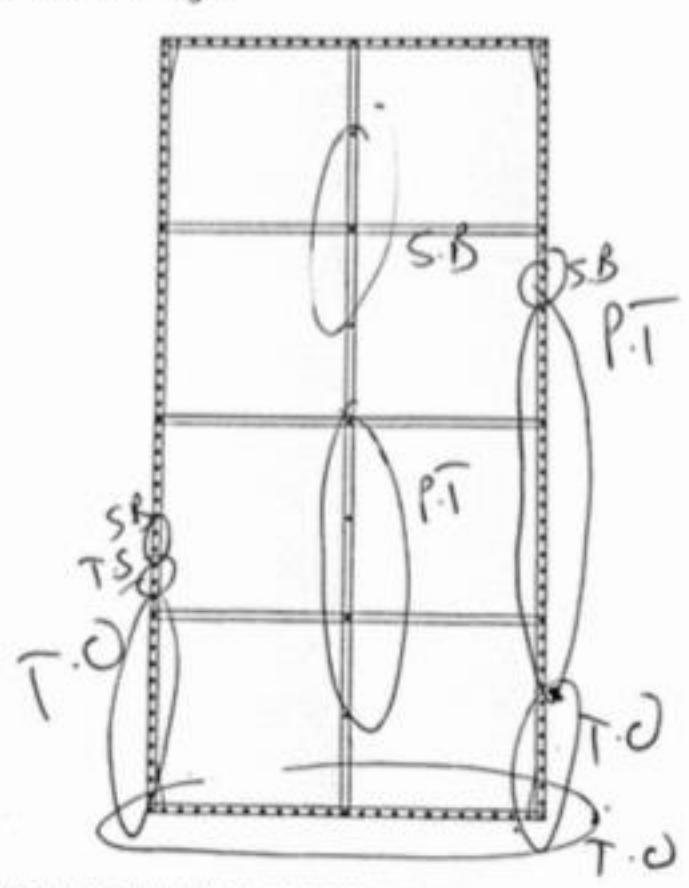
FIGURE C14 : Representative CUREE displacement time history W14

## APPENDIX D OBSERVATION SHEETS





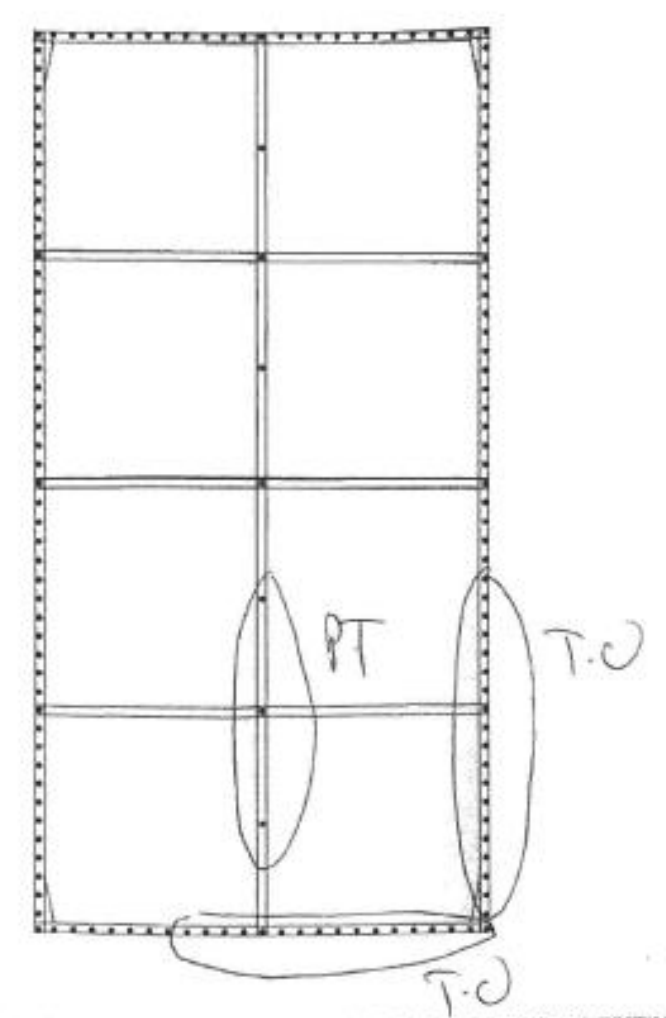
TEST NAME: W. 1 WALL SIZE: LI'V 3 (1220 x2440) SCREW PATTERN: 2" (50--) EDGE DISTANCE: 3/3" TEST MODE: KRUYSAR CY: LIC





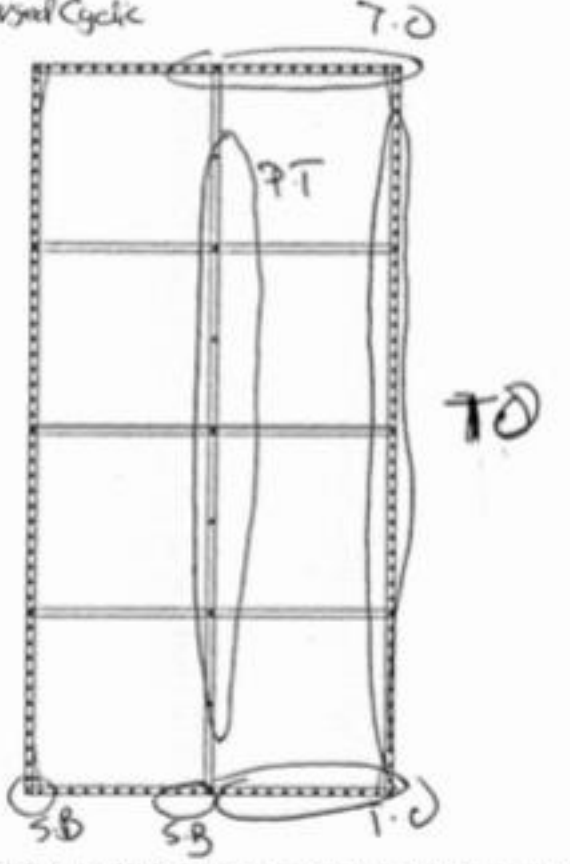
WALL SIZE: 4/23/(1220/2440~~)
SCREW PATTERN: 2"(50~~)
EDGE DISTANCE: 3/3"

TEST MODE: Manatonic



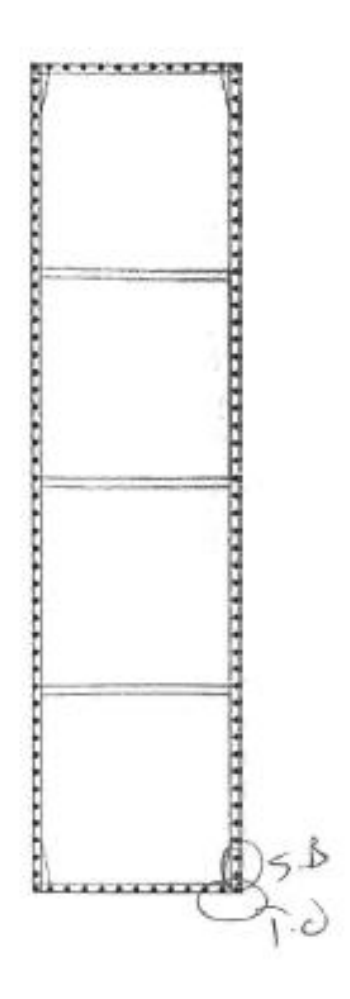


WALL SIZE: 2" (60m)
SCREW PATTERN: 2" (60m)
EDGE DISTANCE: 3/8"
TEST MODE: Lewyal Cycle
7-0 TEST NAME: W2





WALL SIZE: 7'x2' (GOY2440-)
SCREW PATTERN: 2" (50mm)
EDGE DISTANCE: 3/2"
TEST MODE: Hororopic



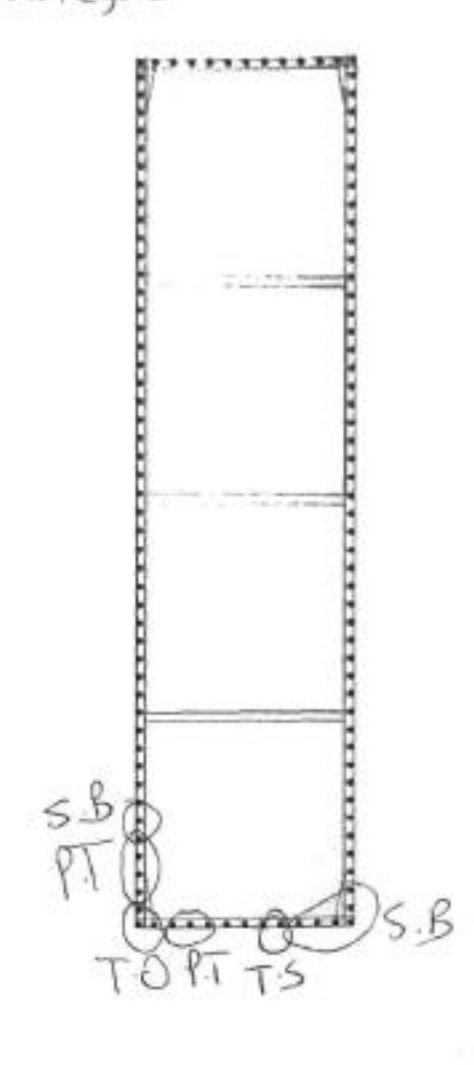


TEST NAME: 43

WALL SIZE: 21821 (GIOXZUYOLL)

SCREW PATTERN: 7" (50-1)

TEST MODE: Reversed Cycle



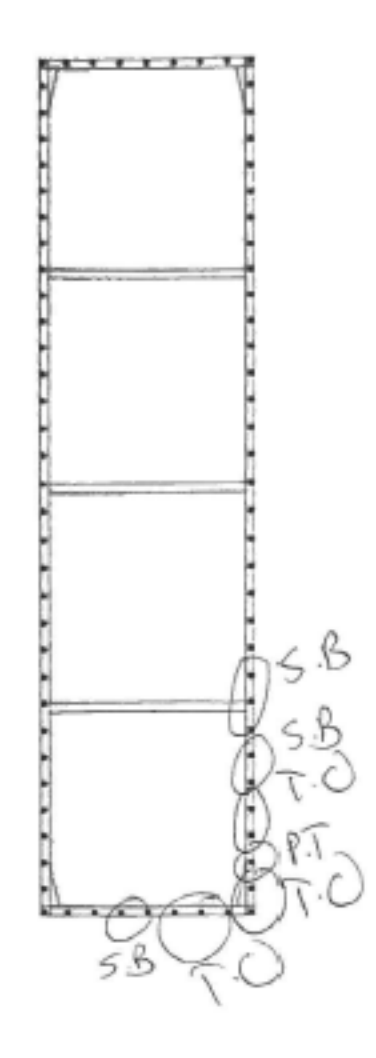


TEST NAME: W4

WALL SIZE: 21/28 (GIOX 2440mm)

SCREW PATTERN: 3" (7-5--)

EDGE DISTANCE: 31 817



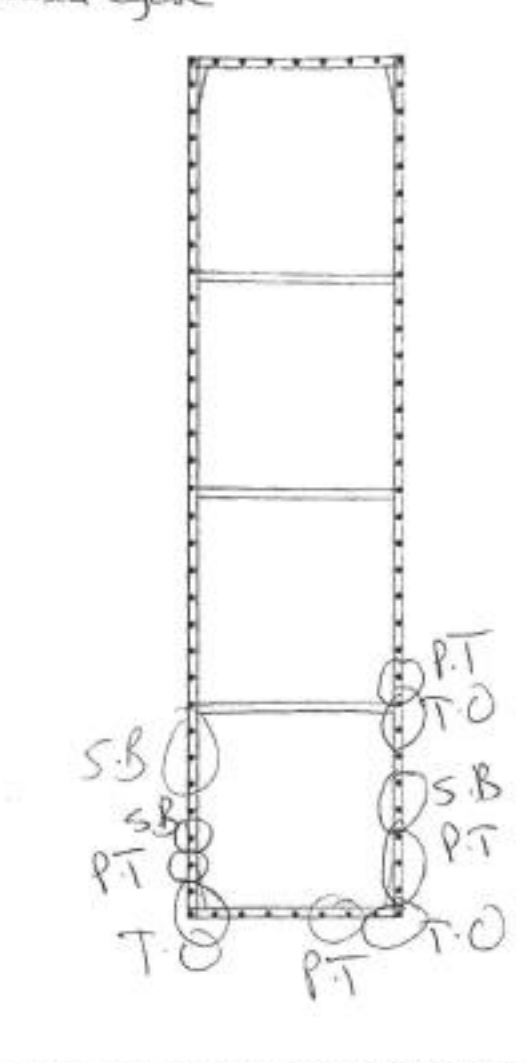


TEST NAME: W4

SCREW PATTERN: 31/75--)

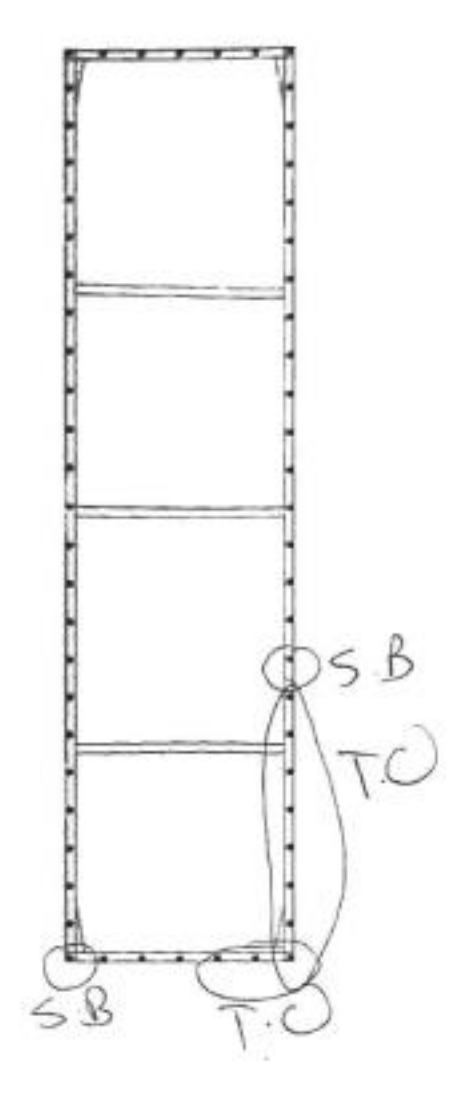
EDGE DISTANCE: 3/8"

TEST MODE: Keressel Cyclic





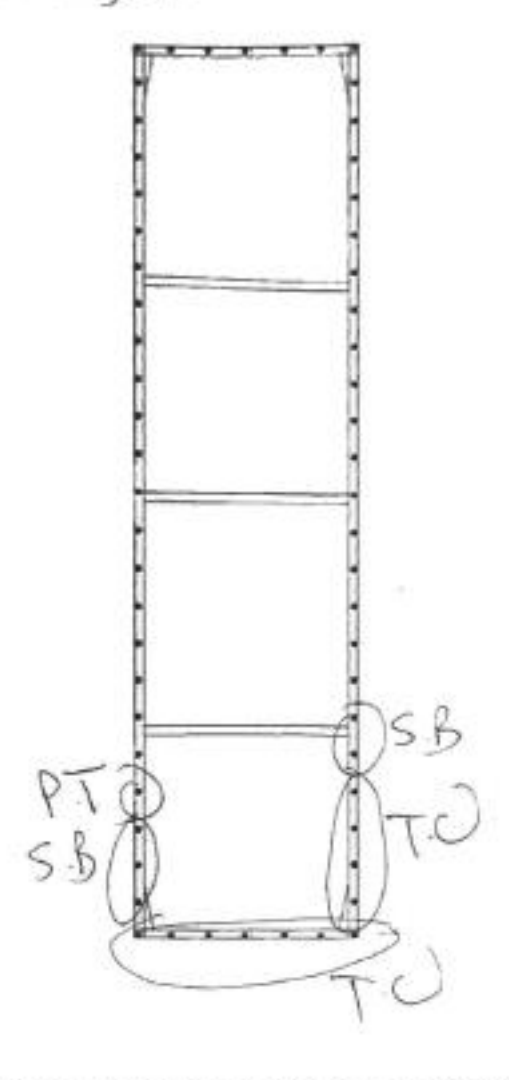
WALL SIZE: 2' B' (GICK Z440~~)
SCREW PATTERN: 4/(100~~)
EDGE DISTANCE: 3/8"
TEST MODE: Manafana





WALL SIZE: Z'x Z'(GICX 244cmm)

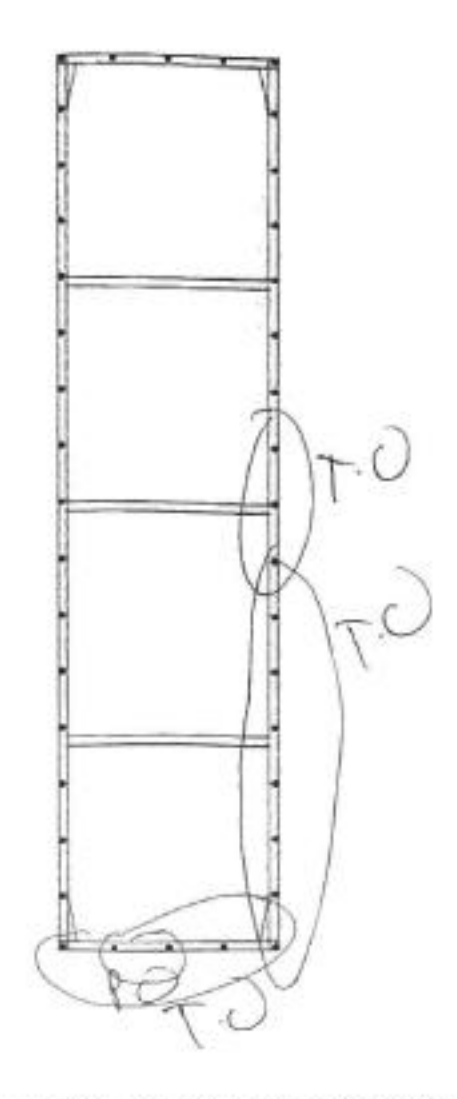
SCREW PATTERN: 100mm (4")
EDGE DISTANCE: 3/8"
TEST MODE: Reversal Cyclic





TEST NAME: WC
WALL SIZE: 2'x 8' (GIOX 2440 -- )
SCREW PATTERN: G"(ISOmn)
EDGE DISTANCE: 3/8"

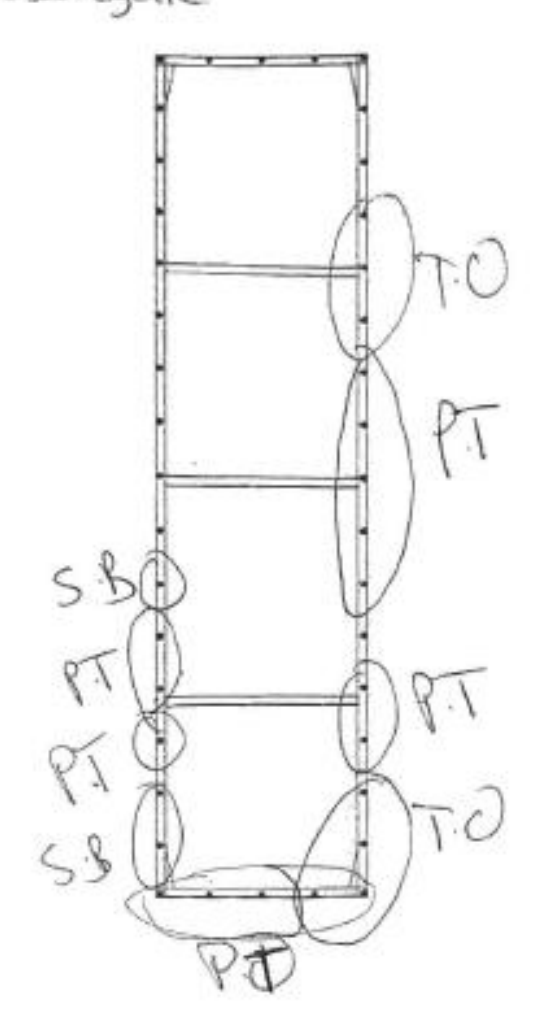
TEST MODE: Monotonic





WALL SIZE: 21/2 (GIOY 2440--)
SCREW PATTERN: 6" (150--)

EDGE DISTANCE: 318"
TEST MODE: REVOSON Cyclic



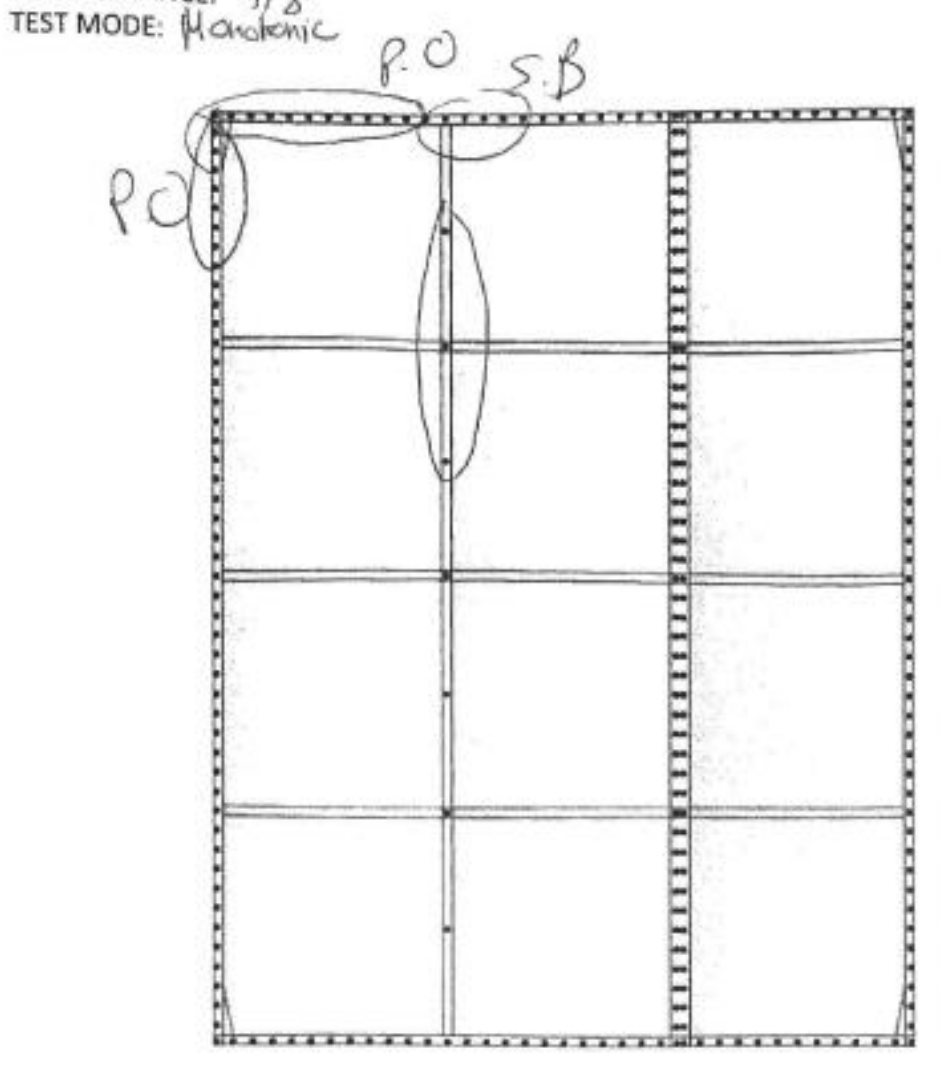


TEST NAME: W7

WALL SIZE: 6/x 2/ (1830×2440mm)

SCREW PATTERN: 2" (50mm)

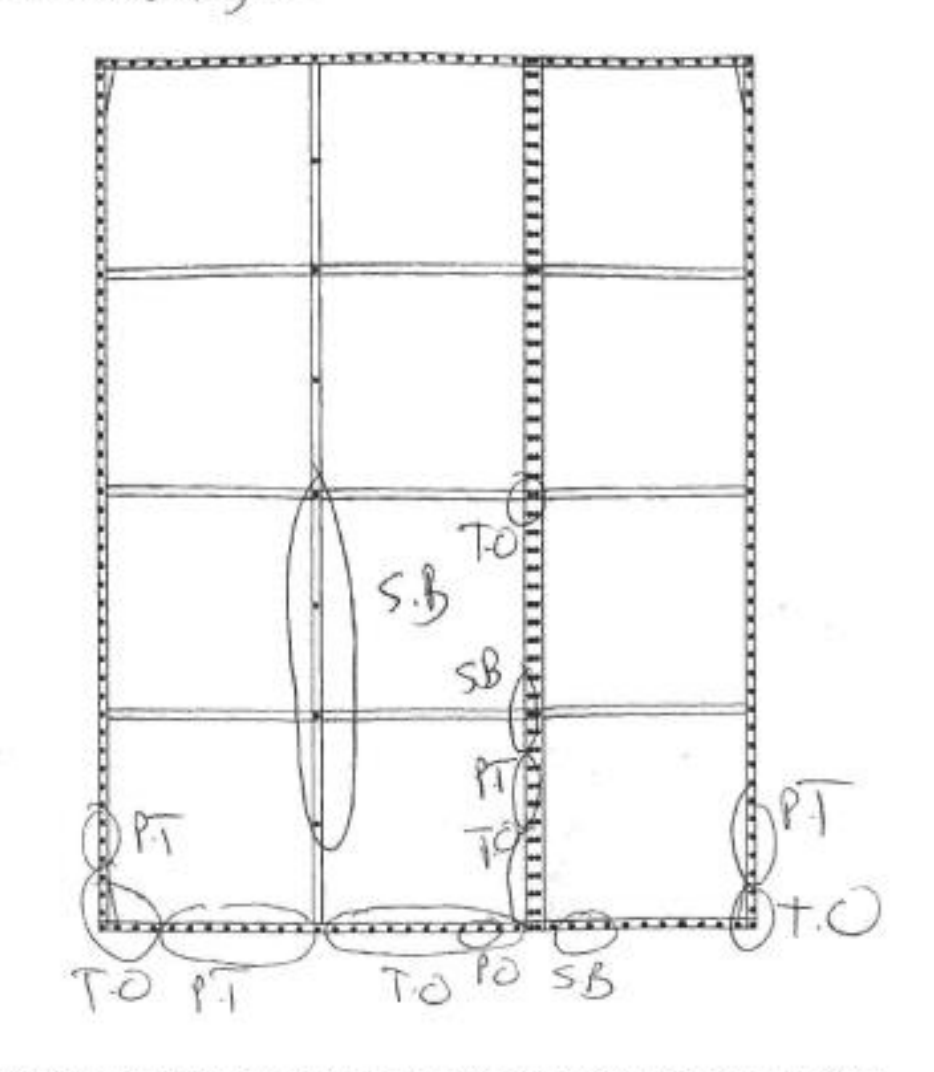
EDGE DISTANCE: 3) 3"



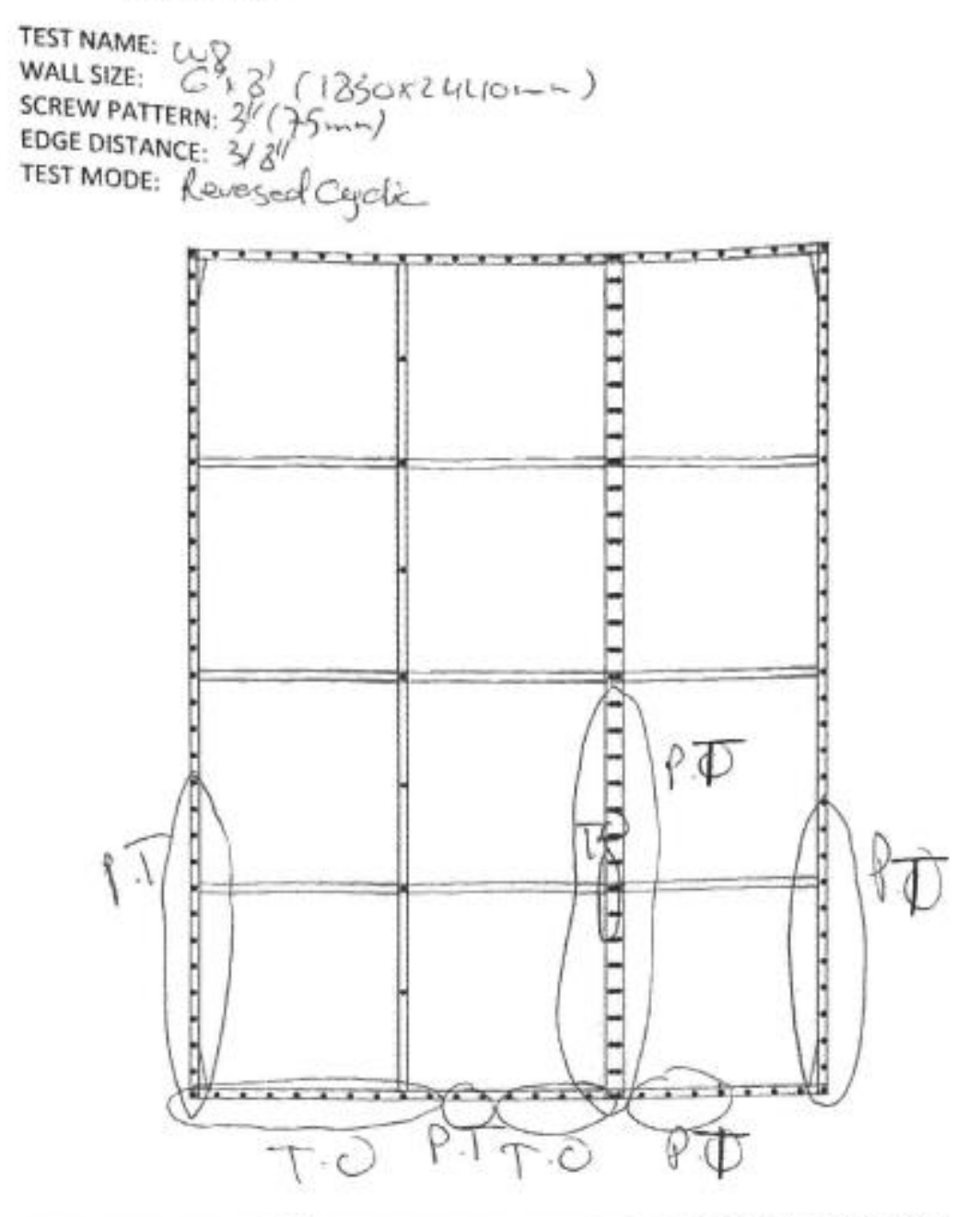


WALL SIZE: G'K 8" (1830x24466mm)
SCREW PATTERN: 2"(50mm)

TEST MODE: KENEYSOLCYCIC







FAILURE MODES: PULL OUT (PO), PULL THROUGH SHEATHING (PT), DAMAGE PROPR TO TESTING (DP), TEAR OUT OF SHEATHING (TO), STEEL BEARING FAILURE (SB)



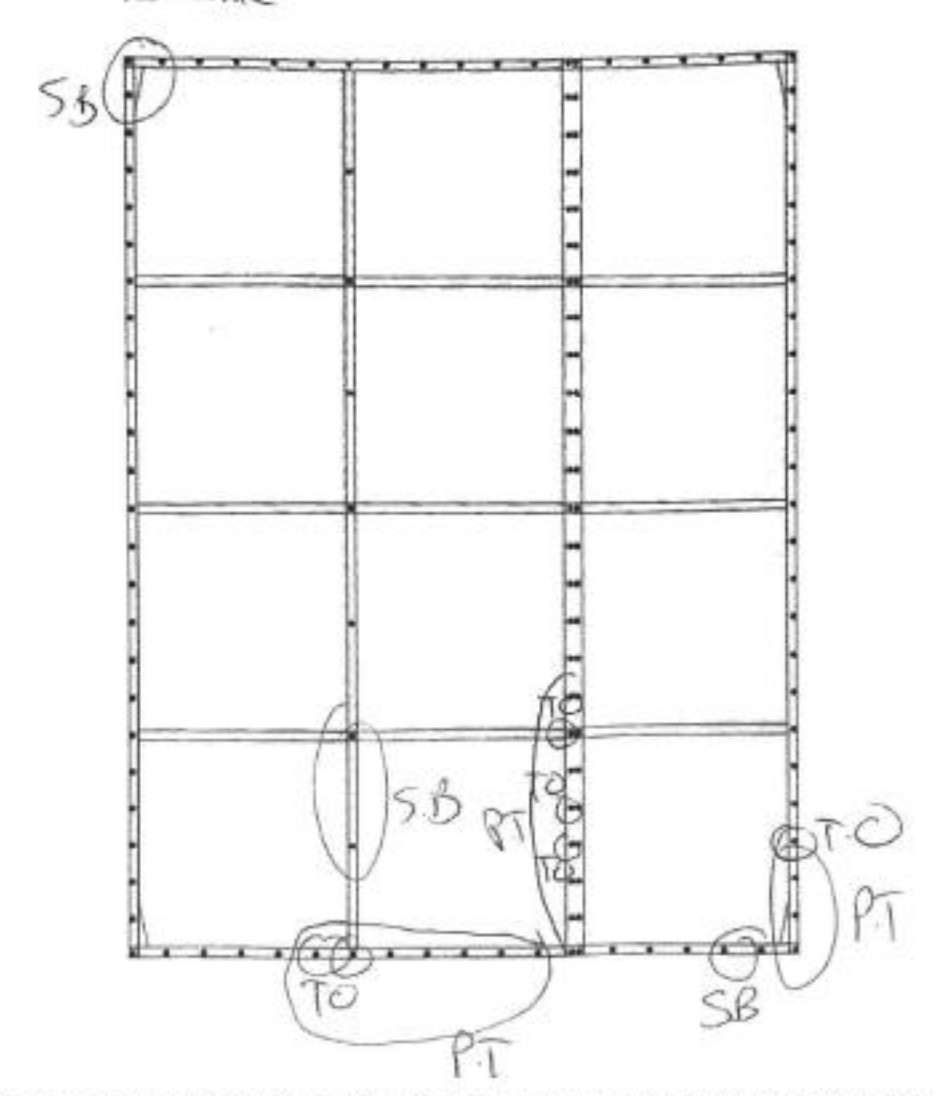
TEST NAME: 109

WALL SIZE: 6'x 8' (1830×2440mm)

SCREW PATTERN: 4/1 (1000mm

EDGE DISTANCE:

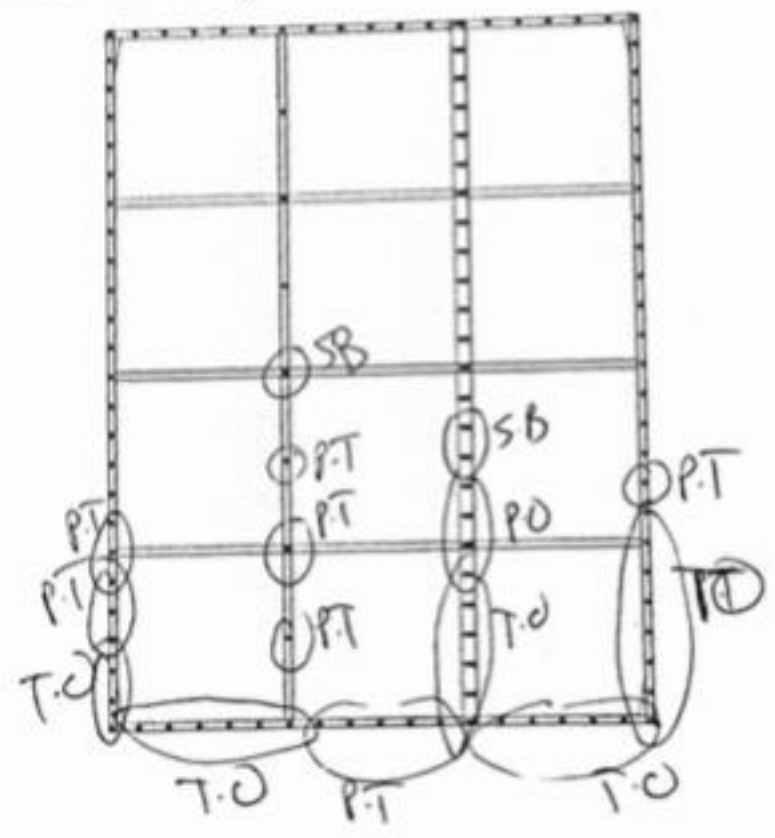
TEST MODE: Konstonic



FAILURE MODES: PULL OUT (PO), PULL THROUGH SHEATHING (PT), DAMAGE PROPR TO TESTING (DP), TEAR OUT OF SHEATHING (TO), STEEL BEARING FAILURE (SB)



TEST NAME: W) G' 13 (1830 XL440 -- )
WALL SIZE: SCREW PATTERN: 4" (100 -- )
EDGE DISTANCE: 3/8"
TEST MODE: RECESSA! Cyclic

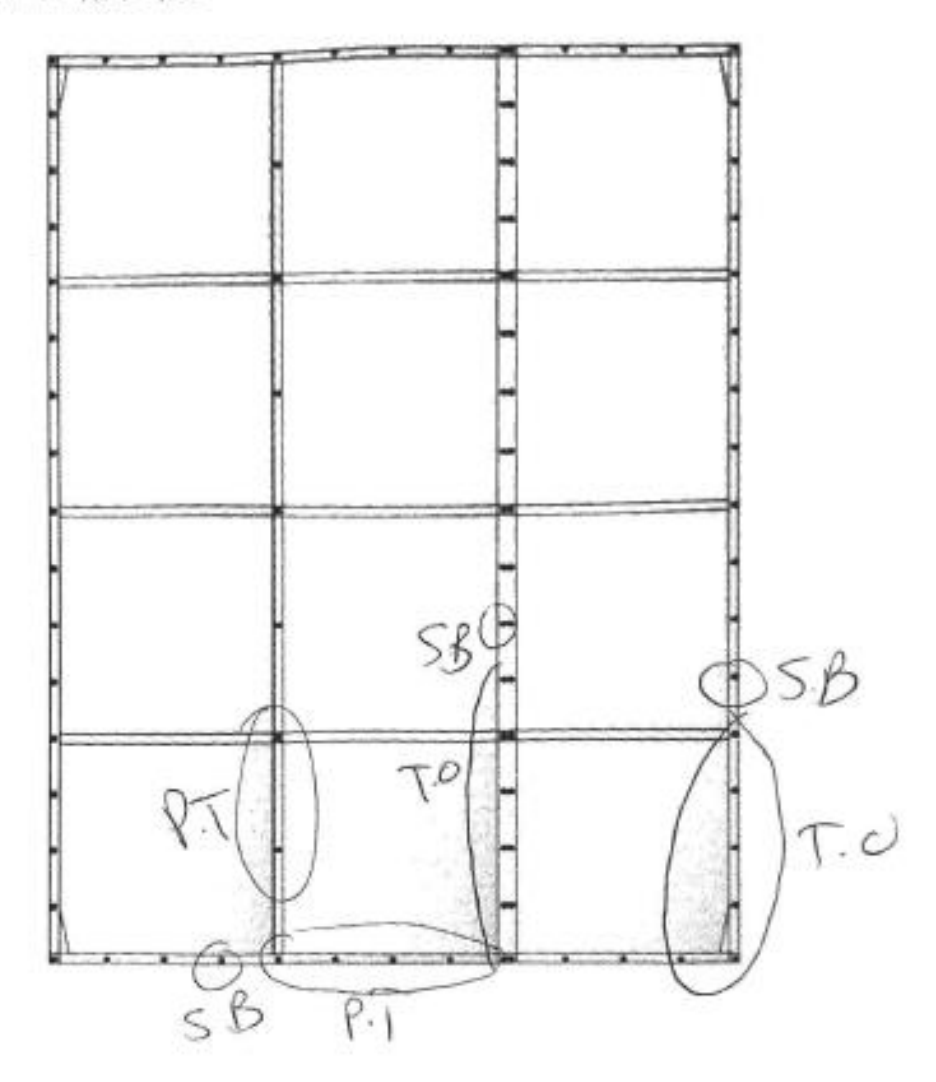




TEST NAME: WIG

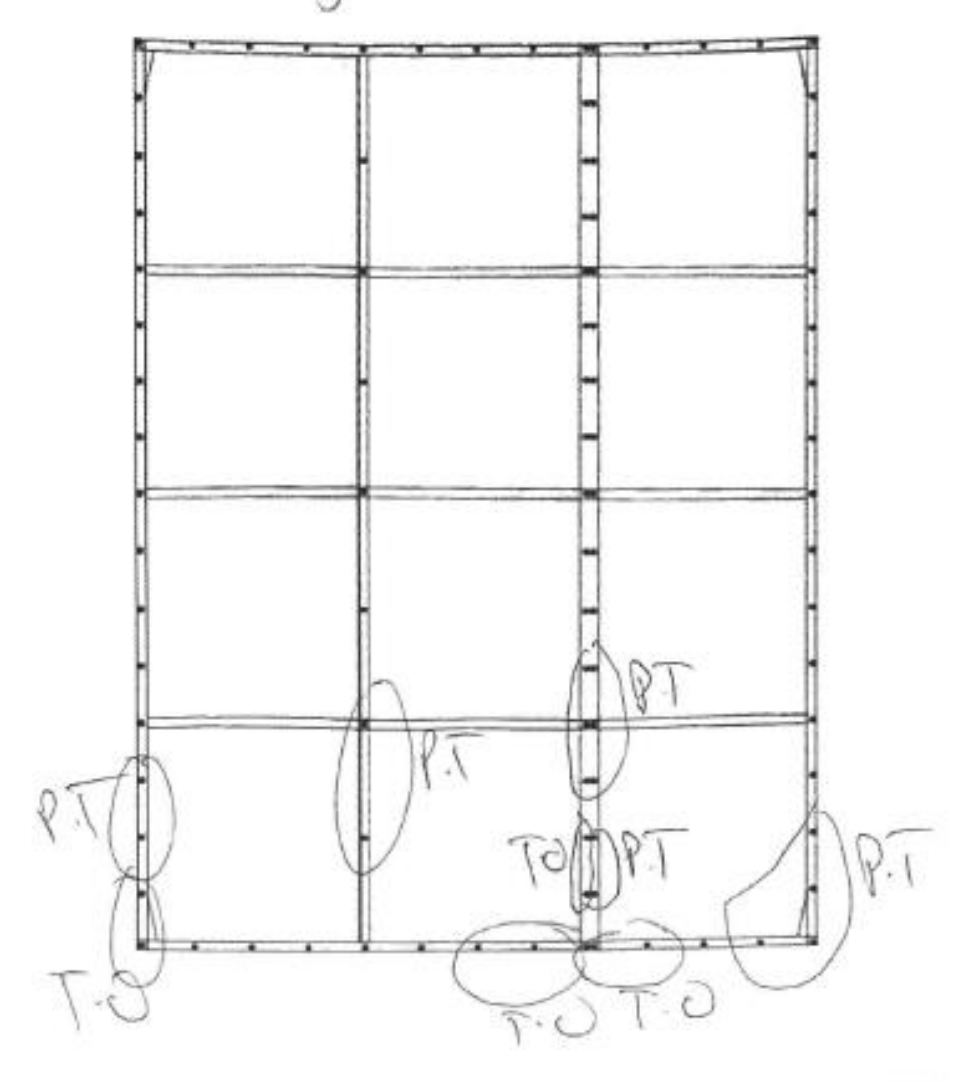
WALL SIZE: 6'x 8' (1830 x2440 mm)
SCREW PATTERN: 6" (150mm)

EDGE DISTANCE: 3/8"! TEST MODE: Mana Panic



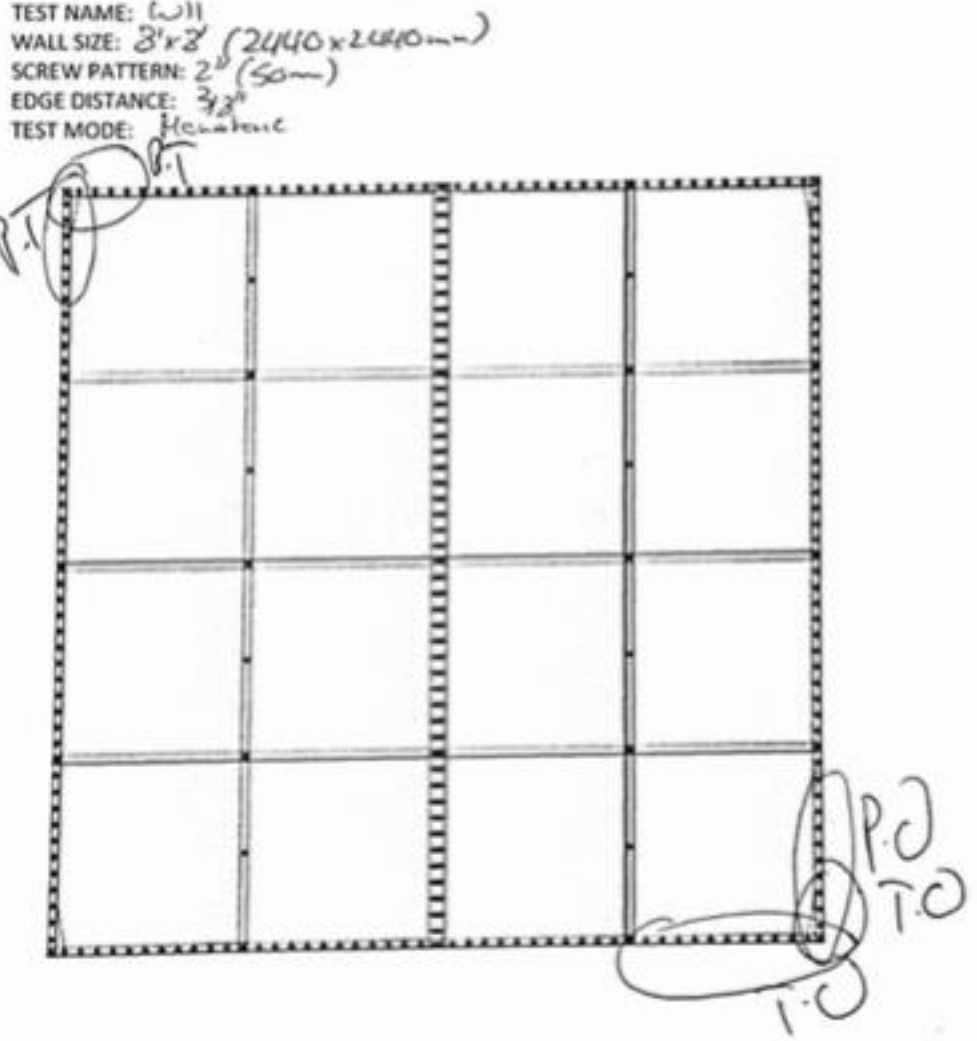


TEST NAME: CU 10
WALL SIZE: G'K 3) (1830x24402-)
SCREW PATTERN: G'(150-)
EDGE DISTANCE: 3/8"
TEST MODE: Leversed Ceptic





TEST NAME: (W)

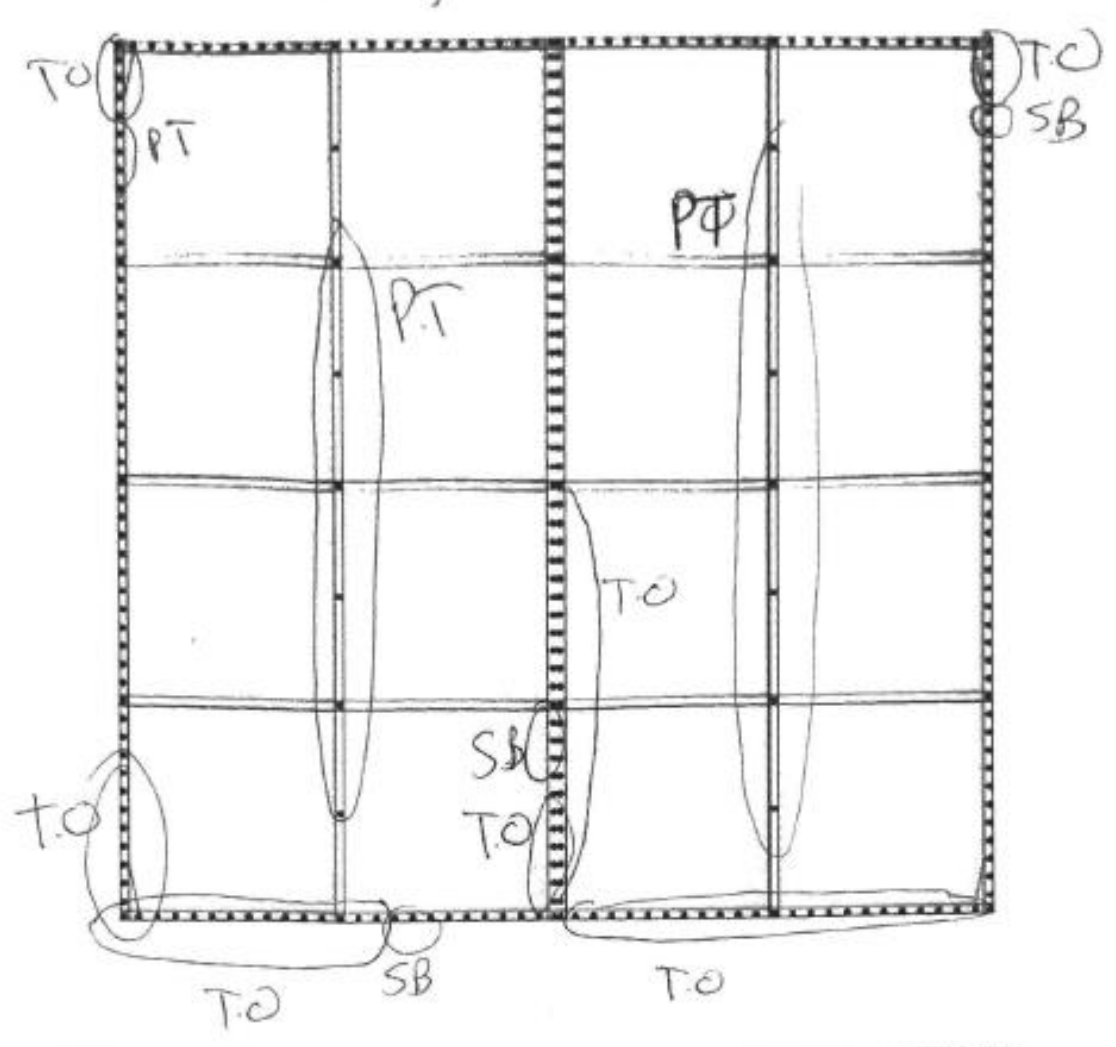




TEST NAME: (UI)

WALL SIZE: 81-8 (2440-2440-) SCREW PATTERN: 2"(50-)

TEST MODE: Reversed Capelic

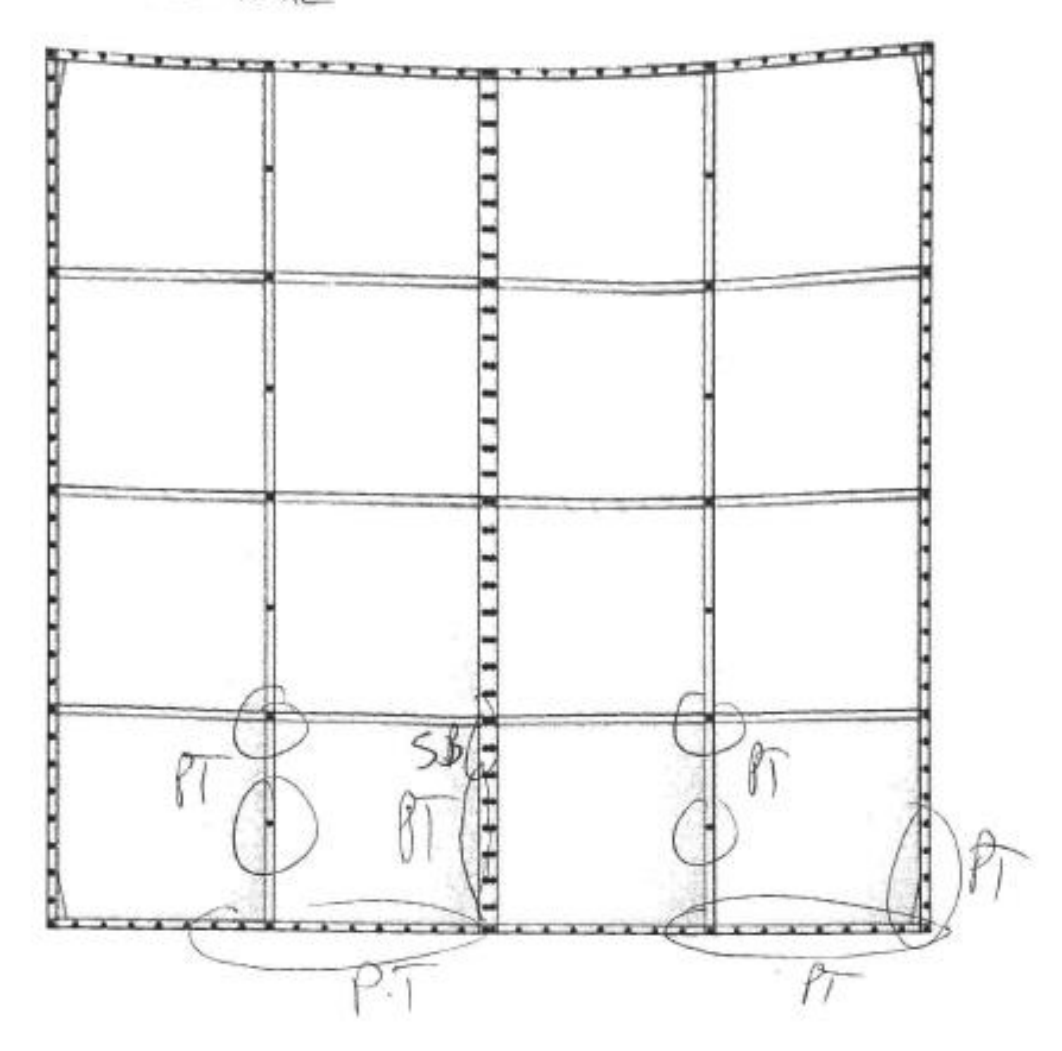


FAILURE MODES: PULL OUT (PO), PULL THROUGH SHEATHING (PT), DAMAGE PROPR TO TESTING (DP), TEAR OUT OF SHEATHING (TO), STEEL BEARING FAILURE (SB)



WALL SIZE: 8 x 8 (2440x 2440--)
SCREW PATTERN: 3" (75--)
EDGE DISTANCE: 3/8"

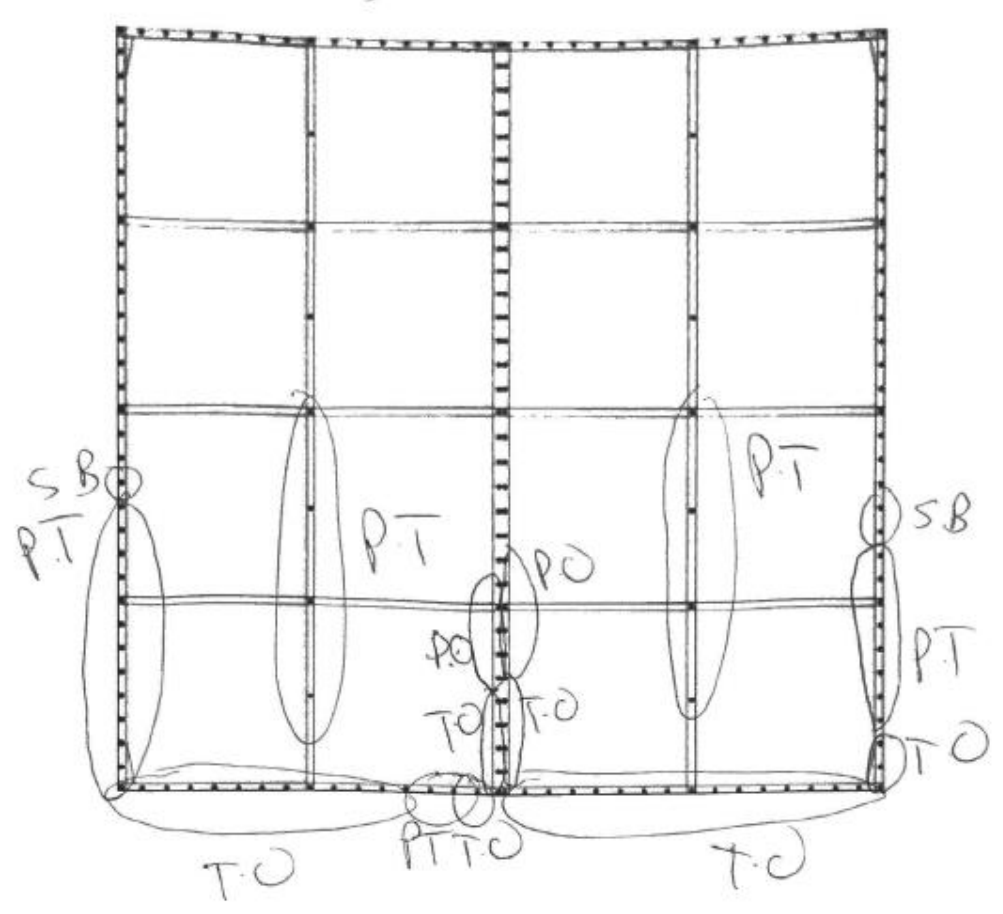
TEST MODE: Monatonic





TEST NAME. WIL

WALL SIZE: 8/8/(2440x 2440m-)
SCREW PATTERN: 3"(75m-)
EDGE DISTANCE: 3/8"
TEST MODE: Reveselyelic

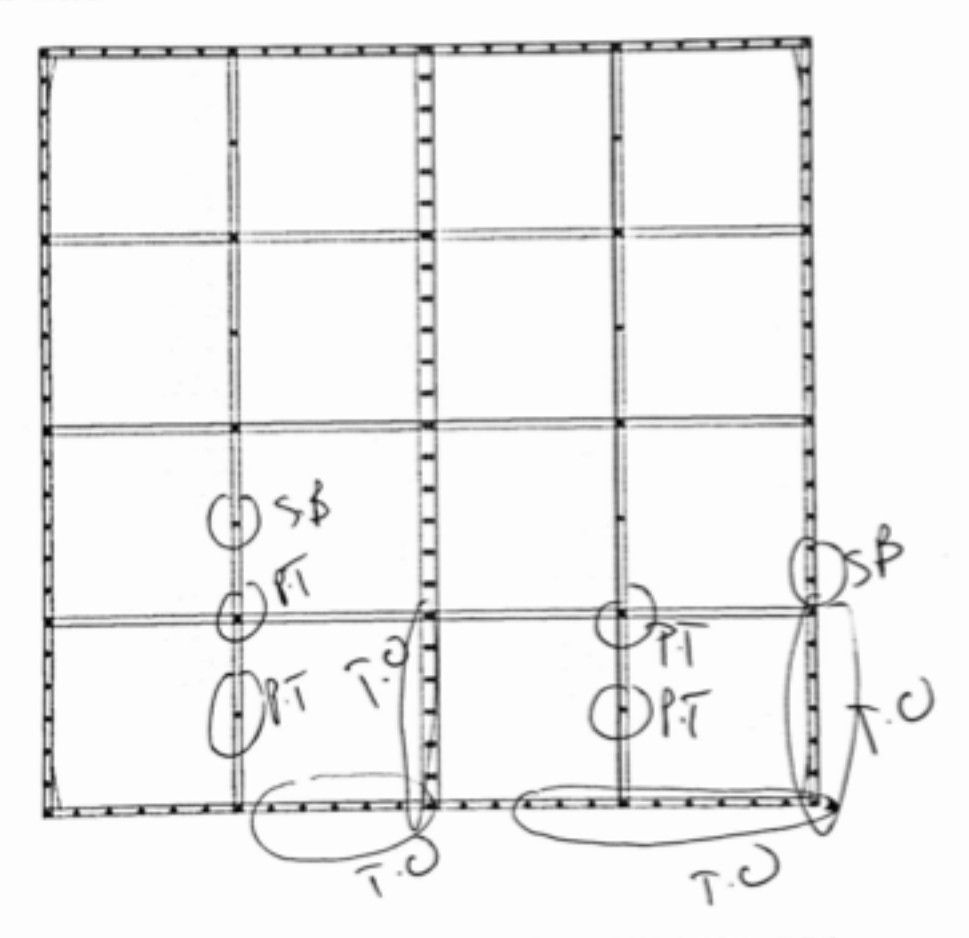


FAILURE MODES: PULL OUT (PO), PULL THROUGH SHEATHING (PT), DAMAGE PROPR TO TESTING (DP), TEAR OUT OF SHEATHING (TO), STEEL BEARING FAILURE (SB)



TEST NAME: WIS 31 (2440-2440-1)
WALL SIZE: 31 81 (100-1)
EDGE DISTANCE: 31 81

TEST MODE: Handra



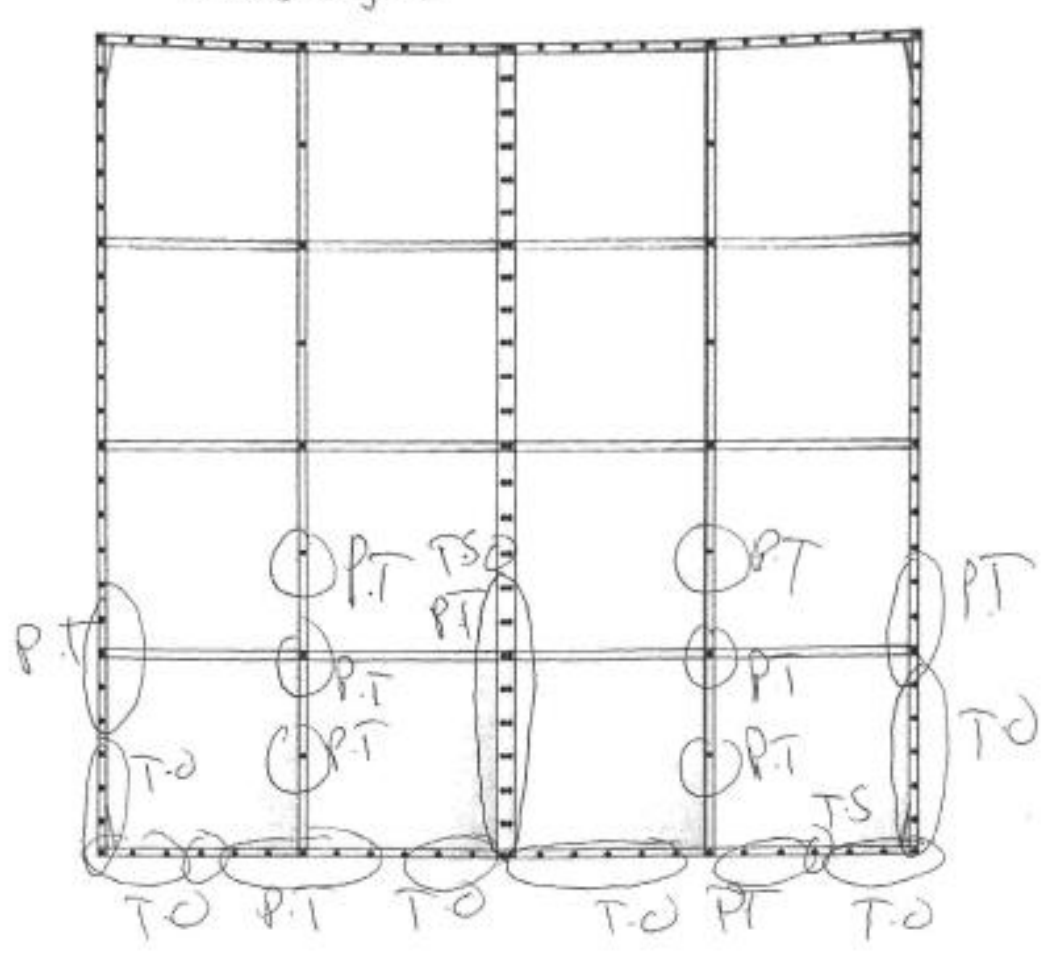


TEST NAME: W12

WALL SIZE: 3/2 8/ (Z4402244000)
SCREW PATTERN: 4///DOME)

EDGE DISTANCE: 3/3

TEST MODE: Revas-lagatic



FAILURE MODES: PULL OUT (PO), PULL THROUGH SHEATHING (PT), DAMAGE PROPE TO TESTING (DP), TEAR OUT OF SHEATHING (TO), STEEL BEARING FAILURE (SB)

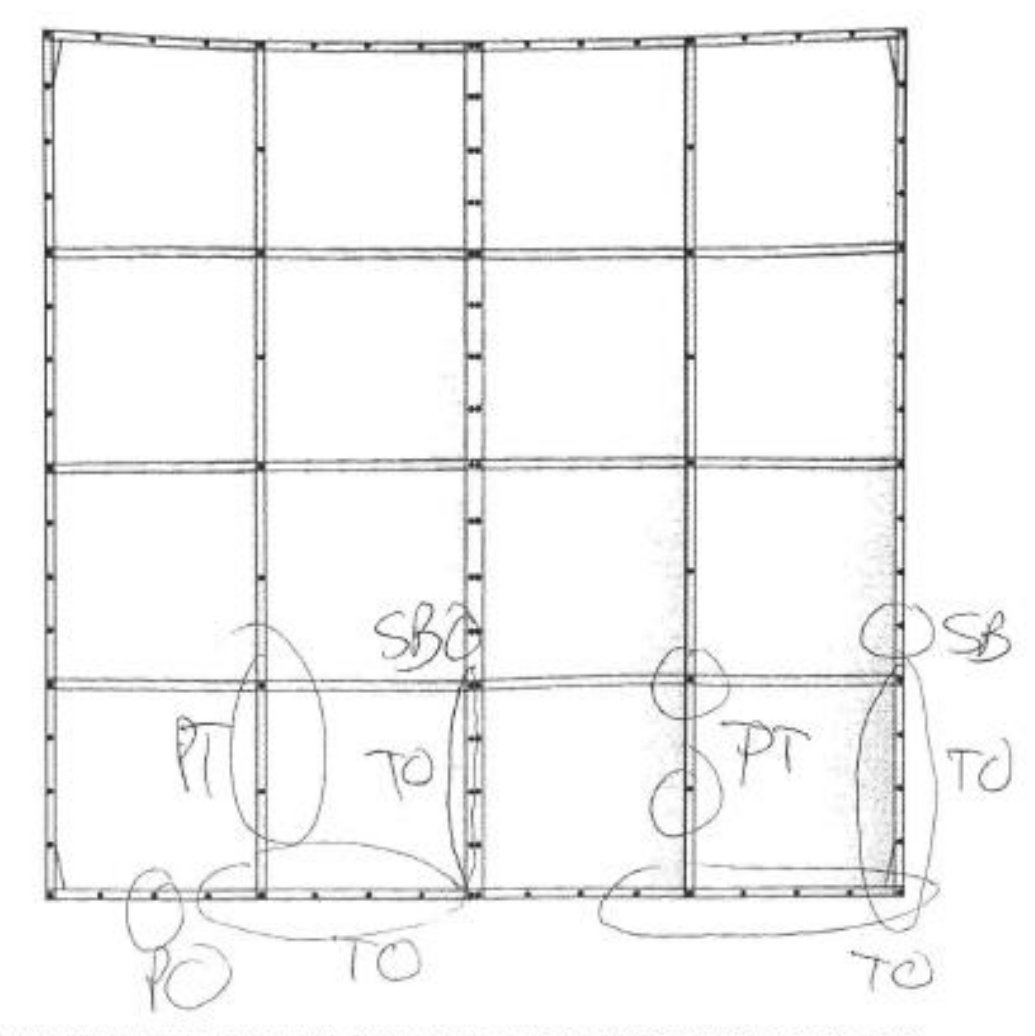


TEST NAME: W14

WALL SIZE: 81/281 (2440 2440 mm)

EDGE DISTANCE: 3/8"

TEST MODE: Manateria



FAILURE MODES: PULL OUT (PO), PULL THROUGH SHEATHING (PT), DAMAGE PROPR TO TESTING (DP), TEAR OUT OF SHEATHING (TO), STEEL BEARING FAILURE (SB)



TEST NAME: LUILY
WALL SIZE: 313 (3446,7446)
SCREW PATTERN: G (150-1)
EDGE DISTANCE; 3/8"
TEST MODE: Peres Cyclic

